Univerza v Ljubljani
Veterinarska fakulteta

Maja Brložnik

VREDNOTENJE PERFUZIJE MIŠJIH IN PASJIH TUMORJEV TER PRAŠIČJIH JETER PO ELEKTROPORACIJI S SLIKOVNO-DIAGNOSTIČNIMI METODAMI

Doktorska disertacija

Ljubljana, 2021

Univerza v Ljubljani
Veterinarska fakulteta

UDK 636.7.09+ 602.6:599.323.451:616.5-006:604.4:615.277.3:612.014.42:615.841(043.3)

mag. Maja Brložnik, dr. vet. med.

VREDNOTENJE PERFUZIJE MIŠJIH IN PASJIH TUMORJEV TER PRAŠIČJIH JETER PO ELEKTROPORACIJI S SLIKOVNO-DIAGNOSTIČNIMI METODAMI

Doktorska disertacija

PERFUSION ASSESSMENT OF MURINE AND CANINE TUMORS AND PORCINE LIVER AFTER ELECTROPORATION WITH DIAGNOSTIC IMAGING METHODS

Doctoral dissertation

Ljubljana, 2021

Maja Brložnik

Vrednotenje perfuzije mišjih in pasjih tumorjev ter prašičjih jeter po elektroporaciji s slikovno-diagnostičnimi metodami

Delo je bilo opravljeno na:

- Kliniki za male živali Veterinarske fakultete Univerze v Ljubljani
- Kliniki za reprodukcijo in velike živali Veterinarske fakultete Univerze v Ljubljani
- Onkološkem inštitutu Ljubljana, Oddelku za eksperimentalno onkologijo.

Mentorica: doc. dr. Darja Pavlin

Somentorica: višja znan. sod. dr. Simona Kranjc

Izjava o delu

Izjavljam, da je doktorska disertacija rezultat lastnega raziskovalnega dela, da so rezultati korektno navedeni in nisem kršila avtorskih pravic in intelektualne lastnine drugih. Izjavljam, da je elektronski izvod identičen tiskanemu.

Člani strokovne komisije za oceno in zagovor:

Predsednica: doc. dr. Ana Nemec

Član: prof. dr. Robert Frangež

Član: prof. dr. Igor Kocijančič

IZVLEČEK

Ključne besede: kožne novotvorbe – slikovna diagnostika; jetra – slikovna diagnostika; elektrokemoterapija – metode; bleomicin – terapevtska raba; elektroporacija – metode; tehnike genskega prenosa; plazmidi – genetika; interlevkin-12 – genetika; ultrasonografija – metode; kontrastna sredstva; računalniška tomografija; izid zdravljenja; živalski modeli; miši; psi; prašiči

Namen doktorske disertacije je bil ovrednotenje rezultatov slikovno-diagnostičnih metod po elektroporaciji (EP) in elektrokemoterapiji (EKT) jeter zdravih prašičev za preučitev varnostnega vidika EKT globoko ležečih jetrnih tumorjev ter rezultatov ultrazvočnega pregleda s kontrastnim sredstvom (UZ-KS) po EKT in genskem elektroprenosu (GEP) mišjih in pasjih tumorjev kot prediktivnih dejavnikov zdravljenja.

Slikovno-diagnostične spremembe po EP in EKT z bleomicinom (BLM) v jetrnem parenhimu in velikih krvnih žilah jeter zdravega prašiča s potencialno nevarno vstavitvijo linearnih in heksagonalnih elektrod v velike jetrne žile smo preučili z ultrazvočno preiskavo takoj po EP/EKT ter z računalniško tomografijo od 60 do 90 minut in en teden po EP/EKT. Rezultati slikovno-diagnostičnih metod jeter prašičev po EK so pokazali zmanjšano perfuzijo tretiranega področja. Spremembe niso bile posledica uporabe BLM, saj so bile enake pri poskusni in kontrolni skupini, kjer smo aplicirali samo električne pulze. Namerna vstavitev elektrod in aplikacija električnih pulzov neposredno v svetlino velikih žil ni povzročila tromboz, krvavitev ali drugih hemodinamskih motenj.

Kot model preiskovanja uporabnosti UZ-KS kot prediktivnega dejavnika zdravljenja s terapevtskimi metodami, ki temeljijo na EP, smo uporabili miši z induciranimi melanomi. V prvi raziskavi smo na mišjem modelu, ki smo ga zdravili z obsevanjem in GEP plazmidne DNA, ki utiša adhezijsko molekulo celic melanoma, opazili značilno zmanjšanje perfuzije tumorjev v terapevtskih skupinah v primerjavi s kontrolnimi skupinami, rezultati UZ-KS pa so korelirali z zmanjšano gostoto žil. Povprečne vrednosti parametra, ki opisuje volumen pretoka, so bile značilno nižje pri tumorjih, ki so se odzvali na terapijo s popolnim odgovorom, in vrednosti PE so pokazale trend korelacije s protitumorsko učinkovitostjo. V drugi raziskavi na mišjih melanomih, zdravljenih z EKT z BLM v kombinaciji z GEP plazmida za interlevkin-12 (pIL-12), je UZ-KS pokazal zmanjšano perfuzijo v skupinah z daljšim časom podvojitve volumna tumorja in prediktivno vrednost UZ-KS smo potrdili s statistično značilnimi Pearsonovimi koeficienti. S krajšim časom podvojitve volumna tumorja je bila povezana tudi večja heterogenost perfuzije tumorja.

V klinični del raziskave smo vključili pse s kožnimi in podkožnimi tumorji, ki so bili zdravljeni s standardnim postopkom kombinacije EKT in GEP pIL-12. Rezultate UZ-KS smo primerjali z izidom zdravljenja. Tudi v klinični raziskavi pri psih smo ugotovili številne razlike v parametrih UZ-KS med tumorji s popolnim odgovorom in tumorji z nepopolnim odgovorom: perfuzija in heterogenost perfuzije sta bili manjši pri tumorjih s popolnim odgovorom.

ABSTRACT

Key words: skin neoplasms – diagnostic imaging; liver – diagnostic imaging; electrochemotherapy – methods; bleomycin – therapeutic use; electroporation – methods; gene transfer techniques; plasmids – genetics; interleukin-12 – genetics; ultrasonography – methods; contrast media; tomography, x-ray computed; treatment outcome; models, animal; mice; dogs; swine

The aim of this dissertation was to evaluate the results of diagnostic imaging after electroporation (EP) and electrochemotherapy (ECT) of porcine liver to investigate the safety aspect of ECT of deep-seated liver tumors and the results of dynamic contrast-enhanced ultrasound (DCE-US) after ECT and gene electrotransfer (GET) of murine and canine tumors as potential predictive factors in treatment.

Radiological findings after EP and ECT with bleomycin (BLM) on the hepatic parenchyma and major blood vessels of the liver of a healthy pig with potentially dangerous insertion of the electrodes into the major hepatic vessels were examined by ultrasound immediately after ECT and by computed tomography from 60 to 90 minutes and one week after ECT with linear and hexagonal electrodes. The results of diagnostic imaging of the porcine liver after ECT showed decreased blood flow in the treated area. The changes were not due to the use of BLM, as they were the same in the experimental and control groups, where only electrical pulses were administered. Intentional insertion of electrodes and application of electrical pulses directly into the lumen of large vessels did not result in thrombosis, haemorrhage, or other hemodynamically significant injury.

Mice with induced melanoma were used as a model to investigate the utility of DCE-US as a prognostic factor for treatment with EP-based therapies. In the first study in a mouse model treated with irradiation and GET of plasmid DNA that silences the melanoma cell adhesion molecule, we observed a decrease in tumor perfusion in the treatment groups compared with the control groups, and the results of DCE-US correlated with decreased vessel density detected histologically. Furthermore, mean values of parameters describing flow volume were significantly lower in tumors with complete response, and they showed a trend toward correlation with antitumor efficacy. In the second study, mouse melanomas were treated with ECT in combination with GET of plasmid DNA encoding interleukin-12 (pIL-12). DCE-US showed reduced perfusion in groups with longer tumor volume doubling time, and the predicted DCE-US value was confirmed by statistically significant Pearson coefficients. In addition, greater tumor perfusion heterogeneity was associated with shorter tumor doubling time.

The clinical study included dogs with cutaneous and subcutaneous neoplasms treated with a standard procedure combining ECT and GET pIL-12. We also found a number of differences in DCE-US parameters between tumors with complete response and tumors with incomplete response in the clinical study: Perfusion and perfusion heterogeneity were lower in tumors with complete response.

Kazalo vsebine

Kazalo slik

Seznam okrajšav

AUC	površina pod krivuljo (angl. area under curve)
BLM	bleomicin (angl. bleomycin)
CT-KS	računalniška tomografija s kontrastnim sredstvom (angl. DCE-CT: dynamic contrast enhanced computed tomography)
EKT	elektrokemoterapija (angl. ECT: electrochemotherapy)
EP	elektroporacija (angl. electroporation)
GEP	genski elektroprenos (angl. GET: gene electrotransfer)
IL-12	interlevkin-12
iRECIST	smernice za kriterije odziva za preskušanje imunoterapevtikov (angl. response evaluation criteria in solid tumors in immunotherapy trials)
MCAM	adhezijska molekula celic melanoma (angl. melanoma cell adhesion molecule)
mRECIST	prilagojeni kriteriji RECIST (angl. modified RECIST)
MRI-KS	magnetnoresonančno slikanje s kontrastnim sredstvom (angl. DCE-MRI dynamic contrast enhanced magnetic resonance imaging)
PE	maksimalna amplituda harmonskega signala oz. vrh ločljivosti (angl. peak enhancement)
pIL-12	plazmidna DNA, ki kodira interlevkin-12
RECIST	kriteriji za oceno odziva pri solidnih tumorjih (angl. response evaluation criteria in solid tumors)
ROI	preiskovano območje (angl. region of interest)
TTP	čas do vrha (angl. time to peak)
UZ-KS	ultrazvočni pregled s kontrastnim sredstvom (angl. DCE-US: dynamic contrast enhanced ultrasound)

1 UVOD

1.1 Pregled literature

1.1.1 Elektroporacija, elektrokemoterapija in genski elektroprenos

Reverzibilna elektroporacija (EP) je metoda, kjer se začasno poveča prepustnost celične membrane z izpostavitvijo celic kratkim visokonapetostnim električnim pulzom, s čimer se molekulam omogoči vstop v celico. Uporablja se pri dveh načinih zdravljenja onkoloških bolnikov: elektrokemoterapiji (EKT) in genskem elektroprenosu (GEP). V primeru EKT se omogoči vstop kemoterapevtikom, v primeru GEP pa plazmidni DNA in drugim nukleinskim kislinam (1,2).

Najpogosteje uporabljana kemoterapevtika za EKT sta cisplatin in bleomicin (BLM) (3, 4, 5, 6). Cisplatin, derivat platine, se uporablja predvsem apliciran intratumorsko, saj je lahko pri intravenski uporabi nefrotoksičen za pse, pri mačkah pa je kontraindiciran zaradi nastanka fulminantnega pljučnega edema (3, 7, 8, 9). Citotoksični antibiotik BLM, ki ga proizvaja bakterija *Streptomyces verticullus* (10), pa se uporablja intravensko in intratumorsko (3, 7, 11, 12). Na mestu, kjer apliciramo pulze, je zaradi prehodno povečane propustnosti celičnih membran dosežena visoka znotrajcelična koncentracija kemoterapevtika in zato močnejše protitumorsko delovanje (2, 13, 14, 15). EKT je lokalno zdravljenje, ki ima učinek tako na tumorske celice kot na ožilje, kar ima za posledico protitumorski učinek pri različnih kožnih, podkožnih in globoko ležečih tumorjih (3, 14). Zdravljenje z EKT je postalo uveljavljen standard zdravljenja različnih človeških tumorjev, kot so melanom, ploščatocelični karcinom, karcinom bazalnih celic, kožne in podkožne metastaze (4, 16, 17, 18, 19, 20, 21, 22, 23, 24, 25), tumorji trebušne slinavke (26, 27, 28, 29), hepatocelularni karcinom in metastaze kolorektalnega karcinoma v jetrih (30, 31, 32, 33, 34, 35), relaps raka dojk (36, 37) idr. Kot samostojno zdravljenje EKT ne povzroča sistemske imunosti, medtem ko lahko EKT v kombinaciji z adjuvantnim GEP povzroči učinek na oddaljene nezdravljene metastaze (angl. abscopal effect) (5, 16, 17, 18, 38, 39, 40, 41, 42).

V primeru GEP s pomočjo EP vnesemo v celice genetski material za terapevtski gen in tako povečamo proizvodnjo želenega proteina (43, 44, 45). Genetski material vnašamo najpogosteje v skeletno mišičje, kožo in tumor. Skeletno mišičje je posebej primerno tarčno tkivo, kadar želimo dolgotrajno izražanje vnešenega gena in proizvodnjo proteina, ki se izloča v krvni obtok in ima sistemske učinke (2, 46, 47, 48, 49). Z GEP v kožo dosežemo tako lokalno intradermalno proizvodnjo proteina kot tudi sistemsko izločanje v krvni obtok (50, 51). Prednost kože kot tarčnega organa za GEP je prisotnost velikega števila imunskih celic, ki so nujne za učinkovit imunski odgovor organizma (51). Omejitev tovrstnega GEP je kratka življenjska doba celic kože, kar onemogoča dolgotrajnejše izražanje vnešenih genov (52, 53). GEP v tumor omogoča proizvodnjo proteinov in tako zagotavlja zadostno lokalno koncentracijo terapevtika brez zaznavnih sistemskih učinkov. To je še zlasti pomembno pri enem najpogosteje uporabljanih terapevtskih genov, genu, ki kodira citokin interlevkin-12 (IL-12) (2, 43, 54, 55), saj je uporaba rekombinantnega IL-12 povezana z resnimi, potencialno življenjsko ogrožujočimi neželenimi sistemskimi učinki (56, 57). Proinflamatorni citokin IL-12, ki ga proizvajajo antigen predstavitvene celice, ima močan protitumorski učinek zaradi vpliva na imunski odziv ter angiogenezo (58, 59, 60). Učinkovitost in varnost GEP plazmidne DNA, ki kodira IL-12 (GEP pIL-12), so potrdile predklinične raziskave na mišjih modelih (46, 61) ter translacijske raziskave pri psih (62, 63). Varno rabo in učinkovanje na metastaze melanoma pa so pokazali tudi pri človeku (64).

V veterinarski medicini sta se EKT in GEP pIL-12 izkazali za učinkoviti pri zdravljenju kožnih, podkožnih in maksilofacialnih tumorjev pri psih (3, 7, 43, 62, 63, 65, 66, 67, 68, 69, 70, 71, 72, 73, 74, 75, 76, 77), ploščatoceličnega karcinoma (78) in sarkoma pri mački (79), kožnih tumorjev pri dihurjih (80), sarkoidnih tumorjev pri konjih (81, 82), različnih tumorjih pri skobčevkah (83, 84) idr.

Kljub klinični učinkovitosti kombiniranega zdravljenja EKT in GEP pIL-12 pa še vedno primanjkuje podatkov o parametrih, ki bi lahko napovedali izid zdravljenja.

1.1.1.1 Prediktivni dejavniki zdravljenja z EKT in GEP

Različne vrste tumorjev se odzivajo na EKT različno: na mišjem modelu so boljši protitumorski učinek EKT opazili pri fibrosarkomu SA-1 kot pri karcinomu EAT in pri slednjem boljši učinek kot pri melanomu B16F1 (13, 85, 86). Različen odziv različnih vrst tumorjev so pripisali intrinzični občutljivosti tumorskih celic na kemoterapevtike in tumorskemu mikrookolju, predvsem ožiljenosti tumorja, ki je imela pomemben vpliv na odgovor tumorjev na EKT. V karcinomih EAT, ki imajo večjo gostoto krvnih žil majhnega premera kot melanomi B16F1, ki imajo žile večjega premera in večjo površino žil, so ugotovili višjo koncentracijo BLM in boljši protitumorski učinek EKT (85).

Rezultati metaanalize zdravljenja tumorjev z EKT so pokazali značilno zmanjšanje učinkovitosti EKT z naraščajočim premerom tumorja (87). Največji padec deleža popolnih odgovorov so ugotovili pri premeru tumorja 2 cm. Pri tumorjih, manjših od 3 cm, se je v primerjavi z večjimi tumorji verjetnost popolnega odgovora značilno povečala za 31 % (87).

Ugotovljeno je tudi, da histološke lastnosti tumorjev, kot so gostota celic, velikost celic ter vsebnost proteoglikana in kolagena, vplivajo na učinkovitost transfekcije električno posredovanega vnosa genov v solidne tumorje pri miših (88).

1.1.1.2 Žilni učinki EP, EKT in GEP

Učinke EP ter EKT na perfuzijo zdravih in tumorskih tkiv so opisali z različnimi indirektnimi ter direktnimi metodami (14, 89, 90, 91, 92, 93, 94, 95, 96, 97, 98, 99, 100), ki so invazivne in zato za klinično uporabo manj zaželene. Ugotovili so, da se po aplikaciji električnih pulzov perfuzija tkiv močno zmanjša zaradi vazokonstrikcije arteriol in nastalega intersticijskega edema; EP povzroči začasno zaporo žilja oz. t. i. "vascular lock" (Slika 1). Trajanje in jakost dinamične zapore žilja sta odvisna od števila, amplitude in trajanja električnih pulzov (14, 90, 91, 92). Pretok se po EP počasi obnovi in se po 24 urah približa stanju pred EP (14, 89, 92, 93, 94). Žilni učinki so bolj izraziti pri EKT kot EP, saj EKT deluje še dodatno citotoksično na endotelijske celice tumorskih žil in povzroči prekinitev integritete njihove stene oz. t. i. "vascular disrupting effect" (89, 97, 98) (Slika 1).

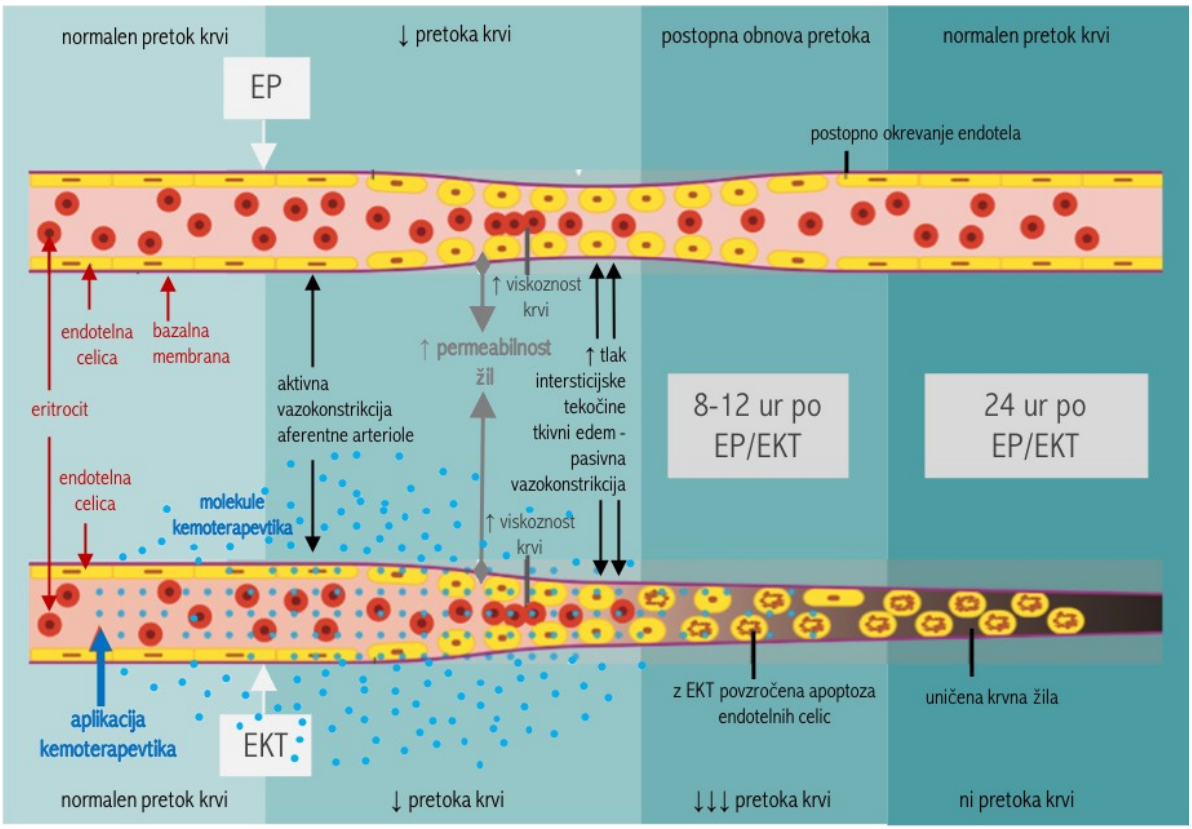

Slika 1. Vpliv elektroporacije in elektrokemoterapije na žile in pretok krvi. Povzeto po Jarm in sod., 2010 (92).

Figure 1. Vascular effects of electroporation and electrochemotherapy. Adapted from Jarm et al., 2010 (92).

1.1.1.3 Učinki EP in EKT na jetrni parenhim in velike jetrne žile

Vpliva EP in EKT na zdrav jetrni parenhim in velike krvne žile jeter, ko so elektrode vstavljene v njihovo svetlino, še niso opisali. Po zdravljenju z ireverzibilno elektroporacijo se slikovno-diagnostične metode uporablja za določitev območja jetrnega tkiva, ki je bilo ireverzibilno elektroporirano (101, 102, 103, 104, 105, 106, 107, 108, 109, 110, 111, 112). Obstaja zgolj eno poročilo o slikovno-diagnostičnih ugotovitvah po EKT tumorjev jeter dveh bolnikov, kjer so UZ spremembe (hiperehogene sledi elektrod in hipoehogenost parenhima) v jetrnih tumorjih opisali kot indikatorje ustrezne pokritosti tumorja z električnim poljem za učinkovito EKT (113).

1.1.2 Ožilje tumorja

Ožilje tumorja je pomembna tarča za zdravljenje in nadziranje raka. Žile so tudi glavna pot za metastatsko širjenje (114). Tumorske žilne mreže so heterogene in pretok skoznje je intermitenten (114, 115, 116). Te značilnosti prispevajo k prostorski in časovni heterogenosti v krvnem pretoku tumorja in zato se ožilje tumorja in perfuzija tumorjev intenzivno raziskujejo kot možni prognostični dejavniki vedenja tumorja in prediktivni dejavniki izida zdravljenja (116).

Ožiljenost tumorja, ki se med histološkimi skupinami tumorjev razlikuje (85, 117, 118), nam da različne informacije. Uporablja se npr. kot merilo za razlikovanje med benignimi in malignimi tumorji (119, 120, 121). Iz večje ožiljenosti tumorja lahko sklepamo o večji možnosti metastaziranja (121, 122). Nenazadnje je lahko povečana ožiljenost pri različnih tumorjih tudi pokazatelj krajšega preživetja (121).

Za rast tumorja je potrebna tvorba novih krvnih žil oz. neovaskularizacija: z vaskulogenezo nastajajo žile *de novo*, z angiogenezo pa nastajajo nove iz že obstoječih (122). Angiogeneza je za rast tumorja nujna in je pomemben prediktivni dejavnik odziva na kemoterapijo pri bolnikih z rakom (121, 122). Poznana so številna antiangiogena zdravila, ki zavirajo nastajanje novih krvnih žil (116, 122), antiangiogeni učinki pa so značilni tudi za EKT in GEP (89, 97, 98, 123, 124). Potreba po oceni učinkovitosti zdravljenja je povzročila večje zanimanje za oceno ožilja tumorja (121).

1.1.3 Ocena perfuzije in ultrazvočni pregled s kontrastnim sredstvom

Perfuzija je celotna porazdelitev krvi v maso ali organ in zlati standard za njeno oceno sta računalniška tomografija s kontrastnim sredstvom (CT-KS) in magnetnoresonančno slikanje s kontrastnim sredstvom (MRI-KS). Z novejšimi ultrazvočnimi kontrastnimi mediji, ki so bolj trpežni, in impulznimi zaporedji, ki so bolj občutljiva na nižje koncentracije kontrastnega medija, se tudi kontrastni harmonski ultrazvok (UZ-KS) razvija kot način perfuzijskega slikanja (121, 125, 126).

1.1.3.1 Kontrastni harmonski ultrazvok

Harmonski ultrazvok je tehnika, ki temelji na principu oddajanja valov pri frekvenci f (prva harmonika) in sprejemanju pri frekvenci 2 f (druga harmonika) ali ½ f (subharmonika). Kakovost slike je izboljšana z uporabo tkivnih harmonikov, saj se tako zmanjšajo artefakti. Ta tehnologija je postala na voljo z razvojem širokopasovnih pretvornikov. Pri vseh ultrazvočnih slikah se oddani signal pri pacientu popači in ustvari zvočne frekvence, ki so večkratniki prvotne osnovne frekvence. Pri harmonskem ultrazvoku se to popačenje uporablja v diagnostične namene (121, 127).

Kontrastno harmonsko slikanje izkorišča lastnosti sodobnih kontrastnih sredstev iz mikromehurčkov, običajno napolnjenih s plinom, ki proizvajajo veliko količino harmonskega signala. Pri določenih valovnih dolžinah, značilnih za kontrastno sredstvo, pride do resonance z ultrazvočnim signalom. Ko se zvočni tlak povečuje, sta širjenje in krčenje mikromehurčka neenaka, kar povzroči izkrivljanje povratnega signala. Ta popačena valovna oblika ima harmonske komponente. Ker kontrastni medij proizvaja več harmonskega signala kot okoliško tkivo, je harmonsko slikanje zelo občutljivo na prisotnost kontrastnega sredstva. Zaradi povečane občutljivosti harmonskega slikanja je s pomočjo ultrazvočnih kontrastnih sredstev mogoče spremljati perfuzijo tkiva na kapilarni ravni (128, 129).

Za izvajanje UZ-KS je potrebna ustrezna programska oprema za kontrastno preiskavo z nizkim mehanskim indeksom, ki pokaže mikromehurčke, ne da bi jih uničila. Za razliko od tkiva imajo mikromehurčki, kadar se ultrazvok uporablja z nizkim mehanskim indeksom, nelinearni odziv in proizvajajo ultrazvočne frekvence druge harmonike, katerih zaznavanje zahteva nekonvencionalne ultrazvočne modalitete, kot je slikanje s pulzno inverzijo (121, 130, 131).

1.1.3.2 Kontrastna sredstva

Najpogosteje dostopni ultrazvočni kontrastni mediji so Sonovue (Bracco, Milano, Italija), Definity (Lantheus Medical Imaging, North Billerica, Massachusetts, ZDA) in Sonozoid (Daiichi Sankyo, Tokio, Japonska). Vsak ima posebne smernice za pripravo in uporabo, ki jih je določil proizvajalec in jih je potrebno natančno upoštevati (131, 132). Radiologi se morajo zavedati krhke narave kontrastnih medijev in si prizadevati za ohranjanje celovitosti mehurčkov v vseh fazah shranjevanja, priprave in aplikacije (127, 131, 137).

Sodobna ultrazvočna kontrastna sredstva so s plinom napolnjeni mikromehurčki: razmeroma netopni plin z visoko molekulsko maso je ujet v fosfolipidni lupini. Mikromehurčki so premera povprečno 2,5 µm, od 1 do 7 µm (132, 133, 134), manjši od premera rdečih krvnih celic približno 6 µm, zato prosto prehajajo skozi pljučno in sistemsko cirkulacijo. V krvi ostajajo nedotaknjeni nekaj minut po intravenski injekciji, kapilarno polnjenje pa vodi do difuznega povečanja nazaj razpršenega ultrazvočnega signala (135). Ko mikromehurčki izginejo iz krvi, jih je mogoče čez približno 30 minut zaznati v jetrnem parenhimu in vranici (pozna faza, specifična za jetra in vranico). Večina kontrastnega sredstva se izloči skozi pljuča v 20 minutah po aplikaciji kot inertni plin, ki je žveplov hidroksid v primeru kontrasta Sonovue, lipoproteinska lupina pa se izloči z žolčem (135, 136).

Prednosti kontrastnih snovi, ki se uporabljajo v UZ-KS, pred tistimi, ki se uporabljajo pri CT-KS, so številne: omogočajo slikanje v realnem času, ni ionizirajočega sevanja, niso nefro- in hepatotoksične in imajo zelo redke in zelo blage stranske učinke (135, 136). Ultrazvočna kontrastna sredstva so v nasprotju z jodiranimi in gadolinijevimi sredstvi strogo žilna, brez kakršne koli intersticijske komponente in kažejo na večje in manjše žile (137).

Kontraindikacije za uporabo mikromehurčkov pri ljudeh vključujejo pljučno hipertenzijo in okvarjeno srčno-pljučno funkcijo (136). Pri velikem številu psov, pri katerih so bili opravljeni pregledi UZ-KS, se je pri manj kot 1 % pojavil takojšen ali zapozneli neželeni učinek (bruhanje, sinkopa) (135). Običajno kontrastni ultrazvočni pregledi trajajo do 2 minuti. Za prikaz več lezij ali organov so pogosto potrebne večkratne aplikacije kontrastnega sredstva, ki pa niso povezane s povečanim tveganjem za neželene učinke (126, 135, 137).

Za razliko od večine oblik slikovnih kontrastnih medijev so ultrazvočna kontrastna sredstva že po naravi krhka. Mikromehurčki se zlahka uničijo z visokoenergijskim zvokom, vključno s tipičnimi energijami ultrazvočne sive lestvice (B-mode) in vsemi Dopplerjevimi signali. Kontrastno sredstvo je mogoče uničiti tudi z neustreznim ravnanjem, na primer s preveč hitrim vbrizgavanjem skozi igle majhnega profila, neustreznim upoštevanjem smernic proizvajalca za pripravo kontrastnega sredstva ali previsoko vpadno energijo med kontrastnim slikanjem.

1.1.3.3 Parametri perfuzijske krivulje

Vgrajena programska oprema ultrazvočnega sistema in/ali računalniški programi pokažejo perfuzijsko krivuljo ali krivuljo, ki predstavlja intenzivnost signala skozi čas, ter naslednje parametre: osnovna intenzivnost, vrh intenzivnosti, in površina pod krivuljo (AUC, angl. area under curve). Maksimalna amplituda harmonskega signala oz. vrh ločljivosti (PE, angl. peak enhancement) se izračuna kot razlika med vrhom intenzivnosti in osnovno intenzivnostjo. PE in AUC sta parametra, ki odražata količino krvi v preiskovanem območju. Parametri, ki odražajo pretok krvi, pa so: čas, ko intenzivnost kontrasta doseže vrh (TTP, angl. time to peak), naraščajoči naklon, čas prihoda, čas od maksimalne vrednosti signala do zmanjšanja amplitude signala na polovico, angl. descend time to one half), in padajoči naklon (DS, angl. descending slope) (Slika 2). Parametri UZ-KS merijo perfuzijo tkiva na ravni kapilar. Na perfuzijske parametre vplivajo srčni, žilni, mikrocirkulacijski in drugi dejavniki. UZ-KS skorje ledvic pri 10 anesteziranih zdravih mačkah je pokazal, da globina preiskovanja ter velikost preiskovanega področja (ROI, angl. region of interest) značilno korelirata s PE (138).

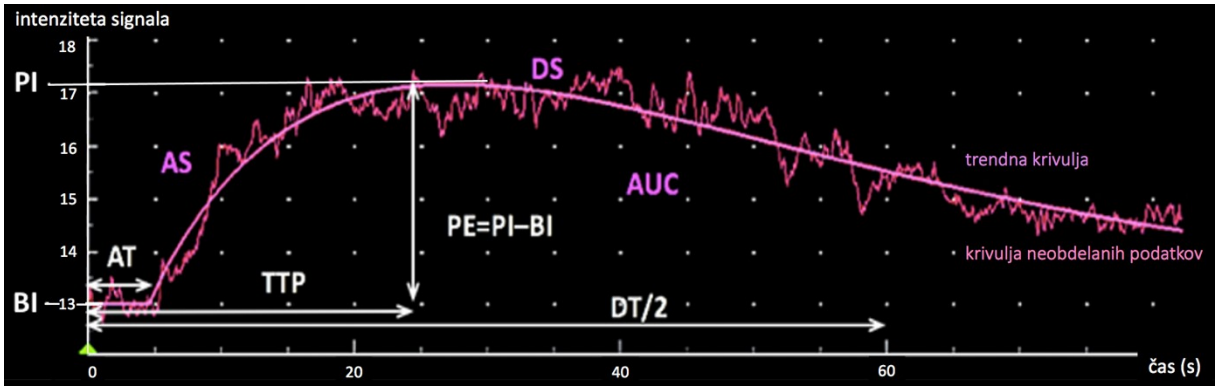

Slika 2. Perfuzijska krivulja. AS = naraščajoči naklon; AT = čas prihoda; AUC = površina pod krivuljo; BI = osnovna intenzivnost; DS = padajoči naklon; DT/2 = čas od maksimalne amplitude do njenega zmanjšanja na polovico; PE = maksimalna amplituda harmonskega signala; PI = vrh intenzivnosti; TTP = čas do vrha. Povzeto po Brložnik in sod., 2021 (str. 133).

Figure 2. Perfusion curve. BI = basic intensity; PI = peak intensity, AUC = area under curve, PE = peak enhancement;; TTP = time to peak, AS = ascending slope), AT = arrival time, DT/2 = half-decay time; DS = descending slope. Adapted from Brloznik et al, 2021 (page 133).

1.1.3.4 Uporaba UZ-KS v onkologiji

UZ-KS se uporablja podobno kot CT-KS in MRI-KS za neinvazivno karakterizacijo lezij (brez biopsije), ugotovljenih med običajnimi ultrazvočnimi preiskavami. V veterinarski medicini se UZ-KS uporablja za razlikovanje spontanih benignih in malignih tumorjev jeter (137, 139, 140, 141, 142, 143), vranice (144, 145, 146, 147, 148), ledvic (149), nadledvičnih žlez (150, 151), bezgavk (152, 153) idr. Prav tako se je UZ-KS izkazal uporaben za določanje sentinelnih bezgavk (154, 155, 156).

Tako v predkliničnih (157, 158, 159, 160) kot tudi v kliničnih raziskavah pri ljudeh in psih (117, 161, 162, 163) so pokazali, da rezultati UZ-KS korelirajo s histološkimi rezultati ožiljenosti tumorja. Poleg tega se je v predkliničnih raziskavah UZ-KS izkazal za dragocenega pri ocenjevanju odziva tumorja na antiangiogeno zdravljenje (158, 159, 164). Tudi v kliničnih raziskavah pri ljudeh se je izkazal kot koristno orodje za oceno učinkovitosti antiangiogenih zdravil (165, 166, 167, 168, 169, 170, 171, 172, 173, 174, 175).

1.1.3.4.1 Uporaba UZ-KS in EP/EKT/GEP

Raziskav, ki navajajo rezultate UZ-KS po EP/EKT/GEP, je le peščica. Pokazali so, da se perfuzija mišjih sarkomov zmanjša 3 in 35 min po EKT, po 48 urah pa se obnovi na izhodiščno stanje (98). UZ-KS so uporabili za določanje področij tumorske nekroze spontanih pasjih tumorjev pred GEP pIL-12 in dokazovanje antiangiogenega učinka GEP pIL-12 8 in 35 dni po zdravljenju (176, 177). Prav tako so z UZ-KS ovrednotili učinek EKT pri človeških tumorjih jeter (113) in pankreasa (27). Vendar v nobeni od raziskav učinka EP, EKT in GEP do sedaj še niso opisali v meri, ki bi omogočala klinično uporabo, predvsem z vidika spremljanja učinkovitosti terapije.

1.1.4 Ocenjevanje odziva na zdravljenje tumorjev z EKT in GEP

Ocena odziva tumorja na zdravljenje temelji predvsem na podlagi ponavljajoče se ocene velikosti tumorja glede na merila za oceno odziva pri solidnih tumorjih (RECIST, angl. response evaluation criteria in solid tumours) (178, 179, 180) in smernice za kriterije odziva za preskušanje imunoterapevtikov (iRECIST, angl. response evaluation criteria in solid tumors in immunotherapy trials) (181). Tumorje uvrstimo mesec dni po zdravljenju v eno od naslednjih skupin:

- popolni odgovor (izginotje tumorja, angl. complete response),
- delni odgovor (vsaj 30-odstotno zmanjšanje tumorja, angl. partial response),
- stabilna bolezen (manj kot 30-odstotno zmanjšanje ali manj kot 20-odstotno povečanje tumorja, angl. stable disease),
- napredovana bolezen (vsaj 20-odstotno povečanje tumorja, angl. progressive disease).

Kriteriji RECIST odražajo le spremembe v velikosti tumorja, ki pa pogosto zaostajajo in zato ne morejo napovedati odziva na terapijo v zgodnji časovni točki (182). Pacient je lahko napačno razvrščen med tiste »brez odgovora na terapijo«, ker ostaja velikost tumorja nespremenjena, ali pa se lahko v zgodnjem času tumor celo poveča zaradi krvavitve, nekroze in edema, kljub temu da je delež tumorja manjši (183). Da bi se izognili tej težavi, so predlagali nove metode za oceno odziva tumorja dva ali več mesecev po antiangiogeni terapiji na osnovi tumorske perfuzije v obliki prilagojenih kriterijev RECIST (mRECIST, angl. modified RECIST) (184). Pojav novih terapij, usmerjenih v tumorsko angiogenezo in vaskularnost tumorja, je poudaril potrebo po natančnih in ponovljivih kvantitativnih tehnikah za oceno zgodnjih sprememb v ožiljenosti tumorjev (183).

1.1.5 Vloga živalskih modelov v translacijskih raziskavah

Pri raziskovanju rakavih obolenj, preizkušanju novih terapij in izida zdravljenja pri človeku so živalski modeli neprecenljivi in nepogrešljivi (185, 186). V predkliničnih raziskavah se za raziskovanje molekulskih procesov in patoloških značilnosti tumorjev zaradi majhne velikosti največ uporabljajo mišji modeli, s katerimi so odkrili številne mehanizme nastanka in razvoja raka (187, 188, 189). Ker so mišji tumorji inducirani, ne odsevajo strukturne in genetske kompleksnosti spontanih tumorjev. Odličen model za translacijo rezultatov raziskav v humano onkologijo so psi. Pri njih se namreč pojavljajo spontani tumorji, ki se razvijajo počasi ob intaktnem imunskem sistemu (185). Ker živijo v današnji družbi psi, hišni ljubljenci, v tesnem stiku z lastniki, si z njimi delijo isto okolje in so del družine, so podvrženi podobnim dejavnikom za razvoj raka kot ljudje, in tudi zato so verjetno tumorji podobni tistim pri ljudeh (190, 191). Prednosti uporabe psa v kliničnih študijah zdravljenje raka je tudi bistveno daljša življenjska doba v primerjavi z mišjimi modeli in posledično možnost proučevanja stranskih učinkov (192) ter hkrati bistveno krajša življenjska doba psov in relativno hitrejši naravni potek bolezni v primerjavi z ljudmi, kar dopušča hitrejše ocenjevanje rezultatov o izidu zdravljenja (193). Prav tako omogoča velikost psa v primerjavi z velikostjo miši odvzem ustrezno velikih vzorcev za analizo tkiva, krvi, ipd. (185, 192). V veterinarski onkologiji je tudi manj uveljavljenih standardov zdravljenja kot v humani medicini, zato je možno preskušati nove načine zdravljenja in prognosticiranja. Zaradi tega postaja veterinarska onkologija vedno bolj pomemben vmesni člen v translaciji rezultatov predkliničnih raziskav v humano onkologijo. Z izvajanjem kliničnih raziskav učinkovitosti novih načinov zdravljenja raka na psih lahko tako pridobimo podatke, ki so pomembni za izvajanje humanih kliničnih raziskav in do njih ne pridemo na eksperimentalnem modelu laboratorijskih živali, saj so lahko značilnosti spontanih in induciranih tumorjev povsem drugačne.

1.2 Namen dela in hipoteze

Namen doktorskega dela je bil ovrednotenje rezultatov perfuzije tumorjev na osnovi rezultatov preiskav UZ-KS in CT-KS po postopku EP in EKT jetrnega tkiva zdravih prašičev ter preiskav UZ-KS po zdravljenju z EKT in GEP pIL-12 mišjih in pasjih tumorjev. Pri mišjih in pasjih tumorjih smo se posvetili predvsem vidiku prediktivne vrednosti diagnostične metode pri zdravljenju induciranih in spontanih tumorjev s pomočjo terapij, ki temelijo na EP. Pri prašičjih jetrih pa nas je zanimal varnostni vidik uporabe EP in EKT pri zdravljenju tumorjev, ki mejino na velike krvne žile.

Hipoteze

(1) »UZ pregled s kontrastnim sredstvom je neinvazivna metoda, s katero lahko vrednotimo vpliv EP, EKT in GEP na perfuzijo tretiranih tumorjev miši in psov.«

(2) »EKT in EP zmanjšata perfuzijo tretiranega področja zdravih prašičjih jeter, vendar ne povzročata z UZ-KS in s CT-KS vidnih sprememb velikih krvnih žil jeter«.

(3) »Z UZ pregledom s kontrastom lahko dokažemo, da imajo tumorji heterogen pretok.«

(4) »Rezultati UZ pregleda s kontrastnim sredstvom korelirajo z lokalnim odgovorom na zdravljenje z EKT/GEP.«

2 OBJAVLJENA ZNANSTVENA DELA

2.1 Radiološke spremembe prašičjih jeter po elektrokemoterapiji z bleomicinom

Radiological findings of porcine liver after electrochemotherapy with bleomycin

Maja Brložnik,[1] Nina Boc,[2] Gregor Serša,[2,3] Jan Žmuc,[2] Gorana Gašljević,[2] Alenka Seliškar,[1] Rok Dežman,[4] Ibrahim Edhemović,[2] Nina Milevoj,[1] Tanja Plavec,[1] Vladimira Erjavec,[1] Darja Pavlin,[1] Maša Bošnjak,[2] Erik Brecelj,[2] Urša Lampreht Tratar,[2] Bor Kos,[6] Jani Izlakar,[2] Marina Štukelj,[1] Damijan Miklavčič,[6] Maja Čemažar.[2,7]*

[1] Univerza v Ljubljani, Veterinarska fakulteta

[2] Onkološki inštitut Ljubljana

[3] Univerza v Ljubljani, Zdravstvena fakulteta

[4] Univerzitetni klinični center Ljubljana

[6] Univerza v Ljubljani, Fakulteta za elektrotehniko

[7] Univerza na Primorskem, Fakulteta za vede o zdravju

* vodilna avtorica: Maja Čemažar

Radiol Oncol 2019; 53(4): 415-426. doi: 10.2478/raon-2019-0049.

Izvleček

Izhodišča. Radiološke spremembe po EP/EKT velikih jetrnih žil ter zdravega jetrnega parenhima še niso bile opisane.

Materiali in metode. V prospektivno raziskavo z izdanim dovoljenjem na živalskem modelu smo vključili devet prašičev pitancev. Pri vsaki živali smo v jetrih ultrazvočno vodeno elektroporirali štiri področja; v treh področjih smo elektrode vstavili v svetline velikih jetrnih žil. Preizkusili smo dve vrsti elektrod; linearne in heksagonalne. Ultrazvočno smo tretirana mesta pregledali takoj in do dvajset minut po postopku, CT-KS pa smo izvedli pred posegom, od 60 do 90 minut po njem ter 1 teden pozneje.

Rezultati. Radiološke preiskave tretiranih področij so pokazale nepoškodovane žilne stene ter normalno prehodne žile – brez krvavitev ali strdkov. Tretirana področja so se ultrazvočno dinamično spreminjala od hiperehogenih mikromehurčkov vzdolž elektrod do hipoehogenosti tretiranega parenhima, difuzije hiperehogenih mikromehurčkov ter izginjanja hipoehogenosti. UZ-KS takoj po postopku in CT-KS od 60 do 90 minut po postopku sta pokazala, da tretirana mesta privzemajo manj kontrasta. Celotna površina mest, ki slabše privzemajo kontrast, je bila v primeru heksagonalnih elektrod manjša kot v primeru linearnih elektrod.

Zaključki. Radiološke preiskave prašičjih jeter po EKT z BLM niso pokazale pomembnih poškodb jeter navkljub tveganemu postopku vstavitve elektrod v svetline velikih jetrnih žil, kar pomeni, da je EKT za zdravljenje jetrnih tumorjev varna.

sciendo Radiology and Oncology | Ljubljana | Slovenia | www.radioloncol.com RADIOLOGY AND ONCOLOGY 415

research article

Radiological findings of porcine liver after electrochemotherapy with bleomycin

Maja Brloznik[1], Nina Boc[2], Gregor Sersa[2,3], Jan Zmuc[2], Gorana Gasljevic[2], Alenka Seliskar[1], Rok Dezman[4], Ibrahim Edhemovic[2], Nina Milevoj[1], Tanja Plavec[1,5], Vladimira Erjavec[1], Darja Pavlin[1], Masa Bosnjak[2], Erik Brecelj[2], Ursa Lampreht Tratar[2], Bor Kos[6], Jani Izlakar[2], Marina Stukelj[7], Damijan Miklavcic[6], Maja Cemazar[2,8]

[1] University of Ljubljana, Veterinary Faculty, Small Animal Clinic, Ljubljana, Slovenia
[2] Institute of Oncology Ljubljana, Ljubljana, Slovenia
[3] University of Ljubljana, Faculty of Health Sciences, Ljubljana, Slovenia
[4] University Medical Centre, Clinical Institute of Radiology, Ljubljana, Slovenia
[5] Small Animal Hospital Hofheim, Katharina-Kemmler-Strasse 7, Hofheim, Germany
[6] University of Ljubljana, Faculty of Electrical Engineering, Ljubljana, Slovenia
[7] University of Ljubljana, Veterinary Faculty, Clinic for Reproduction and Farm Animals, Clinic for Ruminants and Pigs, Ljubljana, Slovenia
[8] University of Primorska, Faculty of Health Sciences, Izola, Slovenia

Radiol Oncol 2019; 53(4): 415-426.

Received 15 August 2019
Accepted 12 September 2019

Correspondence to: Prof. Maja Čemažar, Ph.D., Institute of Oncology Ljubljana, Department of Experimental Oncology, Zaloška 2, Ljubljana, Slovenia. Phone: +386 1 587 94 34; E-mail: mcemazar@onko-i.si

Disclosure: D.M. is an inventor of several patents pending and granted. He is receiving royalties and is consulting for different companies and organizations, which are active in electroporation and electroporation-based technologies and therapies. The remaining authors report no conflicts of interest.

Background. Radiologic findings after electrochemotherapy of large hepatic blood vessels and healthy hepatic parenchyma have not yet been described.

Materials and methods. We performed a prospective animal model study with regulatory approval, including nine grower pigs. In each animal, four ultrasound-guided electroporated regions were created; in three regions, electrodes were inserted into the lumen of large hepatic vessels. Two types of electrodes were tested; variable linear- and fixed hexagonal-geometry electrodes. Ultrasonographic examinations were performed immediately and up to 20 minutes after the procedure. Dynamic computed tomography was performed before and at 60 to 90 minutes and one week after the procedure.

Results. Radiologic examinations of the treated areas showed intact vessel walls and patency; no hemorrhage or thrombi were noted. Ultrasonographic findings were dynamic and evolved from hyperechogenic microbubbles along electrode tracks to hypoechogenicity of treated parenchyma, diffusion of hyperechogenic microbubbles, and hypoechogenicity fading. Contrast-enhanced ultrasound showed decreased perfusion of the treated area. Dynamic computed tomography at 60 to 90 minutes after the procedure showed hypoenhancing areas. The total hypoenhancing area was smaller after treatment with fixed hexagonal electrodes than after treatment with variable linear geometry electrodes.

Conclusions. Radiologic findings of porcine liver after electrochemotherapy with bleomycin did not show clinically significant damage to the liver, even if a hazardous treatment strategy, such as large vessel intraluminal electrode insertion, was employed, and thus further support safety and clinical use of electrochemotherapy for treatment of hepatic neoplasia.

Key words: electrochemotherapy; pig; liver; hepatic vessels; ultrasound; computed tomography

Introduction

Surgical resection is the gold standard for the treatment of hepatic neoplasia. However, the majority of hepatic tumors are unresectable at the time of diagnosis. In these patients, alongside systemic chemotherapy, different local ablative techniques, such as radiofrequency and microwave ablation, are used.[1-3] However, these two techniques are not optimal for tumors located near major bile ducts and larger hepatic vessels due to the heat sink effect or potential damage to vital structures.[2-4] Hence, novel techniques, such as irreversible electroporation (IRE) ablation and electrochemotherapy (ECT), are advantageous for patients with unresectable hepatic neoplasia adjacent to major bile ducts and vessels.[1-3,5] ECT is a method for the delivery of chemotherapeutic drugs by reversible electroporation, which enables the entry of otherwise poorly or nonpermeant exogenous molecules into cells by the application of short high-intensity electric pulses that induce reversible cell membrane permeabilization.[6-8] ECT is nowadays widely used in European centers for the treatment of cutaneous tumors.[9,10]

Clinical studies have shown that ECT is safe and effective also for the treatment of liver metastases and hepatocellular carcinoma (HCC)[3,4,6,7,11–13], and also other deep-seated tumors like pancreatic carcinoma.[14-16] Potentially hazardous electrode insertion into the lumen of major hepatic vessels has been reported in a study with percutaneous ECT of portal vein tumor thrombosis in patients with HCC.[11] From ECT[3,4,6,7,11,12] and IRE[17-22] studies, it is assumed that ECT of large hepatic vessels is safe, but this assumption has not yet been demonstrated with early radiologic examinations, which could reveal possible intra-abdominal hemorrhage or thrombus formation that could prove fatal for the patient.

Radiologic findings after IRE of hepatic tissue have been thoroughly described and used to determine the area that was irreversibly electroporated[22-26], while there has only been one report of radiologic findings after ECT of liver, where ultrasonographic (US) changes in hepatic tumors were described as indicators of adequate electric field tumor coverage for effective ECT.[27] The effect of ECT on healthy hepatic parenchyma and large hepatic vessels has not been previously studied by diagnostic imaging methods. The aim of this study was to characterize radiologic findings after ECT of large hepatic vessels and hepatic parenchyma in a porcine model, and hence to confirm the safety of the procedure.

Materials and methods

Animals and ethics approval

In this prospective animal model study with regulatory approval issued by the National Ethics Committee at The Administration of the Republic of Slovenia for Food Safety, Veterinary, and Plant Protection (Approval number: U34401-1/2017/4, Approval date: 17.03.2017), nine female grower pigs, purchased from an authorized swine breeder (Globocnik, Sencur, Slovenia) 3–17 days before experiment, were included.[28] Experimental animals were reared according to the European Council directive for minimum standards for the protection of pigs (2008/120/EC). All procedures complied with relevant national and European legislation (2010/63/EU).

Animals were 12 weeks old, weighed 31 ± 2.5 kg, and their liver volume estimated from CT images was 865 ± 85 cm^3.

Electrochemotherapy

During open surgery, four US-guided electroporated regions were created.

Insertion of electrodes. Electrodes were inserted into the lumen of the caudal vena cava and surrounding hepatic parenchyma (region 1), into the left median hepatic vein and surrounding parenchyma (region 2), into the left portal vein and parenchyma (region 3), and in the hepatic parenchyma of the left liver lobe (region 4).

Bleomycin and control group. Two pigs served as a control group and received electric pulses (EP) only. In the remaining seven pigs, ECT was performed; bleomycin (Bleomycinum, Heinrich Mack Nachf. GmbH & CO. KG, Illertissen, Germany, 15.000 IE/m^2) was administered intravenously at 8 minutes before the first application of EP.

Types of electrodes. Two types of electrodes routinely used in clinical treatment were tested. Variable linear geometry electrodes consisted of two long needle electrodes (with a diameter of 1.2 mm and a 3 cm long active part), which were 2 cm apart (VG-1230T12, IGEA S.p.A., Carpi, Italy). These electrode were employed in five cases of ECT and the two cases of EP. Fixed hexagonal geometry electrodes consists of seven needle electrodes with a diameter of 0.7 mm that are hexagonally placed 0.73 cm apart in a round plastic holder (N-30-HG, IGEA). These electrodes were used in two cases of ECT.

Electric pulses. EP was delivered with an electric pulse generator (Cliniporator, IGEA), and the

number of pulses for linear and hexagonal geometry electrodes were 8 and 96, respectively (8 between each individual electrode pair). Each pulse was 100 microseconds long, and the voltage was set to 2000 V in the case of linear electrodes and 730 V in the case of hexagonal electrodes. The frequencies for the linear and hexagonal electrode geometries were 1 and 5000 Hz, respectively.

Numerical modeling of electric field distribution

The treated area electric field was calculated by the finite element method using the software package Comsol Multiphysics (COMSOL AB, Stockholm, Sweden) with MATLAB (Mathworks, Natick, MA, USA).[29,30] The electrical parameters and bleomycin dosage were consistent with the European standard operating procedures for the ECT protocol and ECT for colorectal liver metastases clinical trials.[3,31,32]

Study end-point

The animals were euthanized at two or seven days after ECT/EP using 3 ml/10 kg i.v. T61 euthanasia solution (Intervet, Boxmeer, Netherlands); the liver was explanted for histologic analyses, which were reported in a separate paper.[28]

Ultrasonography (US) and computed tomography (CT)

Ultrasonographic examinations (US) were performed immediately and up to 20 minutes after the procedure. Different US machines were used, as available: Resona 7 and/or M9 (Mindray, Shenzhen, China) and/or Logiq S7 Pro (GE, Milwaukee, WI, USA). US examinations included B-mode to provide information about echogenicity and echotexture changes, Doppler (color and pulse-wave) to examine vessel patency and contrast enhanced ultrasound (CEUS) to evaluate the perfusion of hepatic parenchyma. The region of CEUS investigation was chosen according to the available US machine. In the case of the Mindray machine, a linear probe was used and the near-field area was preferred, whereas with the GE machine, the far-field was chosen since contrast works only with a convex probe. CEUS was performed before and after EP/ECT. Low mechanical index (<0.1) was applied, and a transpulmonary contrast agent Sonovue (Bracco, Milan, Italy), based on sulfur hexafluoride microbubbles, was administered into the cephalic vein (2.4 ml), and then flushed with saline (2 ml). From the time of contrast application, a 90-second cine-clip was made for further image analysis.

CT of the liver was performed before and at 60 to 90 minutes after EP/ECT with a Somatom Scope CT scanner (Siemens, Erlangen, Germany) in seven pigs. In two pigs treated with ECT with variable linear geometry electrodes, CT was also performed at 1 week after ECT. The following CT parameters were used: referenced 170 mA, 110 kVp, 3.0 mm slice reconstruction thickness, 2.0 mm reconstruction increment, and beam pitch of 1.4. The dynamic study with the contrast medium iopromide (Ultravist; Bayer, Leverkusen, Germany, 0.5 ml/kg), which was administered intravenously with a Missouri dual chamber injector pump (Ulrich medical, Ulm, Germany) at a velocity of 3 ml/s, consisted of 5 phases: pre-contrast, arterial with bolus tracking in abdominal aorta, and 3 subsequent phases in 30-second intervals (at 30, 60 and 90 seconds after arterial phase).

Image analysis

All radiologic findings were interpreted in consensus by three radiologists (M.B., N.B., R.D.) with more than 10-years of experience in liver imaging.

CEUS perfusion curve, presenting the signal intensity, was analyzed with the US machine built-in software.

CT images were evaluated with a free and open source software program Horos (https://horosproject.org) and Impax 6 (Agfa HealthCare, Mortsel, Belgium). CT findings before and after EP/ECT were compared. Hepatic attenuation, contrast enhancement, vessel patency, diameter and possible extravasation were evaluated. In pre-contrast studies, hepatic attenuation has been evaluated subjectively for homogeneity of hepatic parenchyma and circular ROIs were used to measure the attenuation in Hounsfield units (HU). Vessel patency, diameter and possible extravasation were evaluated subjectively in contrast studies. Dynamic CT showed hypoenhancing areas, which were if compared to untreated areas most clearly seen at 30 or 60 seconds after arterial phase. In each animal, the phase with the most evident hypoenhancing regions was used for further evaluation. Attenuation of untreated hepatic parenchyma was measured with circular ROIs that did not include vessels. Since it was difficult to differentiate individual treatment regions, all hypoenhancing areas were measured; in each of the transverse CT images, all the hypoenhancing regions were carefully delineated (with manual ROIs) to measure the area (in mm^2) and attenuation (in

HU) of the region. The total area, mean area and attenuation of the total area were calculated for each animal. The latter was calculated by a mathematical formula *sum (area x attenuation / total area*). To exclude individual differences in contrast enhancement, attenuation of untreated hepatic parenchyma was also considered; the difference between the attenuation of untreated parenchyma and the attenuation of the total area was divided by the attenuation of untreated parenchyma and multiplied by 100.

Histology

Histologic examinations were performed by an experienced pathologist (G.G.) with more than 10-years of experience in surgical pathology. To provide a comparison of radiologic and histologic data, immediate core biopsies of ECT-treated and untreated areas were performed in two pigs treated with ECT using linear geometry electrodes. In the treated parenchyma, two biopsies located between and oriented parallel to the electrodes were collected: one adjacent to the electrode and one 1 cm away from the electrode to the middle of the treated area. Histologic samples were fixed overnight in 10% buffered formalin, embedded in paraffin, cut into 3- to 4-μm-thick sections and stained with hematoxylin and eosin (H&E).

Statistical analysis

Statistical package computer program SPSS (SPSS Inc., Chicago, Illinois, USA) was used. For analysis of hepatic parenchyma contrast enhancement, the Shapiro-Wilk test was utilized to test the normality. Since the variables were not normally distributed, the Mann-Whitney U test and the Kruskal Wallis H test were used. Statistical significance was defined as $P \leq 0.05$. For other data in this study, descriptive statistics were applied.

Results

Radiologic findings and numerical modeling of electric field distribution

US findings

EP were delivered only after US confirmation of electrode position (Figure 1A). Immediately after

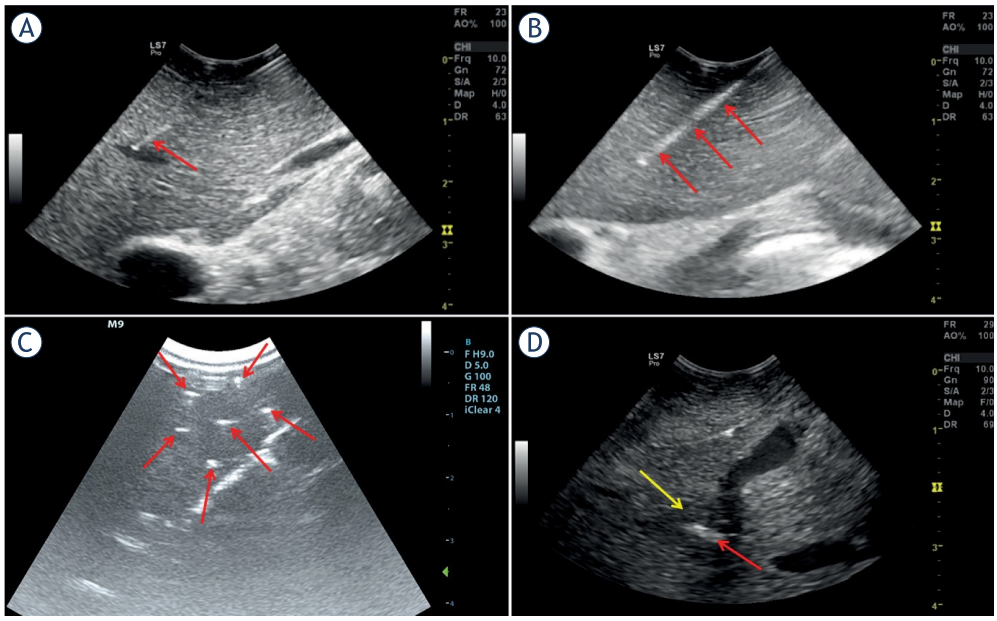

FIGURE 1. B-mode ultrasonography. **(A)** Position of the variable linear geometry electrode in the left middle hepatic vein (arrow). **(B)** Hyperechogenic microbubbles (arrows) observed immediately after electrochemotherapy (ECT) along the track of the linear electrode. **(C)** Hyperechogenic microbubbles observed immediately after ECT along the tracks of hexagonal geometry electrodes (arrows). **(D)** In the next minutes, the hepatic parenchyma of the treated area becomes hypoechogenic (yellow arrow), and hyperechogenic microbubbles (red arrow) start to diffuse.

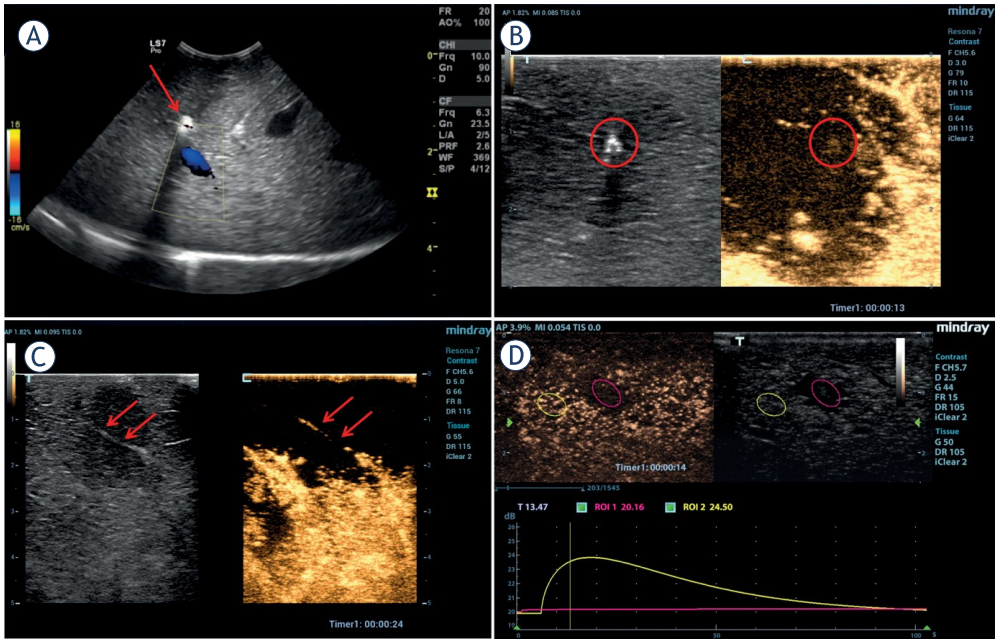

FIGURE 2. Doppler and contrast-enhanced ultrasonography. **(A)** Color Doppler in the left middle hepatic vein (blue) immediately after electrochemotherapy (ECT). Hyperechogenic microbubbles (arrow) can be noted. **(B)** Contrast enhanced ultrasound (CEUS) immediately after ECT and at 13 seconds after contrast administration; the position of the electrode is circled. **(C)** CEUS at 4 minutes after ECT and at 24 seconds after contrast; the larger vessel can be recognized (arrows). **(D)** CEUS at 5 minutes after ECT and at 14 seconds after contrast; a perfusion curve is shown.

the delivery of EP and removal of the electrodes, hyperechogenic microbubbles were observed along the electrode tracks (Figure 1B and C). In the next minutes, the treated parenchyma became hypoechogenic, and the hyperechogenic microbubbles started to diffuse (Figure 1D); the area of hypoechogenicity was larger than the area between the electrodes. In the next 5 to 10 minutes, the hyperechogenic microbubbles diffused through the treated area. There was no obvious difference between EP and ECT with variable linear geometry electrodes, while in the two cases of ECT with fixed hexagonal geometry electrodes, the hypoechogenicity was less evident compared to that with variable linear electrodes. After 10 minutes, the hypoechogenicity started to fade, and in the case of the treatment with hexagonal electrodes, it was no longer visible. The hypoechogenicity of the parenchyma was in contiguity to the treated vessel; however, the vessel wall appeared intact. There was no hemorrhage observed. Furthermore, the patency of the vessel was normal; there were no thrombi, stenotic lesions or extravasation noted, and the Doppler examination showed laminar flow (Figure 2A). CEUS showed that the perfusion of the treated area was significantly decreased (Figure 2B, C and D). The area of the hypoperfused parenchyma was larger than the area between the electrodes (Figure 2B), *i.e.* extending outside the borders of the area encompassed by the electrodes. In the case of the treatment with fixed hexagonal geometry electrodes, the decrease in perfusion was less pronounced compared to the treatment with variable linear geometry electrodes, which was consistent with computer simulation of the larger volume exposed to high strength electric fields in the variable linear geometry electrodes.

CT features

Dynamic contrast enhanced CT at 60 to 90 minutes after EP/ECT showed subtle hypoattenuating electrode tracks in the pre-contrast and arterial phases (Figure 3A and B), while in the 3 subsequent phases, hypoenhancing areas of treated hepatic parenchyma were noted (Figure 3C, D and E). These areas were most clearly observed at 30 or 60 seconds after the arterial phase, and the phase with

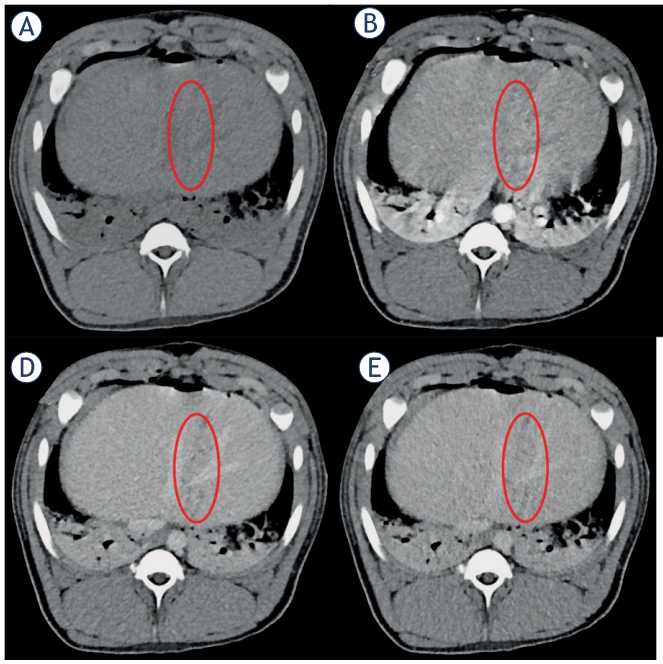

FIGURE 3. Dynamic CT study, area treated with hexagonal electrodes is circled; note that hypoenhancing areas are most clearly seen 30 seconds after arterial phase. **(A)** Pre-contrast. **(B)** Arterial phase. **(C)** At 30 seconds after arterial phase. **(D)** At 60 seconds after arterial phase. **(E)** At 90 seconds after arterial phase.

most evident hypoenhancing areas was used for further evaluation. As can be seen in Table 1, different number of hypoenhancing areas were measured in each animal. In the case of the treatment with linear geometry electrodes, the hypoenhancing regions were larger than those in the case of the treatment with hexagonal geometry electrodes (Figures 4A, B, 5A and 5B). An example of the multiplanar reconstruction (MPR) of one of the areas treated with variable linear geometry electrodes is presented in Figure 4C. All treated vessels were patent with no evidence of thrombosis (Figure 6A). Hypoenhancing areas were in contiguity with the treated vessels. There was no narrowing of the treated vessels, vessel wall and patency were not affected. No contrast extravasation was identified from large vessels in which the electrodes were inserted.

TABLE 1. Area and attenuation of hypoenhancing regions for each animal

		Number of measured hypo-enhancing regions	Total area (in mm²)	Median area (in mm²), IQR	A Attenuation of total area (in HU) ∑ ((area x attenuation) / total area)	B Attenuation of untreated parenchyma (in HU), ± SE 15 measurements in each animal	Difference in attenuation (B – A)	Corrected difference in attenuation (B–A)/B*100
Linear electrodes	ECT	48	8454	94.5, 46–168	72	118 ± 2	46	39
		66	3178	31.5, 19–53	86	114 ± 2	28	25
		91	5146	39, 25–75	82	123 ± 1	41	33
	EP	61	4538	51, 30–104	75	108 ± 1	33	30
		55	3563	32, 18–92	122	165 ± 3	43	26
Hexagonal electrodes	ECT	25	750*	21, 11.5–32*	98	124 ± 2	26	21
		46	2328*	39.5, 25–72*	80	101 ± 1	21*	21*
1 week after ECT with linear electrodes		11	99**	8, 5–11**	74	99 ± 1	24**	25**
		13	300**	19, 12–27.5**	76	101 ± 1	25**	25**

ECT = electrochemotherapy; EP = electroporation; HU = Hounsfield units; IQR = interquartile range; STD = standard deviation; *P < 0.01 compared to groups with variable linear geometry electrodes; **P < 0.01 compared to groups immediately after EP/EC

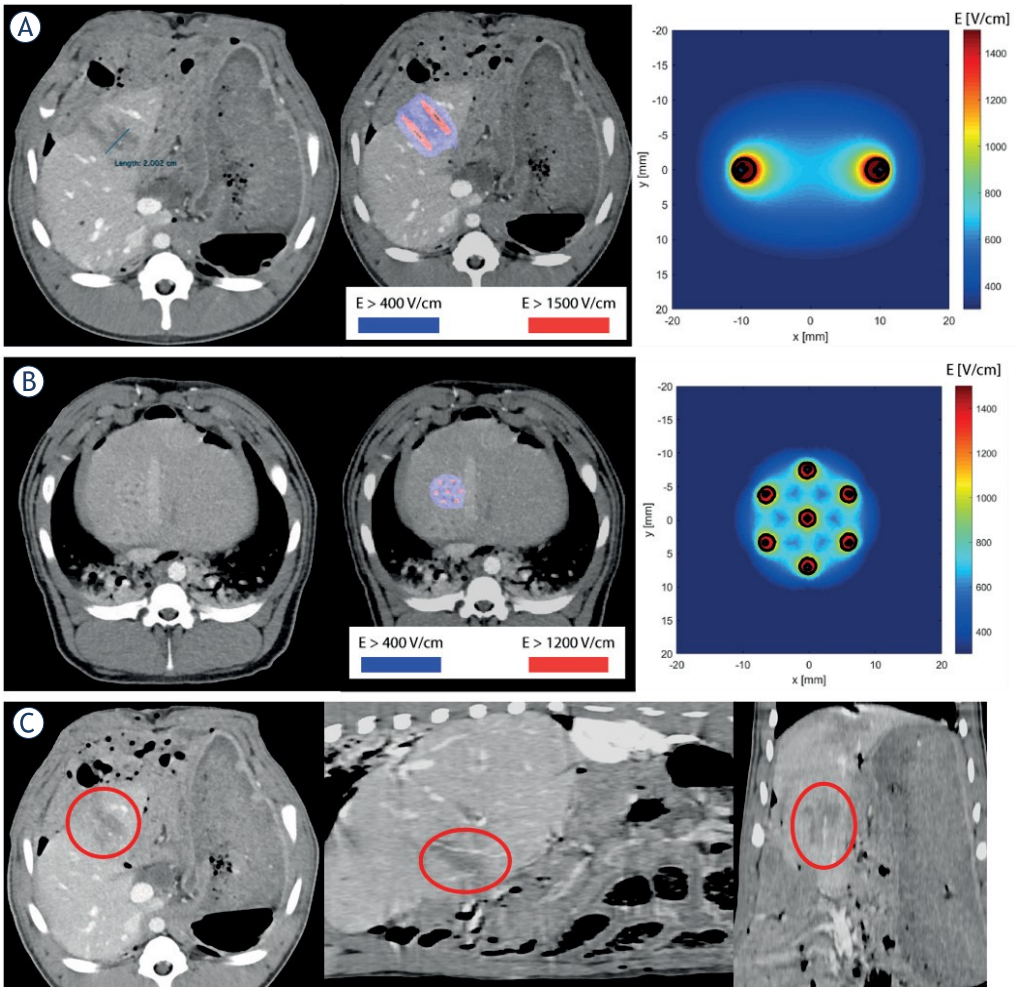

FIGURE 4. (A) Electrochemotherapy (ECT) of the liver with linear electrodes. Left figure is a CT image, where a distance between the hypoenhancing tracks of 2 cm can be noted. Right figure is numerical model of electric field distribution in linear electrodes. Middle figure shows electric field distribution superimposed on the CT image. **(B)** ECT of the liver with hexagonal electrodes. Left figure is a CT image and right figure is numerical model of electric field distribution in hexagonal electrodes. Middle image shows electric field distribution superimposed on the CT image. **(C)** Multiplanar reconstruction (MPR) of Figure 4A. The hypoenhancing area is circled. Note the larger vessel in the middle of the hypoenhancing area in coronal reconstruction.

After careful delineation of the hypoenhancing areas in each of the transverse CT images (Figure 6B), a statistically significant difference between attenuation of untreated parenchyma and attenuation of treated areas was observed in all animals. For each animal, CT measurements and calculations are presented in the Table 1. In the case of the treatment with hexagonal geometry electrodes, the total area of the hypoenhancing regions was smaller than that in the case of the treatment with linear electrodes ($P < 0.001$), which is in accordance with computer simulation. The results of the computer simulations are shown in Figure 4A and B, where the difference in the shape of the local electric field strength produced by the different electrodes is observed. Figure 4A shows that the treated volume produced by the variable linear geometry electrodes measures 30 mm in width and 20 mm in height (corresponding to the distance between the electrodes and the applied voltage) and

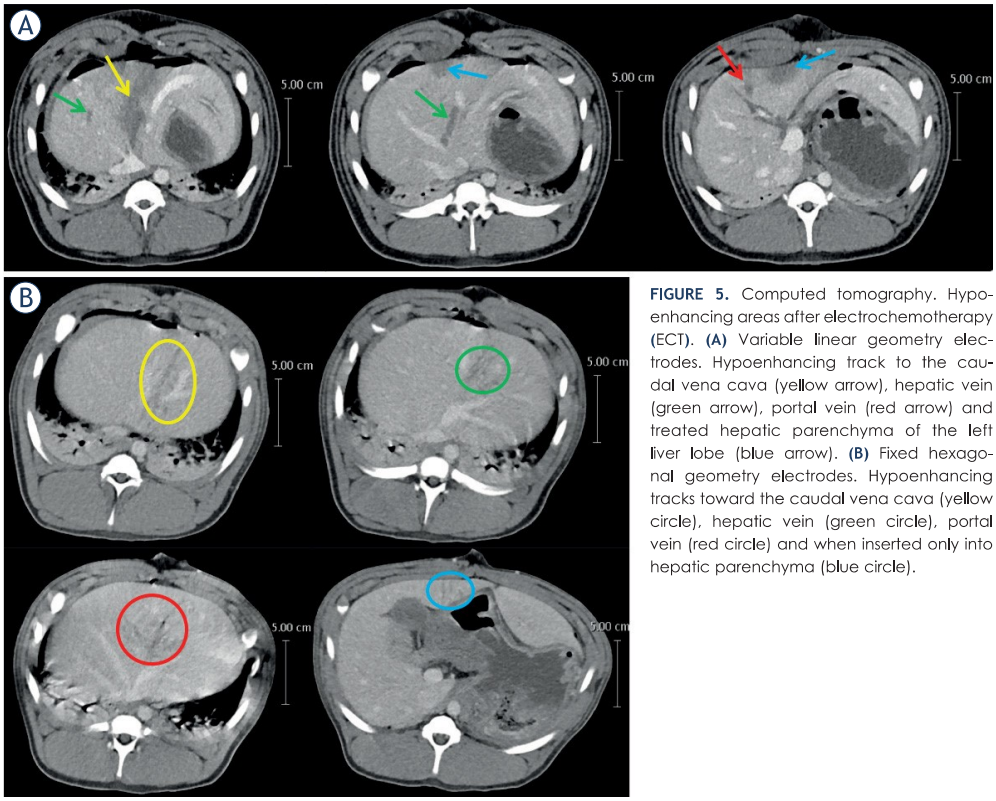

FIGURE 5. Computed tomography. Hypoenhancing areas after electrochemotherapy (ECT). **(A)** Variable linear geometry electrodes. Hypoenhancing track to the caudal vena cava (yellow arrow), hepatic vein (green arrow), portal vein (red arrow) and treated hepatic parenchyma of the left liver lobe (blue arrow). **(B)** Fixed hexagonal geometry electrodes. Hypoenhancing tracks toward the caudal vena cava (yellow circle), hepatic vein (green circle), portal vein (red circle) and when inserted only into hepatic parenchyma (blue circle).

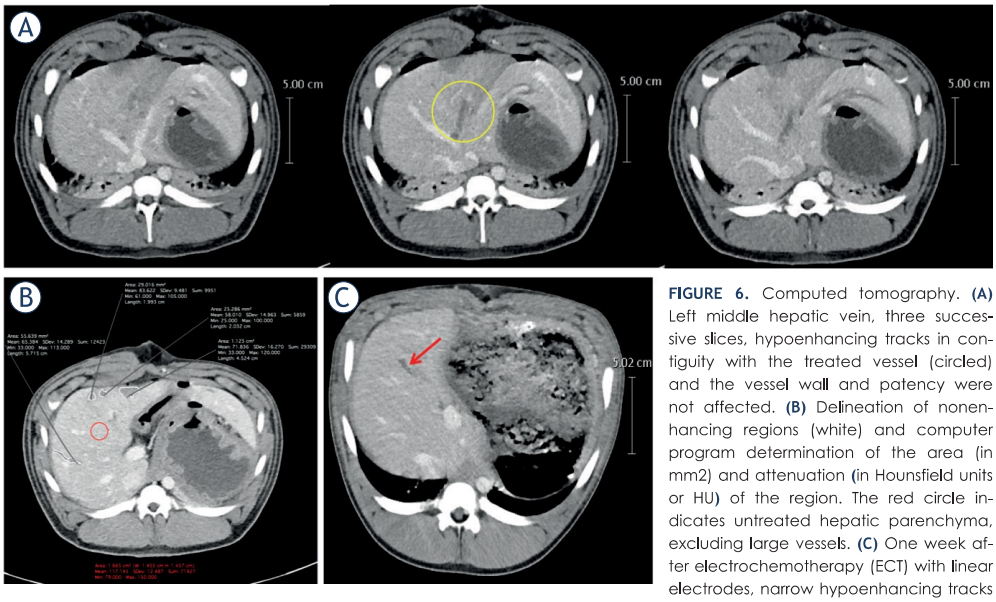

FIGURE 6. Computed tomography. **(A)** Left middle hepatic vein, three successive slices, hypoenhancing tracks in contiguity with the treated vessel (circled) and the vessel wall and patency were not affected. **(B)** Delineation of nonenhancing regions (white) and computer program determination of the area (in mm2) and attenuation (in Hounsfield units or HU) of the region. The red circle indicates untreated hepatic parenchyma, excluding large vessels. **(C)** One week after electrochemotherapy (ECT) with linear electrodes, narrow hypoenhancing tracks were observed (red arrow).

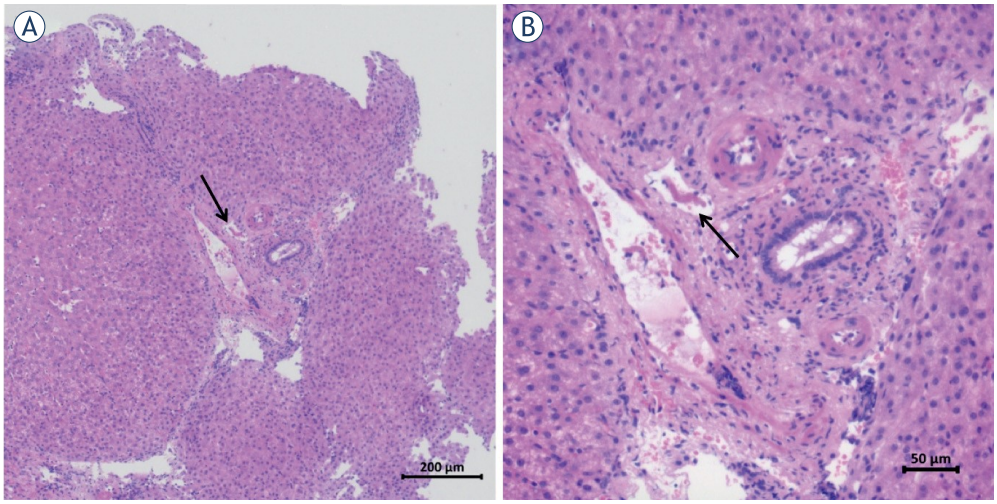

FIGURE 7. Histology of hepatic parenchyma immediately after electrochemotherapy (ECT). Fibrin thrombus in the lumen of a small venule (arrow). **(A)** H&E, 10x. **(B)** H&E, 20x.

is larger than the treated volume produced by the hexagonal electrodes, which is 20 mm by 20 mm (Figure 4B).

Furthermore, the difference and the corrected difference in attenuation were smaller after treatment with fixed hexagonal geometry electrodes than after treatment with variable linear electrodes ($P < 0.001$). There was no significant difference in the total area between the EP and ECT with linear electrodes ($P = 0.908$). In the CT findings at one week after ECT (Figure 6C), a regression of the ECT-induced changes was observed with only small hypoenhancing areas with diameters of up to 6 mm identified, which corresponds to the volume of irreversibly electroporated liver tissue determined by computer simulations, as shown in Figure 4A and B. The total area of the hypoenhancing regions was smaller than that observed immediately after the EP/ECT ($P < 0.001$). The difference and corrected difference in attenuation were both smaller after one week compared to those at 60 to 90 minutes after EP/ECT ($P < 0.001$, $P = 0.007$).

Histologic findings

Histologic findings of treated hepatic parenchyma immediately after ECT showed fibrin thrombi in small venules (Figure 7), with no other histologic changes of other vessels and bile ducts or the hepatic parenchyma.

Discussion

Radiologic findings after EP/ECT of large hepatic vessels and hepatic parenchyma were characterized in a porcine model, which was selected due to anatomical and physiological similarities with the human liver.[1,33] The results showed decreased perfusion in the treated area. This finding was an anticipated result since EP/ECT induces a local blood flow modifying effect or 'vascular lock' characterized by the vasoconstriction and increased wall permeabilization of small blood vessels. The effect on perfusion is shorter in EP compared to that in ECT and shorter in healthy compared to tumor tissue, which is known as the 'vascular disrupting effect'. Chemotherapeutic drugs are cytotoxic to endothelial cells, especially neoplastic endothelial cells, and this effect prolongs decreased perfusion.[34-41] In our case, there was no difference between EP and ECT, and no vascular disrupting effect was observed in healthy hepatic parenchyma[28], which confirms that bleomycin at the doses used has a negligible effect on healthy tissue.[34-36]

All radiologic modalities showed healthy vessel walls and patency, despite direct electrode insertion into the lumen of major hepatic vessels. These findings were consistent with previously published histologic results: no thrombosis was identified at two and seven days after EP/ECT in healthy liver.[28] This result was an expected finding considering

ECT[3,4,8,11-13] and IRE[17-22] clinical studies, where electrodes were inserted in the vicinity of[3,4,8,11-13,17-22] or into major hepatic vessels.[13] The absence of bleeding, even if needles are inserted deep into the hepatic parenchyma, is an important safety aspect of ECT due to the transient local hypoperfusion and possible electrocoagulation related to the high current density at the surface of needle electrodes.[29,35]

The US findings were dynamic. Hyperechogenic bubbles, which initially form around the electrodes, are a consequence of electrochemical reactions on the electrodes and electrocoagulation of the tissue.[27,29] The liberated gases are chlorine at the anode and hydrogen at the cathode.[42,43] Gas bubbles are formed in RFA[44] and IRE[18,45] ablations. Hypoechogenicity of the treated parenchyma indicates a structural change, which presumably occurs due to decreased perfusion caused by the vasoconstriction and increased wall permeability (edema) of small vessels.[34-37] The histologic findings of the treated hepatic parenchyma immediately after ECT showed fibrin thrombi in small venules, which is consistent with decreased perfusion due to vessel spasms.

Decreased perfusion of the treated areas was confirmed with CEUS and dynamic CT studies, the latter proving the decreased contrast enhancement of the treated areas at 30 to 90 seconds after arterial phase. The area of decreased perfusion was smaller after treatment with fixed hexagonal electrodes than after treatment with variable linear geometry electrodes. This effect is due to a larger distance between electrodes in the case of variable geometry electrodes where higher voltage must be applied to achieve same therapeutic effect, and is in accordance with computer simulation and histology.[28] The difference between the two geometry electrodes can be ascribed to a higher local electric field strength adjacent to the electrodes in the case of linear electrodes[46], as shown in Figure 4A and B. Despite the difference in size of hypoperfused hypoenhancing areas due to the higher local electric field, there is no difference in efficacy of electroporation between the variable linear- and fixed hexagonal-geometry electrodes.[29,46] In routine clinical practice hexagonal electrodes are used for smaller and superficial liver tumors, while linear electrodes are used for deep-seated and larger liver tumors.[47] The subtleness of the radiological changes of liver after EP/ECT agrees with laboratory and histologic findings that the procedure is safe, while on the contrary, it could indicate that CT findings might not be a good indicator of procedure efficacy in healthy liver. The vascular structures of the portal spaces as well as branches of the hepatic and portal veins in the liver parenchyma display different changes depending on their size and position in the ablated area: those situated in the central parts of the ablated areas and close to the electrodes show complete necrosis. Smaller structures are more sensitive to electroporation than larger structures with arterioles and bile canaliculi more resistant than venules.[12]

The CT studies at one week after ECT showed only small hypoenhancing areas, which is in accordance with histologic studies showing the existence of scar tissue.[12,28] Where electrodes punctured the wall of the large vessels, the architecture of the vessel wall was effaced with missing endothelium and no thrombosis present.[28]

Our study has several limitations. Due to the time limit of open surgery, there was limited time for US examinations, and the CT studies were performed in a range of 60 to 90 minutes after the EP/ECT. Performing radiologic examinations at different times was a major limitation because radiologic findings were dynamic and evolved in time. Another limitation of this study is the use of various US machines, which precluded numerical and statistical analyses of the US findings. Different heart rates and blood pressures of pigs influenced CEUS assessment of perfusion; therefore, comparisons among animals would be challenging. Another limitation of the study was that CT studies were only performed at 1 week after ECT with variable linear geometry electrodes. Furthermore, in CT studies, various treated areas could not always be differentiated from other areas. This limitation was overcome in the study with the percutaneous ECT of portal vein tumor thrombosis[13] and in a study with IRE of porcine liver[22] with a coaxial angiocatheter to define electrode orientation and position relative to the ablation zone. Only healthy liver was studied, further investigation of other tissues, particularly tumor tissue is required, because it is reasonable to expect that radiologic findings after ECT of hepatic neoplasia differ from radiologic findings after ECT of healthy liver due to differences in vascular and extracellular spaces. Furthermore, relatively small number of animals has been investigated, which prevented further statistical analyses and a better correlation between different groups.

Conclusions

Radiologic findings after EP/ECT of porcine liver did not show clinically significant damage to large

liver vessels and parenchyma; intact vessel walls and patency were observed, the hepatic parenchymal changes indicated by US hypoechogenicity and CT hypoenhancement were subtle. Histologic changes immediately after, and 2 and 7 days after treatment were in accordance with radiologic findings, and these results confirm that ECT is safe for the treatment of tumors that are adjacent to large hepatic vessels. Notably, radiologic features after EP/ECT are dynamic, and further studies are required to thoroughly investigate these features to provide definite answers, which, if any, are useful as indicators of adequate electric field distribution and as possible predictive factors that could guide decisions regarding the course of further treatment.

Acknowledgements

Authors acknowledge the staff of the Small Animal Clinic and Clinic for Ruminants and Pigs (Veterinary Faculty, University of Ljubljana) for their help with animal husbandry, surgery, radiologic examinations, and laboratory tests. Furthermore, we thank Mateja Nagode for the help with statistical analysis. Language editing services for this manuscript were provided by American Journal Experts. The authors acknowledge the financial support of the Slovenian Research Agency (research program No. P3-003, No. P4-0053 and No. P2-0249). The funder had no role in the study design, data collection and analysis, decision to publish, or preparation of the manuscript.

References

1. Ong SL, Gravante G, Metcalfe MS, Dennison AR. History, ethics, advantages and limitations of experimental models for hepatic ablation. *World J Gastroenterol* 2013; **19:** 147-54. doi: 10.3748/wjg.v19.i2.147
2. Au JT, Kingham TP, Jun K, Haddad D, Gholami S, Mojica K, et al. Irreversible electroporation ablation of the liver can be detected with ultrasound B-mode and elastography. *Surgery* 2013; **153:** 787-93. doi: 10.1016/j.surg.2012.11.022
3. Edhemovic I, Brecelj E, Gasljevic G, Music MM, Gorjup V, Mali B, et al. Intraoperative electrochemotherapy of colorectal liver metastases. *J Surg Oncol* 2014; **110:** 320-7. doi: 10.1002/jso.23625
4. Edhemovic I, Gadzijev EM, Brecelj E, Miklavcic D, Kos B, Zupanic A, et al. Electrochemotherapy: a new technological approach in treatment of metastases in the liver. *Technol Cancer Res Treat* 2011; **10:** 475-85. doi: 10.7785/tcrt.2012.500224
5. Kingham TP, Karkar AM, D'Angelica MI, Allen PJ, DeMatteo RP, Getrajdman GI, et al. Ablation of perivascular hepatic malignant tumors with irreversible electroporation. *J Am Coll Surg* 2012; **215:** 379-87. doi: 10.1016/j.jamcollsurg.2012.04.029
6. Colletti L, Battaglia V, De Simone P, Turturici L, Bartolozzi C, Filipponi F. Safety and feasibility of electrochemotherapy in patients with unresectable colorectal liver metastases: a pilot study. *Int J Surg* 2017; **44:** 26-32. doi: 10.1016/j.ijsu.2017.06.033
7. Tafuto S, von Arx C, De Divitiis, Maura CT, Palaia R, Albino V, et al. Electrochemotherapy as a new approach on pancreatic cancer and on liver metastases. *Int J Surg* 2015; **21:** S78-S82. doi: 10.1016/j.ijsu.2015.04.095
8. Miklavcic D, Mali B, Kos B, Heller R, Sersa G. Electrochemotherapy: from the drawing board into medical practice. *Biomed Eng Online* 2014; **13:** 29. doi: 10.1186/1475-925X-13-29
9. Campana LG, Clover JG, Valpione S, Quaglino P, Gehl J, Kunte C, et al. Recommendations for improving the quality of reporting clinical electrochemotherapy studies based on qualitative systematic review. *Radiol Oncol* 2016; **50:** 1-13. doi: 10.1515/raon-2016-0006
10. Campana LG, Marconato R, Valpione S, Galuppo S, Alaibac M, Rossi CR, et al. Basal cell carcinoma: 10-year experience with electrochemotherapy. *J Transl Med* 2017; **15:** 122. doi: 10.1186/s12967-017-1225-5
11. Djokic M, Cemazar M, Popovic P, Kos B, Dezman R, Bosnjak M, et al. Electrochemotherapy as treatment option for hepatocellular carcinoma, a prospective pilot study. *Eur J Surg Oncol* 2018; **44:** 651-7. doi: 10.1016/j.ejso.2018.01.090
12. Gasljevic G, Edhemovic I, Cemazar M, Brecelj E, Gadzijev EM, Music MM, et al. Histopathological findings in colorectal liver metastasis after electrochemotherapy. *PloS One* 2017; **12:** e0180709. doi: 10.1371/journal.pone.0180709
13. Tarantino L, Busto G, Nasto A, Fristachi R, Cacace L, Talamo M, et al. Percutaneous electrochemotherapy in the treatment of portal vein tumor thrombosis at hepatic hilum in patients with hepatocellular carcinoma in cirrhosis: a feasibility study. *World J Gastroenterol* 2017; **23:** 906-18. doi: 10.3748/wjg.v23.i5.906
14. Granata V, Fusco R, Piccirillo M, Palaia R, Petrillo A, Lastoria S, Izzo F. Electrochemotherapy in locally advanced pancreatic cancer: Preliminary results. *Int J Surg* 2015; **18:** 230-6. doi: 10.1016/j.ijsu.2015.04.055
15. Bimonte S, Leongito M, Granata V, Barbieri A, del Vecchio V, Falco M, et al. Electrochemotherapy in pancreatic adenocarcinoma treatment: preclinical and clinical studies. *Radiol Oncol* 2016; **50:** 14-20. doi: 10.1515/raon-2016-0003
16. Granata V, Fusco R, Setola SV, Palaia R, Albino V, Piccirillo M, et al. Diffusion kurtosis imaging and conventional diffusion weighted imaging to assess electrochemotherapy response in locally advanced pancreatic cancer. *Radiol Oncol* 2019; **53:** 415-24. doi: 10.2478/raon-2019-0004
17. Cannon R, Ellis S, Hayes D, Narayanan G, Martin RCG. Safety and early efficacy of irreversible electroporation for hepatic tumors in proximity to vital structures. *J Surg Oncol* 2013; **107:** 544-9. doi: 10.1002/jso.23280
18. Lee EW, Chen C, Prieto VE, Dry SM, Loh CT, Kee ST. Advanced hepatic ablation technique for creating complete cell death: irreversible electroporation. *Radiology* 2010; **255:** 426-33. doi: 10.1148/radiol.10090337
19. Lee YJ, Lu DS, Osuagwu F, Lassman C. Irreversible electroporation in porcine liver: short- and long-term effect on the hepatic veins and adjacent tissue by CT with pathological correlation. *Invest Radiol* 2012; **47:** 671-5. doi: 10.1097/RLI.0b013e318274b0df
20. Narayanan G, Bhatia S, Echenique A, Suthar R, Barbery K, Yrizarry J. Vessel patency post irreversible electroporation. *Cardiovasc Intervent Radiol* 2014; **37:** 1523-9. doi: 10.1007/s00270-014-0988-9
21. Kasivisvanathan V, Thapar A, Oskrochi Y, Picard J, Leen EL. Irreversible electroporation for focal ablation at the porta hepatis. *Cardiovasc Intervent Radiol* 2012; **35:** 1531-4. doi: 10.1007/s00270-012-0363–7
22. Lee YJ, Lu DS, Osuagwu F, Lassman C. Irreversible electroporation in porcine liver: acute computed tomography appearance of ablation zone with histopathologic correlation. *J Comput Assist Tomogr* 2013; **37:** 154-8. doi: 10.1097/RCT.0b013e31827dbf9b
23. Appelbaum L, Ben-David E, Sosna J, Nissenbaum Y, Goldberg SN. US findings after irreversible electroporation ablation: radiologic-pathologic correlation. *Radiology* 2012; **262:** 117-25. doi: 10.1148/radiol.11110475
24. Abdelsalam ME, Chetta JA, Harmoush S, Ensor J Jr, Javadi S, Dixon K, et al. CT findings after irreversible electroporation ablation in a porcine model: radiologic-pathologic correlation. *J Vasc Interv Radiol* 2013; **24:** S161. doi: 10.1016/j.jvir.2013.01.405
25. Charpentier KP, Wolf F, Noble L, Winn B, Resnick M, Dupuy DE. Irreversible electroporation of the liver and liver hilum in swine. *HPB (Oxford)* 2011; **13:** 168-73. doi: 10.1111/j.1477-2574.2010.00261.x

26. Chung DJ, Sung K, Osuagwu FC, Wu HH, Lassman C, Lu DS. Contrast enhancement patterns after irreversible electroporation: experimental study of CT perfusion correlated to histopathology in healthy porcine liver. *J Vasc Interv Radiol* 2016; **27:** 104-11. doi: 10.1016/j.jvir.2015.09.005

27. Boc N, Edhemovic I, Kos B, Music MM, Brecelj E, Trotovsek B, et al. Ultrasonographic changes in the liver tumors as indicators of adequate tumor coverage with electric field for effective electrochemotherapy. *Radiol Oncol* 2018; **52:** 383-91. doi: 10.2478/raon-2018-0041

28. Zmuc J, Gasljevic G, Sersa G, Edhemovic I, Boc N, Seliskar A, et al. Large liver blood vessels and bile ducts are not damaged by electrochemotherapy with bleomycin in pigs. *Sci Rep* 2019: **9:** 3649. doi: 10.1038/s41598-019-40395-y

29. Kos B, Voigt P, Miklavcic D, Moche M. Careful treatment planning enables safe ablation of liver tumors adjacent to major blood vessels by percutaneous irreversible electroporation (IRE). *Radiol Oncol* 2015; **49:** 234-41. doi: 10.1515/raon-2015-0031

30. Marčan M, Pavliha D, Kos B, Forjanič T, Miklavčič D. Web-based tool for visualization of electric field distribution in deep-seated body structures and planning of electroporation-based treatments. *Biomed Eng Online* 2015; **14 Suppl 3:** S4. doi: 10.1186/1475-925X-14-S3-S4

31. Marty M, Sersa G, Rémi Garbay J, Gehl J, Collins CG, Snoj M, et al. Electrochemotherapy – an easy, highly effective and safe treatment of cutaneous and subcutaneous metastases: results of ESOPE (European Standard Operating Procedures of Electrochemotherapy) study. *EJC Supplements* 2006; **4:** 3-13. doi: 10.1016/j.ejcsup.2006.08.002

32. Mir LM, Gehl J, Sersa G, Collins CG, Garbay JR, Billard V, et al. Standard operating procedures of the electrochemotherapy: instructions for the use of bleomycin or cisplatin administered either systemically or locally and electric pulses delivered by Cliniporator by means of invasive or non-invasive electrodes. *Eur J Cancer Suppl* 2006; **4:** 14-25. doi: 10.1016/j.ejcsup.2006.08.003

33. Nykonenko A, Vavra P, Zonca P. Anatomic peculiarities of pig and human liver. *Exp Clin Transplant* 2017; **15:** 21-6. doi: 10.6002/ect.2016.0099

34. Bellard E, Markelc B, Pelofy S, Le Guerroué, Sersa G, et al. Intravital microscopy at the single vessel level brings new insights of vascular modification mechanisms induced by electropermeabilization. *J Control Release* 2012; **163:** 396-403. doi: 10.1016/j.jconrel.2012.09.010

35. Jarm T, Cemazar M, Miklavcic D, Sersa G. Antivascular effects of electrochemotherapy: implications in treatment of bleeding metastases. *Expert Rev Anticancer Ther* 2010; **10:** 729-46. doi: 10.1586/era.10.43

36. Gehl J, Skovsgaard T, Mir LM. Vascular reactions to in vivo electroporation: characterization and consequences for drug and gene delivery. *Biochim Biophys Acta* 2002; **1569:** 51-8. doi: 10.1016/s0304-4165(01)00233-1

37. Markelc B, Bellard E, Sersa G, Jesenko T, Pelofy S, Teissié, et al. Increased permeability of blood vessels after reversible electroporation is facilitated by alterations in endothelial cell-to-cell junctions. *J Control Release* 2018; **276:** 30-41. doi: 10.1016/j.jconrel.2018.02.032

38. Ivanusa T, Beravs K, Cemazar M, Jevtic V, Demsar F, Sersa G. MRI macromolecular contrast agents as indicators of changed tumor blood flow. *Radiol Oncol* 2001; **35:** 139-47.

39. Sersa G, Cemazar M, Miklavcic D. Tumor blood flow modifying effects of electrochemotherapy: a potential vascular targeted mechanism. *Radiol Oncol* 2003; **37:** 43-8.

40. Sersa G, Cemazar M, Miklavcic D, Chaplin DJ. Tumor blood flow modifying effect of electrochemotherapy with bleomycin. *Anticancer Res* 1999; **19:** 4017-22.

41. Sersa G, Cemazar M, Parkins CS, Chaplin DJ. Tumour blood flow changes induced by application of electric pulses. *Eur J Cancer* 1999; **35:** 672-7. doi: 10.1016/s0959-8049(98)00426-2

42. Li K, Xin Y, Gu Y, Xu B, Fan D, Ni B. Effects of direct current on dog liver: possible mechanisms for tumor electrochemical treatment. *Bioelectromagnetics* 1997; **18:** 2-7. doi: 10.1002/(sici)1521-186x(1997)18:1<2::aid-bem2>3.0.co;2-6

43. Stehling MK, Guenther E, Mikus P, Klein N, Rubinsky L, Rubinsky B. Synergistic combination of electrolysis and electroporation for tissue ablation. *PloS One* 2016; **11:** e0148317. doi: 10.1371/journal.pone.0148317

44. Oei T, vanSonnenberg E, Shankar S, Morrison PR, Tuncali K, Silverman SG. Radiofrequency ablation of liver tumors: a new cause of benign portal venous gas. *Radiology* 2005; **237:** 709-17. doi: 10.1148/radiol.2372041295

45. Faroja M, Ahmed M, Appelbaum L, Ben-David E, Moussa M, Sosna J. Irreversible electroporation ablation: is all the damage non thermal? *Radiology* 2013; **266:** 462-70. doi: 10.1148/radiol.12120609

46. Miklavcic D, Semrov D, Mekid H, Mir LM. A validated model of in vivo electric field distribution in tissues for electrochemotherapy and for DNA electrotransfer for gene therapy. *Biochim Biophys Acta* 2000; **1523:** 73-83. doi: 10.1016/s0304-4165(00)00101-x

47. Miklavcic D, Sersa G, Brecelj E, Gehl J, Soden D, Bianchi G, et al. Electrochemotherapy: technological advancements for efficient electroporation-based treatment of internal tumors. *Med Biol Eng Comput* 2012; **50:** 1213-25. doi: 10.1007/s11517-012-0991-8

2.2 Ultrazvočni pregled s kontrastnim sredstvom za oceno perfuzije tumorjev in izida zdravljenja na modelu mišjih melanomov

Contrast-enhanced ultrasound for evaluation of tumor perfusion and outcome following treatment in a murine melanoma model

Maja Brložnik,[1] Nina Boc,[2] Maja Čemažar,[2,5] Maša Bošnjak,[2] Monika Savarin,[2] Nataša Kejžar,[3] Gregor Serša,[2,4] Darja Pavlin,[1]* Simona Kranjc Brezar.[2,3]*

[1] Univerza v Ljubljani, Veterinarska fakulteta

[2] Onkološki inštitut Ljubljana

[3] Univerza v Ljubljani, Medicinska fakulteta

[4] Univerza v Ljubljani, Zdravstvena fakulteta

[5] Univerza na Primorskem, Fakulteta za vede o zdravju

* vodilni avtorici: Darja Pavlin in Simona Kranjc Brezar

Bioelectrochemistry 2021; 142: 107932. doi: 10.1016/j.bioelechem.2021.107932.

Izvleček

Zaradi pomanjkanja podatkov o prediktivnih dejavnikih zdravljenja na osnovi EP smo raziskali možno prediktivno vlogo UZ-KS za oceno perfuzije tkiva pri miših z melanomom B16F10, zdravljenih z obsevanjem in GEP plazmidne DNA, ki utiša adhezijsko molekulo celic melanoma (MCAM, angl. melanoma cell adhesion molecule). Rezultate UZ-KS smo primerjali s histološko analizo tumorja (barvanje žilja). Miši z induciranimi podkožnimi tumorji smo zdravili z GEP za utišanje MCAM, obsevanjem ali kombiniranim zdravljenjem obsevanja in GEP za utišanje MCAM. UZ-KS preiskava, ki je bila uporabljena za oceno tumorske perfuzije, smo izvedli pred in do 10 dni po začetku eksperimenta, rezultate UZ-KS pa smo primerjali z rastjo tumorja in številom krvnih žil, analiziranih v histoloških odsekih tumorja. UZ-KS je pokazal značilno zmanjšanje perfuzije tumorja v kombiniranih terapevtskih skupinah v primerjavi s kontrolnimi skupinami in je koreliral s histološkimi analizami tumorjev, ki so pokazale zmanjšano gostoto žilja. V tej raziskavi je bil opažen trend inverzne korelacije med perfuzijo tumorja in učinkovitostjo zdravljenja. Večja kot je bila perfuzija tumorja, krajši je bil pričakovani čas podvojitve. Pokazali smo, da lahko UZ-KS uporabimo na osnovi ocene perfuzije, za ugotavljanje žilne gostote tumorjev in učinkovitosti zdravljenja.

Bioelectrochemistry 142 (2021) 107932

Contents lists available at ScienceDirect

Bioelectrochemistry

journal homepage: www.elsevier.com/locate/bioelechem

Contrast-enhanced ultrasound for evaluation of tumor perfusion and outcome following treatment in a murine melanoma model

Maja Brloznik [a], Nina Boc [b], Maja Cemazar [b,e], Masa Bosnjak [b], Monika Savarin [b], Natasa Kejzar [c], Gregor Sersa [b,d], Darja Pavlin [a,*], Simona Kranjc Brezar [b,f,*]

[a] Small Animal Clinic, Veterinary Faculty, University of Ljubljana, Gerbiceva 60, Ljubljana, Slovenia
[b] Institute of Oncology Ljubljana, Zaloska 2, Ljubljana, Slovenia
[c] Institute for Biostatistics and Medical Informatics, Faculty of Medicine, University of Ljubljana, Vrazov trg 2, Ljubljana, Slovenia
[d] Faculty of Health Sciences, University of Ljubljana, Zdravstvena pot 5, Ljubljana, Slovenia
[e] Faculty of Health Sciences, University of Primorska, Polje 42, Izola, Slovenia
[f] Faculty of Medicine, University of Ljubljana, Vrazov trg 2, Ljubljana, Slovenia

ARTICLE INFO

Article history:
Received 1 November 2020
Received in revised form 10 August 2021
Accepted 13 August 2021
Available online 18 August 2021

Keywords:
Murine melanoma B16F10
Gene electrotransfer
Melanoma cell adhesion molecule
Irradiation
Antivascular effects
Contrast-enhanced harmonic ultrasound

ABSTRACT

Due to a lack of data on predictors of electroporation-based treatment outcomes, we investigated the potential predictive role of contrast-enhanced harmonic ultrasound (CEUS) in mice B16F10 melanoma treated by gene electrotransfer (GET) to silence melanoma cell adhesion molecule (MCAM) and radiotherapy, which has not been evaluated yet. CEUS evaluation was verified by tumor histological analysis. Mice bearing subcutaneous tumors were treated with GET to silence MCAM, irradiation or the combination of GET to silence MCAM and irradiation (combined treatment). CEUS of the tumors used to evaluate tumor perfusion was performed before and up to 10 days after the beginning of the experiment, and the CEUS results were compared with tumor growth and the number of blood vessels analyzed in the histological tumor sections. CEUS revealed a decrease in tumor perfusion in the combined therapy groups compared with the control groups and correlated with tumor histological analyses, which showed a decreased vascular density. In this study a trend of inverse correlation was observed between tumor perfusion and treatment efficacy. The greater the perfusion of the tumor, the shorter the expected doubling time. Furthermore, decreased perfusion showed a trend to correlate with higher antitumor efficacy. Thus, CEUS could be used to predict tumoral vascular density and treatment effectiveness.

1. Introduction

The tumor vasculature is an attractive target for cancer therapy. A single vessel facilitates the survival of multiple tumor cells and provides the main route for metastatic spread [1]. Therefore, tumor vessel density and certain tumor perfusion aspects have been intensively investigated as possible predictors of tumor behavior and treatment outcome. A method to detect tissue perfusion at the capillary level is contrast-enhanced harmonic ultrasound (CEUS). In preclinical studies, it was shown to be an accurate predictor of tumor vascularization compared with histological results [2–4], and it correlated with advanced diagnostic imaging methods [5]. Furthermore, CEUS proved to be valuable in assessing the tumor response to treatment and as a possible means to guide the drug dosages [3–5]. In human and canine clinical studies, CEUS was able to determine microvessel density [6–9]. In humans, it has been proven to be a useful tool to evaluate the efficacy of anti-angiogenic treatments [10–13]. CEUS parameters measure tissue perfusion at the capillary level: some of them describe blood volume and others blood flow rate. Perfusion parameters are influenced by cardiac, vascular, microcirculatory and other factors [13].

Gene electrotransfer (GET) is a physical method of plasmid DNA delivery into cells, enabling the entry of large molecules by application of short high-voltage electric pulses that induce cell membrane permeabilization [14–16]. Melanoma cell adhesion molecule (MCAM) or CD146 is a multifunctional transmembrane glycoprotein, which is overexpressed in melanoma and is involved in melanoma development and progression, the latter including invasiveness, metastatic potential, and angiogenesis. Therefore, the silencing of MCAM, using plasmid DNA encoding shRNA

* Corresponding authors at: Small animal clinic, Veterinary Faculty, University of Ljubljana, Gerbiceva 60, Ljubljana (D. Pavlin); Institute of Oncology Ljubljana, Zaloska 2, Ljubljana, Slovenia (S. Kranjc Brezar).
E-mail addresses: darja.pavlin@vf.uni-lj.si (D. Pavlin), skranjc@onko-i.si (S. Kranjc Brezar).

https://doi.org/10.1016/j.bioelechem.2021.107932
1567-5394/

against MCAM, is a potential target for the gene therapy of melanoma [17–19].

Vascular targeted therapies aim at normalizing the tumor vasculature and therefore promote radiosensitizing effects because they facilitate increased oxygenation of the remaining tumor tissue [1,21–23]. GET of plasmid DNA exhibits a radiosensitizing effect in murine tumors [19–23], and studies have shown that both therapeutic and control plasmid DNA devoid of therapeutic genes have antitumor action [19,24–26].

Despite clinical effectiveness of electroporation-based therapies there is still a lack of data on predictors of treatment outcome. Thus, this study aimed to compare the results of CEUS with histological analysis of the tumor vascular density and evaluate them as possible predictive factors for the therapeutic outcome in an experimental model of radioresistant murine melanoma B16F10 treated with irradiation and gene electrotransfer (GET) of plasmid DNA encoding shRNA against MCAM.

2. Materials and methods

2.1. Animals

Female C57Bl/6JOlaHsd mice (Envigo RMS SrL, San Pietro al Natisone, Italy), 7 weeks old, weighing 18–20 g, were housed under specific pathogen-free conditions at a temperature of 20–24 °C and with a relative humidity of 55 ± 10%, a 12-hour light/dark cycle, and food and water provided ad libitum. All the procedures were performed according to the guidelines for animal experiments of the EU directive (2010/63/EU). Regulatory approval was issued by the Veterinary Administration of the Ministry of Agriculture and the Environment of the Republic of Slovenia (No. U34401-1/2015/38).

2.2. Tumors

The subcutaneous tumors were induced on the back of the mice by the subcutaneous injection of 100 μl of B16F10 cell suspension containing one million cells (American Type Culture Collection, Manassas, VA, USA). The cells were cultured in advanced minimum essential medium (AMEM) supplemented with 5% fetal bovine serum (FBS), 10 mM/l L-glutamine GlutaMAX (all Gibco, Fisher Scientific, Waltham, MA, USA), 100 U/ml of penicillin (Grünenthal, Aachen, Germany) and 50 mg/ml of gentamicin (Krka, Novo mesto, Slovenia) in a 5% CO_2 humidified incubator at 37 °C. At 80% confluence, trypsinization was performed with 0.25% trypsin/EDTA in Hank's buffer and the cells were then washed with AMEM with FBS and collected by centrifugation. The cells were routinely checked for the presence of *Mycoplasma sp* (MycoAlertTM PLUS Mycoplasma Detection Kit; Pharma & Biotech, Lonza, Basel, Switzerland).

2.3. Experimental protocol

The tumors were allowed to reach a volume of approximately 40 mm^3, which corresponds to a diameter of approximately 6 × 6 × 2 mm (day 0). The tumors were measured every second day with a Vernier-caliper, and the tumor volume was calculated from the measured perpendicular diameters ($V = a \times b \times c \times \pi/6$).

The mice were randomly divided into twelve groups, each containing nine or ten mice. The procedures performed in the treatment groups are presented in Table 1.

Irradiation was delivered by a Darpac 2000 X-ray unit (Gulmay Medical Ltd, Surrey, UK) operating at 220 kV, 10 mA, with 1.8-mm aluminum filtration. Possible acute skin reactions in the irradiated field were monitored as described previously [21,27,28].

Electric pulses were generated by an electric pulse generator ELECTRO CELL B10 HVLV (Betatech, L'Union, France) and delivered through two parallel stainless steel electrodes 6–7 mm apart, depending on the tumor volume. After the delivery of four pulses, the electrodes were turned for 90° to deliver four additional pulses. The selection of voltage, duration and frequency of EP was chosen based on previous studies [14,15].

For EP and CEUS, the mice were anesthetized using inhalation anesthesia with isoflurane (2% v/v), and the heating pad was used to prevent hypothermia. For CEUS examinations, the tumors were fixed in a plastic holder to improve tumor display and for more stable probe holding.

CEUS examinations were performed in three to seven animals of each group on days 0, 1, 2, 5, 6, 7 and/or 10. On days 0, 1 and 2, CEUS examinations were performed before other procedures. The schedule of the experiment is shown in Scheme 1. The mice used for tumor histology were humanely sacrificed on day 6. Mice were humanely sacrificed due to disease burden when tumor diameter was larger than 12 mm. Most of the statistical analyses were performed until day 7; however, from day 6, the sample of mice is biased toward mice with a lower disease burden.

The contrast agent Sonovue (Bracco, Milan, Italy), ultrasonographic machine M9 (Mindray, Shenzhen, China) and linear probe (L3-13.5; Mindray, Shenzhen, China) with a frequency of 3 to 13.5 MHz and harmonic ultraband nonlinear contrast display at a low mechanical index were used. The clinical guidelines for CEUS to quantify tumor perfusion were followed [29–31]. After applying 50 μl of the topical anesthetic Alcaine ophthalmic solution (Alcon, Basel, Switzerland) to the mice cornea, 0.1 ml of contrast agent was administered to the retroorbital sinus [32]. From the time of contrast application, a 90-second-long recording was made. Each tumor was carefully delineated, and 6 to 8 ellipsoid regions of interest (ROIs) were drawn to cover the whole area of the tumor (Supplementary Figure S1). For the whole tumor and ROIs, the perfusion curve or time-intensity curve, presenting the signal intensity, was analyzed using an ultrasound (US) system with built-in software.

Animal weight was monitored as a sign of the systemic toxicity of the treatments. The animals were weighed on the treatment starting date before plasmid injections and thereafter every second day until the end of the experiment when the tumor grew up to 450 mm^3 on average. To determine the antitumor effect of the treatment, a tumor growth delay evaluation was performed. Based on the tumor volume calculations (described in the paragraph above), a tumor doubling time (DT) was determined as the time in which the tumor doubled the volume from the initial day of the experiment. Growth delay (GD) was determined as the difference in the DT of each tumor in the therapeutic and mean DT in the control group [33]. The tumor growth delay assay was performed in the same animals used for CEUS measurements.

Mice with tumor regression were examined for tumor presence for 100 days after the treatment. If they were tumor free 100 days after the treatment, they were considered complete responders (CRs). They were challenged with a second subcutaneous injection of the melanoma cells as previously described. Animals without tumor growth in the subsequent 100 days were considered resistant to secondary challenges.

2.4. Histological analysis

From each experimental group, three tumors were collected for immunohistological (IHC) analysis on day 6 from the beginning of the therapy. The tumors were fixed in IHC zinc fixative (BD Biosciences, San Diego, CA, USA), embedded in paraffin blocks, and cut into 2-μm-thick sections, which were stained to determine blood vessels in the tumors. The sections were incubated with pri-

Table 1
Procedures performed in the twelve groups of mice with melanoma B16F10 treated with irradiation and gene electrotransfer (GET) of plasmid DNA encoding shRNA against MCAM.

	Treatment group	No. of included mice	Treatment	Treatment schedule
1	CTRL	9	no therapies performed	
2	pC	9	intratumoral injection of control plasmid DNA (pENTR/U6 pControl, 4 μg/μl) [17,19,22], 50 μg (12.5 μl)	on days 0, 2 and 4
3	pMCAM	9	intratumoral injection of plasmid DNA encoding shRNA MCAM (pENTR/U6 CD146, 4 μg/μl) [18], 50 μg (12.5 μl)	on days 0, 2 and 4
4	EP	9	8 square electric pulses of 600 V/cm, a pulse duration of 5 ms, and a frequency of 1 Hz	on days 0, 2 and 4
5	IR	9	irradiation in special lead holders with the apertures of 10 mm: a single dose of 15 Gy at a dose rate of 2.16 Gy/min	on day 1
6	GET pC	9	as described above for GET and pC: EP were delivered 10 min after intratumoral plasmid DNA injection	on days 0, 2 and 4
7	GET pMCAM	10	as described above for GET and pMCAM: EP were delivered 10 min after intratumoral plasmid DNA injection	on days 0, 2 and 4
8	EP IR	9	as described above for EP and IR	EP on days 0, 2, 4 IR on day 1
9	pMCAM IR	9	as described above for pMCAM and IR	pMCAM on days 0, 2, 4 IR on day 1
10	pC IR	9	as described above for pC and IR	pC on days 0, 2, 4 IR on day 1
11	GET pMCAM IR	10	as described above for GET pMCAM and IR	GET on days 0, 2, 4 IR on day 1
12	GET pC IR	9	as described above for GET pC and IR	GET pC on days 0, 2, 4 IR on day 1

LEGEND: CTRL = untreated control; GET = gene electrotransfer; EP = electric pulses; IR = single-dose irradiation; pC = intratumoral injection of control plasmid; pMCAM = intratumoral injection of plasmid DNA encoding shRNA for MCAM.

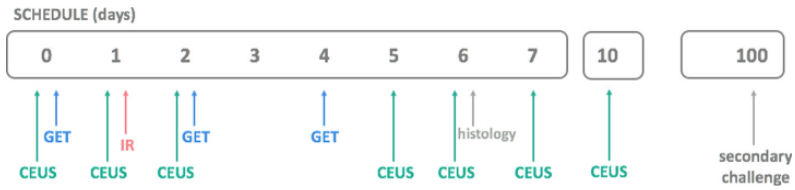

Scheme 1. Schedule of the experiment. CEUS = contrast-enhanced ultrasound, GET = gene electrotransfer of plasmid DNA, IR = irradiation (15 Gy).

mary rabbit polyclonal antibodies against CD31 (ab28364; Abcam, USA) at a dilution of 1:1000. Next, the sections were incubated with biotinylated goat anti-rabbit antibodies, streptavidin-peroxidase conjugate, and peroxidase substrate (rabbit-specific HRP/DAB detection IHC kit; ab64261; Abcam, USA), followed by hematoxylin counterstaining, as described previously [19]. Five randomly selected viable parts of each tumor were examined using a BX-51 microscope under 40 × magnification (numerical aperture 0.85) and captured using a DP72 CCD camera (both Olympus, Hamburg, Germany). The images were analyzed by two independent researchers and presented as the vascular density (the number of vessels per analyzed area, i.e., the number of vessels divided by the area of the acquired image).

2.5. Statistical analysis

The mean and standard deviation or error are considered measures of centrality and variability in numerical variables. One-way analysis of variance followed by the Holm–Sidak corrected t-tests were used to exploratory compare the mean differences in DT or vascular density between the treatment groups (Systat Software, Chicago, IL, USA). Generalized Bland–Altman plots were used to inspect the possible correlation between the mean values and their variability. Independent samples *t*-test was used to explore the possible daily difference between mean peak enhancement (PE) values in groups (CR vs. non-CR). The daily association between the PE and (log) DT values were explored using linear regression models and presented in scatterplots with linear regression lines. The p-values for each day were adjusted using Hommel's correction for the familywise error rate due to multiple comparisons. Additionally, to model a possible association of PE measurements over time with the status CR or non-CR, mixed-effect logistic regression was applied (considering each mouse and each treatment as random effects). Statistical package R was used [34]. Statistical significance was set to $p < 0.05$.

3. Results

To evaluate the capacity of CEUS to assess tumor perfusion/vascularization and outcome following electroporation treatment, we used mice bearing B16F10 melanoma tumors subjected to electroporation gene therapy and ionizing radiation as a that was previously observed to be a relevant model [18], where different levels of response were determined after monotherapies and after the combined treatment with radiation therapy. Ultrasound (US) system built-in software showed the perfusion curve and the following parameters: Base Intensity (BI: the basic intensity of non-contrast perfusion status), Peak Intensity (PI) and Area Under Curve (AUC). Peak Enhancement (PE) was calculated as the difference between PI and BI. PE and AUC are blood volume parameters. The parameters describing blood flow rate are Time To Peak (TTP:

the time at which contrast intensity reaches a peak), Ascending Slope (AS: the slope between the starting point of lesion perfusion and the peak), Arrival Time (AT: the time at which the contrast intensity appears, generally the current time value is 110% higher than the baseline intensity), Descend Time to one-half (DT/2: the time at which the intensity is half the value of the peak intensity), and Descending Slope (DS: the slope between the and the peak and ending point of lesion perfusion) (Fig. 1). No evident association was observed between vascular density (measured by IHC) and tumor growth (assessed by a caliper) and CEUS blood flow parameters (AT, AS, TTP, DT/2, DS) and AUC blood volume parameter; thus, only PE as the CEUS result was analyzed and is reported below.

3.1. Correlation of the CEUS results with the vascular density in tumors

To determine if CEUS could be used as a method to evaluate an antivascular response to treatment using GET of pMCAM and irradiation, the CEUS results were compared with the vascular density in histological tumor sections (Table 2). The mean vascular density for the combined therapeutic groups GET pMCAM IR, GET pMCAM and GET pC IR was significantly lower, from 1.4- to 3.8-fold than that in the pertinent control groups and untreated control group. The mean PE values for the combined therapeutic groups GET pMCAM IR, GET pMCAM and GET pC IR were significantly lower, from 1.8- to 6.9-fold, than those of the pertinent control groups (and untreated control group) (Table 2). The correlation of the histological results (vascular density) and PE was found for all the treatment groups (Supplementary Figure S2). Because the measurements of vascular density were mostly taken from different mice compared with the measurements of PE, none of the standard correlation measures between these two methods could be reported.

Comparing to pertinent and untreated control groups, in the combined therapeutic groups GET pMCAM IR, GET pMCAM and GET pC IR, a decrease in perfusion and a smaller number of blood vessels were observed by CEUS and histological analyses, respectively (Supplementary Figs. S1 and S2).

3.2. Heterogeneity of perfusion in tumors

Perfusion curves for different ROIs of the same tumor showed that the tumors that were larger than 40 mm^3 were commonly heterogeneously perfused (Supplementary Figure S3). Heterogeneous perfusion was more pronounced with the increased tumor volume in all the treatment groups. To inspect this heterogeneity, Bland–Altman plots of the means and standard deviations for each treatment group are presented in Fig. 2A for vascular density and Fig. 2B for PE. The variabilities increased in the treatment groups with a larger mean PE—i.e., the mice in groups with higher values of PE were more heterogeneous than mice in groups with lower PE values.

Heterogenous perfusion of the tumors in the same therapeutic group on the same day is also observed in Supplementary Figure S4. Heterogeneity of perfusion was also commonly observed for the same tumor during the time of observation and an example of such a tumor, where complete response was observed, can be seen in Supplementary Figure S5.

Table 2
Mean values and standard errors for CEUS peak enhancement (PE) and vessel density in the twelve treatment groups on day 6 after the treatment.

Treatment group	CEUS PE		Vessel density (number/mm^2)	
	Mean	SE	Mean	SE
CTRL	10.4	0.7	364.3	21.1
pC	9.6	1.9	331.1	33.2
pMCAM	9.3	0.8	326.8	20.6
EP	8.4	2.2	280.9	18.4
IR	6.5	0.5	211.5*	12.1
GET pC	6.7	2.2	248.5*	29.8
GET pMCAM	2.4*	0.8	127.1*	11.7
pC IR	4.2*	0.2	172.1*	12.9
pMCAM IR	5.1	2.2	175.8*	13.9
EP IR	5.7	1.1	203.0*	16.3
GET pC IR	2.3*	1.1	127.4*	13.2
GET pMCAM IR	1.5*	0.5	96.0*	7.7

LEGEND: CTRL = untreated control; GET = gene electrotransfer; IR = single-dose irradiation, 15 Gy; pC = intratumoral injection of control plasmid; pMCAM = intratumoral injection of plasmid DNA encoding shRNA for MCAM; PE = peak enhancement; SE = standard error of arithmetic mean.
* $p < 0.05$ = statistically significant mean difference compared with untreated control group.

3.3. Tumor growth delay after the silencing of MCAM and irradiation

The growth of B16F10 melanoma after silencing MCAM and irradiation is shown in Table 3 and Supplementary Figure S6. Monotherapies, EP or IR or the injection of either plasmid showed no significant effect on tumor growth compared with control untreated tumors. Furthermore, partially combined treatments of

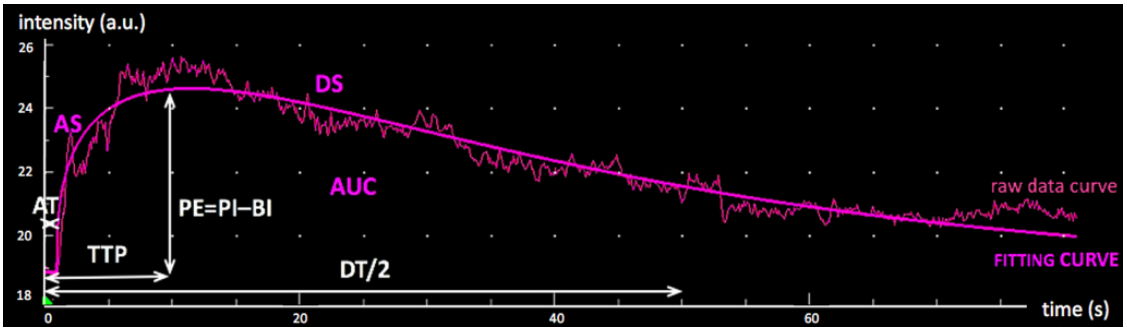

Fig. 1. CEUS perfusion curve with a schematic representation of the dynamic parameters. Raw data and fitting curves are displayed by the built-in software of the M9 ultrasound device (Mindray). Peak enhancement (PE) is the difference between peak (PI) and Base Intensity (BI). Arrival Time (AT) is the time after contrast injection until the contrast agent appears. Time to peak (TTP) is the time at which the contrast intensity reaches a peak value. Descend Time to one-half (DT/2) is the time when the intensity is one-half the value of the peak intensity. Ascending and dDescending Slope (AS and DS) refer to slope coefficients. Area Under the Curve (AUC) is the area under the perfusion curve.

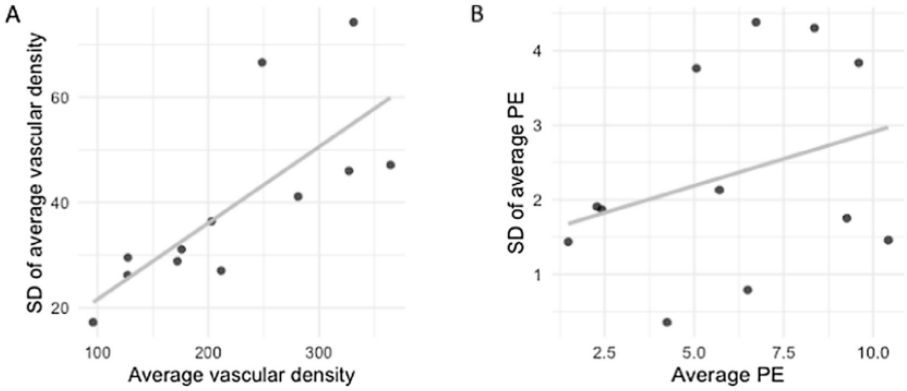

Fig. 2. Bland-Altman Plots of the means and standard deviations of vascular density (A) and CEUS peak enhancement (PE) at day 6 for all treatment groups. The gray lines are for visual inspection only.

Table 3
Antitumor response of B16F10 melanoma after different treatment modalities.

Group	n	DT (days)		GD (days)		CR		resistant to SC	
		Mean	SE	Mean	SE	n	%	n	%
CTRL	6	1.3[#]	0.2	/	/	0	0	0	0
pC	6	2.6[#]	0.3	1.3[#]	0.3	0	0	0	0
pMCAM	6	2.5[#]	0.5	1.2[#]	0.5	0	0	0	0
EP	6	3.6[#]	1.6	2.3[#]	1.6	0	0	0	0
IR	6	1.4[#]	0.3	0.1[#]	0.3	0	0	0	0
GET pC	6	34.3[*,#]	0.8	33.0[*,#]	0.8	1	20.0	0	0
GET pMCAM	7	37.1[*]	20.7	35.8[*]	20.7	1	14.3	1	100
pC IR	6	5.8[*,#]	1.7	4.5[*,#]	1.7	0	0	0	0
pMCAM IR	6	23.0[*,#]	14.7	21.6[*,#]	14.7	1	16.7	1	100
EP IR	6	8.5[*,#]	2.3	7.2[*,#]	2.3	0	0	0	0
GET pC IR	5	74.2[*]	23.8	72.9[*]	23.8	2	40.0	2	100
GET pMCAM IR	7	80.4[*]	19.6	79.1[*]	19.6	3	42.9	3	100

LEGEND: CR = complete response, tumor-free animal at day 100; CTRL = untreated control; DT = tumor doubling time; EP = application of electrical pulses; GD = tumor growth delay (=$DT_{tumor\ in\ experimental\ group}$–mean of DT_{ctrl}); GET = gene electrotransfer; IR = single-dose irradiation, 15 Gy; n = number of all mice in group; pC = intratumoral injection of control plasmid; pMCAM = intratumoral injection of plasmid DNA encoding shRNA for MCAM; SC = mice resistant to secondary challenge; SE = standard error of arithmetic mean; / = not applicable.
[*] $p < 0.05$ = statistically significant mean difference compared to control.
[#] $p < 0.05$ = statistically significant mean difference compared to GET pMCAM IR, GET pC IR.

tumors (EP IR, GET pMCAM, GET pC, pMCAM IR, pC IR, GET pMCAM, GET pC) significantly prolonged tumor growth delay compared with the control tumors. Additionally, tumor cures were obtained in the controls of GET pMCAM, GET pC and pMCAM IR, ranging from 14% to 20% (Table 3). When a single dose of IR was combined with GET pMCAM or GET pC, pronounced radiosensitization was observed compared with the control, monotherapy, EP IR, pMCAM IR, and pC IR groups, resulting in a significant reduction of tumor growth (43%) and a tumor cure rate of 40%; additionally, the tumors were resistant to secondary challenge (Table 3).

Irradiation alone or combined treatments resulted in hair loss, but no skin desquamation was observed. Additionally, no systemic toxicity was observed after the treatments.

3.4. CEUS PE capacity to predict antitumor response to treatment

To explore the capacity of CEUS to predict tumor outcome, we compared CEUS PE values and growth parameters (CR, DT, GD, resistance to secondary challenge). Among the mice with CEUS results (n = 49), 8 were complete responders: three in the GET pMCAM IR group, one in the GET pMCAM group, one in the GET pC group, two in the GET pC IR group, and one in the pMCAM IR group (Table 3).

The comparisons of mean PE values between the CR and non-CR groups demonstrated that the mean PE values were significantly lower in the CR group from day 5 (Supplementary Table S1). The association between the daily CEUS PE parameter and logarithmically transformed DT is explored graphically in Fig. 3. Note that the mice with the most advanced tumors (with the shortest DT values) were excluded from the analyses early (as shown on days 6 and 7 by the lack of dots with small DT values); the CR mice had DT ceiled to 100. The results of linear regression analyses for each day of measurement associating PE with logarithmically transformed DT are presented in Supplementary Table S2. Negative regression coefficients suggest that the larger is the PE of a mouse the lower is the expected (log) DT. Similar findings were observed as above, when evaluating the association with CR.

An additional attempt to model a possible association of PE measurements over time with the status CR or non-CR by mixed-effects logistic regression showed no statistically significant predictors. This finding can be partially attributed to the lack of strength in detecting a difference in the early days and bias introduced in the sample in the later days. However, the trends for our data set stayed the same as in the simpler analyses above—i.e., the larger is the PE, the less probable is the CR at a fixed day.

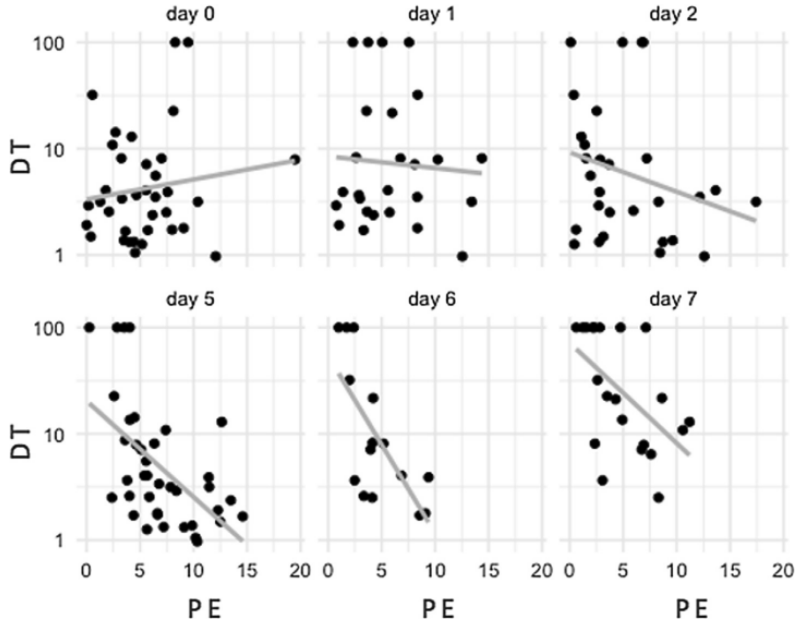

Fig. 3. Association between CEUS peak enhancement (PE) and logarithmically transformed doubling time (DT). The lines serve as visual inspection.

4. Discussion

In the current study, among the CEUS parameters only PE was an indicator of treatment response in the murine model and correlated with mean vascular density in histological analyses of treated tumors. The mean PE values were significantly lower in the tumors that responded to therapy with CR. In addition, PE values showed a trend toward correlation with antitumor efficacy (the greater the PE value of a mouse, the lower the expected DT value and a lower probability of CR). Thus, this study confirms that CEUS could be used to evaluate perfusion and treatment response in mice treated with vascular targeted therapies that have anti-angiogenic and anti-vascular activities [1,35].

Tumor perfusion can be assessed by various methods investigating tumor vasculature and tumor perfusion, either invasively (e.g., histological analyses) or less invasively (e.g., contrast-enhanced imaging). CEUS is a simple method of perfusion assessment, and our data show that CEUS evaluation agrees with the histological analyses of tumor blood vessels abundance, a finding that is consistent with other studies, both preclinical [2–4] and clinical [6–9]. The significantly lower PE values for CR tumors and the tendency for CEUS results to correlate with treatment outcome in our study are consistent with preclinical murine [3,4] and human clinical studies [10–13] in which CEUS results are a useful predictor of antiangiogenic treatment. However, in studies of canine tumors treated with radiotherapy, CEUS was not found to be predictive [36,37]. The canine studies included a small number of dogs with different tumor types treated with radiotherapy, and the reason why CEUS was not predictive may also be due to the different mechanism of antitumor action between radiotherapy alone and in combination with EP–based treatment. Radiation therapy is more efficient in areas with increased perfusion because hypoxic cells are resistant to treatment. Furthermore, only combined therapy is an antiangiogenic treatment [18–20].

In human clinical studies [10–13], different CEUS parameters (AUC, TTP, AS, and PE) showed trends toward a correlation with survival. In our study, the CEUS parameter that correlated with histology and tumor growth was PE, a parameter that describes the blood volume of the investigated area. On the other hand, parameters that describe the blood flow rate did not show associations with tumor growth and histological results. Possible reasons for this lack of correlation could be the retroorbital injections of contrast without the use of an infusion pump and different planes of anesthesia. The latter influences physiologic parameters such as the systemic blood pressure, body temperature, heart rate, cardiac contractility, and others, which all affect tissue perfusion, which depends on cardiac, vascular, microcirculatory, and humoral factors. Retroorbital injections of contrast agents were shown to be comparable with tail injections in mice [38]; however, in that study, contrast agents were administered via a catheter; in our study, the operator inserted the needle into the retro-orbital sinus [32]. Furthermore, the rate of contrast injection was less unified than that using an infusion pump.

The tumor vasculature differs from the normal vasculature; the former is immature with a poorly developed discontinuous endothelial-cell lining, and the basement membrane is irregular and structurally abnormal. Tumor vascular networks are chaotic, and the flow through many of the tumor vessels is only intermittent [1,35,39]. These characteristics of tumor vessels contribute to spatial and temporal heterogeneity in the tumor blood flow [39], as observed in our study; the tumors were commonly heterogeneously perfused, and the perfusion of the same tumor was different on different days. Regions of the tumor that are poorly perfused are radioresistant; therefore, combined treatments with vascular targeted therapies aiming to normalize the tumor vasculature are intensively investigated. In our study, the CEUS results and histological vascular density showed that GET of plasmid DNA encoding shRNA for MCAM and GET of control plasmid both exhibit radiosensitizing effects. Electric pulses of a voltage higher than 560 V induce a local blood flow modifying effect or ‘vascular lock’, which is characterized by vasoconstriction and increased wall permeabilization of small blood vessels, resulting in tissue

edema [40–50]. The duration and strength of vascular lock depend on EP (number, amplitude, and duration), type of tissue (healthy versus tumor cells), and use of chemotherapeutics [43–46]. Blood flow is slowly restored after EP; in 24 h, it approaches the flow before EP [45–49]. CEUS has been used to describe decreased perfusion after electrochemotherapy (ECT) of human hepatic tumors [51] and after the ECT of healthy porcine liver [52]. However, these immediate effects after EP were not evident in this study because CEUS was performed on each day before the therapies to evaluate the vascular effects of 24-hour combined treatment.

The reasons for the first major limitation of this study—the small number of animals and measurements—were the principle of 3Rs (Reduce, Reuse and Recycle) and exclusion of measurements due to the unpredictable contrast stability. The chemical and physical stabilities of the Sonovue microbubble dispersion last for 6 h, and ultrasound contrast agents are easily destroyed in small-gauge needles [53]. Both reasons for the first major limitation are also reasons for the second major limitation of this study, which was that not all of the measurements of vascular density measurements were obtained from the same mice that were subjected to the PE measurements; therefore, none of the standard correlation measures could be reported. However, the mice were inbred syngenic animals, indicating more genetic uniformity and pathophysiological similarity among individuals [54]. In the treatment groups using therapeutic plasmid—i.e., GET pMCAM and GET pMCAM IR—vascular density and PE were determined in the same mice. The scatterplot of these measurements and Pearson's correlation are reported in the Supplementary Information (Supplementary Figure S7).

5. Conclusion

CEUS results for tumors correlated with histological analysis of blood vessel density, demonstrating they could be a valuable method of tissue perfusion assessment. Furthermore, CEUS results for tumors that responded to therapy with CR were significantly different from those without CR and CEUS results showed a trend toward correlation with antitumor effectiveness. In a patient evaluation, simple methods such as CEUS, which provide readily available data during therapy and can be repeated frequently are advantageous because they could provide beneficial prognostic and predictive information, assisting the clinician in deciding whether the repetition of therapy is necessary for the response to therapy. Had the number of mice in this study been larger, the observed tendency of CEUS results to correlate with antitumor efficacy could have been more categorical. The potential value of CEUS as a technique to determine prognosis and predict outcome of neoplastic disease warrants further studies in scientific research and clinical practice to confirm whether it can predict the disease outcome and assist in the planning of repeated therapy or different treatment combinations in individual patients.

Declaration of Competing Interest

The authors declare that they have no known competing financial interests or personal relationships that could have appeared to influence the work reported in this paper.

Acknowledgments

The authors thank Miha Melinec and Tone Jamnik (DIPROS d.o.o.) for their assistance and ultrasonographic machines that enabled contrast studies. Language editing services for this manuscript were provided by American Journal Experts.

Funding

Furthermore, we acknowledge the financial support of the Slovenian Research Agency (research program No. P3-003 and No. P4-0053). The funder had no role in the study design, data collection and analysis, decision to publish, or preparation of the manuscript.

Authors' contributions

Study concepts/study design, S.K.B., D.P., M.C., G.S.; data acquisition, M.B., S.K.B, M.Bo.; data analysis/interpretation, M.B., N.B., D. P., N.K., S.K.B,; manuscript drafting, M.B., N.B., D.P., S.K.B; manuscript revision for important intellectual content, M.C., G.S., S.K.B, D.P.; approval of the final submitted manuscript, all authors; and manuscript editing, all authors.

References

[1] G.M. Tozer, C. Kanthou, B.C. Baguley, Disrupting tumour blood vessels, Nat. Rev. Cancer 5 (6) (2005) 423–435, https://doi.org/10.1038/nrc1628.
[2] E.F. Donnelly, L. Geng, W.E. Wojcicki, A.C. Fleischer, D.E. Hallahan, Quantified power Doppler US of tumor blood flow correlates with microscopic quantification of tumor blood vessels, Radiol 219 (1) (2001) 166–170, https://doi.org/10.1148/radiology.219.1.r01ap38166.
[3] J.H. Zhou, L.H. Cao, J.B. Liu, W. Zheng, M. Liu, R.Z. Luo, F. Han, A. Li, Quantitative assessment of tumor blood flow in mice after treatment with different doses of an antiangiogenic agent with contrast-enhanced destruction-replenishment US, Radiology 259 (2) (2011) 406–413, https://doi.org/10.1148/radiol.10101339.
[4] J.H. Zhou, L.H. Cao, W. Zheng, M. Liu, F. Han, A.H. Li, Contrast-enhanced gray-scale ultrasound for quantitative evaluation of tumor response to chemotherapy: preliminary results with a mouse hepatoma model, AJR Am. J. Roentgenol. 196 (1) (2011) W13–7, https://doi.org/10.2214/AJR.10.4734.
[5] K.J. Nierman, A.C. Fleischer, J. Huamani, T.E. Yankeelov, D.W. Kim, W.D. Wilson, D.E. Hallahan, Measuring tumor perfusion in control and treated murine tumors: correlation of microbubble contrast-enhanced sonography to dynamic contrast-enhanced magnetic resonance imaging and fluorodeoxyglucose positron emission tomography, J. Ultrasound Med. 26 (6) (2007) 749–756, https://doi.org/10.7863/jum.2007.26.6.749.
[6] J.P. Sedelaar, G.J. van Leenders, C.A. Hulsbergen-van de Kaa, H.G. van der Poel, J. A. van der Laak, F.M. Debruyne, H. Wijkstra, J.J. de la Rosette, Microvessel density: correlation between contrast ultrasonography and histology of prostate cancer, Eur. Urol. 40 (3) (2001) 285–293, https://doi.org/10.1159/000049788.
[7] X. Leng, G. Huang, F. Ma, L. Yao, Regional Contrast-Enhanced Ultrasonography (CEUS) characteristics of breast cancer and correlation with Microvessel Density (MVD), Med. Sci. Monit. 23 (2017) 3428–3436, https://doi.org/10.12659/MSM.901734.
[8] X. Li, Y. Li, Y. Zhu, L. Fu, P. Liu, Association between enhancement patterns and parameters of contrast-enhanced ultrasound and microvessel distribution in breast cancer, Oncol Lett 15 (4) (2018) 5643–5649, https://doi.org/10.3892/ol.2018.8078.
[9] S. Ohlerth, M. Wergin, C.R. Bley, F. Del Chicca, D. Laluhova, B. Hauser, M. Roos, B. Kaser-Hotz, Correlation of quantified contrast-enhanced power Doppler ultrasonography with immunofluorescent analysis of microvessel density in spontaneous canine tumours, Vet. J. 183 (1) (2010) 58–62, https://doi.org/10.1016/j.tvjl.2008.08.026.
[10] N. Lassau, S. Koscielny, L. Albiges, L. Chami, B. Benatsou, M. Chebil, A. Roche, B. J. Escudier, Metastatic Renal Cell Carcinoma Treated with Sunitinib: Early Evaluation of Treatment Response Using Dynamic Contrast-Enhanced Ultrasonography, Clin Canc Res 16 (4) (2010) 1216–1225, https://doi.org/10.1158/1078-0432.CCR-09-2175.
[11] N. Lassau, S. Koscielny, L. Chami, M. Chebil, B. Benatsou, A. Roche, M. Ducreux, D. Malka, V. Boige, Advanced hepatocellular carcinoma: early evaluation of response to bevacizumab therapy at dynamic contrast-enhanced US with quantification – preliminary results, Radiology 258 (1) (2011) 291–300, https://doi.org/10.1148/radiol.10091870.
[12] N. Lassau, J. Bonastre, M. Kind, V. Vilgrain, J. Lacroix, M. Cuinet, S. Taieb, R. Aziza, A. Sarran, C. Labbe-Devilliers, B. Gallix, O. Lucidarme, Y. Ptak, L. Rocher, L.M. Caquot, S. Chagnon, D. Marion, A. Luciani, S. Feutray, J. Uzan-Augui, B. Coiffier, B. Benastou, S. Koscielny, Validation of dynamic contrast-enhanced ultrasound in predicting outcomes of antiangiogenic therapy for solid tumors: the French multicenter support for innovative and expensive techniques study, Invest. Radiol. 49 (12) (2014) 794–800, https://doi.org/10.1097/RLI.0000000000000085.
[13] N. Lassau, B. Coiffier, M. Kind, V. Vilgrain, J. Lacroix, M. Cuinet, S. Taieb, R. Aziza, A. Sarran, C. Labbe-Devilliers, B. Gallix, O. Lucidarme, Y. Ptak, L. Rocher, L.M. Caquot, S. Chagnon, D. Marion, A. Luciani, S. Feutray, J. Uzan-Augui, B. Benatsou, J. Bonastre, S. Koscielny, Selection of an early biomarker for vascular

normalization using dynamic contrast-enhanced ultrasonography to predict outcomes of metastatic patients treated with bevacizumab, Ann. Oncol. 27 (10) (2016) 1922–1928, https://doi.org/10.1093/annonc/mdw280.
[14] M. Cemazar, T. Jarm, G. Sersa, Cancer electrogene therapy with interleukin-12, Curr Gene Ther 10 (4) (2010) 300–311, https://doi.org/10.2174/156652310791823425.
[15] M. Cemazar, J. Ambrozic Avgustin, D. Pavlin, G. Sersa, A. Poli, A. Krhac Levacic, N. Tesic, U. Lampreht Tratar, M. Rak, N. Tozon, Efficacy and safety of electrochemotherapy combined with peritumoral IL-12 gene electrotransfer of canine mast cell tumours, Vet. Comp. Oncol. 15 (2) (2017) 641–654, https://doi.org/10.1111/vco.2017.15.issue-210.1111/vco.12208.
[16] A.I. Daud, R. DeConti, S. Andrews, P. Urbas, A.I. Riker, V.K. Sondak, P.N. Munster, D.M. Sullivan, K.E. Ugen, J.L. Messina, R. Heller, Phase I trial of interleukin-12 plasmid electroporation in patients with metastatic melanoma, J Clin Oncol 26 (36) (2008) 5896–5903, https://doi.org/10.1200/JCO.2007.15.6794.
[17] L. Prosen, B. Markelc, T. Dolinsek, B. Music, M. Cemazar, G. Sersa, Mcam silencing with RNA interference using magnetofection has antitumor effect in murine melanoma, Mol. Ther. Nucleic Acids 3 (2014) e205, https://doi.org/10.1038/mtna.2014.56.
[18] S. Kranjc Brezar, V. Mrak, M. Bosnjak, M. Savarin, G. Sersa, M. Cemazar, Intratumoral gene electrotransfer of plasmid DNA encoding shRNA against melanoma cell adhesion molecule radiosensitizes tumors by antivascular effects and activation effects and activation of an immune response, Vaccines 135 (2020), https://doi.org/10.3390/vaccines8010135.
[19] M. Savarin, U. Kamensek, M. Cemazar, R. Heller, G. Sersa, Electrotransfer of plasmid DNA radiosensitizes B16F10 tumors through activation of immune response, Radiol. Oncol. 51 (2017) 30–39, https://doi.org/10.1515/raon-2017-0011.
[20] G. Tevz, S. Kranjc, M. Cemazar, U. Kamensek, A. Coer, M. Krzan, S. Vidic, D. Pavlin, G. Sersa, Controlled systemic release of interleukin-12 after gene electrotransfer to muscle for cancer gene therapy alone or in combination with ionizing radiation in murine sarcomas, J. Gene. Med. 11 (12) (2009) 1125–1137, https://doi.org/10.1002/jgm.v11:1210.1002/jgm.1403.
[21] A. Sedlar, S. Kranjc, T. Dolinšek, M. Čemažar, A. Coer, G. Serša, Radiosensitizing effect of intratumoral interleukin-12 gene electrotransfer in murine sarcoma, BMC Cancer 13 (2013) 38, https://doi.org/10.1186/1471-2407-13-38.
[22] M. Stimac, U. Kamensek, M. Cemazar, S. Kranjc, A. Coer, G. Sersa, Tumor radiosensitization by gene therapy against endoglin, Cancer Gene Ther 23 (7) (2016) 214–220, https://doi.org/10.1038/cgt.2016.20.
[23] M. Savarin, A. Prevc, M. Rzek, M. Bosnjak, I. Vojvodic, M. Cemazar, T. Jarm, G. Sersa, Intravital monitoring of vasculature after targeted gene therapy alone or combined with tumor irradiation, Technol Cancer Res Treat 17 (2) (2018), https://doi.org/10.1177/1533033818784208.
[24] M. Bosnjak, T. Jesenko, U. Kamensek, G. Sersa, J. Lavrencak, L. Heller, M. Cemazar, Electrotransfer of different control plasmids elicits antitumor effectiveness in B16.F10 melanoma, Cancers 10 (2) (2018) 37, https://doi.org/10.3390/cancers10020037.
[25] L.C. Heller, R. Heller, Electroporation gene therapy preclinical and clinical trials for melanoma, Curr Gene Ther 10 (4) (2010) 312–317, https://doi.org/10.2174/156652310791823489.
[26] L. Heller, V. Todorovic, M. Cemazar, Electrotransfer of single-stranded or double-stranded DNA induces complete regression of palpable B16.F10 mouse melanomas, Cancer Gene Ther. 20 (12) (2013) 695–700, https://doi.org/10.1038/cgt.2013.71.
[27] S. Kranjc, M. Cemazar, A. Grosel, M. Sentjurc, G. Sersa, Radiosensitising effect of electrochemotherapy with bleomycin in LPB sarcoma cells and tumors in mice, BMC Cancer 5 (2005) 115–123, https://doi.org/10.1186/1471-2407-5-115.
[28] S. Kranjc, G. Tevz, U. Kamensek, S. Vidic, M. Cemazar, G. Sersa, Radiosensitizing effect of electrochemotherapy in a fractionated radiation regimen in radiosensitive murine sarcoma and radioresistant adenocarcinoma tumor model, Radiat. Res. 172 (6) (2009) 677–685.
[29] C. Dietrich, M. Averkiou, J.-M. Correas, N. Lassau, E. Leen, F. Piscaglia, An EFSUMB introduction into Dynamic Contrast- Enhanced Ultrasound (DCE-US) for quantification of tumour perfusion, Ultraschall Med. 33 (04) (2012) 344–351, https://doi.org/10.1055/s-0032-1313026.
[30] F. Piscaglia, C. Nolsoe, C.F. Dietrich, D.O. Cosgrove, O.H. Gilja, M. Bachmann Nielsen, T. Albrecht, L. Barozzi, M. Bertolotto, O. Catalano, M. Claudon, D.A. Clevert, J.M. Correas, M. D'Onofrio, F.M. Drudu, Y. Eyding, M. Giovannini, M. Hocke, A. Ignee, E.M. Jung, A.S. Klauser, N. Lasssau, E. Leen, G. Mathis, A. Saftoiu, G. Seidel, P.S. Sidhu, G. ter Haar, D. Timmerman, H.P. Weskott, The EFSUMB Guidelines and Recommendations on the Clinical Practice of Contrast Enhanced Ultrasound (CEUS): update 2011 on non-hepatic applications, Ultraschall Med. 33 (1) (2012) 33–59, https://doi.org/10.1055/s-0031-1281676.
[31] M. Westwood, M. Joore, J. Grutters, K. Redekop, N. Armstrong, K. Lee, V. Gloy, H. Raatz, K. Misso, J. Severens, J. Kleijnen, Contrast-enhanced ultrasound using SonoVue® (sulphur hexafluoride microbubbles) compared with contrast-enhanced computed tomography and contrast-enhanced magnetic resonance imaging for the characterisation of focal liver lesions and detection of liver metastases: a systematic review and cost-effectiveness analysis, Health Technol. Assess. 17 (16) (2013) 1–243, https://doi.org/10.3310/hta17160.
[32] T. Yardeni, M. Eckhaus, H.D. Morris, M. Huizing, S. Hoogstraten-Miller, Retro-orbital injections in mice, Lab Anim (NY) 40 (5) (2011) 155–160, https://doi.org/10.1038/laban0511-155.
[33] Demidenko E. Three endpoints of in vivo tumour radiobiology and their statistical estimation. Int J Radiat Biol 2010; 86(2): 164–73. doi: 10.3109/09553000903419304.
[34] R Core Team (2020). R: A language and environment for statistical computing. R Foundation for Statistical Computing, Vienna, Austria. https://www.R-project.org [15th June 2020].
[35] R.K. Jain, Normalization of tumor vasculature: an emerging concept in antiangiogenic therapy, Science 307 (5706) (2005) 58–62, https://doi.org/10.1126/science.1104819.
[36] C. Rohrer Bley, D. Laluhova, M. Roos, B. Kaser-Hotz, S. Ohlerth, Correlation of pretreatment polarographically measured oxygen pressures with quantified contrast-enhanced power doppler ultrasonography in spontaneous canine tumors and their impact on outcome after radiation therapyKorrelation des polarographisch gemessenen Sauerstoffdrucks mit quantifiziertem, kontrastverstärktem Power-Doppler-Ultraschall bei spontanen kaninen Tumoren und deren Einfluss auf das Tumorverhalten nach Strahlentherapie, Strahlenther. Onkol. 185 (11) (2009) 756–762, https://doi.org/10.1007/s00066-009-1988-6.
[37] S. Ohlerth, C.R. Bley, D. Laluhová, M. Roos, B. Kaser-Hotz, Assessment of changes in vascularity and blood volume in canine sarcomas and squamous cell carcinomas during fractionated radiation therapy using quantified contrast-enhanced power Doppler ultrasonography: a preliminary study, Vet. J. 186 (1) (2010) 58–63, https://doi.org/10.1016/j.tvjl.2009.07.006.
[38] F. Wang, M. Nojima, Y. Inoue, K. Ohtomo, S. Kiryu, Assessment of MRI contrast agent kinetics via retro-orbital injection in mice: comparison with tail vein injection, PLoS One 10 (6) (2015), https://doi.org/10.1371/journal.pone.0129326 e0129326.
[39] D.W. Siemann, The unique characteristics of tumor vasculature and preclinical evidence for its selective disruption by tumor-vascular disrupting agents, Cancer Treat. Rev. 37 (1) (2011) 63–74, https://doi.org/10.1016/j.ctrv.2010.05.001.
[40] G. Sersa, M. Cemazar, D. Miklavcic, DJ. Chaplin, Tumor blood flow modifying effect of electrochemotherapy with bleomycin, Anticancer Res 19 (1999) 4017–4022, https://doi.org/10.1007/978-3-540-73044-6 152.
[41] G. Sersa, M. Cemazar, C.S. Parkins, D.J. Chaplin, Tumour blood flow changes induced by application of electric pulses, Eur J Cancer 35 (1999) 672–677, https://doi.org/10.1016/S0959-8049(98)00426-2.
[42] J. Gehl, T. Skovsgaard, L.M. Mir, Vascular reactions to in vivo electroporation: characterization and consequences for drug and gene delivery, BBA 1569 (1–3) (2002) 51–58, https://doi.org/10.1016/s0304-4165(01)00233-1.
[43] G. Sersa, M. Cemazar, D. Miklavcic, Tumor blood flow modifying effects of electrochemotherapy: a potential vascular targeted mechanism, Radiol Oncol 37 (2003) 43–48, https://doi.org/10.1007/978-3-540-73044-6_153.
[44] G. Sersa, T. Jarm, T. Kotnik, A. Coer, M. Podkrajsek, M. Sentjurc, D. Miklavcic, M. Kadivec, S. Kranjc, A. Secerov, M. Cemazar, Vascular disrupting action of electroporation and electrochemotherapy with bleomycin in murine sarcoma, Br. J. Cancer 98 (2) (2008) 388–398, https://doi.org/10.1038/sj.bjc.6604168.
[45] T. Jarm, M. Cemazar, D. Miklavcic, G. Sersa, Antivascular effects of electrochemotherapy: implications in treatment of bleeding metastases, Expert Rev. Anticancer Ther. 10 (5) (2010) 729–746, https://doi.org/10.1586/era.10.43.
[46] E. Raesi, S.M.P. Firoozabadi, S. Hajizadeh, H. Rajabi, Z.M. Hassan, The effect of high-frequency electric pulses on tumor blood flow in vivo, J. Membrane Biol. 236 (1) (2010) 163–166, https://doi.org/10.1007/s00232-010-9288-8.
[47] E. Bellard, B. Markelc, S. Pelofy, F. Le Guerroué, G. Sersa, J. Teissié, M. Cemazar, M. Golzio, Intravital microscopy at the single vessel level brings new insights of vascular modification mechanisms induced by electropermeabilization, J. Control. Release 163 (3) (2012) 396–403, https://doi.org/10.1016/j.jconrel.2012.09.010.
[48] B. Markelc, E. Bellard, G. Serša, S. Pelofy, J. Teissie, A. Coer, M. Golzio, M. Cemazar, In vivo molecular imaging and histological analysis of changes induced by electric pulses used for plasmid DNA electrotransfer to the skin: a study in a dorsal window chamber in mice, J. Membr. Biol. 245 (9) (2012) 545–554, https://doi.org/10.1007/s00232-012-9435-5.
[49] B. Markelc, G. Sersa, M. Cemazar, Differential mechanisms associated with vascular disrupting action of electrochemotherapy: intravital microscopy on the level of single normal and tumor blood vessels, PLoS One 8 (2013), https://doi.org/10.1371/journal.pone.0059557 e59557.
[50] B. Markelc, E. Bellard, G. Sersa, T. Jesenko, S. Pelofy, J. Teissie, R. Frangez, M.P. Rols, M. Cemazar, M. Golzio, Increased permeability of blood vessels after reversible electroporation is facilitated by alterations in endothelial cell-to-cell junctions, J. Control. Release 276 (2018) 30–41, https://doi.org/10.1016/j.jconrel.2018.02.032.
[51] N. Boc, I. Edhemovic, B. Kos, M.M. Music, E. Brecelj, B. Trotovsek, M. Bosnjak, M. Djokic, D. Miklavcic, M. Cemazar, G. Sersa, Ultrasonographic changes in the liver tumors as indicators of adequate tumor coverage with electric field for effective electrochemotherapy, Radiol Oncol 52 (2018) 383–391, https://doi.org/10.2478/raon-2018-0041.
[52] M. Brloznik, N. Boc, G. Sersa, J. Zmuc, G. Gasljevic, A. Seliskar, R. Dezman, I. Edhemovic, N. Milevoj, T. Plavec, V. Erjavec, D. Pavlin, M. Bosnjak, E. Brecelj, U. Lampreht Tratar, B. Kos, J. Izlakar, M. Stukelj, D. Miklavcic, M. Cemazar, Radiological findings of porcine liver after electrochemotherapy with bleomycin, Radiol. Oncol. 53 (4) (2019) 415–426.
[53] D.B. Erlichman, A. Weiss, M. Koenigsberg, M.W. Stein, Contrast enhanced ultrasound: A review of radiology applications, Clin. Imaging 60 (2) (2019) 209–215, https://doi.org/10.1016/j.clinimag.2019.12.013.

[54] E. Costa, T. Ferreira-Gonçalves, G. Chasqueira, A.S. Cabrita, I.V. Figueiredo, R.C. Pinto, Experimental models as refined translational tools for breast cancer research, Sci. Pharm. 88 (2020) 32, https://doi.org/10.3390/scipharm88030032.

Maja Brloznik graduated as a Doctor of Veterinary Medicine and received her M.Sc. from the University of Ljubljana. She graduated at the University of Luxembourg as European Master of Small Animal Veterinary Medicine in 2018. She works in cardiology and diagnostic ultrasound at Small Animal Clinic of Veterinary Faculty of the University in Ljubljana and at International Veterinary Services in Asia. She is currently enrolled in PhD studies and her main research interests are radiologic methods as predictive factors of electrochemotherapy and gene therapy of murine and spontaneous canine tumors.

Nina Boc graduated as a Medical Doctor from the Medical faculty of University of Ljubljana. She earned her specialist degree in Radiology with honour in 2010. She is currently the head of the Radiology Department of Institute of Oncology in Ljubljana. Her main research interest is use of radiologic methods in electrochemotherapy. She is involved in various multicentre clinical studies.

Maja Cemazar received her Ph.D. in Basic Medical Sciences from the Medical Faculty, the University of Ljubljana in 1998. She works at the Department of Experimental Oncology, Institute of Oncology Ljubljana, and teaches at the Faculty of Health Sciences, University of Primorska, Slovenia. Her main research interests are in the field of gene electrotransfer employing plasmid DNA encoding different immunomodulatory and antiangiogenic therapeutic genes. In 2006 she received the Award of the Republic of Slovenia for important achievements in scientific research and development in the field of experimental oncology.

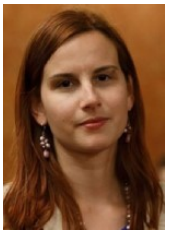

Masa Bosnjak received her Ph.D. in Basic Medical Sciences from the Medical Faculty, the University of Ljubljana in 2015. She is employed at the Institute of Oncology Ljubljana at the Department of Experimental Oncology. Her main research interest is *in vitro* and *in vivo* preclinical oncology focused on delivery of drug and genes to the cells and tumors with electrochemotherapy and gene electrotransfer.

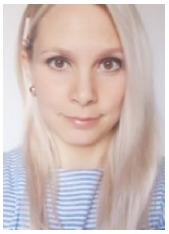

Monika Savarin is a Ph.D. in Basic Medical Sciences, and since 2012 employed at the Department of Experimental Oncology, Institute of Oncology Ljubljana. Currently, her main focus is on her Post Doc project, combining radiotherapy and gene therapy for modulating tumor blood vessels. She is also involved in other preclinical studies, focusing on electroporation, immunohistology and vascular targeting genes.

Natasa Kejzar, Ph.D. in Statistics, is employed at the Institute for Biostatistics and Medical Informatics, Faculty of Medicine, University of Ljubljana as an assistant professor and researcher. Her research is in biostatistical methodology, more precisely in clustering, classification and measures of explained variation for different statistical models

Gregor Sersa graduated from the Biotechnical Faculty at theUniversity of Ljubljana in 19 78, where he is currently a professor of molecular biology. He is employed at the Institute of Oncology in Ljubljana as a head of the Department of Experimental Oncology. His specific field of interest is the effect of the electric field on tumor cells and tumors as drug and gene delivery system in different therapeutic approaches. Besides experimental work, he is actively involved in the education of undergraduate and postgraduate students at the University of Ljubljana.

Darja Pavlin graduated from Veterinary faculty at University of Ljubljana in 2000 and obtained her PhD in the field of gene therapy of canine tumors. At the moment she is employed at Clinic for companion animals at Veterinary faculty Ljubljana as an assistant professor, involved in clinical work, research and as a lecturer in different undergraduate programs.

Simona Kranjc, Ph.D. in Basic Medical Sciences, is employed at the Department of Experimental Oncology, Institute of Oncology Ljubljana since 1998. Her main interest of research is preclinical oncology, *in vitro* and *in vivo*. Precisely, she is experienced in research of tumor biology, radiotherapy, electrochemotherapy, gene electrotransfer with different antiangiogenic and immunomodulatory targets, three-dimensional cultures, testing of new drugs and investigating of new gene and drug delivery methods.

2.3 Ovrednotenje tumorske perfuzije z dinamično ultrazvočno kontrastno preiskavo kot prediktivnega dejavnika razvoja mišjih melanomov, zdravljenih z elektrokemoterapijo in genskim elektroprenosom plazmidne DNA z zapisom za mišji interlevkin-12

Tumor perfusion evaluation using dynamic contrast-enhanced ultrasound after electrochemotherapy and IL-12 plasmid electrotransfer in murine melanoma

Maja Brložnik,[1] Nina Boc,[2] Maja Čemažar,[2,3] Gregor Serša,[2,4] Maša Bošnjak,[2]
Simona Kranjc Brezar,[2,5*] Darja Pavlin.[1*]

[1] Univerza v Ljubljani, Veterinarska fakulteta
[2] Onkološki inštitut Ljubljana
[3] Univerza na Primorskem, Fakulteta za vede o zdravju
[4] Univerza v Ljubljani, Zdravstvena fakulteta
[5] Univerza v Ljubljani, Medicinska fakulteta

* vodilni avtorici: Simona Kranjc Brezar in Darja Pavlin

Sci Rep 2021; 11(1):m13446. doi: 10.1038/s41598-021-92820-w.

Izvleček

EKT z BLM je učinkovito protitumorsko zdravljenje, ki se že uporablja v klinični onkologiji. Vendar sama EKT še vedno velja za lokalno protitumorsko terapijo, ker ne more povzročiti sistemske imunosti. Zdravljenje EKT z adjuvantnim GEP pIL-12 ima sistemski učinek na netretirane tumorje oziroma oddaljene metastaze. Čeprav je bila protitumorska učinkovitost obeh terapij samostojno ali v kombinaciji dokazana tako na predkliničnih kot kliničnih poskusih, še vedno manjkajo podatki o prediktorjih učinkovitosti zdravljenja. V naši raziskavi smo ovrednotili rezultate UZ-KS kot prediktivnega dejavnika za EKT z BLM in GEP pIL-12 pri mišjem melanomu. Tumorje melanoma B16F10 pri samicah miši linije C57Bl/6NCrl, smo zdravili z GEP pIL-12 in EKT z BLM. Z UZ-KS smo jih pregledali takoj po terapiji, 6 ur in 1, 3, 7 in 10 dni pozneje. Za preverjanje korelacije med časom podvojitve tumorja in meritvami UZ-KS smo uporabili semilinearne regresijske modele in Bland-Altmanovo analizo. Zdravljene skupine, pri katerih je UZ-KS pokazal zmanjšano perfuzijo tumorja, so imele daljše čase podvojitve volumna tumorja. Potrdili smo, da je imelo povečanje parametra PE, ki odraža relativno količino krvi, prediktivno vrednost za izid terapije: večji PE je bil povezan s krajšim časom podvojitve tumorja. Poleg tega je bila z izidom povezana tudi heterogenost perfuzije: tumorji z bolj heterogeno perfuzijo so imeli hitrejšo rast, torej značilno krajše čase podvojitve. Ta raziskava kaže, da lahko UZ-KS uporabimo kot metodo za napovedovanje učinkovitosti zdravljenja na osnovi elektroporacije.

scientific reports

OPEN

Tumor perfusion evaluation using dynamic contrast-enhanced ultrasound after electrochemotherapy and IL-12 plasmid electrotransfer in murine melanoma

Maja Brloznik[1], Nina Boc[2], Maja Cemazar[2,3], Gregor Sersa[2,4], Masa Bosnjak[2], Simona Kranjc Brezar[2,5]✉ & Darja Pavlin[1]✉

Electrochemotherapy with bleomycin (ECT BLM) is an effective antitumor treatment already used in clinical oncology. However, ECT alone is still considered a local antitumor therapy because it cannot induce systemic immunity. When combined with adjuvant gene electrotransfer of plasmid DNA encoding IL-12 (GET pIL-12), the combined therapy leads to a systemic effect on untreated tumors and distant metastases. Although the antitumor efficacy of both therapies alone or in combination has been demonstrated at both preclinical and clinical levels, data on the predictors of efficacy of the treatments are still lacking. Herein, we evaluated the results of dynamic contrast-enhanced ultrasound (DCE-US) as a predictive factor for ECT BLM and GET pIL-12 in murine melanoma. Melanoma B16F10 tumors grown in female C57Bl/6NCrl mice were treated with GET pIL-12 and ECT BLM. Immediately after therapy, 6 h and 1, 3, 7 and 10 days later, tumors were examined by DCE-US. Statistical analysis was performed to inspect the correlation between tumor doubling time (DT) and DCE-US measurements using semilinear regression models and Bland–Altman plots. Therapeutic groups in which DCE-US showed reduced tumor perfusion had longer tumor DTs. It was confirmed that the DCE-US parameter peak enhancement (PE), reflecting relative blood volume, had predictive value for the outcome of therapy: larger PE correlated with shorter DT. In addition, perfusion heterogeneity was also associated with outcome: tumors that had more heterogeneous perfusion had faster growth, i.e., shorter DTs. This study demonstrates that DCE-US can be used as a method to predict the efficacy of electroporation-based treatment.

Electrochemotherapy with bleomycin (ECT BLM) has been shown to be an effective antitumor treatment in numerous clinical trials[1–6]. It is a local treatment that combines the use of electroporation (EP) and chemotherapeutic agents and has a dual effect on tumor cells and the vasculature, resulting in an antitumor effect in various solid tumors[5–7]. Many studies have indicated the contribution of the immune system to the efficiency of ECT, which induces immunogenic cell death by activating molecular signals called danger-associated molecular patterns (DAMPs) that strengthen the innate immune cells that drive the production of specific antitumor immunity[7–12]. However, ECT alone is unable to induce systemic immunity, whereas ECT in combination with adjuvant gene electrotransfer (GET) results in an 'abscopal effect' on untreated distant metastases[7,8]. Recent preclinical and clinical studies have shown that the effect of ECT can be potentiated by GET using plasmid DNA encoding IL-12 (GET pIL-12)[7,8,10,13–17].

[1]Clinic for Small Animals, Veterinary Faculty, University of Ljubljana, Gerbičeva 60, Ljubljana, Slovenia. [2]Institute of Oncology Ljubljana, Zaloška 2, Ljubljana, Slovenia. [3]Faculty of Health Sciences, University of Primorska, Polje 42, Izola, Slovenia. [4]Faculty of Health Sciences, University of Ljubljana, Zdravstvena 5, Ljubljana, Slovenia. [5]Faculty of Medicine, University of Ljubljana, Vrazov trg 2, Ljubljana, Slovenia. ✉email: skranjc@onko-i.si; darja.pavlin@vf.uni-lj.si

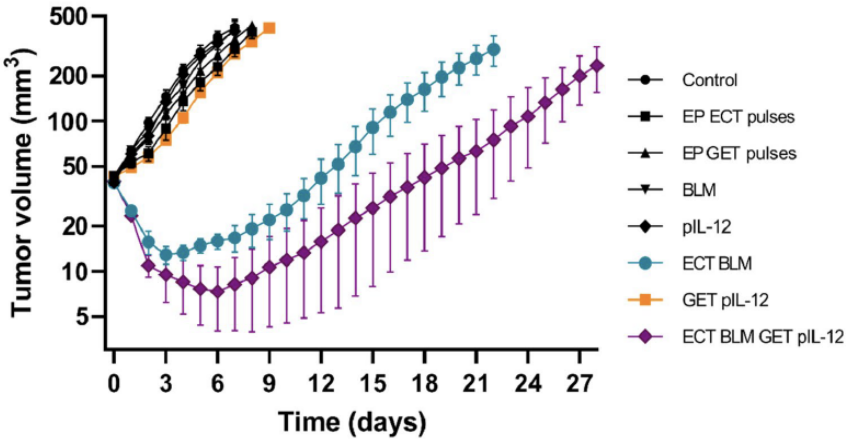

Figure 1. Mean tumor volume in mouse melanoma B16F10 cells treated with electrochemotherapy with bleomycin and gene electrotransfer of plasmid DNA encoding IL-12. Data are presented as the mean and standard error of the mean (SE) (n = 66). BLM = bleomycin, 7.5 µg/mouse; ECT = electrochemotherapy; EP = electric pulses; GET = gene electrotransfer; pIL-12 = plasmid DNA encoding mouse interleukin-12. Note that significant tumor growth delay was observed in the mice treated with ECT BLM and ECT BLM combined with GET pIL-12. In GET pIL-12 and other groups (untreated control and pertinent controls) no antitumor efficiacy was observed.

Based on the results of clinical trials[1–4], ECT BLM has been listed in several national and international guidelines as an effective treatment option for various tumor types in human[5,6,18] and veterinary oncology[19]. Clinical trials using GET pIL-12 have been performed in human[20–22] and veterinary patients[7,13,14,23–25], but standard operating procedures for GET pIL-12 are still pending.

High-amplitude electrical pulses induce a local reduction in blood flow or 'vascular lock' characterized by vasoconstriction and increased wall permeability of small blood vessels[10,26–29]. Furthermore, the vascular effects of EP-based therapies are not only caused by the direct effect of electrical pulses on cells but are further enhanced by the use of chemotherapeutic agents in ECT treatment. The effect on perfusion lasts longer in ECT than in EP alone and longer in tumors than in healthy tissues, which is referred to as the 'vascular disrupting effect'[10,26,29].

Despite the known clinical efficacy of combined treatments of ECT and GET, there is still a lack of data on parameters that could predict outcome of these treatments. One of the possible methods to determine the predictive factors of therapy is dynamic contrast-enhanced ultrasound (DCE-US), a noninvasive method used to assess tissue perfusion at the capillary level, which correlates with histological results of vascular density in preclinical[30–32] and clinical studies[33–36]. DCE-US has been used to predict the efficacy of various antiangiogenic treatments in both human[37–42] and preclinical studies[31].

Current ultrasound contrast agents are gas-filled microbubbles: a relatively insoluble gas core is stabilized within a phospholipid shell that provides relative stability in plasma for several minutes[43]. Microbubbles are 1–3 µm in diameter, smaller than mouse red blood cells, which are approximately 6 µm in diameter. Microbubbles pass freely throughout the pulmonary and systemic circulation, and capillary filling leads to diffuse enhancement of the perfused tissue. To perform DCE-US, contrast-specific software with a low mechanical index (MI) is required to visualize microbubbles without destroying them. Unlike tissue, microbubbles have a nonlinear response when used with a low MI[43,44].

Investigating perfusion is an attractive method for predicting antitumor effects, especially in antiangiogenic treatments, e.g., ECT combined with GET. In combined ECT and GET treatments, it is reasonable to assume that repetition of the therapy is appropriate if the therapy does not result in the expected 'vascular lock' and/or the antiangiogenic effects are not evident in the days after treatment.

This study aimed to evaluate the results of DCE-US, including tumor perfusion heterogeneity, as predictive factors of ECT BLM and GET pIL-12 on murine B16F10 melanoma growth.

Results

Tumor growth delay (GD) after ECT BLM and GET pIL-12. For the DCE-US studies, murine B16F10 melanoma tumors treated with ECT BLM and GET pIL-12 were used as a model, which has previously been shown to be feasible for studying the antitumor effect of EP-based treatments.

Monotherapies, i.e., pIL-12, BLM and application of electrical pulses (EP ECT; EP GET), and combined treatment with GET pIL-12 had no significant antitumor effect and resulted in tumor GD of up to only 1.9 days compared to untreated tumors (Fig. 1, Supplementary Table S1). However, the growth of B16F10 melanoma tumors was significantly delayed when ECT BLM was performed either alone or in combination with GET pIL-12. Tumor GD after ECT BLM treatment was 14 days, and after ECT BLM GET, pIL-12 was 26.7 days.

DCE-US results. To monitor the effect of treatment on tumor perfusion, DCE-US measurements were performed at different time points after therapy.

There was no correlation between tumor growth and blood flow parameters (AT, AS, TTP, DT/2, DS) or AUC blood volume parameters. Only a correlation between tumor growth and PE was confirmed; therefore, only PE was further analyzed and is reported below.

Of note, mice in the untreated CTRL and pertinent CTRL groups were not measured on days seven and ten because they were humanely sacrificed on day six due to disease burden.

DCE-US results in the treatment groups. Immediately after therapy, the PE values in the groups in which electrical pulses for ECT were applied alone (EP ECT pulses; 2.0 ± 0.8) combined with an intratumoral injection of BLM (ECT BLM, 2.4 ± 0.8) or combined with an intratumoral injection of BLM and GET pIL-12 (ECT BLM GET pIL-12;1.7 ± 0.5) were lower than those in the untreated CTRL group (CTRL; 6.5 ± 0.7) (Fig. 2, Supplementary Table S2). This result was confirmed by DCE-MRI imaging of the tumors, which demonstrated decreased perfusion in the tumors immediately and 6 h after ECT compared to untreated CTRL tumors (Supplementary Fig. S1).

Furthermore, six hours, one day and three days after therapy, the PE values were significantly lower in the ECT BLM (1.6 ± 0.4, 2.0 ± 0.3, 2.2 ± 0.5) and ECT BLM GET pIL-12 groups (2.2 ± 0.7, 2.0 ± 0.6, 2.7 ± 0.7) than in the untreated CTRL group (6.5 ± 1.2, 6.2 ± 1.0, 8.4 ± 1.3).

The Bland–Altman plots presented in Fig. 3 show good agreement between PE and DT. The confidence intervals were narrower on days 1, 7 and 10.

DCE-US results as predictive factors for response to treatment. The association between PE and logarithmically transformed DT for all groups is shown in Fig. 4. Note that mice with the most advanced tumors (the shortest DT values) were excluded from the analyses early (no dots for small DT values at days 7 and 10). Negative regression coefficients (r) indicated that the larger the PE of a mouse was, the lower the expected DT. Statistically significant Pearson coefficients showed a weaker correlation at the second and third time points of the DCE-US measurements (6 h and 1 day after therapy) (− 0.5 and − 0.4, respectively) and a stronger correlation immediately after treatment and on days 3 and 7 (− 0.6) and the strongest correlation on day 10 (− 0.8) (Supplementary Table S3). The association between DCE-US PE and logarithmically transformed DT of mice in the two therapeutic groups showed the weakest correlation on day 1 ($r = -0.3$) and the strongest correlation on days 0 and 10 ($r = -0.7$ and $r = -0.8$, respectively) (Fig. 5, Supplementary Table S4).

DCE-US results for heterogeneity of tumor perfusion. Perfusion curves for different ROIs of the same tumor showed that tumors larger than 40 mm^3 were often heterogeneously perfused; note the different perfusion curves for different ROIs in Supplementary Fig. S2. In larger tumors, the PE values were higher (Fig. 6), and heterogeneous perfusion was more pronounced with increasing tumor volume in all the treatment groups; the SD of PE versus tumor volume showed that the larger the tumor volume, the greater the SD of PE (Fig. 7). In addition, mice in the same treatment group exhibited heterogeneous PE values; the SD of PE was large (± 25.9% on average and up to ± 52.6%). It should also be noted that the variability of perfusion for the same tumor on different days was high (Fig. 2).

The SD of PE for ROIs in the same tumor was compared with DT (Fig. 8); the greater the perfusion heterogeneity (i.e., SD of PE), the shorter the DT. In the ECT BLM group, there was a significant correlation for measurements immediately after therapy ($p = 0.0014$), 6 h after therapy ($p = 0.049$), and on day 1 ($p = 0.038$) and day 10 ($p = 0.043$). Negative regression coefficients (r) indicated that the larger the SD of PE of a tumor the shorter the expected DT. For ECT BLM GET pIL-12, the correlation was significant only on days 0 and 7 ($p = 0.024$ and $p = 0.034$, respectively), with Pearson coefficients of − 0.8 and − 0.7, respectively.

Discussion

Our study confirmed that DCE-US can be used to predict the outcome of EP-based treatments in a mouse melanoma model. Our study also shows that tumor perfusion heterogeneity correlates with treatment outcome. The ultrasonographically determined mean PE values were significantly lower in the groups with shorter tumor DT, and the larger the PE of a mouse, the slower the tumor growth. In our study, the correlation between PE and DT increased with time, with the highest Pearson coefficient at day 10, when only mice of both therapeutic groups were still alive. Immediately after therapy, decreased mean PE values were obtained for the three groups treated with EP for ECT. This local blood flow altering effect or 'vascular lock' characterized by vasoconstriction and increased wall permeability of small blood vessels is induced by high-voltage electrical pulses[10,26–29,45,46], and they were used only in three groups and not in the other groups. Blood flow is slowly restored after EP and approaches the previous flow within 24 h[10,27,29]. The vascular effects of EP are exacerbated by the use of chemotherapeutic agents that are cytotoxic to neoplastic endothelial cells, and this effect prolongs reduced blood flow[26,27]. The results of DCE-US as predictors of EP-based treatments and tumor heterogeneity correlated with tumor growth have not been previously reported. However, for the clinical use of DCE-US for tumor perfusion and antitumor effect prediction, further studies are needed to determine appropriate cutoff values for DCE-US parameters and tumor perfusion conditions that take into account tumor size, perfusion heterogeneity and others to effectively decide on prognosis and the need for repeated therapy. The results of our study are consistent with preclinical studies in which DCE-US results were predictive of treatment success with cisplatin and thalidomide[30,31] and with human clinical studies in which DCE-US results were predictive of antiangiogenic chemotherapeutic treatment[37–42], whereas DCE-US had no predictive value for the radiation outcome in canine tumors[47,48]. Our results are encouraging; previous methods for assessing vascularity in tumors after EP-based treatment are mostly invasive, e.g.,

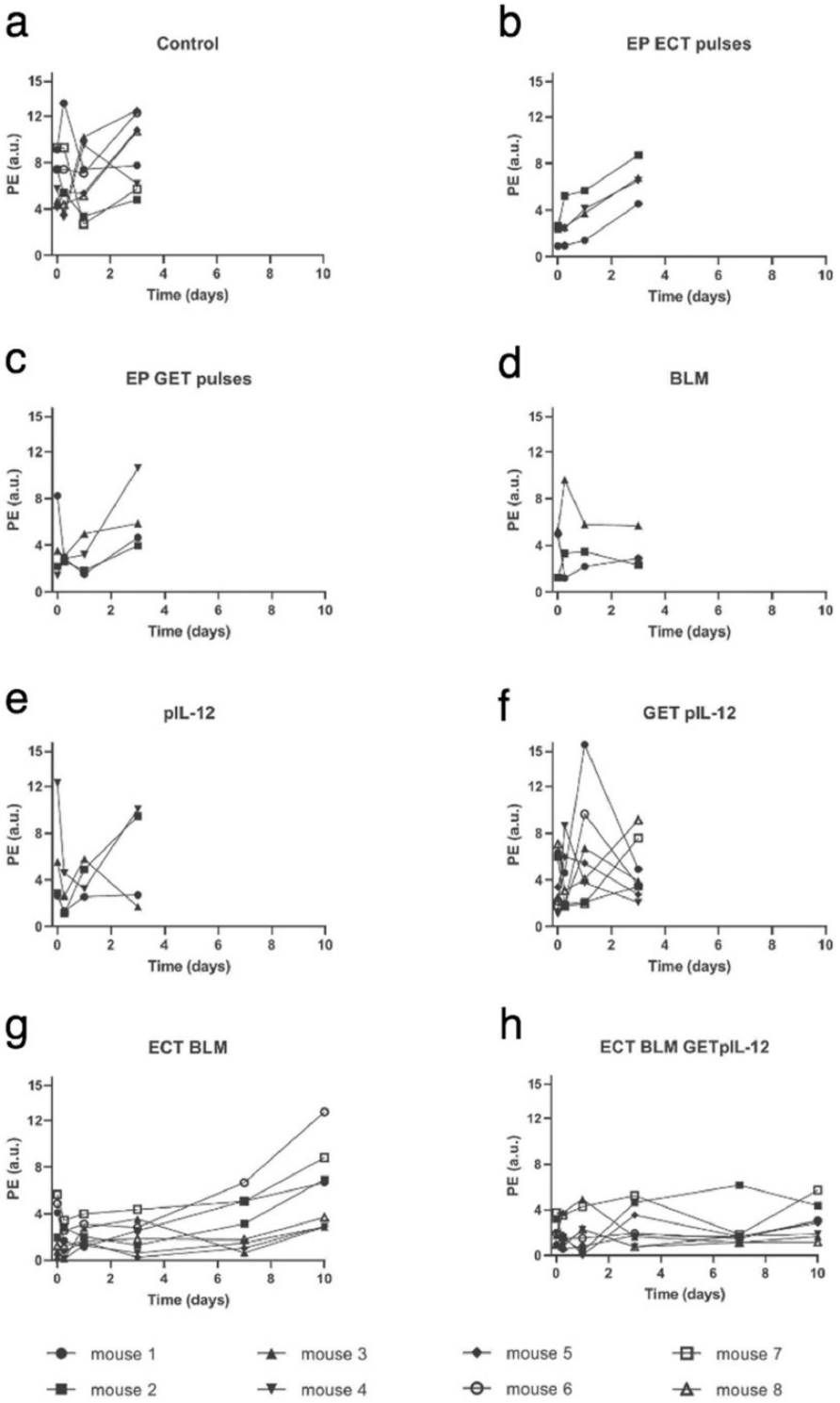

Figure 2. Peak enhancement on different days in mouse melanoma B16F10 cells treated with electrochemotherapy with bleomycin and gene electrotransfer of plasmid DNA encoding plasmid IL-12. Based on dynamic contrast-enhanced ultrasound (DCE-US) measurements, peak enhancement was calculated as the difference between peak intensity and base intensity. Note that mice in the control and pertinent control groups were not measured on days 7 and 10 because they were humanely sacrificed on day 6 due to disease burden. BLM = bleomycin, 7.5 µg/mouse; ECT = electrochemotherapy; EP = electric pulses; GET = gene electrotransfer; pIL-12 = plasmid DNA encoding mouse interleukin-12; PE = peak enhancement. Note that PE values are lower for ECT BLM group (G) and ECT BLM GET pIL-12 group (H) than for other groups.

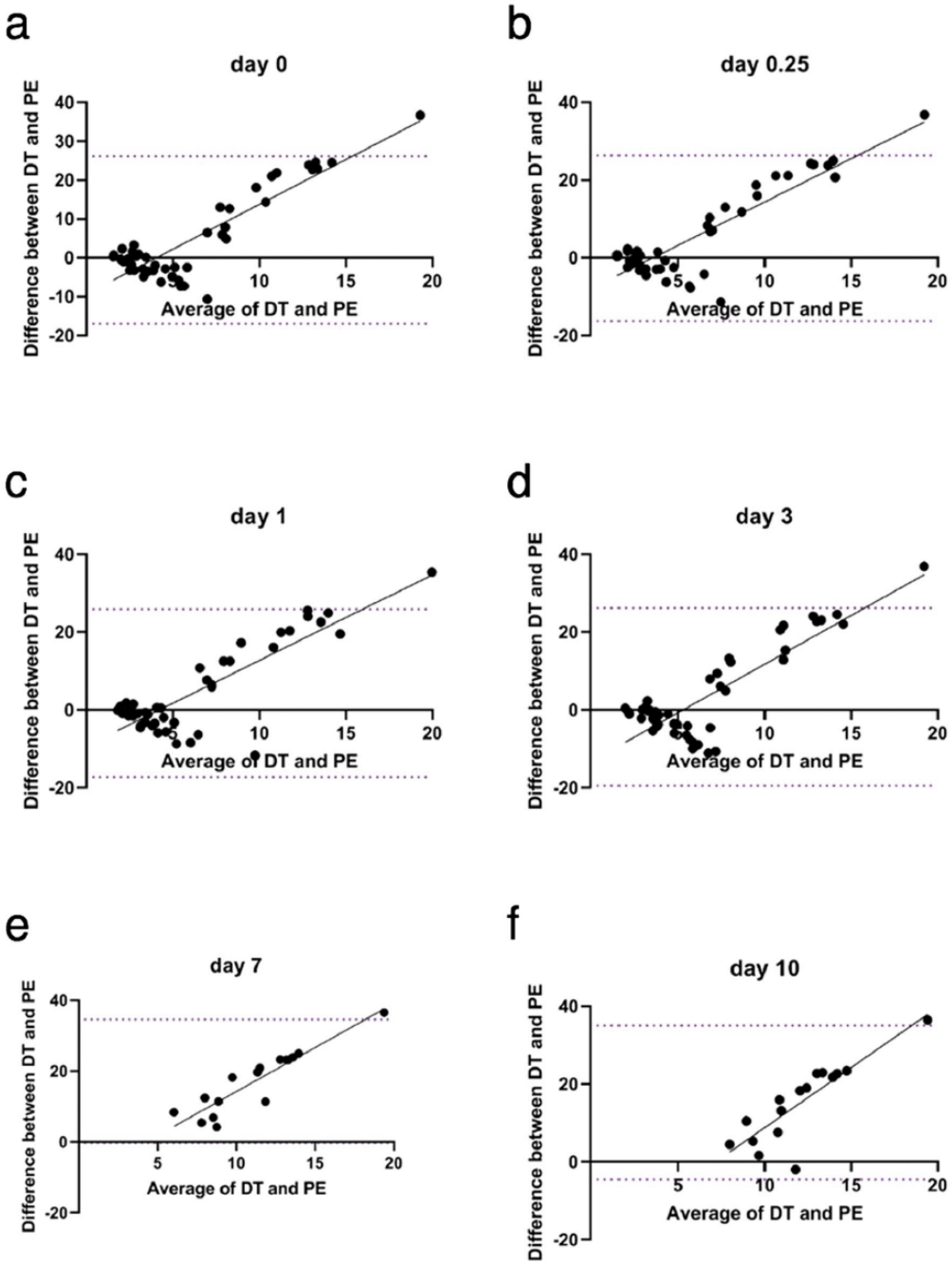

Figure 3. Bland–Altman plot of differences between tumor doubling time and peak enhancement vs. the average of the two measurements at different time points (a – f). Dotted lines represent the 95% confidence interval. Gray lines are for visual inspection only. BLM = bleomycin, 7.5 µg/mouse; DT = doubling time; ECT = electrochemotherapy; EP = electric pulses; GET = gene electrotransfer; pIL-12 = plasmid DNA, encoding mouse interleukin-12; PE = peak enhancement. Note that on days 7 and 10, only mice in the therapeutic groups (ECT BLM and ECT BLM combined with GET pIL-12) were measured because mice in the control groups were humanely sacrificed on day 6 due to the disease burden. Each group consisted of 3–8 animals.

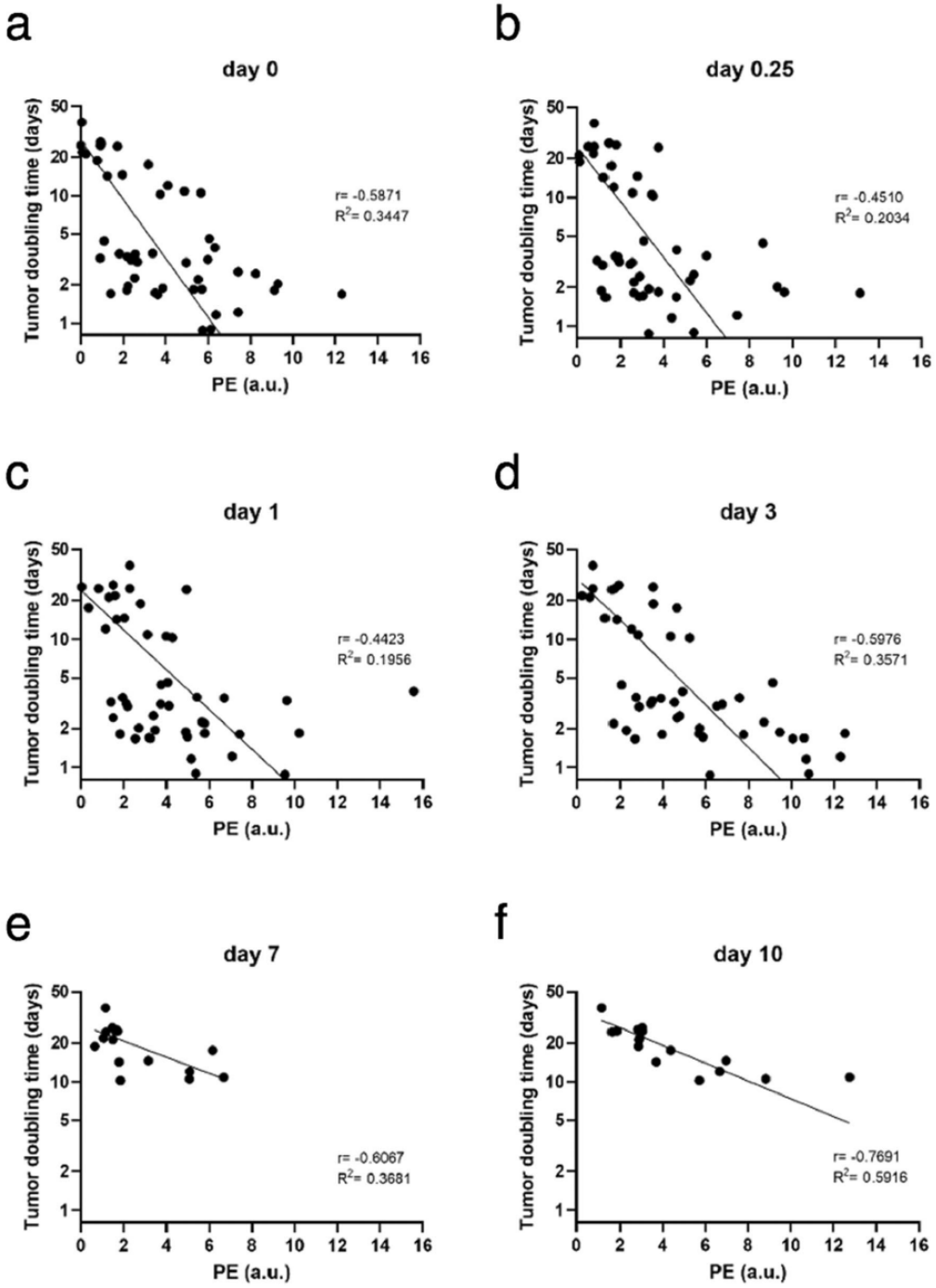

Figure 4. Correlation between peak enhancement and logarithmically transformed doubling time in B16F10 melanoma at different time points (a – f) after treatment with bleomycin electrochemotherapy and gene electrotransfer of a plasmid encoding mouse interleukin-12. BLM = bleomycin, 7.5 µg/mouse; DT = doubling time; ECT = electrochemotherapy; EP = electric pulses; GET = gene electrotransfer; pIL-12 = plasmid DNA encoding mouse interleukin-12; PE = peak enhancement. On days 0, 0.25, 1 and 3, DCE-US was performed in all the treatment groups: control, electroporation (EP) of tumors or the skin using a different set of pulses, intratumoral injection of BLM, intradermal injection of pIl-12, ECT BLM, GET pIl-12, and ECT BLM combined with GET pIL-12. Note that on days 7 and 10, only mice in the therapeutic groups (ECT BLM and ECT BLM combined with GET pIL-12) were measured because mice in the control groups were humanely sacrificed on day 6 due to the disease burden.

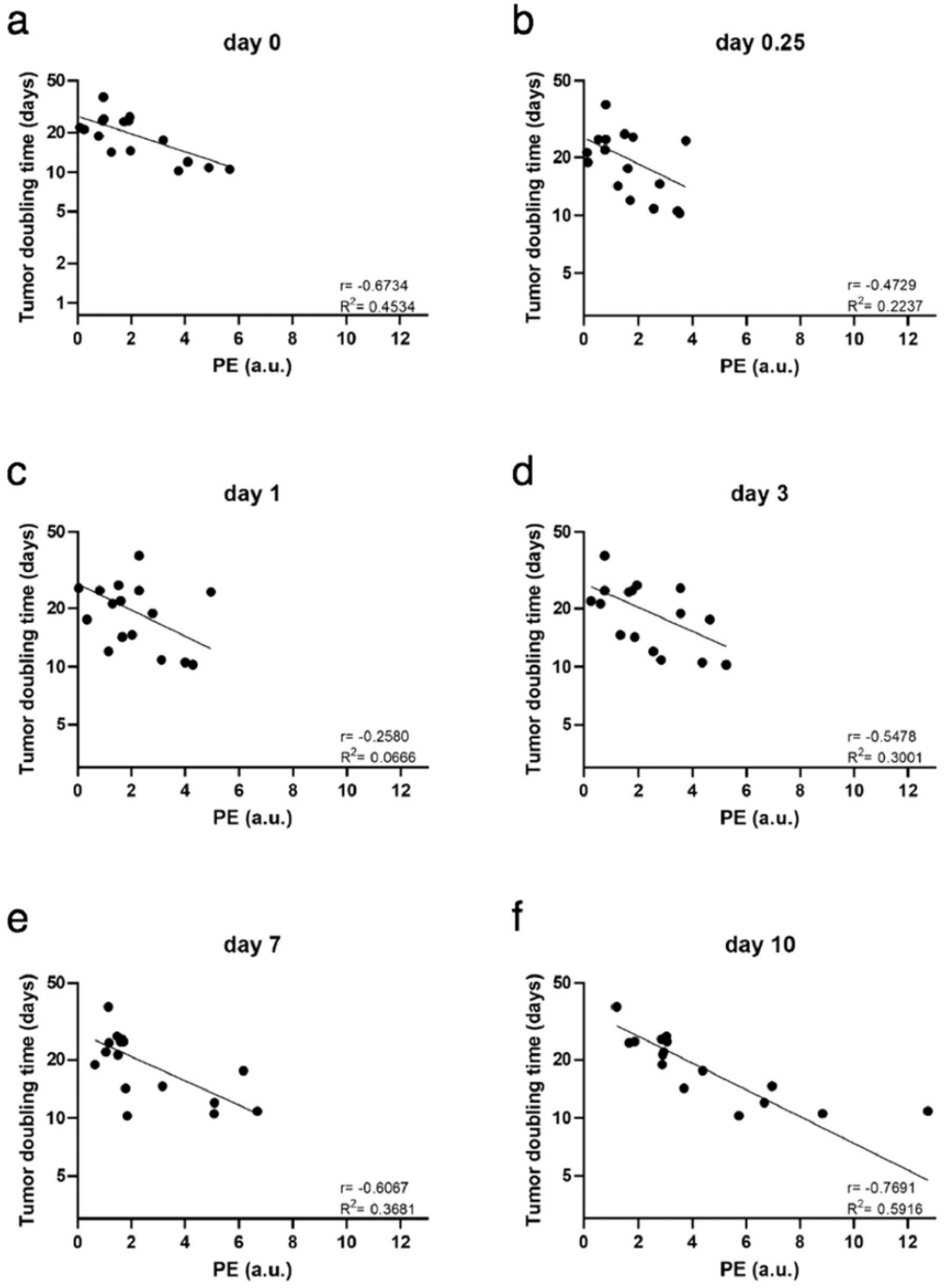

Figure 5. Correlation between peak enhancement and logarithmically transformed doubling time in B16F10 melanoma at different time points (a–f) after treatment with bleomycin electrochemotherapy and gene electrotransfer of plasmid encoding mouse interleukin-12. BLM = bleomycin, 7.5 µg/mouse; DT = doubling time; ECT = electrochemotherapy; EP = electric pulses; GET = gene electrotransfer; pIL-12 = plasmid DNA encoding mouse interleukin-12; PE = peak enhancement. Note that only data for mice in the therapeutic groups (ECT BLM and ECT BLM combined with GET pIL-12) are presented.

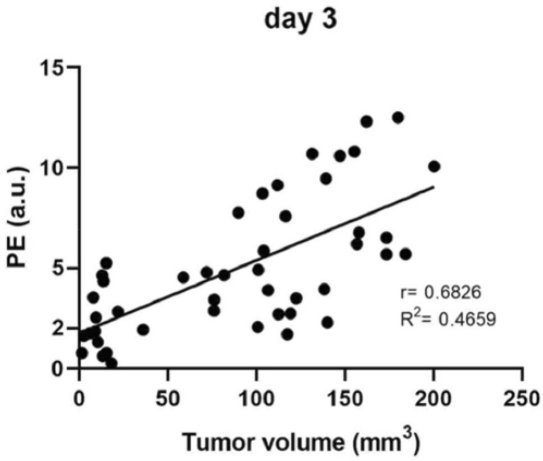

Figure 6. Correlation between peak enhancement and tumor volume at day 3 in melanoma B16F10 cells after treatment with bleomycin electrochemotherapy and gene electrotransfer of a plasmid DNA encoding mouse interleukin-12. Dots represent data obtained from all 47 animals in the experiment. PE = peak enhancement.

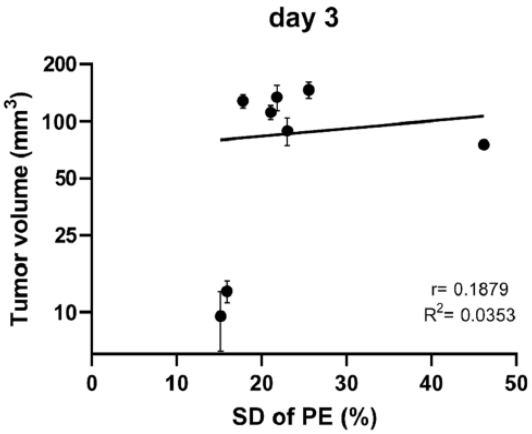

Figure 7. Correlation between tumor volume and the standard deviation of peak enhancement on day 3 after treatment with bleomycin electrochemotherapy and gene electrotransfer of plasmid DNA encoding mouse interleukin-12. PE = peak enhancement; SD = standard deviation. Data were obtained from 66 animals included in the experiment. Note that the larger the tumor volume is, the larger the SD of PE.

immunohistochemistry, and have not been shown to be predictive of EP-based treatment success. In contrast, DCE-US is noninvasive and repeatable and therefore could be used for longitudinal tumor monitoring and decision making when using EP-based therapy in a patient. If therapy does not result in the expected 'vascular lock' or decreased perfusion in the following days, as shown in our study, then therapy should be repeated if needed.

The concept of tumor heterogeneity has not yet been incorporated into current clinical oncology practice or the evidence-based cancer treatment paradigm[48]. Nevertheless, there is evidence that heterogeneous functional/biological characteristics of tumors significantly influence treatment outcomes[49]. Perfusion heterogeneity is common in solid aggressive tumors[50,51], and this was also observed for melanoma tumors in this study, with perfusion heterogeneity becoming more pronounced with increasing tumor volume across all treatment groups. The heterogeneity of tumors could be explained by impaired mechanisms regulating vascular growth. Tumor vessels are abnormal—immature—with chaotic tumor vascular networks and only intermittent flow through many vascular branches[52,53]. Such an aberrant vasculature was observed by DCE-US in our study; in general, the periphery of the tumors was more perfused, and rapid wash-in and wash-out were observed. Moreover, mice of the same group exhibited heterogeneous PE values with high standard deviations (up to ± 41.5%). In addition, we demonstrated a correlation between perfusion heterogeneity and tumor response; the SD of PE for different ROIs of the tumor was correlated with DT; the more heterogeneously perfused the tumors were, the shorter the

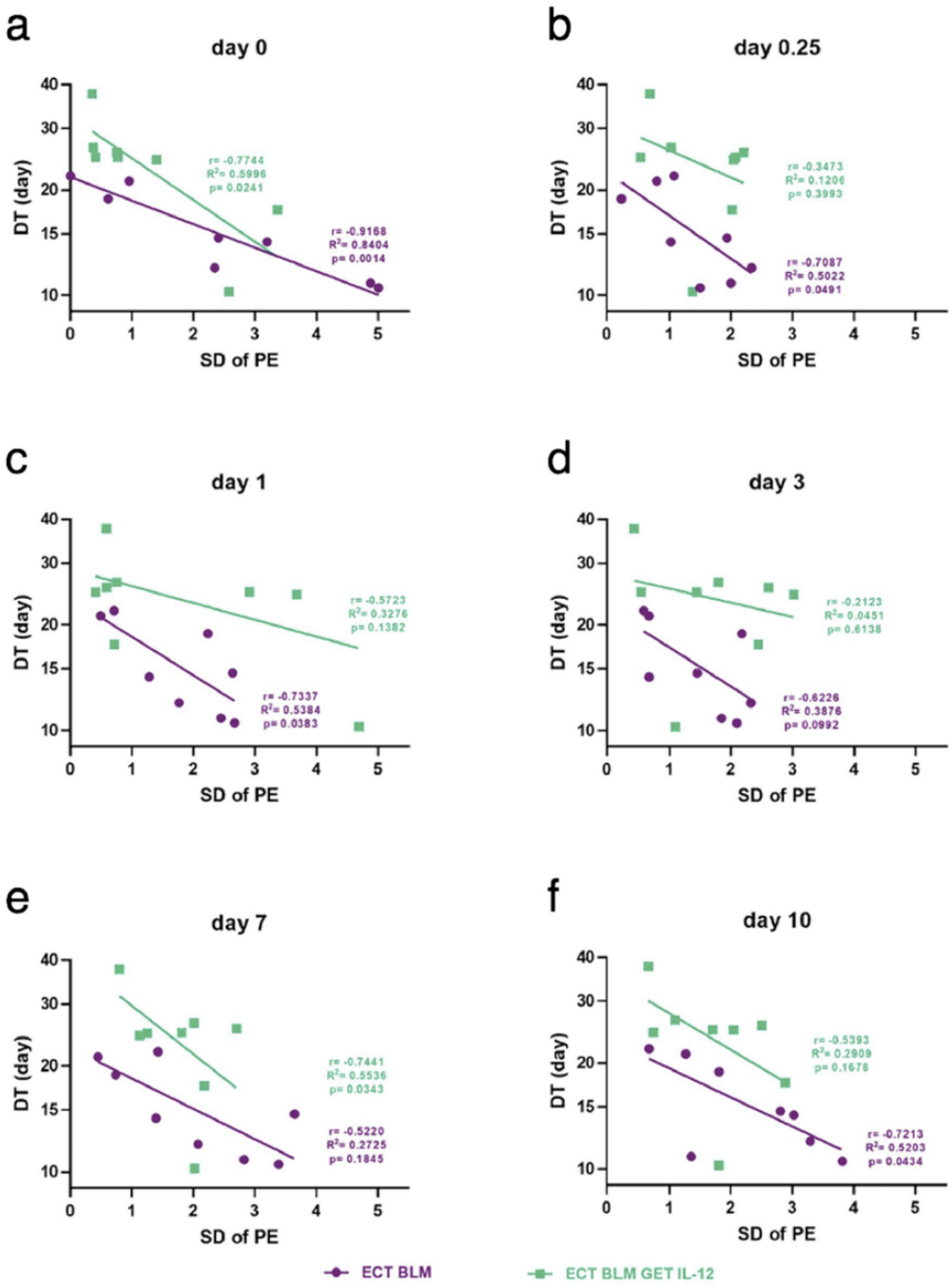

Figure 8. Correlation between the standard deviation of peak enhancement for different regions of interest of a tumor and DT in B16F10 melanoma at different time points (a – f) after treatment with bleomycin electrochemotherapy and gene electrotransfer of a plasmid encoding mouse interleukin 12. BLM = bleomycin, 7.5 µg/mouse; DT = doubling time; ECT = electrochemotherapy; EP = electric pulses; GET = gene electrotransfer; pIL-12 = plasmid DNA encoding mouse interleukin-12; PE = peak enhancement; ROI = region of interest; SD = standard deviation. The presented data were obtained from tumors treated with ECT BLM and ECT BLM combined with GET pIL-12 (n = 16).

DT. This was particularly true for the ECT BLM group, in which we observed a statistically significant correlation between the two parameters throughout the observation period. In contrast, in the group that received GET in addition to ECT, there were only two statistically significant time points (immediately after therapy and on day 7). This could mean that we affected the tumor vasculature and perfusion heterogeneity when GET p-IL12 was added to ECT BLM. Similar to our results, perfusion heterogeneity evaluated by DCE-MRI in cervical cancer treated with radio- and chemotherapy[49] and by DCE-CT in hepatic neoplasia treated with antiangiogenic therapy has been shown to correlate with local tumor control and survival[54]. The first mentioned study showed an opposite result to ours, reporting that decreased perfusion correlated with a worse treatment outcome for radiotherapy in cervical cancer because the response to radiation therapy is lower in parts of the tumor that are hypoxic due to decreased perfusion[49]. The results of the second study were similar to ours, in which a negative percentage change in the heterogeneity parameter correlated with better treatment outcomes of hepatic neoplasia treated with antiangiogenic therapy[54]. Perfusion heterogeneity may lead to unfavorable drug delivery and an increasing hypoxic environment that accelerates cancer progression[54]. Although a heterogeneous response is typical of many cancer treatments, the treatment regimen remains largely uniform, which may be why treatment failure is so common in different cancers where recommended guidelines for the most appropriate treatment have been followed[49]. Predicting treatment outcome is challenging when performed as early as possible during treatment, when targeted adjustments to therapy are generally more effective[49]. Our tumor heterogeneity results show that not only tumor perfusion intensity but also perfusion heterogeneity can be used to assess treatment outcome in ECT BLM treatment; if tumors are still heterogeneous after treatment, then repeated therapy should be considered. In the combined ECT BLM GET pIL-12 treatment, perfusion heterogeneity correlated with tumor growth at two time points only; therefore, further studies are needed to evaluate whether GET p-IL12 affects tumor vasculature in such a way that tumor perfusion heterogeneity is less predictive of tumor growth.

A major limitation of our study was that there were no complete responders. This could be due to the low BLM dose; we used 7.5 µg of BLM per mouse, whereas in previous studies, higher dosages were used[26]. This lower BLM dose was chosen to avoid too many CRs due to the high antitumor effect of ECT BLM. Our goal was to achieve a broad spectrum of different responders: CR, partial response, response with stable disease, and response with varying progress. The pharmacokinetics of BLM depend on tumor vascularity, which affects the accumulation and distribution of the drug in the tumor: the more vascularized the tumors are with small vessels, the better the effect of ECT, and conversely, when the vessels are larger, the washout of the chemotherapeutic drug is greater and the effect of ECT is lower[55]. In addition, no significant antitumor effect was observed when treated with peritumoral GET p-IL12. This result is in contrast to studies reporting the antitumor efficacy of intratumoral GET p-IL12[56] and GET with control plasmid DNA[9,11]. The most likely reasons for the lower antitumor efficacy of GET p-IL12 in our study are the peritumoral application of pIL-12, a different dose of pIL-12 and/or a different protocol of application of electrical pulses (56). In our study, the GD of the two therapeutic groups was 15 days and 28 days, which is consistent with preclinical and clinical studies reporting the efficacy of ECT with BLM[1–5] and potentiation of ECT with GET[6–8,13,14].

This study demonstrates that DCE-US, a simple, noninvasive, safe, and inexpensive method of tissue perfusion, can be used to predict tumor growth after EP-based therapy. The information obtained with DCE-US is readily available and DCE-US can be easily repeated during therapy. Due to its potential value as a prognostic and predictive factor of disease, further preclinical and clinical studies are needed to confirm these preclinical study results in mice. If confirmed, the results of DCE-US can be used to predict the course of the disease and thus can even be used as a decision-making tool for planning repeated therapy or different treatment combinations in individual patients.

Methods

The study was carried out in compliance with the ARRIVE guidelines.

Tumor cells. Melanoma B16F10 cells were cultured in Advanced Minimal Essential Medium (AMEM) containing 5% fetal bovine serum (FBS) (Gibco, Fisher Scientific, Waltham, MA, USA), 10 mM/L L-glutamine GlutaMAX (Gibco, Fisher Scientific, Waltham, MA, USA), 100 U/mL penicillin (Gruenenthal, Aachen, Germany) and 50 mg/mL gentamicin (Krka, Novo Mesto, Slovenia) in an incubator humidified with 5% CO_2 at 37 °C. At 80% confluence, trypsinization was performed with 0.25% trypsin/EDTA in Hank's buffer. Cells were then washed with AMEM containing 5% FBS and collected by centrifugation. Tumors were induced on the backs of mice by a subcutaneous injection of 100 µl of a B16F10 cell suspension containing one million cells prepared in a 0.9% NaCl solution (B Braun, Melsungen AG, Melsungen, Germany).

Animals. Female C57Bl/6NCrl mice (Envigo RMS SrL, San Pietro al Natisone, Italy) that were 7 weeks old and weighed 18–20 g were housed under specific pathogen-free conditions at a temperature of 20–24 °C, a relative humidity of 55 ± 10%, a 12-h light–dark cycle and ad libitum food and water. All procedures were performed according to the guidelines for animal experiments of the EU Directive (2010/63/EU). Official approval was granted by the Veterinary Administration of the Ministry of Agriculture, Forestry and Food of the Republic of Slovenia (No. U34401-1/2015/43).

BLM. BLM (Bleomycin medac, Medac, Wedel, Germany, BLM) was dissolved to 3 mg/mL in sterile water (B Braun, Melsungen AG, Melsungen, Germany), aliquoted and frozen at -20 °C until use. A fresh BLM solution of 0.375 mg/mL in 0.9% NaCl was prepared (B Braun, Melsungen AG, Melsungen, Germany) before intratumoral injection (7.5 µg of BLM in 20 µl).

IL-12 plasmid. The pORF-mIL-12-ORT (pIL-12) plasmid, which encodes the mouse gene IL-12 and lacks an antibiotic resistance gene, was used. Construction of the plasmid has been previously described[57]. The plasmid was isolated from a bacterial culture using an EndoFree Plasmid Mega kit (Qiagen, Hilden, Germany) and diluted to a concentration of 0.625 mg/mL in endotoxin-free water (Qiagen, Hilden, Germany). Purity and yield were determined spectrophotometrically (Epoch Microplate Spectrophotometer, Take3™ microvolume plate, BioTek, Bad Friedrichshall, Germany). Before experiments, the concentration and identity of the plasmid were confirmed by restriction analysis on an electrophoresis gel.

Experimental design and DCE-US examinations. The experiment began when tumors reached approximately 40 mm^3 (6 × 6 × 2 mm in orthogonal diameters) (considered day 0). Mice were randomly divided into eight groups with 8–12 mice each. There was no tumor manipulation in the control group (CTRL). There were two groups in which only different electrical pulses were applied: in the EP ECT group, electrical pulses were applied for ECT (8 square electrical pulses with a voltage-distance ratio of 1300 V/cm, a pulse duration of 100 µs and a frequency of 1 Hz), and in the EP GET group, electrical pulses were applied in GET to the skin (12 electrical pulses, 150 ms long with a voltage-distance ratio of 170 V/cm at 2.82 kHz). The selection of the voltage, duration and frequency of the electrical pulses was based on ECT[2,3,5–7,17,18,58] and GET guidelines[15,19–24,59,60]. The electrical pulses for EP ECT were generated using the electrical pulse generator ELECTRO CELL B10 HVLV (Betatech, L'Union, France) and delivered through two parallel stainless-steel electrodes 6 mm apart. After delivery of 4 pulses, the electrodes were rotated 90°, and four more electrical pulses were applied to expose the entire tumor to the electrical pulses. The electrical pulses for EP GET were generated using the Cliniporator electrical pulse generator (IGEA S.p.A., Carpi, Italy); 12 electrical pulses were delivered to the skin through a noninvasive multielectrode array (MEA) consisting of six spring-loaded pins arranged in a hexagonal mesh 3.5 mm apart[59]. In the BLM group, BLM was administered intratumorally (7.5 µg/mouse, 20 µl). In the pIL-12 group, the plasmid IL-12 was injected intradermally into the peritumoral region (4 sites around the tumor, 4 × 20 µl, 0.625 mg/mL, 50 µg). In the combined treatment of the intratumoral BLM injection and application of electrical pulses (ECT BLM), electrical pulses were delivered 2 min after the injection of BLM. In the combined treatment of IL-12 plasmid injection and application of electrical pulses (GET pIL-12), the delivery of electrical pulses was performed immediately after the intradermal injection of IL-12 plasmid in the peritumoral area. In the combined treatment of electrochemotherapy with gene electrotransfer (ECT BLM GET pIL-12) group, the IL-12 plasmid was first administered intradermally in the peritumoral region, and immediately thereafter, electrical pulses were administered as described above for the GET group. Then, 5 min later, BLM was injected intratumorally, and 2 min later, electrical pulses, as for the ECT group, were delivered (Supplementary Fig. S3).

DCE-US examinations were performed in all animals immediately after therapy, 6 h and 1, 3, 7 and 10 days after therapy (Supplementary Fig. S2). SonoVue contrast agent (Bracco, Milan, Italy), a M9 ultrasound machine (Mindray, Shenzhen, China) and a linear probe (L3-13.5, Mindray, Shenzhen, China) with a frequency of 3 to 13.5 MHz and harmonic nonlinear ultraband contrast imaging at a low mechanical index were used. After applying 50 µl of the Alcaine topical ophthalmic anesthetic solution (Alcon, Basel, Switzerland) to the mouse cornea, 0.1 mL of contrast agent was administered into the retro-orbital sinus of the mouse. A 90-s recording was made from the time of contrast agent application. Each tumor was carefully delineated. In addition, 6 to 8 ellipsoidal regions of interest (ROIs) were plotted to cover the entire area of the tumor. For the tumor and ROIs, the perfusion curve or time-intensity curve was analyzed using software integrated in the US device, which displayed the following parameters: BI (base intensity; the baseline intensity when no contrast agent was present), PI (peak intensity), TTP (time to peak; the time at which the contrast intensity reached the peak value), AS (ascending slope; the slope between the starting point of lesion perfusion and the peak value), AT (arrival time; time point at which contrast intensity appeared, generally the time when intensity was 110% higher than the baseline), DT/2 (descend time to half; a time point at which the intensity was half the value of the peak intensity), DS (descending slope) and AUC (area under the curve). PE (peak enhancement) was calculated as the difference between PI and BI (Supplementary Fig. S4). PE and AUC are blood volume parameters, while all others (TTP, AS, AT, DT/2 and DS) describe the blood flow rate. Tumor heterogeneity was assessed using the standard deviation (SD) of parameters for different ROIs of the tumor.

For GET and DCE-US studies, mice were anesthetized under inhalation anesthesia with isoflurane (2% v/v), and heating pads were used to prevent hypothermia.

The weight of the animals was monitored as a sign of systemic toxicity of the treatments. Mice were weighed before the first treatment and then every other day until the end of the experiment.

Tumors were measured every other day using Vernier caliper and tumor volume was calculated from the measured perpendicular diameters ($V = a \times b \times c \times \pi/6$). Tumor doubling time (DT) was determined as the time the tumor doubled in volume from the first day of the experiment. Growth delay (GD) was determined as the difference between the tumor doubling time of the individual tumor in the tested group and the mean tumor doubling time in the untreated CTRL group. Mice with tumor regression were examined for the presence of tumors 100 days after treatment. If they were tumor-free 100 days after treatment, then they were considered complete responders (CRs). The results of DCE-US were compared to tumor growth (CR, DT, GD).

In addition, nine mice underwent dynamic contrast-enhanced magnetic resonance imaging (DCE-MRI): two from the CTRL group (on day 1) and seven from the ECT group (immediately, 6, 12, and 36 h after ECT and on day ten in two mice). For DCE-MRI examinations, mice were anesthetized with intraperitoneal application of ketamine (75 mg/kg) and xylazine (3 mg/kg). Gadolinium contrast agent, 100 µL per mouse (gadobutrol 500 mg/kg, Gadovist, 1 mmol/mL (Bayer, Leverkusen, Germany)), was administered via a catheter inserted into the retro-orbital sinus.

Statistical analysis. One-way analysis of variance followed by the Holm-Sidak test was used to compare differences in tumor growth and DCE-US results among treatment groups (Systat Software, Chicago, IL, USA). Statistical significance was defined as $p < 0.05$. Daily associations between the PE and (log) DT values or tumor volume and tumor perfusion heterogeneity were examined using linear regression models and are presented in scatterplots with linear regression lines and Pearson correlation analysis. In addition, Bland–Altman plots were used to show differences between DT and PE and the average of these two measurements within each treatment according to the time points of the PE measurements. All analyses and graphical presentations were performed using GraphPad Prism 8.4 (GraphPad software, San Diego, CA).

Data availability

The datasets generalised during and/or analysed during the current study are available from the corresponding author on reasonable request.

Received: 14 February 2021; Accepted: 24 May 2021
Published online: 29 June 2021

References

1. Mali, B., Jarm, T., Snoj, M., Sersa, G. & Miklavcic, D. Antitumor effectiveness of electrochemotherapy: A systematic review and meta-analysis. *Eur. J. Surg. Oncol.* **39**(1), 4–16 (2013).
2. Edhemovic, I. *et al.* Intraoperative electrochemotherapy of colorectal liver metastases: A prospective phase II study. *Eur. J. Surg. Oncol.* **46**(9), 1628–1633 (2020).
3. Cadossi, R., Ronchetti, M. & Cadossi, M. Locally enhanced chemotherapy by electroporation: Clinical experiences and perspective of use of electrochemotherapy. *Future Oncol.* **10**(5), 877–890 (2014).
4. Cemazar, M. *et al.* Electrochemotherapy in veterinary oncology. *J. Vet. Intern. Med.* **22**(4), 826–831 (2008).
5. Marty, M. *et al.* Electrochemotherapy—an easy, highly effective and safe treatment of cutaneous and subcutaneous metastases: Results of ESOPE (European Standard Operating Procedures of Electrochemotherapy) study. *EJC Suppl.* **4**, 3–13 (2006).
6. Bertino, G. *et al.* European Research on Electrochemotherapy in Head and Neck Cancer (EURECA) project: Results of the treatment of skin cancer. *Eur. J. Cancer* **63**, 41–52 (2016).
7. Cemazar, M. *et al.* Efficacy and safety of electrochemotherapy combined with peritumoral IL-12 gene electrotransfer of canine mast cell tumours. *Vet. Comp. Oncol.* **15**(2), 641–654 (2017).
8. Sersa, G. *et al.* Electrochemotherapy of tumors as in situ vaccination boosted by immunogene electrotransfer. *Cancer Immunol. Immunother.* **64**(10), 1315–1327 (2015).
9. Bosnjak, M. *et al.* Electrotransfer of different control plasmids elicits antitumor effectiveness in B16.F10 melanoma. *Cancers* **10**(2), 37 (2018).
10. Gehl, J., Skovsgaard, T. & Mir, L. M. Vascular reactions to in vivo electroporation: Characterization and consequences for drug and gene delivery. *Biochim. Biophys. Acta* **1569**(1–3), 51–58 (2002).
11. Kranjc Brezar, S., Mrak, V., Bosnjak, M., Savarin, M., Sersa, G. & Cemazar, M. Intratumoral gene electrotransfer of plasmid DNA encoding shRNA against melanoma cell adhesion molecule radiosensitizes tumors by antivascular effects and activation effects and activation of an immune response. *Vaccines* **8**(1), 135 (2020).
12. Polajzer, T., Jarm, T. & Miklavcic, D. Analysis of damage-associated molecular pattern molecules due to electroporation of cells in vitro. *Radiol. Oncol.* **54**(3), 317–328 (2020).
13. Pavlin, D., Cemazar, D., Sersa, G. & Tozon, N. IL-12 based gene therapy in veterinary medicine. *J. Transl. Med.* **10**, 234–244 (2012).
14. Cutrera, J. *et al.* Safe and effective treatment of spontaneous neoplasms with interleukin 12 electro-chemo-gene therapy. *J. Cell Mol. Med.* **19**(3), 664–675 (2015).
15. Sedlar, A. *et al.* Potentiation of electrochemotherapy by intramuscular IL-12 gene electrotransfer in murine sarcoma and carcinoma with different immunogenicity. *Radiol. Oncol.* **46**(4), 302–311 (2012).
16. Milevoj, N. *et al.* A combination of electrochemotherapy, gene electrotransfer of plasmid encoding canine IL-12 and cytoreductive surgery in the treatment of canine oral malignant melanoma. *Res. Vet. Sci.* **122**, 40–49 (2019).
17. Kishida, T. *et al.* Electrochemo-gene therapy of cancer: intratumoral delivery of interleukin-12 gene and bleomycin synergistically induced therapeutic immunity and suppressed subcutaneous and metastatic melanomas in mice. *Mol. Ther.* **8**(5), 738–745 (2003).
18. Mir, L. M. *et al.* Standard operating procedures of the electrochemotherapy: instructions for the use of bleomycin or cisplatin administered either systemically or locally and electrical pulses delivered by Cliniporator by means of invasive or non-invasive electrodes. *Eu. J. Cancer Suppl.* **4**, 14–25 (2006).
19. Tozon, N. *et al.* Operating procedures of the electrochemotherapy for treatment of tumor in dogs and cats. *J. Vis. Exp.* **116**, 54760 (2016).
20. Daud, A. I. *et al.* Phase I trial of interleukin-12 plasmid electroporation in patients with metastatic melanoma. *J. Clin. Oncol.* **26**(36), 5896–5903 (2008).
21. Shirley, S. A., Lundberg, C. G., Li, F., Burcus, N. & Heller, R. Controlled gene delivery can enhance therapeutic outcome for cancer immune therapy for melanoma. *Curr. Gene. Ther.* **15**(1), 32–43 (2015).
22. Heller, R. & Heller, L. C. Gene electrotransfer clinical trials. *Adv. Gen.* **89**, 235–262 (2015).
23. Cicchelero, L. *et al.* Intratumoural interleukin 12 gene therapy stimulates the immune system and decreases angiogenesis in dogs with spontaneous cancer. *Vet Comp Oncol* **15**, 1187–1205 (2016).
24. Salvadori, C. *et al.* Effects of electrochemotherapy with cisplatin and peritumoral IL-12 gene electrotransfer on canine mast cell tumors: A histopathologic and immunohistochemical study. *Radiol. Oncol.* **51**(3), 286–294 (2017).
25. Pavlin, D. *et al.* Electrogene therapy with interleukin-12 in canine mast cell tumors. *Radiol. Oncol.* **45**, 30–39 (2011).
26. Sersa, G., Cemazar, M. & Miklavcic, D. Tumor blood flow modifying effects of electrochemotherapy: A potential vascular targeted mechanism. *Radiol. Oncol.* **37**, 43–48 (2003).
27. Jarm, T., Cemazar, M., Miklavcic, D. & Sersa, G. Antivascular effects of electrochemotherapy: Implications in treatment of bleeding metastases. *Expert. Rev. Anticancer. Ther.* **10**(5), 729–746 (2010).
28. Bellard, E. *et al.* Intravital microscopy at the single vessel level brings new insights of vascular modification mechanisms induced by electropermeabilization. *J. Control. Release* **163**(3), 396–403 (2012).
29. Markelc, B., Sersa, G. & Cemazar, M. Differential mechanisms associated with vascular disrupting action of electrochemotherapy: intravital microscopy on the level of single normal and tumor blood vessels. *PLoS ONE* **8**, e59557 (2013).
30. Zhou, J. H. *et al.* Quantitative assessment of tumor blood flow in mice after treatment with different doses of an antiangiogenic agent with contrast-enhanced destruction-replenishment US. *Radiology* **259**(2), 406–413 (2011).
31. Zhou, J. H. *et al.* Contrast-enhanced gray-scale ultrasound for quantitative evaluation of tumor response to chemotherapy: Preliminary results with a mouse hepatoma model. *Am. J. Roentgenol.* **196**(1), W13–W17 (2011).

32. Arteaga-Marrero, N. *et al.* Radiation treatment monitoring with DCE-US in CWR22 prostate tumor xenografts. *Acta Radiol.* **60**(6), 788–797 (2019).
33. Sedelaar, J. P. *et al.* Microvessel density: correlation between contrast ultrasonography and histology of prostate cancer. *Eur. Urol.* **40**(3), 285–293 (2001).
34. Leng, X., Huang, G., Ma, F. & Yao, L. Regional Contrast-Enhanced Ultrasonography (DCE-US) characteristics of breast cancer and correlation with Microvessel Density (MVD). *Med. Sci. Monit.* **23**, 3428–3436 (2017).
35. Li, X., Li, Y., Zhu, Y., Fu, L. & Liu, P. Association between enhancement patterns and parameters of contrast-enhanced ultrasound and microvessel distribution in breast cancer. *Oncol. Lett.* **15**(4), 5643–5649 (2018).
36. Ohlerth, S. *et al.* Correlation of quantified contrast-enhanced power Doppler ultrasonography with immunofluorescent analysis of microvessel density in spontaneous canine tumours. *Vet. J.* **183**(1), 58–62 (2010).
37. Lassau, N. *et al.* Dynamic contrast-enhanced ultrasonography (DCE-US): a new tool for the early evaluation of antiangiogenic treatment. *Target. Oncol.* **5**(1), 53–58 (2010).
38. Lassau, N. *et al.* Advanced hepatocellular carcinoma: early evaluation of response to bevacizumab therapy at dynamic contrast-enhanced US with quantification—preliminary results. *Radiology* **258**(1), 291–300 (2011).
39. Lassau, N. *et al.* Standardization of dynamic contrast-enhanced ultrasound for the evaluation of antiangiogenic therapies: The French multicenter Support for Innovative and Expensive Techniques Study. *Invest. Radiol.* **47**(12), 711–716 (2012).
40. Lassau, N., Cosgrove, D. & Armand, J. P. Early evaluation of targeted drugs using dynamic contrast-enhanced ultrasonography for personalized medicine. *Future Oncol.* **8**(10), 1215–1218 (2012).
41. Lassau, N. *et al.* Validation of dynamic contrast-enhanced ultrasound in predicting outcomes of antiangiogenic therapy for solid tumors: The French multicenter support for innovative and expensive techniques study. *Invest. Radiol.* **49**(12), 794–800 (2014).
42. Kim, Y. *et al.* Early prediction of response to neoadjuvant chemotherapy using Dynamic Contrast-Enhanced MRI and Ultrasound in breast cancer. *Korean J. Radiol.* **19**, 682–691 (2018).
43. Fetzer, D. T. *et al.* Artifacts in contrast-enhanced ultrasound: a pictorial essay. *Abdom. Radiol.* **43**(4), 977–997 (2018).
44. Erlichman, D. B., Weiss, A., Koenigsberg, M. & Stein, M. W. Contrast enhanced ultrasound: A review of radiology applications. *Clin. Imaging* **60**(2), 209–215 (2019).
45. Boc, N. *et al.* Ultrasonographic changes in the liver tumors as indicators of adequate tumor coverage with electric field for effective electrochemotherapy. *Radiol. Oncol.* **52**(4), 383–391 (2018).
46. Brloznik, M. *et al.* Radiological findings of porcine liver after electrochemotherapy with bleomycin. *Radiol. Oncol.* **53**(4), 415–426 (2019).
47. Rohrer Bley, C., Laluhova, D., Roos, M., Kaser-Hotz, B. & Ohlerth, S. Correlation of pretreatment polarographically measured oxygen pressures with quantified contrast-enhanced power doppler ultrasonography in spontaneous canine tumors and their impact on outcome after radiation therapy. *Strahlenther Onkol.* **185**(11), 756–762 (2009).
48. Ohlerth, S., Bley, C. R., Laluhová, D., Roos, M. & Kaser-Hotz, B. Assessment of changes in vascularity and blood volume in canine sarcomas and squamous cell carcinomas during fractionated radiation therapy using quantified contrast-enhanced power Doppler ultrasonography: A preliminary study. *Vet. J.* **186**(1), 58–63 (2010).
49. Mayr, N. A. *et al.* Characterizing tumor heterogeneity with functional imaging and quantifying high-risk tumor volume for early prediction of treatment outcome: Cervical cancer as a model. *Int. J. Radiat. Oncol. Biol. Phys.* **83**(3), 972–979 (2012).
50. Yankeelov, T. E. *et al.* Correlation between estimates of tumor perfusion from microbubble contrast-enhanced sonography and dynamic contrast-enhanced magnetic resonance imaging. *J. Ultrasound. Med.* **25**(4), 487–497 (2006).
51. Graff, B. A., Benjaminsen, I. C., Melas, E. A., Brurberg, K. G. & Rofstad, E. K. Changes in intratumor heterogeneity in blood perfusion in intradermal human melanoma xenografts during tumor growth assessed by DCE-MRI. *Magn. Reson. Imaging* **23**(9), 961–966 (2005).
52. Tozer, G. M., Kanthou, C. & Baguley, B. C. Disrupting tumour blood vessels. *Nat. Rev. Cancer* **5**(6), 423–435 (2005).
53. Siemann, D. W. The unique characteristics of tumor vasculature and preclinical evidence for its selective disruption by tumor-vascular disrupting agents. *Cancer Treat. Rev.* **37**(1), 63–74 (2011).
54. Hayano, K., Lee, S. H., Yoshida, H., Zhu, A. X. & Sahani, D. V. Fractal analysis of CT perfusion images for evaluation of antiangiogenic treatment and survival in hepatocellular carcinoma. *Acad. Radiol.* **21**(5), 654–660 (2014).
55. Groselj, A. *et al.* Vascularization of the tumours affects the pharmacokinetics of bleomycin and the effectiveness of electrochemotherapy. *Basic Clin. Pharmacol. Toxicol.* **123**(3), 247–256 (2018).
56. Pavlin, D. *et al.* Local and systemic antitumor effect of intratumoral and peritumoral IL-12 electrogene therapy on murine sarcoma. *Cancer Biol. Ther.* **8**, 2114–2122 (2009).
57. Kamensek, U., Tesic, N., Sersa, G., Kos, S. & Cemazar, M. Tailor-made fibroblast-specific and antibiotic-free interleukin 12 plasmid for gene electrotransfer-mediated cancer immunotherapy. *Plasmid* **89**, 9–15 (2017).
58. Campana, L. G. *et al.* Recommendations for improving the quality of reporting clinical electrochemotherapy studies based on qualitative systematic review. *Radiol. Oncol.* **50**(1), 1–13 (2016).
59. Kos, S. *et al.* Electrotransfer parameters as a tool for controlled and targeted gene expression in skin. *Mol. Ther.* **5**, e356 (2016).
60. Shi, G., Edelblute, C., Arpag, S., Lundberg, C. & Heller, R. IL-12 gene electrotransfer triggers a change in immune response within mouse tumors. *Cancers* **10**, 498 (2018).

Acknowledgements

The authors thank Miha Melinec and Tone Jamnik (DIPROS d.o.o.) for their assistance and ultrasonographic machines that enabled contrast studies. The authors acknowledge the financial support of the Slovenian Research Agency (Research Program No P3-003 and No P4-0053). The funder had no influence on the study design, data collection and analysis, the decision to publish, or the preparation of the manuscript. The language editing of this manuscript was done by American Journal Experts.

Author contributions

Study concepts/study design, S.K.B., D.P., M.C., G.S.; data acquisition, M.B., S.K.B., M.Bo., N.B.; data analysis/interpretation, M.B., N.B., D.P., S.K.B.; manuscript drafting, M.B., D.P., S.K.B.; manuscript revision for important intellectual content, M.C., G.S., S.K.B., D.P.; approval of the final version of submitted manuscript, M.B., N.B., M.C., G.S., M.Bo., D.P., S.K.B.; and manuscript editing, M.B., N.B., M.C., G.S., M.Bo., D.P., S.K.B.

Competing interests

The authors declare no competing interests.

Additional information

Supplementary Information The online version contains supplementary material available at https://doi.org/10.1038/s41598-021-92820-w.

Correspondence and requests for materials should be addressed to S.K.B. or D.P.

Reprints and permissions information is available at www.nature.com/reprints.

Publisher's note Springer Nature remains neutral with regard to jurisdictional claims in published maps and institutional affiliations.

2.4 Rezultati dinamične ultrazvočne kontrastne preiskave korelirajo z izidom zdravljenja pasjih tumorjev, zdravljenih z elektrokemoterapijo in genskim elektroprenosom plazmidne DNA z zapisom za pasji interlevkin-12

Results of dynamic contrast-enhanced ultrasound correlate with treatment outcome in canine neoplasia treated with electrochemotherapy and interleukin-12 plasmid electrotransfer

Maja Brložnik[1], Simona Kranjc Brezar[2,3], Nina Boc[2], Tanja Knific[1], Maja Čemažar[2,6], Nina Milevoj[1], Gregor Serša[2,7], Nataša Tozon[1], Darja Pavlin.[1*]

[1] Univerza v Ljubljani, Veterinarska fakulteta

[2] Onkološki inštitut Ljubljana

[3] Univerza v Ljubljani, Medicinska fakulteta

[4] Univerza na Primorskem, Fakulteta za vede o zdravju

[5] Univerza v Ljubljani, Zdravstvena fakulteta

* vodilna avtorica: Darja Pavlin

Front Vet Sci 2021; 8: 679073. doi: 10.3389/fvets.2021.679073.

Izvleček

EKT in/ali GEP pIL-12 sta učinkovit način zdravljenja pasjih kožnih, podkožnih in maksilofacialnih tumorjev. Kljub klinični učinkovitosti kombiniranega zdravljenja z EKT in GEP pIL-12 pa še vedno manjkajo podatki o parametrih, ki bi lahko napovedali izid zdravljenja. Cilj te raziskave je bil raziskati, ali se rezultati UZ-KS podkožnih tumorjev razlikujejo med tumorji, ki so se odzvali s popolnim odgovorom, in tumorji, ki se niso odzvali popolnoma pri psih, zdravljenih z EKT in GEP pIL-12. Zdravili smo osem psov s skupno 12 tumorji. Preiskave UZ-KS so bile opravljene pri vseh živalih pred in takoj po terapiji ter čez 8 ur in 1., 3. in 7. dan. Nadaljnji klinični pregledi so bili opravljeni 7. in 14. dan, ter 1 in 6 mesecev ter 1 leto po zdravljenju. Opažene so bile številne pomembne razlike v parametrih UZ-KS med tumorji s popolnim odgovorom in tumorji brez popolnega odgovora; perfuzija in heterogenost perfuzije sta bili pri tumorjih s popolnim odgovorom značilno nižji kot pri tumorjih, ki se niso odzvali popolnoma. Potrebne so raziskave z večjim številom psov, da bi ugotovili, ali je mogoče rezultate UK-KS uporabiti za napovedovanje izidov zdravljenja in za učinkovito odločanje o potrebi po ponavljajočem se zdravljenju ali različnih kombinacijah zdravljenja pri posameznih psih.

frontiers in Veterinary Science

ORIGINAL RESEARCH
published: 20 May 2021
doi: 10.3389/fvets.2021.679073

Results of Dynamic Contrast-Enhanced Ultrasound Correlate With Treatment Outcome in Canine Neoplasia Treated With Electrochemotherapy and Interleukin-12 Plasmid Electrotransfer

*Maja Brloznik[1], Simona Kranjc Brezar[2,3], Nina Boc[4], Tanja Knific[5], Maja Cemazar[2,6], Nina Milevoj[1], Gregor Sersa[2,7], Natasa Tozon[1] and Darja Pavlin[1]**

[1] Veterinary Faculty, Small Animal Clinic, University of Ljubljana, Ljubljana, Slovenia, [2] Department of Experimental Oncology, Institute of Oncology Ljubljana, Ljubljana, Slovenia, [3] Faculty of Medicine, University of Ljubljana, Ljubljana, Slovenia, [4] Department of Radiology, Institute of Oncology Ljubljana, Ljubljana, Slovenia, [5] Institute of Food Safety, Feed and Environment, Veterinary Faculty, University of Ljubljana, Ljubljana, Slovenia, [6] Faculty of Health Sciences, University of Primorska, Izola, Slovenia, [7] Faculty of Health Sciences, University of Ljubljana, Ljubljana, Slovenia

OPEN ACCESS

Edited by:
Tommaso Banzato,
University of Padua, Italy

Reviewed by:
Andrej Cör,
Orthopaedic Hospital Valdoltra, Slovenia
Takehiko Kakizaki,
Kitasato University, Japan

***Correspondence:**
Darja Pavlin
darja.pavlin@vf.uni-lj.si

Specialty section:
This article was submitted to Veterinary Imaging, a section of the journal Frontiers in Veterinary Science

Received: 10 March 2021
Accepted: 09 April 2021
Published: 20 May 2021

Citation:
Brloznik M, Kranjc Brezar S, Boc N, Knific T, Cemazar M, Milevoj N, Sersa G, Tozon N and Pavlin D (2021) Results of Dynamic Contrast-Enhanced Ultrasound Correlate With Treatment Outcome in Canine Neoplasia Treated With Electrochemotherapy and Interleukin-12 Plasmid Electrotransfer. Front. Vet. Sci. 8:679073. doi: 10.3389/fvets.2021.679073

Electrochemotherapy (ECT) and/or gene electrotransfer of plasmid DNA encoding interleukin-12 (GET pIL-12) are effective treatments for canine cutaneous, subcutaneous, and maxillofacial tumors. Despite the clinical efficacy of the combined treatments of ECT and GET, data on parameters that might predict the outcome of the treatments are still lacking. This study aimed to investigate whether dynamic contrast-enhanced ultrasound (DCE-US) results of subcutaneous tumors differ between tumors with complete response (CR) and tumors without complete response (non-CR) in dogs treated with ECT and GET pIL-12. Eight dogs with a total of 12 tumor nodules treated with ECT and GET pIL-12 were included. DCE-US examinations were performed in all animals before and immediately after therapy as well as 8 h and 1, 3, and 7 days later. Clinical follow-up examinations were performed 7 and 14 days, 1 and 6 months, and 1 year after treatment. Numerous significant differences in DCE-US parameters were noted between tumors with CR and non-CR tumors; perfusion and perfusion heterogeneity were lower in CR tumors than in non-CR tumors. Therefore, studies with larger numbers of patients are needed to investigate whether DCE-US results can be used to predict treatment outcomes and to make effective decisions about the need for repeated therapy or different treatment combinations in individual patients.

Keywords: dog, contrast-enhanced ultrasonography, electrochemotherapy, immunotherapy, gene electrotransfer, bleomycin, cisplatin, IL-12 plasmid

INTRODUCTION

Dynamic contrast-enhanced ultrasound (DCE-US) is a simple, readily available, non-invasive, safe, and inexpensive method for assessing tissue perfusion at the capillary level and correlates with histological results of vessel density in preclinical (1–3) and clinical studies (4–7). Moreover, DCE-US has been used to predict the efficacy of antiangiogenic treatments of various tumors in preclinical (3) and human clinical trials (8–17), whereas DCE-US had no predictive value in canine tumors treated with radiotherapy (18). Furthermore, DCE-US results correlated with the results of advanced diagnostic imaging (19). The contrast agents used in DCE-US are gas-filled microbubbles stabilized in a lipoprotein shell that have a diameter of 1–3 μm, which is small enough to migrate freely through the circulation and large enough to remain in the vascular space (20–22). Capillary filling results in diffuse enhancement of perfused tissue. Most of the contrast agent is excreted through the lungs within 20 min after administration (23). The advantages of contrast agents used in DCE-US over those used in dynamic contrast-enhanced computed tomography (DCE-CT) are numerous: the contrast agents allow real-time imaging, there is no ionizing radiation, they are neither nephro- nor hepatotoxic, and they have very few, very mild side effects (22–24). In humans, contraindications to microbubble administration include pulmonary hypertension and impaired cardiopulmonary function (24). In a large number of dogs in which DCE-US examinations were performed, <1% developed an immediate effect, including vomiting and/or syncope, or delayed adverse effects, including vomiting (23).

Electrochemotherapy (ECT) and/or gene electrotransfer of plasmid DNA encoding interleukin-12 (GET pIL-12) are effective treatments for cutaneous, subcutaneous and maxillofacial tumors in dogs (25–41), superficial cell carcinoma in cats (42), cutaneous tumors in ferrets (43) and sarcoid tumors in horses (44, 45). Several preclinical (46–49) and clinical studies in veterinary patients (26–28, 33, 36, 50) have shown that the effect of ECT is potentiated by GET pIL-12, and ECT has become an established standard of care for a variety of human cancers: cutaneous and subcutaneous tumors, including melanoma, squamous cell carcinoma, basal cell carcinoma, and other metastases (51–58); hepatocellular carcinoma and colorectal liver metastases (59–63); pancreatic neoplasia (64–66); and others. A portion of the antitumor efficacy of electroporation (EP)-based therapies arises from the effect of EP on the vasculature of the treated tumor, inducing a local blood flow effect, namely, "vascular lock," i.e., small blood vessel vasoconstriction and increased wall permeabilization (67–74). The vascular effects of EP are enhanced by the use of chemotherapeutic agents in ECT treatment, and the effect lasts longer in tumors than in healthy tissue, namely, the "vascular disrupting effect" (67, 68, 72).

Despite the clinical efficacy of the combined treatments of ECT and GET pIL-12, there is still a lack of data on parameters that might predict the outcome of the treatments. For EP-based treatments, it could be assumed that the therapy should be repeated if it does not reflect in the expected "vascular lock" immediately after the treatment and/or anti-angiogenic effects in the days after.

This pilot study aimed to investigate whether the DCE-US results from subcutaneous tumors correlate with treatment outcomes in dogs treated with ECT combined with GET pIL-12.

MATERIALS AND METHODS

Design and Setting

Eight dogs (seven females and one male) with a total of 12 superficial tumor nodules (11 mast cell tumors and 1 neurofibrosarcoma) treated with ECT and GET pIL-12 were included (**Table 1**). Their mean age with standard deviation was 8.0 ± 2.3 years. Six dogs had one tumor, and two dogs had three tumors. Each nodule was measured in three perpendicular directions (a, b, c), and tumor volume was calculated using the formula: $V = a \times b \times c \times \pi/6$. Owners of the dogs signed an informed consent form before inclusion.

ECT Combined With GET pIL-12

The procedures were performed under general anesthesia: the dogs received 0.2 mg/kg midazolam (Midazolam Torrex, Torrex Pharma GesmbH, Vienna, Austria) intravenously, and anesthesia was induced by 3–6 mg/kg propofol (Diprivan, Zeneca, Grangemouth, United Kingdom) administered intravenously and maintained with isoflurane (Isoflurin, Vetpharma Animal Health, Barcelona, Spain). All patients received fluid therapy throughout the procedure by administering Hartmann's solution (B Braun Melsungen AG, Melsungen, Germany) at a rate of 5 mL/kg/h.

An electrical pulse generator, CliniporatorTM (IGEA s.r.l., Carpi, Italy), was used to deliver electrical pulses through either plate, hexagonal, or needle electrodes. The selection of electrode type, voltage, duration, and frequency of the electrical pulses was based on ECT (23, 35, 48–52) and GET studies (25–28, 33) (**Table 2**).

For the ECT procedure, two dogs received bleomycin (Blenoxane, Bristol-Myers, NY, USA) at a concentration of 3 mg/mL intravenously at a dose of 0.3 mg/kg, and six dogs received cisplatin (cis-diammine dichloroplatin II, Cisplatin Accord 1 mg/mL, Accord Health Care, Warsaw, Poland) at a concentration of 1 mg/mL and at a dose of 1 mg/cm^3 intratumorally (**Table 2**).

For the GET procedure, the pCMVcaIL-12 plasmid encoding canine IL-12 was used, isolated using the Qiagen Endo-Free kit (Qiagen, Hilden, Germany), and diluted to a concentration of 1 mg/mL in endotoxin-free water (Qiagen). Quality control and quantification were performed (28). The plasmid was injected at a dose of 2 mg per patient (27, 28, 33) peritumorally in two dogs and intratumorally in six dogs (**Table 2**). When more than one tumor was present in a patient, the dose of pIL-12 was divided among the tumors proportional to the tumor volume (**Table 2**).

DCE-US

DCE-US examinations were performed in all animals before and immediately after therapy as well as 8 h and 1, 3, and 7 days later (**Figure 1**). For the first two measurements, the dogs were under general anesthesia (described above for ECT combined with GET) but were awake for the DCE-US measurements at 8 h and 1, 3, and 7 days after therapy. The contrast agent Sonovue

TABLE 1 | Characteristics of the eight dogs treated with electrochemotherapy (ECT) combined with gene electrotransfer of plasmid DNA encoding canine interleukin-12 (GET pIL-12).

Patient no.	Age	Sex	Breed	Weight (kg)	Tumor	No of tumors	Tumor volume (cm^3)
1	9 y 11 m	Female	Mixed breed	25.0	Mast cell tumor	1	0.38
2	9 y 7 m	Female	German hunting terrier	11.3	Mast cell tumor	3	0.04; 0.004; 0.01
3	9 y 10 m	Female	Beagle	17.3	Neurofibrosarcoma	1	23.00
4	10 y 8 m	Female	Mixed breed	34.4	Mast cell tumor	3	1.10; 0.10; 0.004
5	6 y 5 m	Female	Basset hound	29.0	Mast cell tumor	1	5.00
6	4 y 10 m	Female	Golden retriever	34.2	Mast cell tumor	1	0.92
7	5 y 11 m	Male	Boston terrier	10.7	Mast cell tumor	1	0.37
8	6 y 7 m	Female	Bernese mountain dog	40.3	Mast cell tumor	1	0.27

TABLE 2 | Electrochemotherapy (ECT) combined with gene electrotransfer of plasmid DNA encoding canine interleukin-12 (GET pIL-12) treatment regimens (dosages, route of administration, type of electrodes and pulse parameters) and outcome per patient.

Patient no.	ECT					GET pIL12			Outcome
	Drug	Dose (mg)	Administration	Type of electrodes	Pulse parameters	pIL-12 administration (2 mg)	Type of electrodes	Pulse parameters	
1	BLM	6.90	i.v.	Plate	ECT pulses	p.t.	MEA	GET pulses	CR
2	CDDP	T1: 0.60	i.t.	Plate	ECT pulses	p.t.	MEA	GET pulses	Non-CR (PD)
		T2: 0.20							Non-CR (PD)
		T3: 0.20							CR
3	CDDP	12.00	i.t.		/	i.t.	Hexagonal	ECT pulses	Non-CR (PR)
4	BLM	10.47	i.v.		/	i.t.	Hexagonal	ECT pulses	Non-CR (PD)
									CR
									CR
5	CDDP	5.00	i.t.		/	i.t.	Hexagonal	ECT pulses	CR
6	CDDP	0.90	i.t.		/	i.t.	Hexagonal	ECT pulses	CR
7	CDDP	0.37	i.t.		/	i.t.	Needle	ECT pulses	Non-CR (PR)
8	CDDP	0.27	i.t.		/	i.t.	Plate	ECT pulses	CR

BLM, bleomycin; CDDP, cisplatin; i.v., intravenously; i.t., intratumorally; p.t., peritumorally; T, tumor nodule; ECT pulses, 8 pulses of 100 μs duration with an amplitude to electrode distance ratio of 1,300 V/cm and a frequency of repetition of 5 kHz; GET pulses = 150 ms pulse of amplitude 170 V/cm; / = electroporation was performed simultaneously for ECT and GET; CR, tumor with complete response; MEA, multielectrode array; non-CR, tumor without complete response; PD, progressive disease; PR, partial response.

FIGURE 1 | Schedule for electrochemotherapy combined with gene electrotransfer of plasmid DNA encoding interleukin IL-12 (ECT+GET), dynamic contrast-enhanced ultrasound (DCE-US) examinations and clinical follow-up examinations, which included tumor volume measurement.

(Bracco, Milan, Italy) was administered into the cephalic vein at dose 0.5–1.5 mL per dog, depending on the weight of the animal (<10 kg: 0.06 mL/kg, 10–20 kg: 0.05 mL/kg, 20–30 kg: 0.04 mL/kg, and >30 kg: 0.03 mL/kg).

Ultrasound examinations were performed with a Resona 7 ultrasound scanner and a linear probe L11-3u with a frequency of 3–10 MHz (Mindray, Shenzhen, China). Low mechanical index harmonic non-linear ultraband contrast imaging was used. From

the time of contrast application, a 90-s recording was made. The Dicom files of the examinations were imported into the free software Vuebox^{TM} (Bracco, Milan, Italy) to quantify tissue perfusion with DCE-US. Each tumor was carefully delineated, and two additional regions of interest (ROIs), each representing half of the tumor and the reference region representing the tissue below the tumor, were drawn. The arrival time of the contrast agent was manually selected. For each of the perfusion or time-intensity curves representing signal intensity over time, the following was recorded: basic intensity (BI) when no contrast agent was present, peak intensity (PI), and time to peak (TTP) in ms, the time at which the contrast intensity reached its peak. PE (peak enhancement) was calculated as the difference between PI and BI.

The dogs were closely monitored for adverse effects of contrast administration: vomiting, respiratory distress, syncope, nausea, and other effects. The dogs were hospitalized for the first three measurements. For the last three measurements, the dogs were monitored as outpatients for immediate effects (<1 h) and by the owner for delayed effects.

Clinical Follow-Up Examinations

Clinical follow-up examinations that included measurement of the three perpendicular tumor dimensions were performed at 7 and 14 days, 1 and 6 months and 1 year after treatment (**Figure 1**). Tumors were classified as having a complete response (CR) or not having a complete response (non-CR) with the latter including partial response (at least 30% decrease in tumor size), progressive disease (>20% increase in tumor size), and stable disease (neither sufficient shrinkage to qualify for partial response nor sufficient increase to qualify for progressive disease) according to RECIST (75) and iRECIST (76) criteria.

Statistical Analysis

Statistical software R, version 3.6.2, was used for the statistical analysis (77). The parameters of interest are defined in **Table 3**.

The normality of the data was tested using the Shapiro Wilk test. Data were not normally distributed; therefore, the comparison between CR and non-CR tumors for each variable was calculated using the Wilcoxon rank-sum test. Statistical significance was set at 5%.

RESULTS

Response to Therapy

The size of the tumors varied from 0.004 to 23.0 cm^3 (median 0.32 cm^3). The median baseline tumor volume did not differ between CR and non-CR tumors. Furthermore, none of the DCE-US parameters correlated with pretherapy tumor volume.

There were seven tumors with CR in six dogs: dogs 1, 2, 4, 5, 6, and 8. Clinical follow-up examination of the tumor of dog 1 is presented in **Figure 2**. There were five tumors without CR in four dogs (dogs 2, 3, 4, and 7; **Table 2**). Three of the non-CR tumors were classified as progressive disease, and two showed a partial response (**Table 2**).

No adverse effects of contrast administration were noted in our study.

DCE-US Results

The PE values were significantly lower in tumors with CR than in tumors with non-CR at all time points after therapy, except on day 3 (**Figure 3**). The difference in PE between CR and non-CR tumors was highest 8 h after therapy and gradually decreased in the following days but remained statistically significant on days 3 and 7. Note that the CR tumors showed no contrast enhancement immediately and 8 h after therapy; this finding is in contrast to non-CR tumors, which were still filled with microbubbles (**Figure 4**).

The PE ratio (**Table 3**) was significantly reduced in CR tumors compared to non-CR tumors immediately, 8 h and 7 days after therapy. The difference steadily increased over time, reaching a 45-fold decrease by day 7 (**Figure 5**).

The PE change (**Table 3**) was significantly reduced in CR tumors at four time points: immediately, 8 h, and 1 and 7 days after therapy. The highest difference between the two tumor groups (20-fold decrease) was observed immediately after therapy. With time, the difference decreased but remained statistically significant (**Figure 6**).

The percentage change in TTP from baseline TTP (TTP ch) was more than three times greater 7 days after therapy in tumors with CR than in tumors without CR (**Figure 7**) because TTP increased from baseline in CR tumors and decreased from baseline in non-CR tumors.

The percentage difference in the change in PE between the two parts of the tumor (PE_{ROI} dif_{ch}), which describes tumor heterogeneity in PE, was more than 10–13 times lower immediately, 8 h and 3 days after therapy in tumors with CR compared to tumors with non-CR (**Figure 8**).

The parameters TTP, TTP_{ROI} dif, PE_{ROI} dif, and TTP ratio (**Table 3**) were not significantly different between CR and non-CR tumors.

When results for both groups (CR vs. non-CR tumors) regardless of the time were compared, PE, PE ratio, PE ch, TTP_{ROI} dif, and TTP_{ROI} dif_{ch} were significantly lower, and TTP ch was significantly higher in tumors with CR than in tumors with non-CR (**Tables 3**, **4**).

DISCUSSION

This study shows a significant difference in DCE-US results between canine tumors that achieved a CR to ECT combined with GET pIL-12 and non-CR tumors. After therapy, perfusion of tumors was lower in the CR group, and perfusion heterogeneity was greater in non-CR tumors.

To the best of our knowledge, this is the first study to compare DCE-US results with treatment outcomes in canine tumors treated with ECT combined with GET pIL-12. Our results are consistent with human studies that have shown DCE-US results to be a useful tool for predicting the efficacy of other antiangiogenic treatments in metastatic renal cell carcinoma, advanced hepatocellular carcinoma, colorectal carcinoma, metastatic breast cancer, gastrointestinal stromal

TABLE 3 | Definition of tumor volume and dynamic contrast-enhanced ultrasound parameters (DCE-US) and their calculation.

Parameter	Symbol	Calculation
Volume of tumor before the treatment (cm^3)	V	a × b × c × π/6 (a,b,c = perpendicular tumor dimensions)
Peak enhancement	PE	= Peak Intensity (PI) – Basic Intensity (BI)
Time to peak	TTP	
Ratio between PE of the tumor and PE of the reference (PE_{ref})	*PE ratio*	$= \frac{PE}{PE_{ref}}$
Ratio between TTP of the tumor and TTP of the reference	*TTP ratio*	$= \frac{TTP}{TTP\ ref}$
Percentage change in PE	*PE ch*	$= \frac{PE_t}{PE_{t0}} \times 100 - 100$
Percentage change in TTP	*TTP ch*	$= \frac{TTP_t}{TTP_{t0}} \times 100 - 100$
Percentage difference in PE between ROI1 and ROI2	PE_{ROI} *dif*	$= \frac{PE_{ROI1} - PE_{ROI2}}{(PE_{ROI1} + PE_{ROI2})/2} \times 100$
Percentage difference in TTP between ROI1 and ROI2	TTP_{ROI} *dif*	$= \frac{TTP_{ROI1} - TTP_{ROI2}}{(TTP_{ROI1} - TTP_{ROI2})/2} \times 100$
Percentage difference in change of PE between ROI1 and ROI2	PE_{ROI} dif_{ch}	$= \frac{PE\ ch_{ROI1} - PE\ ch_{ROI2}}{(PE\ ch_{ROI1} + PE\ ch_{ROI2})/2} \times 100$
Percentage difference in change of TTP between ROI1 and ROI2	TTP_{ROI} dif_{ch}	$= \frac{TTP\ ch_{ROI1} - TTP\ ch_{ROI2}}{(TTP\ ch_{ROI1} - TTP\ ch_{ROI2})/2} \times 100$

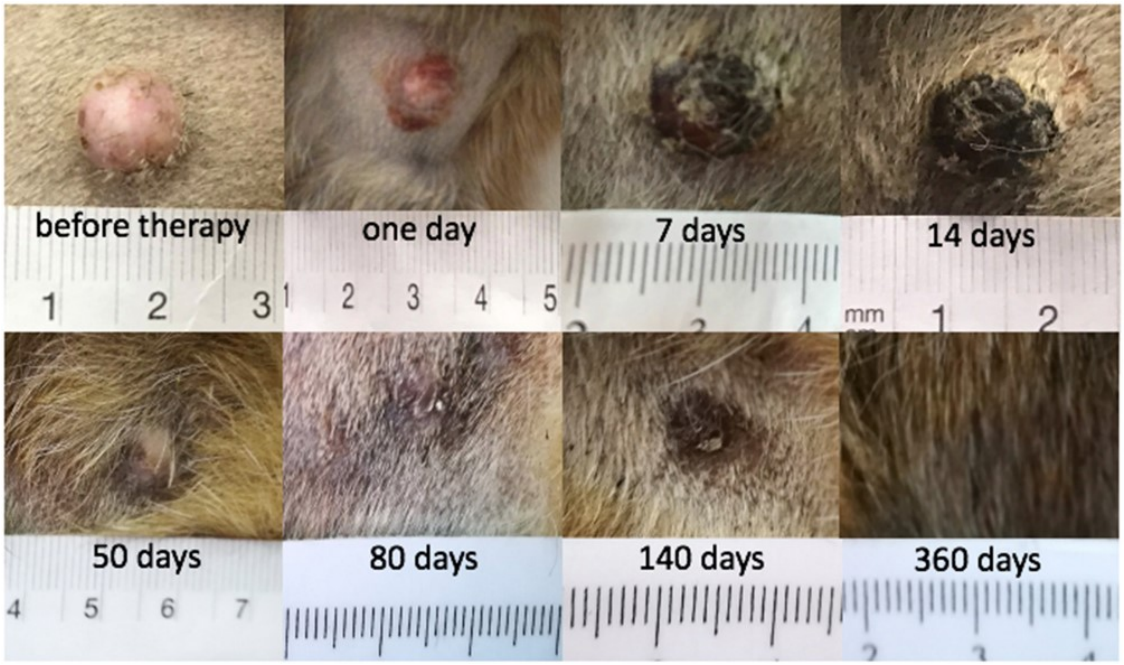

FIGURE 2 | Mast cell tumor in dog 1 where a complete response (CR) was achieved after electrochemotherapy (ECT) combined with gene electrotransfer of plasmid DNA encoding interleukin IL-12 (GET pIL-12).

tumors, and metastatic melanoma (9–11, 14–16). Tumors included in this study were compared between the two groups regarding tumor perfusion and perfusion heterogeneity. Before therapy, no differences in perfusion parameters and perfusion heterogeneity were noted between CR and non-CR tumors. Perfusion decreased after therapy in all CR tumors, which is consistent with previously described vascular lock and vascular disrupting action of EP-based therapies (63–74). The decrease in tumor perfusion was greater in CR compared with non-CR tumors, supporting the assumption that therapy is more likely to be effective if it is reflected in immediate "vascular lock." Furthermore, the difference remained statistically significant until day 7 with the exception of day 3. This finding is consistent with the expectation that the outcome of therapy is less likely to be favorable when therapy does not show antiangiogenic effects that result in decreased perfusion in the days after treatment. A similar trend was observed on day 3. However, due to owner non-compliance and thus missing data from one dog with three tumors, the difference was not statistically significant.

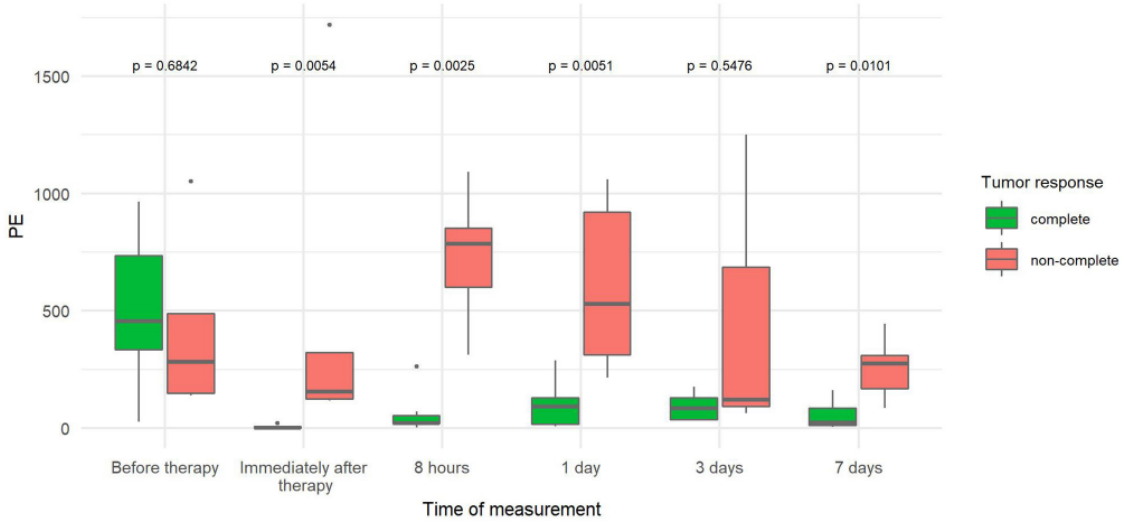

FIGURE 3 | Comparison of peak enhancement (PE) at different time points between canine tumors with complete (CR) and non-complete (non-CR) responses to combined electrochemotherapy treatment with gene electrotransfer of plasmid DNA encoding interleukin IL-12 (ECT GET pIL-12). Note the *p*-values presented at the top of the image. Note that PE is significantly lower for complete response tumors than for non-complete response tumors at all time points after therapy except at 3 days.

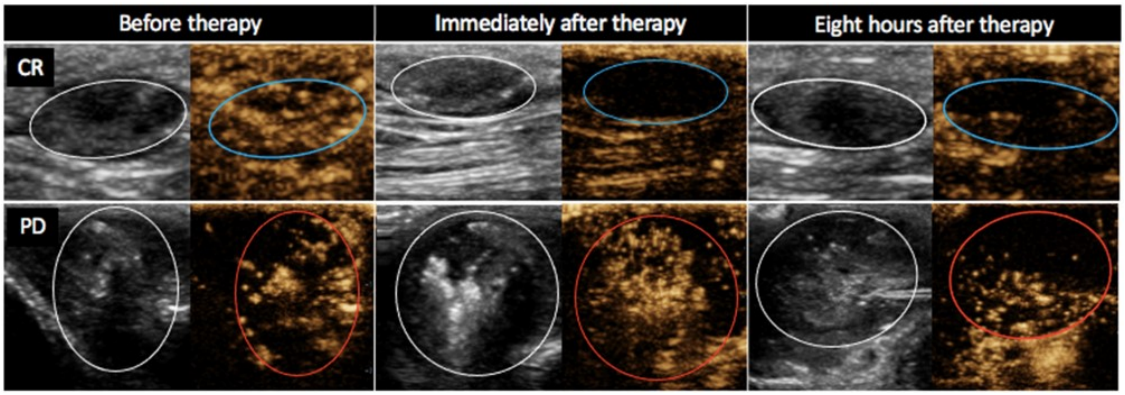

FIGURE 4 | Contrast-enhanced ultrasound images (B mode image to the left and non-linear contrast mode to the right of each image) of two mast cell tumors in dog 4. Images were obtained 20 s after contrast administration at different time points after electrochemotherapy (ECT) combined with gene electrotransfer of plasmid DNA encoding interleukin IL-12 (GET pIL-12) as noted at the top of the figure. Note the difference between tumors with complete response (CR) and tumors with progressive disease (PD) after therapy. Non-CR tumors (red circles) are filled with microbubbles, whereas CR tumors (blue circles) show no contrast enhancement immediately and 8 h after therapy.

In a study of nine spontaneous canine tumors treated with GET pIL-12 (25), a significant decrease in the DCE-US parameters wash-in area under the curve describing relative blood volume and wash-in rate describing blood flow velocity was observed at days 8 and 35 compared to baseline, consistent with the results of our study. Similar parameters reflecting relative blood volume and blood flow velocity, namely PE and TTP, respectively, were investigated by the same authors in a study of five dogs treated with GET pIL-12 in combination with metronomic cyclophosphamide (30). They observed a significant decrease in PE and prolonged TTP 35 days after treatment, which is consistent with our results, while in contrast to our results, an increase in PE was observed 8 days after treatment. The difference in the dynamics of PE can most likely be attributed to the fact that the study by Cicchelero et al. (30) investigated GET pIL-12 (without ECT), which does not

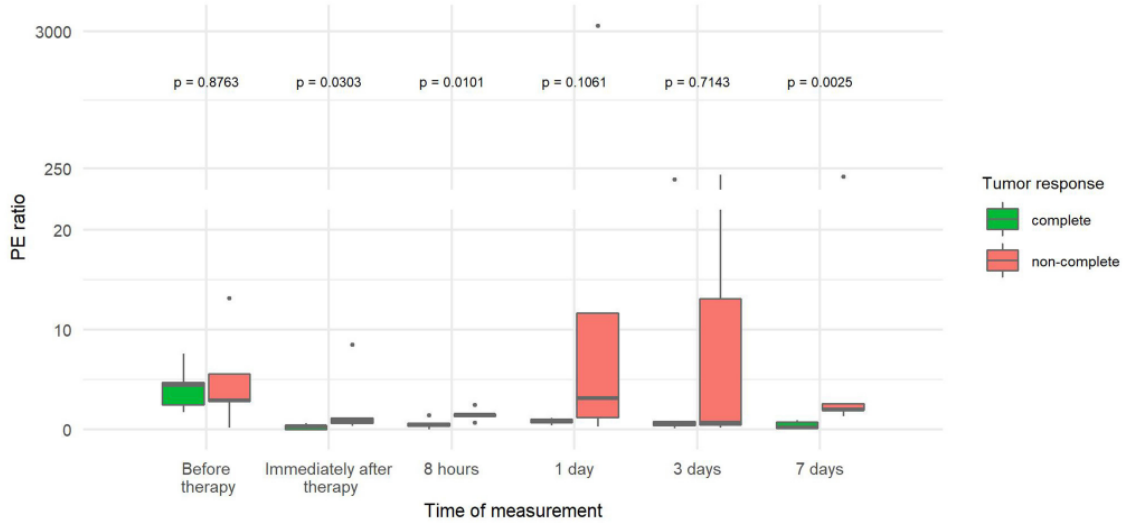

FIGURE 5 | Comparison of ratios between tumor peak enhancement and reference peak enhancement (PE ratio) at different time points between canine tumors with a complete and non-complete response to electrochemotherapy (ECT) with gene electrotransfer of plasmid DNA encoding interleukin IL-12 (GET pIL-12). Note the *p*-values presented at the top of the image. PE ratio is significantly lower for complete response tumors compared with non-complete response tumors immediately after therapy and at 8 h and 7 days.

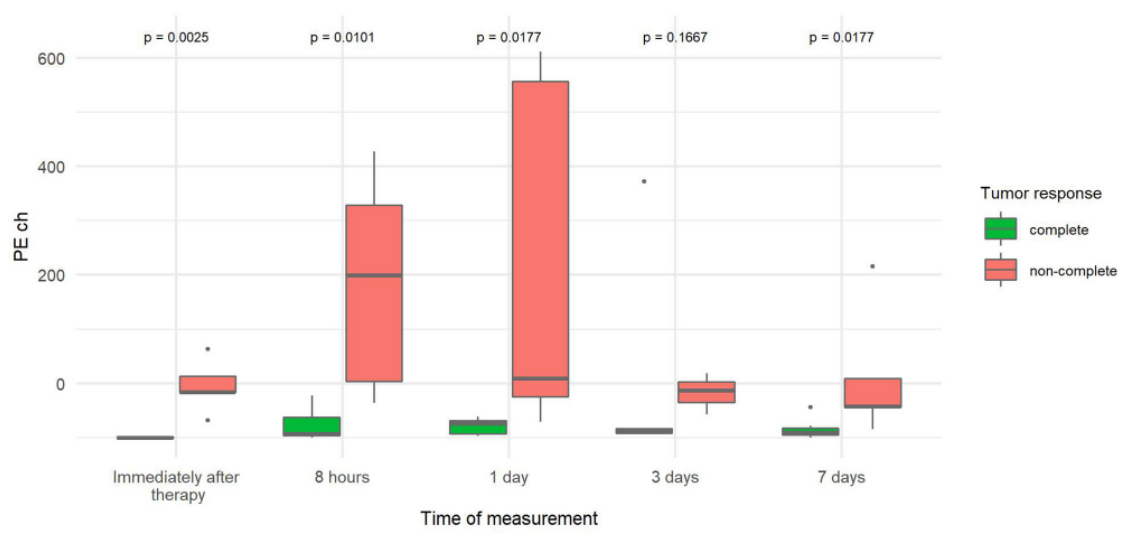

FIGURE 6 | Comparison of the percentage change in peak enhancement of tumor (PE ch) at different time points between canine tumors with a complete and non-complete response to electrochemotherapy (ECT) with gene electrotransfer of plasmid DNA encoding interleukin IL-12 (GET pIL-12). Note the *p*-values presented at the top of the image. PE ch is significantly lower for complete response tumors compared with non-complete response tumors immediately after therapy and at 8 h and 7 days.

induce a "vascular disrupting effect," i.e., cytotoxic effect of chemotherapeutic drugs on vascular endothelial cells (67, 68, 72) that can be observed after treatment with ECT. Treatment with GET pIL-12 results in a much less pronounced antitumor effect (27), also observed in this study, as no clinically relevant outcome was observed (30). However, it is likely that the decrease

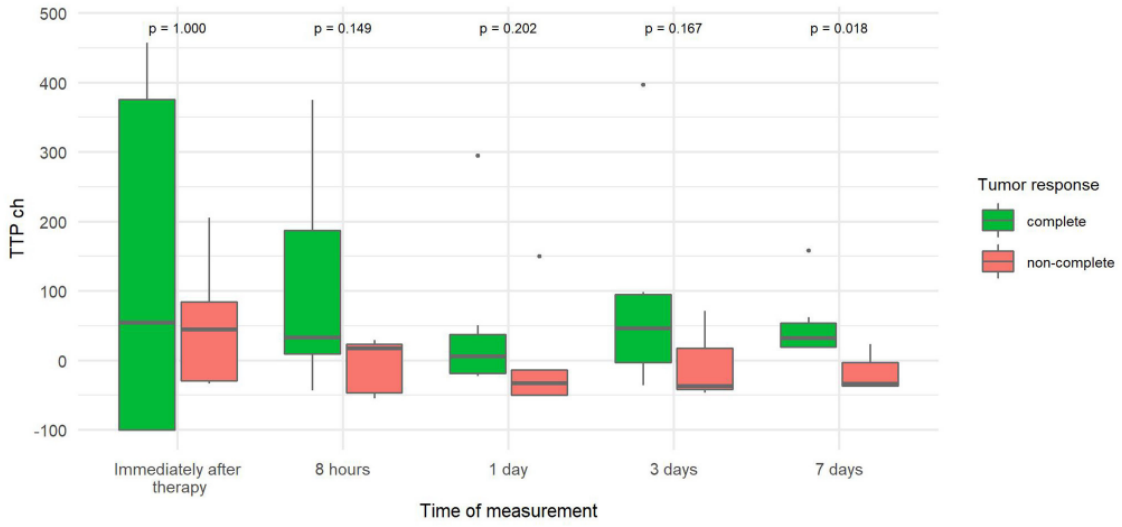

FIGURE 7 | Comparison of the percentage change in time to peak of tumor (TTP ch) at different time points canine tumors with complete and non-complete response to electrochemotherapy (ECT) with gene electrotransfer of plasmid DNA encoding interleukin IL-12 (GET pIL-12). Note the *p*-values presented at the top of the image. TTP ch is significantly lower for complete response tumors compared with non-complete response tumors 7 days after therapy.

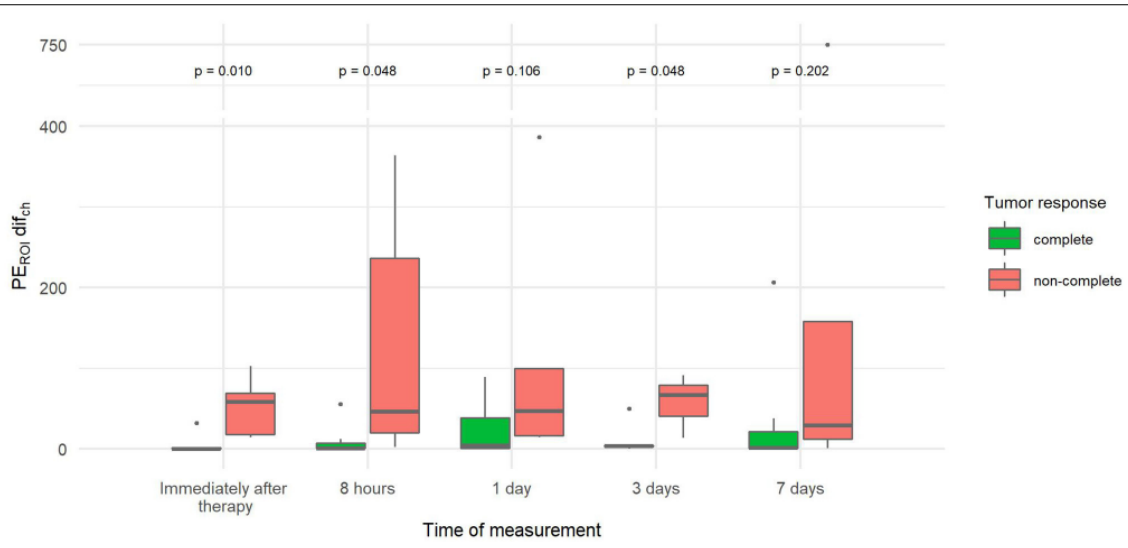

FIGURE 8 | Comparison of the percentage difference in change of peak enhancement of the two tumor parts (PE_{ROI} dif_{ch}) at different time points between canine tumors with a complete and non-complete response to electrochemotherapy (ECT) with gene electrotransfer of plasmid DNA encoding interleukin IL-12 (GET pIL-12). Note the *p*-values presented at the top of the image. PE_{ROI} dif_{ch} is significantly lower for complete response tumors compared with non-complete response tumors immediately after therapy and at 8 h and 3 days after therapy.

in PE and prolongation of TTP 35 days after treatment is a consequence of the antiangiogenic effect of gene therapy. An additional difference between our studies is also the fact that the latter study (30) included five different tumor types and DCE-US was performed only at three time points, i.e., before therapy and at days 8 and 35; our data cannot be directly compared because they were collected at different time points and after different treatments.

TABLE 4 | Comparison of overall results of dynamic contrast-enhanced ultrasound parameters (DCE-US) between tumors with complete response (CR) and tumors without complete response (non-CR) treated with electrochemotherapy (ECT) combined with gene electrotransfer (GET pIL-12).

Parameter		Tumor response		Wilcoxon rank sum test
		CR	Non-CR	
		Median (1st and 3rd quartile)	Median (1st and 3rd quartile)	*p*-value
V	Volume of tumor before the treatment (cm^3)	0.27 (0.06, 0.65)	0.37 (0.04, 1.10)	0.8072
PE	Peak enhancement	32.50 (14.87, 150.90)	312.56 (155.21, 803.50)	<0.0001
TTP	Time to peak	9.41 (6.70, 17.07)	8.90 (6.36, 13.42)	0.1242
PE ratio	Ratio between PE of the tumor and PE of the reference	0.64 (0.34, 1.10)	1.77 (0.84, 3.77)	<0.0001
TTP ratio	Ratio between TTP of the tumor and TTP of the reference	0.96 (0.57, 1.24)	0.79 (0.60, 1.29)	0.6926
PE ch	Percentage change in PE	−92.36 (−97.21, −79.13)	3.69 (−39.22, 131.43)	<0.0001
TTP ch	Percentage change in TTP	27.91 (−6.49, 94.75)	29.06 (−37.56, −26.51)	<0.0001
PE_{ROI} *dif*	Percentage difference in PE between ROI1 and ROI2	17.09 (5.81, 33.75)	30.20 (9.35, 38.07)	0.0892
TTP_{ROI} *dif*	Percentage difference in TTP between ROI1 and ROI2	5.71 (0.92, 15.69)	12.34 (7.02, 20.08)	0.0673
PE_{ROI} dif_{ch}	Percentage difference in change of PE between ROI1 and ROI2	1.59 (0.29, 10.15)	47.01 (15.34, 100.99)	<0.0001
TTP_{ROI} dif_{ch}	Percentage difference in change of TTP between ROI1 and ROI2	16.17 (11.06, 59.41)	50.00 (21.41, 130.35)	0.0577

A common feature of malignant tumors compared with non-malignant tumors is rapid wash-in (78, 79), which may be associated with shorter TTP. In our study, 7 days after therapy, the percentage change in TTP was greater in CR tumors, i.e., the time to peak increased significantly compared with the measurement before therapy, which may indicate that the tumors became "less malignant" with the treatment performed. These results are similar to those of human studies examining various chemotherapeutic antiangiogenic treatments, in which TTP and wash-in rate decreased after therapy (10, 17, 80). In a study of the efficacy of sorafenib treatment of metastatic renal cancer in humans, the correlation between treatment outcome and the percentage of perfused tissue decreased 3 weeks after treatment (15). In contrast, in studies evaluating DCE-US after radiotherapy for spontaneous tumors in dogs (18, 81), DCE-US results were not predictive of disease outcome. This difference can be explained by an important difference in the mechanism of action of radiotherapy compared to ECT combined with GET pIL-12. Radiotherapy is less efficient in regions of lower perfusion due to the resistance of hypoxic cells to treatment, whereas the presented EP-based treatment exerts antiangiogenic and cytotoxic effects that do not depend on cell oxygenation.

Perfusion heterogeneity is a hallmark of malignant tumors and provides valuable information for discriminating between malignant and benign lesions (82). We demonstrated a significant difference in perfusion heterogeneity between the two different groups based on the clinical response: tumors reaching CR were less heterogeneously perfused than non-CR tumors. This is an important finding as it indicates a possible predictive value of perfusion heterogeneity in therapies based on antiangiogenic effects. Similar results were obtained by DCE-CT in human hepatic neoplasia treated with antiangiogenic therapy; reduced perfusion heterogeneity correlated with better local tumor control and longer survival (83). In contrast, in human cervical cancer treated with radiotherapy and chemotherapy and evaluated with dynamic contrast-enhanced magnetic resonance imaging (DCE-MRI), decreased perfusion heterogeneity correlated with poorer outcomes due to a lower response to radiotherapy in those parts of the tumor that are hypoxic due to decreased perfusion (82). Therefore, perfusion and perfusion heterogeneity evaluated with DCE-US appear to be useful for predicting the results of antiangiogenic treatments but cannot be used for all types of anticancer therapy.

Investigation of perfusion is an appealing method to predict outcome in tumors treated with antiangiogenic therapies. Our results show that DCE-US is safe for the patient; no adverse effects of contrast administration were noted despite repeated administration. Furthermore, it is a simple method to assess tumor perfusion that can be easily repeated during and after treatment and, based on our study, is associated with treatment outcome in canine tumors treated with a combination of ECT and GET pIL-12. The next clinically applicable step would be to investigate the predictive ability of DCE-US to distinguish between tumors that were successfully treated and those in which the therapy is unlikely to lead to a complete response after EP-based therapies. This information would allow a clinician to perform such a therapeutic procedure on a patient to evaluate if and when the therapy should be repeated, preferably in the early stages of the treatment when targeted therapy adjustments are generally more effective. This was not possible in our study given that a much larger number of patients are needed for logistic regression models. If a predictive value is to be confirmed, appropriate cutoff values for DCE-US parameters should be ascertained to make effective decisions about prognosis and the need for repeated or additional therapy in individual patients.

DATA AVAILABILITY STATEMENT

The original contributions presented in the study are included in the article/supplementary material, further inquiries can be directed to the corresponding author/s.

ETHICS STATEMENT

The animal study was reviewed and approved by National Ethics Committee at the Administration of the Republic of Slovenia for Food Safety, Veterinary, and Plant Protection (U34401-24/2014/4). Written informed consent was obtained from the owners for the participation of their animals in this study.

AUTHOR CONTRIBUTIONS

DP, MC, GS, NT, and MB: conception and design. MB, NB, NM, and DP: acquisition of data. MB, NB, NM, TK, DP, and SKB: analysis and interpretation of data. MB, NB, DP, and SKB: drafting the article. GS, MC, NT, DP, and SKB: revising the article for intellectual content. All authors: final approval of the completed article.

FUNDING

The authors acknowledge the financial support of the Slovenian Research Agency (research program grant numbers P3-0003, P4-0053, and J3-6796). The funder had no role in the study design, data collection and analysis, decision to publish, or preparation of the manuscript.

ACKNOWLEDGMENTS

The authors are grateful to Miha Melinec and Tone Jamnik (DIPROS d.o.o.) for their assistance and ultrasonographic machines that enabled contrast studies. Furthermore, authors thank Urša Lampreht Tratar for second row of photos in **Figure 2**. Language editing services for this manuscript were provided by American Journal Experts.

REFERENCES

1. Donelly EF, Geng L, Wojcicki WE, Fleischer AC, Hallahan DE. Quantified power Doppler US of tumor blood flow correlates with microscopic quantification of tumor blood vessels. *Radiology.* (2001) 219:166–70. doi: 10.1148/radiology.219.1.r01ap38166
2. Zhou JH, Cao LH, Liu JB, Zheng W, Liu M, Luo RZ, et al. Quantitative assessment of tumor blood flow in mice after treatment with different doses of an antiangiogenic agent with contrast-enhanced destruction-replenishment US. *Radiology.* (2011) 259:406–13. doi: 10.1148/radiol.10101339
3. Zhou JH, Cao LH, Zheng W, Liu M, Han F, Li AH. Contrast-enhanced gray-scale ultrasound for quantitative evaluation of tumor response to chemotherapy: preliminary results with a mouse hepatoma model. *AJR Am J Roentgenol.* (2011) 196:W13–7. doi: 10.2214/AJR.10.4734
4. Sedelaar JP, van Leenders GJ, Hulsbergen-van de Kaa CA, van der Poel HG, van der Laak JA, Debruyne FM, et al. Microvessel density: correlation between contrast ultrasonography and histology of prostate cancer. *Eur Urol.* (2001) 40:285–93. doi: 10.1159/000049788
5. Leng X, Huang G, Ma F, Yao L. Regional Contrast-Enhanced Ultrasonography (DCE-US) characteristics of breast cancer and correlation with Microvessel Density (MVD). *Med Sci Monit.* (2017) 23:3428–36. doi: 10.12659/MSM.901734
6. Li X, Li Y, Zhu Y, Fu L, Liu P. Association between enhancement patterns and parameters of contrast-enhanced ultrasound and microvessel distribution in breast cancer. *Oncol Lett.* (2018) 15:5643–9. doi: 10.3892/ol.2018.8078
7. Ohlerth S, Wergin M, Bley CR, Del Chicca F, Laluhová D, Hauser B, et al. Correlation of quantified contrast-enhanced power Doppler ultrasonography with immunofluorescent analysis of microvessel density in spontaneous canine tumours. *Vet J.* (2010) 183:58–62. doi: 10.1016/j.tvjl.2008.08.026
8. Lassau N, Chebil M, Chami L. A new functional imaging technique for the early functional evaluation of antiangiogenic treatment: dynamic contrast-enhanced ultrasonography (DCE-US). *Target Oncol.* (2008) 3:111–7. doi: 10.1007/s11523-008-0081-x
9. Lassau N, Chebil M, Chami L, Bidault S, Girard E, Roche A. Dynamic contrast-enhanced ultrasonography (DCE-US): a new tool for the early evaluation of antiangiogenic treatment. *Target Oncol.* (2010) 5:53–8. doi: 10.1007/s11523-010-0136-7
10. Lassau N, Koscielny S, Chami L, Chebil M, Benatsou B, Roche A, et al. Advanced hepatocellular carcinoma: early evaluation of response to bevacizumab therapy at dynamic contrast-enhanced US with quantification - preliminary results. *Radiology.* (2011) 258:291–300. doi: 10.1148/radiol.10091870
11. Lassau N, Chapotot L, Benatsou B, Vilgrain V, Kind M, Lacroix J, et al. Standardization of dynamic contrast-enhanced ultrasound for the evaluation of antiangiogenic therapies: the French multicenter Support for Innovative and Expensive Techniques Study. *Invest Radiol.* (2012) 47:711–66. doi: 10.1097/RLI.0b013e31826dc255
12. Lassau N, Cosgrove D, Armand JP. Early evaluation of targeted drugs using dynamic contrast-enhanced ultrasonography for personalized medicine. *Future Oncol.* (2012) 8:1215–8. doi: 10.2217/fon.12.114
13. Lassau N, Bonastre J, Kind M, Vilgrain V, Lacroix J, Cuinet M, et al. Validation of dynamic contrast-enhanced ultrasound in predicting outcomes of antiangiogenic therapy for solid tumors: the French multicenter support for innovative and expensive techniques study. *Invest Radiol.* (2014) 49:794–800. doi: 10.1097/RLI.0000000000000085
14. Lassau N, Coiffier B, Kind M, Vilgrain V, Lacroix J, Cuinet M, et al. Selection of an early biomarker for vascular normalization using dynamic contrast-enhanced ultrasonography to predict outcomes of metastatic patients treated with bevacizumab. *Ann Oncol.* (2016) 27:1922–8. doi: 10.1093/annonc/mdw280
15. Lamuraglia M, Escudier B, Chami L, Schwartz B, Leclere J, Roche A, et al. To predict progression-free survival and overall survival in metastatic renal cancer treated with sorafenib: pilot study using dynamic contrast-enhanced Doppler ultrasound. *Eur J Cancer.* (2006) 42:2472–9. doi: 10.1016/j.ejca.2006.04.023
16. Escudier B, Lassau N, Angevin E, Soria JC, Chami L, Lamuraglia M, et al. Phase I trial of sorafenib in combination with IFN alpha-2a in patients with unresectable and/or metastatic renal cell carcinoma or malignant melanoma. *Clin Cancer Res.* (2007) 13:1801–9. doi: 10.1158/1078-0432.CCR-06-1432
17. Kim Y, Kim SH, Song BJ, Kang BJ, Yim KI, Lee A, et al. Early prediction of response to neoadjuvant chemotherapy using Dynamic Contrast-Enhanced MRI and Ultrasound in breast cancer. *Korean J Radiol.* (2018) 19:682–91. doi: 10.3348/kjr.2018.19.4.682
18. Rohrer Bley C, Laluhova D, Roos M, Kaser-Hotz B, Ohlerth S. Correlation of pretreatment polarographically measured oxygen pressures with quantified contrast-enhanced power doppler ultrasonography in spontaneous canine tumors and their impact on outcome after radiation therapy. *Strahlenther Onkol.* (2009) 185:756–62. doi: 10.1007/s00066-009-1988-6
19. Nierman KJ, Fleischer AC, Huamani J, Yankeelov TE, Kim DW, Wilson WD, et al. Measuring tumor perfusion in control and treated murine tumors: correlation of microbubble contrast-enhanced sonography to dynamic contrast-enhanced magnetic resonance imaging and fluorodeoxyglucose positron emission tomography. *J Ultrasound Med.* (2007) 26:749–56. doi: 10.7863/jum.2007.26.6.749
20. Denham SL, Alexander LF, Robbin ML. Contrast-enhanced ultrasound: practical review for the assessment of hepatic and renal lesions. *Ultrasound Q.* (2016) 32:116–25. doi: 10.1097/RUQ.0000000000000182
21. Fetzer DT, Rafailidis V, Peterson C, Grant EG, Sidhu P, Barr RG. Artifacts in contrast-enhanced ultrasound: a pictorial essay. *Abdom Radiol.* (2018) 43:977–97. doi: 10.1007/s00261-017-1417-8

22. Erlichman DB, Weiss A, Koenigsberg M, Stein MW. Contrast enhanced ultrasound: a review of radiology applications. *Clin Imaging.* (2019) 60:209–15. doi: 10.1016/j.clinimag.2019.12.013
23. Seiler GS, Brown JC, Reetz JA, Taeymans O, Bucknoff M, Rossi F, et al. Safety of contrast-enhanced ultrasonography in dogs and cats: 488 cases (2002-2011). *J Am Vet Med Assoc.* (2013) 242:1255–9. doi: 10.2460/javma.242.9.1255
24. Dolan MS, Gala SS, Dodla S, Abdelmoneim SS, Xie F, Cloutier D, et al. Safety and efficacy of commercially available ultrasound contrast agents for rest and stress echocardiography: a multicenter experience. *J Am Coll Cardiol.* (2009) 53:32–8. doi: 10.1016/j.jacc.2008.08.066
25. Cicchelero L, Denies S, Vanderperren K, Stock E, Van Brantegem L, de Rooster H, et al. Intratumoural interleukin 12 gene therapy stimulates the immune system and decreases angiogenesis in dogs with spontaneous cancer. *Vet Comp Oncol.* (2017) 15:1187–205. doi: 10.1111/vco.12255
26. Salvadori C, Svara T, Rocchigiani G, Millanta F, Pavlin D, Cemazar M, et al. Effects of electrochemotherapy with cisplatin and peritumoral il-12 gene electrotransfer on canine mast cell tumors: a histopathologic and immunohistochemical study. *Radiol Oncol.* (2017) 51:286–94. doi: 10.1515/raon-2017-0035
27. Pavlin D, Cemazar M, Cör A, Sersa G, Pogačnik A, Tozon N. Electrogene therapy with interleukin-12 in canine mast cell tumors. *Radiol Oncol.* (2011) 45:30–9. doi: 10.2478/v10019-010-0041-9
28. Milevoj N, Lampreht Tratar U, Nemec A, Brozic A, Znidar K, Sersa G, et al. A combination of electrochemotherapy, gene electrotransfer of plasmid encoding canine IL-12 and cytoreductive surgery in the treatment of canine oral malignant melanoma. *Res Vet Sci.* (2019) 122:40–9. doi: 10.1016/j.rvsc.2018.11.001
29. Milevoj N, Tozon N, Licen S, Lampreht Tratar U, Sersa G, Cemazar M. Health-related quality of life in dogs treated with electrochemotherapy and/or interleukin-12 gene electrotransfer. *Vet Med Sci.* (2020) 6:290–8. doi: 10.1002/vms3.232
30. Cicchelero L, Denies S, Vanderperren K, Stock E, Van Brantegem L, de Rooster H, et al. Immunological, anti-angiogenic and clinical effects of intratumoral interleukin 12 electrogene therapy combined with metronomic cyclophosphamide in dogs with spontaneous cancer: a pilot study. *Cancer Lett.* (2017) 400:205–18. doi: 10.1016/j.canlet.2016.09.015
31. Cutrera J, King G, Jones P, Kicenuik K, Gumpel E, Xia X, et al. Safe and effective treatment of spontaneous neoplasms with interleukin 12 electro-chemo-gene therapy. *J Cell Mol Med.* (2015) 19:664–75. doi: 10.1111/jcmm.12382
32. Cemazar M, Jarm T, Sersa G. Cancer electrogene therapy with interleukin-12. *Curr Gene Ther.* (2010) 10:300–11. doi: 10.2174/156652310791823425
33. Cemazar M, Ambrozic Avgustin J, Pavlin D, Sersa G, Poli A, Levacic Krhač A, et al. Efficacy and safety of electrochemotherapy combined with peritumoral IL-12 gene electrotransfer of canine mast cell tumours. *Vet Comp Oncol.* (2017) 15:641–54. doi: 10.1111/vco.12208
34. Cemazar M, Tamzali Y, Sersa G, Tozon N, Mir LM, Miklavcic D, et al. Electrochemotherapy in veterinary oncology. *J Vet Intern Med.* (2008) 22:826–31. doi: 10.1111/j.1939-1676.2008.0117.x
35. Nemec A, Milevoj N, Lampreht Tratar U, Sersa G, Cemazar M, Tozon N. Electroporation-based treatments in small animal veterinary oral and maxillofacial oncology. *Front Vet Sci.* (2020) 7:575911. doi: 10.3389/fvets.2020.575911
36. Reed SD, Fulmer A, Buckholz J, Zhang B, Cutrera J, Shiomitsu K, et al. Bleomycin/interleukin-12 electrochemogenetherapy for treating naturally occurring spontaneous neoplasms in dogs. *Cancer Gene Ther.* (2010) 17:571–8. doi: 10.1038/cgt.2010.13
37. Impellizeri J, Aurisicchio L, Forde P, Soden DM. Electroporation in veterinary oncology. *Vet J.* (2016) 217:18–25. doi: 10.1016/j.tvjl.2016.05.015
38. Kodre V, Cemazar M, Pecar J, Sersa G, Cor A, Tozon N. Electrochemotherapy compared to surgery for treatment of canine mast cell tumours. *In Vivo.* (2009) 23:55–62.
39. Spugnini EP, Di Tosto G, Salemme S, Pecchia L, Fanciulli M, Baldi A. Electrochemotherapy for the treatment of recurring aponeurotic fibromatosis in a dog. *Can Vet J.* (2013) 54:606–9.
40. Spugnini EP, Vincenzi B, Citro G, Dotsinsky I, Mudrov T, Baldi A, 2011. Evaluation of cisplatin as an electrochemotherapy agent for the treatment of incompletely excised mast cell tumors in dogs. *J Vet Intern Med.* (2011) 25:407–11. doi: 10.1111/j.1939-1676.2011.0678.x
41. Tellado MN, Maglietti FH, Michinski SD, Marshall GR, Signori E. Predictive factors of response to electrochemotherapy in canine oral malignant melanoma. *Radiol Oncol.* (2020) 54:68–78. doi: 10.2478/raon-2020-0014
42. Tozon N, Pavlin D, Sersa G, Dolinsek T, Cemazar M. Electrochemotherapy with intravenous bleomycin injection: an observational study in superficial squamous cell carcinoma in cats. *J Feline Med Surg.* (2014) 16:291–9. doi: 10.1177/1098612X13507071
43. Racnik J, Svara T, Zadravec M, Gombac M, Cemazar M, Sersa G, et al. Electrochemotherapy with bleomycin of different types of cutaneous tumours in a ferret (Mustela Putorius Furo). *Radiol Oncol.* (2017) 52:98–104. doi: 10.1515/raon-2017-0057
44. Tamzali Y, Borde L, Rols MP, Golzio M, Lyazrhi F, Teissie J. Successful treatment of equine sarcoids with cisplatin electrochemotherapy: a retrospective study of 48 cases. *Equine Vet J.* (2012) 44:214–20. doi: 10.1111/j.2042-3306.2011.00425.x
45. Tozon N, Kramaric P, Kos Kadunc V, Sersa G, Cemazar M. Electrochemotherapy as a single or adjuvant treatment to surgery of cutaneous sarcoid tumours in horses: a 31-case retrospective study. *Vet Rec.* (2016) 179:1–6. doi: 10.1136/vr.103867
46. Glass LF, Pepine ML, Fenske NA, Jaroszeski M, Reintgen DS, Heller R. Bleomycin-mediated electrochemotherapy of metastatic melanoma. *Arch Dermatol.* (1996) 132:1353–7. doi: 10.1001/archderm.1996.03890350095015
47. Pavlin D, Cemazar D, Sersa G, Tozon N. IL-12 based gene therapy in veterinary medicine. *J Transl Med.* (2012) 10:234–44. doi: 10.1186/1479-5876-10-234
48. Sedlar A, Dolinšek T, Markelc B, Prosen L, Kranjc S, Bosnjak M, et al. Potentiation of electrochemotherapy by intramuscular IL-12 gene electrotransfer in murine sarcoma and carcinoma with different immunogenicity. *Radiol Oncol.* (2012) 46:302–11. doi: 10.2478/v10019-012-0044-9
49. Kishida T, Asada H, Itokawa Y, Yasutomi K, Shin-Ya M, Gojo J, et al. Electrochemo-gene therapy of cancer: intratumoral delivery of interleukin-12 gene and bleomycin synergistically induced therapeutic immunity and suppressed subcutaneous and metastatic melanomas in mice. *Mol Ther.* (2003) 8:738–45. doi: 10.1016/j.ymthe.2003.08.002
50. Maglietti F, Tellado M, De Robertis M, Michinski S, Fernandez J, Signori E, et al. Electroporation as the immunotherapy strategy for cancer in veterinary medicine: state of the art in Latin America. *Vaccines (Basel).* (2020) 8:537. doi: 10.3390/vaccines8030537
51. Heller R, Jaroszeski MJ, Reintgen DS, Puleo CA, DeConti RC, Gilbert RA, et al. Treatment of cutaneous and subcutaneous tumors with electrochemotherapy using intralesional bleomycin. *Cancer.* (1998) 83:148–157. doi: 10.1002/(SICI)1097-0142(19980701)83:1<148::AID-CNCR20>3.0.CO;2-W
52. Sersa G, Stabuc B, Cemazar M, Miklavcic D, Rudolf Z. Electrochemotherapy with cisplatin: clinical experience in malignant melanoma patients. *Clin Cancer Res.* (2000) 6:863–7.
53. Byrne CM, Thompson JF, Johnston H, Hersey P, Quinn MJ, Michael Hughes T, et al. Treatment of metastatic melanoma using electroporation therapy with bleomycin (electrochemotherapy). *Melanoma Res.* (2005) 15:45–51. doi: 10.1097/00008390-200502000-00008
54. Gaudy C, Richard MA, Folchetti G, Bonerandi JJ, Grob JJ. Randomized controlled study of electrochemotherapy in the local treatment of skin metastases of melanoma. *J Cutan Med Surg.* (2006) 10:115–21. doi: 10.2310/7750.2006.00037
55. Marty M, Serša G, Rémi Garbay J, Gehl J, Collins CG, Snoj M, et al. Electrochemotherapy - an easy, highly effective and safe treatment of cutaneous and subcutaneous metastases: results of ESOPE (European Standard Operating Procedures of Electrochemotherapy) study. *EJC Suppl.* (2006) 4:3–13. doi: 10.1016/j.ejcsup.2006.08.002
56. Mir LM, Gehl J, Sersa G, Collins CG, Garbay JR, Billard V, et al. Standard operating procedures of the electrochemotherapy: instructions for the use of bleomycin or cisplatin administered either systemically or locally and electrical pulses delivered by Cliniporator by means of invasive or non-invasive electrodes. *Eur J Cancer Suppl.* (2006) 4:14–25. doi: 10.1016/j.ejcsup.2006.08.003

57. Bertino G, Serša G, De Terlizzi F, Occhini A, Plaschke CC, Groselj A, et al. European research on electrochemotherapy in head and neck cancer (EURECA) project: results of the treatment of skin cancer. *Eur J Cancer.* (2016) 63:41–52. doi: 10.1016/j.ejca.2016.05.001
58. Campana LG, Marconato R, Valpione S, Galuppo S, Alaibac M, Rossi CR, et al. Basal cell carcinoma: 10-year experience with electrochemotherapy. *J Transl Med.* (2017) 15:122. doi: 10.1186/s12967-017-1225-5
59. Colletti L, Battaglia V, De Simone P, Turturici L, Bartolozzi C, Filipponi F. Safety and feasibility of electrochemotherapy in patients with unresectable colorectal liver metastases: a pilot study. *Int J Surg.* (2017) 44:26–32. doi: 10.1016/j.ijsu.2017.06.033
60. Djokic M, Cemazar M, Popovic P, Kos B, Dezman R, Bosnjak M, et al. Electrochemotherapy as treatment option for hepatocellular carcinoma, a prospective pilot study. *Eur J Surg Oncol.* (2018) 44:651–7. doi: 10.1016/j.ejso.2018.01.090
61. Edhemovic I, Brecelj E, Gasljevic G, Marolt Music M, Gorjup V, Mali B, et al. Intraoperative electrochemotherapy of colorectal liver metastases. *J Surg Oncol.* (2014) 110:320–7. doi: 10.1002/jso.23625
62. Ruers T, van Coevorden F, Punt CJA, Pierie JPEN, Borel-Rinkes I, Ledermann JA, et al. Local treatment of unresectable colorectal liver metastases: results of a randomized phase II trial. *J Natl Cancer Inst.* (2017) 109:djx015. doi: 10.1093/jnci/djx015
63. Edhemovic I, Brecelj E, Cemazar M, Boc N, Trotovsek B, Djokic M, et al. Intraoperative electrochemotherapy of colorectal liver metastases: a prospective phase II study. *Eur J Surg Oncol.* (2020) 46:1628–33. doi: 10.1016/j.ejso.2020.04.037
64. Tafuto S, von Arx C, De Divitiis, Maura CT, Palaia R, Albino V, et al. Electrochemotherapy as a new approach on pancreatic cancer and on liver metastases. *Int J Surg.* (2015) 21:S78–S82. doi: 10.1016/j.ijsu.2015.04.095
65. Granata V, Fusco R, Piccirillo M, Palaia R, Petrillo A, Lastoria S, et al. Electrochemotherapy in locally advanced pancreatic cancer: Preliminary results. *Int J Surg.* (2015) 18:230–6. doi: 10.1016/j.ijsu.2015.04.055
66. Bimonte S, Leongito M, Granata V, Barbieri A, Vecchio VD, Falco M, et al. Electrochemotherapy in pancreatic adenocarcinoma treatment: pre-clinical and clinical studies. *Radiol Oncol.* (2016) 50:14–20. doi: 10.1515/raon-2016-0003
67. Sersa G, Cemazar M, Miklavcic D, Chaplin DJ. Tumor blood flow modifying effect of electrochemotherapy with bleomycin. *Anticancer Res.* (1999) 19:4017–22.
68. Sersa G, Cemazar M, Miklavcic D. Tumor blood flow modifying effects of electrochemotherapy: a potential vascular targeted mechanism. *Radiol Oncol.* (2003) 37:43–8.
69. Sersa G, Jarm T, Kotnik T, Coer A, Podkrajsek M, Sentjurc M, et al. Vascular disrupting action of electroporation and electrochemotherapy with bleomycin in murine sarcoma. *Br J Cancer.* (2008) 98:388–98. doi: 10.1038/sj.bjc.6604168
70. Jarm T, Cemazar M, Miklavcic D, Sersa G. Antivascular effects of electrochemotherapy: implications in treatment of bleeding metastases. *Expert Rev Anticancer Ther.* (2010) 10:729–46. doi: 10.1586/era.10.43
71. Gehl J, Skovsgaard T, Mir LM. Vascular reactions to in vivo electroporation: characterization and consequences for drug and gene delivery. *Biochim Biophys Acta.* (2002) 1569:51–8. doi: 10.1016/S0304-4165(01)00233-1
72. Markelc B, Sersa G, Cemazar M. Differential mechanisms associated with vascular disrupting action of electrochemotherapy: intravital microscopy on the level of single normal and tumor blood vessels. *PLoS One.* (2013) 8:e59557. doi: 10.1371/journal.pone.0059557
73. Boc N, Edhemovic I, Kos B, Marolt Music M, Brecelj E, Bosnjak M, et al. Ultrasonographic changes in the liver tumors as indicators of adequate tumor coverage with electric field for effective electrochemotherapy. *Radiol Oncol.* (2018) 52:383–391. doi: 10.2478/raon-2018-0041
74. Brloznik M, Boc N, Sersa G, Zmuc J, Gasljevic G, Seliskar A, et al. Radiological findings of porcine liver after electrochemotherapy with bleomycin. *Radiol Oncol.* (2019) 53:415–26. doi: 10.2478/raon-2019-0049
75. Schwarz LH, Litiere S, de Vries E, Ford R, Gwyther S, Mandrekar S, et al. RECIST 1.1 - update and clarification: from the RECIST Committee. *Eur J Cancer.* (2016) 62:132–7. doi: 10.1016/j.ejca.2016.03.081
76. Seymour K, Bogaerts J, Perrone A, Ford R, Schwartz LH, Mandrekar S, et al. iRECIST: guidelines for response criteria for use in trials testing immunotherapeutics. *Lancet Oncol.* (2017) 18:e143–e52. doi: 10.1016/S1470-2045(17)30074-8
77. R Core Team. *R: A Language and Environment for Statistical Computing, version 3.5.0.* Vienna: R Foundation for Statistical Computing (2019). Available online at: https://www.R-project.org (November 15, 2020).
78. Kong WT, Wang WP, Huang BJ, Ding H, Mao F. Value of wash-in and wash-out time in the diagnosis between hepatocellular carcinoma and other hepatic nodules with similar vascular pattern on contrast-enhanced ultrasound. *J Gastroenterol Hepatol.* (2014) 29:576–80. doi: 10.1111/jgh.12394
79. Li YJ, Wen G, Wang Y, Wang DX, Yang L, Deng YJ, et al. Perfusion heterogeneity in breast tumors for assessment of angiogenesis. *J Ultrasound Med.* (2013) 32:1145–55. doi: 10.7863/ultra.32.7.1145
80. Lassau N, Koscielny S, Albiges L, Chami L, Benatsou B, Chebil M, et al. Metastatic renal cell carcinoma treated with sunitinib: early evaluation of treatment response using dynamic contrast-enhanced ultrasonography. *Clin Cancer Res.* (2010) 16:1216–25. doi: 10.1158/1078-0432.CCR-09-2175
81. Ohlerth S, Bley CR, Laluhová D, Roos M, Kaser-Hotz B. Assessment of changes in vascularity and blood volume in canine sarcomas and squamous cell carcinomas during fractionated radiation therapy using quantified contrast-enhanced power Doppler ultrasonography: a preliminary study. *Vet J.* (2010) 186:58–63. doi: 10.1016/j.tvjl.2009.07.006
82. Mayr NA, Huang Z, Wang JZ, Lo SS, Fan JM, Grecula JC, et al. Characterizing tumor heterogeneity with functional imaging and quantifying high-risk tumor volume for early prediction of treatment outcome: cervical cancer as a model. *Int J Radiat Oncol Biol Phys.* (2012) 83:972–9. doi: 10.1016/j.ijrobp.2011.08.011
83. Hayano K, Lee SH, Yoshida H, Zhu AX, Sahani DV. Fractal analysis of CT perfusion images for evaluation of antiangiogenic treatment and survival in hepatocellular carcinoma. *Acad Radiol.* (2014) 21:654–60. doi: 10.1016/j.acra.2014.01.020

Conflict of Interest: The authors declare that the research was conducted in the absence of any commercial or financial relationships that could be construed as a potential conflict of interest.

3 RAZPRAVA

Zdravljenje z EKT je uveljavljen standard zdravljenja različnih kožnih, podkožnih in globoko ležečih tumorjev pri ljudeh (4, 16, 17, 18, 19, 20, 21, 22, 23, 24, 25, 26, 27, 28, 29, 30, 31, 32, 33, 34, 35, 36, 37). Zdravljenje z GEP pIL-12 kot samostojna terapija ali pa v kombinaciji z EKT je učinkovit način zdravljenja različnih tumorjev pri psih (61, 62, 63, 65, 66, 67, 68, 69, 70, 71, 72, 73, 74, 75, 76, 77).

S preiskavo UZ-KS tumorjev lahko vrednotimo spremembe v perfuziji tkiv (161, 162, 163, 164) in tako lahko določimo mesta zmanjšane perfuzije zaradi tumorske nekroze, edema in tromboze ter mesta povečane perfuzije zaradi reaktivne hiperemije in neovaskularizacije (158, 159, 194, 195, 196, 197, 198). Vrednotenje perfuzije in njene heterogenosti je pomembno za napoved uspešnosti zdravljenja (199, 200).

Kljub učinkovitosti in uveljavljenosti terapij na osnovi EP še vedno primanjkuje podatkov o varnostnih vidikih zdravljenja jeter, ko so elektrode vstavljene v svetline velikih jetrnih žil ter o parametrih, ki bi lahko napovedali izid zdravljenja, zato smo v doktorskem delu:

1. ovrednotili rezultate UZ-KS in CT-KS po EKT jeter zdravih prašičev z vstavitvijo elektrod in aplikacijo električnih pulzov neposredno v svetlino velikih žil in tako proučili varnost EKT tudi v primeru potencialno nevarne vstavitve elektrod v svetlino velikih jetrnih žil in
2. analizirali rezultate UZ-KS po EKT in GEP induciranih mišjih in spontanih pasjih tumorjev: rezultate UZ-KS smo primerjali z rezultati imunohistoloških analiz (barvanje ožilja) ter z izidom zdravljenja. Tako smo proučili uporabnost rezultatov UZ-KS kot prediktivnega dejavnika zdravljenja z EKT in GEP.

3.1 Slikovno-diagnostične spremembe prašičjih jeter po EKT z BLM

Vpliva EP in EKT na zdrav jetrni parenhim in velike krvne žile jeter (kavdalno veno kavo, levo srednjo hepatično veno in levo portalno veno), ko so elektrode vstavljene v njihovo svetlino, s slikovno-diagnostičnimi metodami še niso opisali. Zato smo na modelu prašičjih jeter, ki smo jih izbrali zaradi anatomskih in fizioloških podobnosti z jetri človeka (201, 202), želeli pokazati, da je namerna vstavitev elektrod in aplikacija električnih pulzov neposredno v svetlino velikih žil varna. Ugotovili smo, da ne povzročita tromboz, krvavitev ali drugih hemodinamsko

pomembnih poškodb in je skladna z rezultati histoloških preiskav jeter prašičev 2 in 7 dni po EP/EKT (203) ter z raziskavami EKT, kjer so elektrode vstavili v bližino (30, 31, 32, 35, 204, 205) ali v svetlino velikih jetrnih žil (206). Odsotnost krvavitve, tudi če so bile elektrode vstavljene globoko v jetrni parenhim in v svetlino velikih žil, je pomemben varnostni vidik EKT. Najverjetnejši razlog za to ugotovitev je prehodna lokalna hipoperfuzija in elektrokoagulacija, povezana z visoko gostoto električnega toka na površini elektrod (207).

Ugotovitve UZ prikaza v svetlostnem načinu predstavitve (angl. B-mode) so bile dinamične: najprej so se pojavili hiperehogeni mikromehurčki vzdolž elektrodnih sledi, potem je postalo tretirano področje hipoehogeno, hiperehogeni mikromehurčki pa so se enakomerno porazdelili. Hipoehogenost področja je pričela potem bledeti, mikromehurčki pa izginjati. Hiperehogeni mikromehurčki, ki se sprva tvorijo okoli elektrod, so posledica elektrokemijskih reakcij na elektrodah in elektrokoagulacije tkiva (92, 207). Plinski mehurčki nastajajo tudi v ablacijah ireverzibilne elektroporacije (107, 208).

Hipoehogenost tretiranega parenhima jeter kaže na strukturno spremembo zaradi zmanjšane perfuzije, ki jo povzroči prehodna vazokonstrikcija in prehodna povečana prepustnost stene majhnih žil (edem) (92). Vazokonstrikcija žil ob aplikaciji električnih pulzov je opisana v že objavljenih kliničnih raziskavah in prispeva k učinkovitosti zdravljenja z EKT, saj vodi do učinkovitega ujetja ali vsaj oviranega izpiranja kemoterapevtika, nabranega v tumorju zaradi zmanjšanega pretoka krvi in zato so tumorske celice dalj časa izpostavljene visoki koncentraciji zdravila (14, 90, 91, 92, 93, 94, 95, 209, 210).

Rezultati histološke analize poriranega jetrnega parenhima takoj po EKT so pokazali fibrinske trombe v majhnih venulah, kar je skladno z zmanjšano perfuzijo zaradi zastojne kongestije zaradi spazma venul.

Obe dinamični preiskavi s kontrastom, UZ-KS in CT-KS, sta pokazali, da porirana področja privzemajo manj kontrasta, kar dodatno potrjuje prej opisano zmanjšanje perfuzije tretiranega tkiva kot sta pokazali preiskavi UZ prikaz v svtlostnem načinu ter histološka analiza parenhima takoj po EKT. Uporabili smo dve vrsti elektrod: linearne s spremenljivo geometrijo in fiksne heksagonalne. V rutinski klinični praksi se heksagonalne elektrode uporabljajo za manjše in površinske jetrne tumorje, linearne elektrode pa za globoko ležeče in večje tumorje jeter (211).

Pri linearnih elektrodah so bila območja zmanjšane perfuzije značilno večja v primerjavi s heksagonalnimi elektrodami. To je posledica večje razdalje med elektrodami v primeru elektrod z linearno spremenljivo geometrijo, kjer je potrebno uporabiti višjo lokalno napetost električnega polja, da dosežemo enak terapevtski učinek (212). Razlika v velikosti področij z zmanjšano perfuzijo pri uporabi različnih elektrod je bila v skladu z računalniško simulacijo lokalne napetosti električnega polja in prej objavljenimi histološkimi analizami (203). Vendar pa kljub omenjeni razliki v velikosti omenjenih območij ni razlik v učinkovitosti elektroporacije med elektrodami različne geometrije (204, 207). Poleg tega opažene slikovno-diagnostične spremembe niso bile posledica uporabe BLM, saj so bile enake pri poskusni in kontrolni skupini, kjer smo aplicirali samo električne pulze, kar je skladno z že znanim dejstvom, da ima BLM na zdravo tkivo zanemarljiv učinek (14, 92, 93, 203).

Preiskave CT-KS en teden po EKT so pokazale le majhna območja zmanjšanja privzemanja kontrasta, kar je v skladu z rezultati histološke analize tkiv, kjer je bila ugotovljena proliferacija granulacijskega tkiva (203, 205). Histološke spremembe takoj po EP/EKT ter 2 in 7 dni pozneje (203) so bile blage in zato v skladu z radiološkimi ugotovitvami v naši raziskavi, ki niso pokazale klinično pomembnih poškodb velikih jetrnih žil in parenhima: stene tretiranih žil so bile nepoškodovane in prehodnost žil primerna, spremembe jetrnega parenhima pa blage. Ti rezultati potrjujejo, da je EKT za zdravljenje tumorjev, ki mejijo na velike jetrne žile, varna.

Radiološke značilnosti jeter po EP/EKT so dinamične in potrebne so nadaljnje raziskave z večjim številom živali v postopkih, da se te značilnosti temeljito preučijo, s čimer bi zagotovili odgovore, katere radiološke ugotovitve so koristni kazalci ustrezne porazdelitve električnega polja in možni prediktivni dejavniki, ki bi lahko bistveno vplivali na odločitve glede poteka nadaljnjega zdravljenja.

3.2 Vrednotenje tumorske perfuzije na modelu mišjih melanomov B16F10 z UZ-KS

Kot poskusni model za optimizacijo metode UZ-KS za oceno perfuzije živalskih tkiv po EKT in GEP smo v prvi raziskavi uporabili miši z melanom B16F10, zdravljenim s kombinacijo obsevanja in GEP s plazmidno DNA. Ta kodira shRNA proti CD146 oz. MCAM. MCAM je transmembranski glikoprotein, ki je prekomerno izražen v melanomu in je pomemben v patogenezi bolezni, ki vključuje invazivnost, metastatski potencial in angiogenezo tumorja (123, 213). MCAM, z

uporabo plazmidne DNA, ki kodira shRNA proti MCAM, je zato potencialna tarča za gensko terapijo melanoma (213). Z analizo rezultatov UZ-KS tumorjev po različnih zdravljenjih smo opisali učinke zdravljenja na perfuzijo tumorjev, rezultate UZ-KS pa smo primerjali z rastnimi krivuljami tumorjev, deležem popolnih ozdravitev in rezultati histoloških preiskav (barvanje žilja, pozitivnega na označevalec CD31, ki je močneje izražen pri nekaterih vrstah tumorjev).

V drugi raziskavi na mišjem modelu melanoma B16F10 smo miši zdravili z EKT z BLM in GEP pIL--12. Omenjeno zdravljenje ima učinkovit protitumorski učinek zaradi vpliva kemoterapevtika na tumorske in endotelne celice ter zaradi vpliva GEP na imunski odziv ter angiogenezo (77). Rezultate UZ-KS smo primerjali s podvojitvenim časom volumna tumorja, saj smo želeli proučiti, ali je UZ-KS uporaben za napovedovanje izida zdravljenja mišjih melanomov B16F10 z EKT in GEP pIL-12.

Iz rezultatov UZ-KS lahko pridobimo vrednosti za različne parametre, ki jih je mogoče razdeliti na parametre, ki opisujejo pretok krvi (AT, AS, TTP, DS, DT/2) in parametre, ki opisujejo količino krvi (AUC, PE). Iz trenutno dostopne literature je razvidno, da so v humanih kliničnih raziskavah (168, 169, 170, 173) pokazali trend v smeri korelacije s preživetjem različni parametri UZ-KS (AUC, TTP, AS in PE). V naših raziskavah na mišjem modelu je bil z rastjo tumorja povezan le parameter PE. Za razliko od humanih raziskav, parametri, ki opisujejo hitrost pretoka krvi, niso pokazali značilne povezave z rastjo tumorja in s histološkimi rezultati. Možni razlogi za ugotovitev so lahko povsem tehnične narave: živali v postopkih so bile v različnih ravneh anestezije in retroorbitalne injekcije kontrasta smo izvedli brez uporabe infuzijske črpalke, kar lahko oboje vpliva na rezultate meritev pretoka krvi skozi tkiva. Globina anestezije vpliva na fiziološke parametre, kot so sistemski krvni tlak, telesna temperatura, srčni utrip, krčljivost srca in drugi, ki vplivajo na perfuzijo tkiva, odvisno od srčnih, žilnih, mikrocirkulacijskih in humoralnih dejavnikov. Retroorbitalne aplikacije kontrastnih snovi so se sicer pokazale primerljive z aplikacijami v veno repa (214), vendar so v tej raziskavi kontrastna sredstva aplicirali skozi kanile, v naši raziskavi pa smo iglo vstavili v retro-orbitalni sinus (215). Kadar kontrast apliciramo ročno in ne z infuzijsko črpalko, ne moremo doseči popolnoma enakomerne hitrosti vbrizgavanja med bolusom, ki traja nekaj sekund. Poleg tega se lahko hitrost vbrizgavanja kontrasta zelo razlikuje tudi med posamičnimi aplikacijami pri eni živali oziroma med različnimi živalmi.

Korelacija rezultatov UZ-KS s histološkimi analizami tumorskih krvnih žil, ki smo jo potrdili v prvi raziskavi na mišjem modelu, je v skladu s predkliničnimi (157, 158, 159) in kliničnimi (148, 161, 162, 163, 216) raziskavami na drugih histoloških vrstah tumorjev, ki so jih zdravili z drugimi vrstami antiangiogene terapije. Povprečne vrednosti PE so bile značilno večje v skupinah s krajšim časom podvojitve volumna tumorja. Nižji kot je bil PE, kar pomeni manjšo količino krvi v tumorju, počasnejša je bila njegova rast. To je pomembna ugotovitev, saj potrjuje prediktivno vrednost rezultatov UZ-KS po zdravljenju z EKT in/ali GEP. Rezultati obeh raziskav so skladni s predkliničnimi raziskavami, izvedenimi z drugimi vrstami protitumorskega zdravljenja. Rezultati UZ-KS so bili na primer uporabni za napoved izida zdravljenja induciranih mišjih hepatomov s talidomidom (158) in cisplatinom (159). Tudi v humanih kliničnih raziskavah, kjer so preučevali antiangiogeno zdravljenje z različnimi kemoterapevtiki (169, 170, 171, 172, 173, 175), so pokazali, da rezultati UZ-KS kolerirajo z rastjo tumorja. Nasprotno pa UZ-KS ni imel prediktivne vrednosti za izid obsevanja pri pasjih tumorjih (217, 218). To je mogoče razložiti s pomembno razliko v mehanizmu delovanja radioterapije v primerjavi z EKT v kombinaciji z GEP pIL-12; radioterapija je manj učinkovita v regijah z nižjo perfuzijo zaradi večje odpornosti hipoksičnih celic na zdravljenje, medtem ko ima terapija na osnovi EP antiangiogene in citotoksične učinke, ki niso odvisni od celične oksigenacije. Žilno usmerjene terapije lahko učinkovito normalizirajo vaskularno strukturo tumorja in za določeno obdobje, ki je znano kot okno za normalizacijo, oslabijo rast žil. V tem času postanejo dodatne terapije, kot sta kemoterapija in obsevanje, učinkovitejše (219), ker povečajo oksigenacijo preostalega tumorskega tkiva (220, 221, 222). Sinergistični učinki med radioterapijo in žilno usmerjenimi terapijami, ki vključujejo imunoterapijo (prepoznavanje in ciljanje tumorskih celic z imunskimi), kemoterapijo, žilno usmerjena zdravila, idr. se izkoriščajo pri kombiniranih zdravljenjih (122, 223). Žilno usmerjena zdravila razvrščamo v dve skupini: tista, ki zavirajo angiogenezo (preprečujejo nastanek novih žil iz že obstoječih) in tista, ki vplivajo na obstoječe tumorsko žilje. Čeprav obe skupini zdravil ciljata tumorsko žilje, se razlikujeta po mehanizmu delovanja: prva zavira nastanek novih žil in zmanjša oksigenacijo, druga pa normalizira tumorsko žilje, poveča perfuzijo in oksigenacijo in ima zato sinergističen učinek s kemoterapijo in radioterapijo (219). Na mišjih tumorjih so pokazali, da ima tudi GEP plazmidne DNA radiosenzibilizirajoči učinek (48, 220, 221, 222).

3.3 Tumorska perfuzija, ovrednotena z UZ-KS kot prediktivni dejavnik zdravljenja spontanih pasjih tumorjev z EKT in GEP pIL-12

V trenutno dostopni literaturi je zelo malo podatkov o tem, ali se UZ-KS lahko uporabi za napovedovanje odziva spontanih pasjih tumorjev na zdravljenje z EKT in/ali GEP pIL-12. V raziskavah, objavljenih leta 2017, so preučili uporabo UZ-KS pri 9 psih, zdravljenih z GEP pIL-12 (176) in 5 psih, zdravljenih z GEP pIL-12 in metronomsko kemoterapijo (177). V obeh omenjenih raziskavah niso dosegli popolnih ozdravitev, zato niso mogli proučiti, ali rezultati lahko služijo kot možen prediktivni dejavnik zdravljenja.

V klinični del naše raziskave smo vključili 8 psov z 12 kožnimi in podkožnimi novotvorbami, od katerih je bilo 11 mastocitomov in 1 nevrofibrosarkom. Rezultate UZ-KS smo primerjali s kliničnim odgovorom glede na kriterije RECIST. Eden od naših ciljev je bil z UZ-KS ovrednotiti vpliv EKT z GEP pIL-12 na perfuzijo tumorjev. Poleg tega smo želeli s pridobljenimi rezultati UZ-KS ugotoviti, ali obstajajo razlike med tumorji, ki so se na zdravljenje odzvali s popolnim odgovorom, in tumorji, ki so se odzvali z nepopolnim odgovorom.

Podobno kot v predkliničnih raziskavah na mišjem modelu smo tudi pri psih ugotovili, da je PE tumorjev s popolnim odgovorom značilno nižji v primerjavi s PE tumorjev, ki so se odzvali z nepopolnim odgovorom. Za razliko od raziskav pri miših, kjer smo povezavo z rastjo tumorja potrdili le za PE, smo pri psih sedem dni po terapiji ugotovili, da je odstotek sprememb TTP večji pri tumorjih s popolnim odgovorom kot pri tistih, ki se niso odzvali popolnoma. To pomeni, da so tumorji s popolnim odgovorom značilno počasneje privzemali kontrast. Skupna značilnost malignih tumorjev v primerjavi z benignimi je hitro privzemanje kontrasta (216, 224) in z njim povezan krajši TTP. Naši rezultati lahko kažejo, da so tumorji po zdravljenju postali "manj maligni", glede na to, da so začeli počasneje privzemati kontrast. Ti rezultati so podobni rezultatom raziskav pri ljudeh, ki so preučevale različna kemoterapevtska antiangiogena zdravljenja, pri katerih sta se TTP in hitrost izpiranja kontrasta po terapiji zmanjšali (169, 170, 175). V raziskavi učinkovitosti zdravljenja sorafeniba pri metastatskem raku ledvic pri ljudeh se je povezava med izidom zdravljenja in deležom prekrvljenega dela tumorja zmanjšala tri tedne po zdravljenju (165). V nasprotju pa v raziskavah, ki so ocenjevale UZ-KS po radioterapiji spontanih tumorjev pri psih (218), rezultati UZ-KS niso napovedali izida bolezni. Tudi tu je

možen razlog za slednji rezultat razlika v mehanizmu delovanja radioterapije v primerjavi z EKT v kombinaciji z GEP pIL-12, kot smo razpravljali v prejšnjem podpoglavju.

V raziskavi devetih psov s spontanimi tumorji, zdravljenih z GEP pIL-12 (176), so z UZ-KS opazili znatno zmanjšanje območja površine pod krivuljo harmonskega signala v času merjenja (AUC), kar odraža relativno količino krvi preiskovanega območja v času merjenja. Prav tako je bila v primerjavi z izhodiščnimi vrednostmi 8. in 35. dan znatno nižja hitrost izpiranja (angl. wash-out), ki opisuje hitrost pretoka krvi, kar je skladno z rezultati naše raziskave. Podobne parametre, ki odražajo relativno količino krvi in hitrost pretoka krvi, in sicer PE oziroma TTP, so isti avtorji raziskali v raziskavi petih psov, zdravljenih z GEP pIL-12 v kombinaciji z metronomskim ciklofosfamidom (177). Opazili so znatno zmanjšanje PE in podaljšan TTP 35 dni po zdravljenju, kar je v skladu z našimi rezultati, medtem ko so v nasprotju z našimi rezultati 8 dni po zdravljenju opazili povečanje PE. Razliko v dinamiki PE lahko najverjetneje pripišemo dejstvu, da so Cicchelero in sod. (177) raziskali GEP pIL-12 (brez EKT), ki ne povzroča prekinitve integritete endotelijske stene (angl., vascular disrupting effect), to je citotoksičnega učinka kemoterapevtskih zdravil na endotelijske celice žil (89, 91, 92), ki ga lahko opazimo po zdravljenju z EKT. Zdravljenje z GEP pIL-12 ima za posledico bistveno manj izrazit protitumorski učinek (62), opažen tudi v slednji raziskavi, saj niso opazili nobenega klinično pomembnega izida (177). Vendar pa je verjetno, da je zmanjšanje PE in podaljšanje TTP 35 dni po zdravljenju posledica antiangiogenega učinka genske terapije. Dodatna razlika med našimi raziskavami je tudi dejstvo, da je slednja raziskava (177) vključevala pet različnih vrst tumorjev, UZ-KS pa je bil opravljen le v treh časovnih točkah, torej pred terapijo ter v 8. in 35. dnevu, zato naših podatkov tako ni mogoče neposredno primerjati, ker so bili zbrani ob različnih časovnih točkah in po različnih terapijah.

Naši rezultati so v skladu z raziskavami pri ljudeh, ki so pokazale, da so rezultati UZ-KS koristno orodje za napovedovanje učinkovitosti različnih antiangiogenih zdravljenj pri metastatskem karcinomu ledvic, napredovalem hepato-celularnemu karcinomu, kolorektalnem karcinomu, metastatskem raku dojk, gastro-intestinalnih stromalnih tumorjih ter metastatskem melanomu (165, 166, 169, 170, 171, 172, 173, 174, 175). V naši raziskavi se je perfuzija po terapiji zmanjšala pri vseh tumorjih s popolnim odgovorom, kar je v skladu z znanimi žilnimi učinki EP, EKT in GEP (14, 89, 92, 97, 98, 113). Zmanjšanje perfuzije tumorja takoj po terapiji je

bilo večje pri tumorjih s popolnim odgovorom, kar podpira domnevo, da je terapija bolj učinkovita, če se odraža v takojšnji "žilni zapori" (angl. vascular lock). Razlika je bila značilna vse do sedmega dne, z izjemo tretjega dne. To je pomembna ugotovitev, skladna s pričakovanjem, da je manj verjetno, da bo izid terapije ugoden, če terapija ne pokaže antiangiogenih učinkov, ki povzročijo zmanjšano perfuzijo v dneh po zdravljenju. Podoben trend smo opazili tudi tretji dan, vendar razlika ni bila značilna. Najverjetnejši razlog za slednje je nesodelovanja lastnika in s tem manjkajoči podatki enega psa s tremi tumorji. Pokazali smo, da lahko rezultate UZ-KS uporabimo za napovedovanje izida zdravljenja pri pacientih, ki smo jih zdravili s kombiniranim zdravljenjem EKT in GEP.

3.4 Heterogenost perfuzije tumorjev

Koncept heterogenosti tumorjev še ni vključen v sedanjo klinično onkološko prakso ali paradigmo zdravljenja raka, obstajajo pa raziskave, da heterogene funkcionalne/biološke značilnosti tumorjev pomembno vplivajo na izid zdravljenja (199). Heterogeno odzivanje je značilno za več načinov zdravljenja raka, vendar ostaja režim zdravljenja večinoma enoten, zato je neuspeh zdravljenja tako pogost pri različnih vrstah raka, kjer so bile upoštevane priporočene smernice za najprimernejše zdravljenje (199).

V naši raziskavi smo heterogenost perfuzije skozi tumorje določili s standardno deviacijo izbranih ROI. Te smo primerjali z izidom zdravljenja z namenom, da bi ugotovili, ali lahko tudi heterogenost perfuzije, in ne le njeno intenzivnost, uporabimo za napovedovanje izida. Tako v raziskavi pri psih kot tudi pri mišjih melanomih, zdravljenih z EKT in GEP pIL-12, smo pokazali, da sta heterogenost perfuzije in izid zdravljenja povezana. To je pomembna ugotovitev, saj kaže na možno prediktivno vrednost heterogenosti perfuzije pri terapijah, ki temeljijo na antiangiogenih učinkih. Podobne rezultate je pokazal CT-KS tumorjev jeter pri človeku, ki so bili zdravljeni z antiangiogeno terapijo; zmanjšana heterogenost perfuzije je bila povezana z boljšo lokalno kontrolo tumorja in daljšim preživetjem (200). V nasprotju pa je bila pri raku maternične vratu, zdravljenem z radioterapijo in kemoterapijo ter ocenjenim z MRI-KS, zmanjšana heterogenost perfuzije povezana s slabšim izidom zaradi manjšega odziva na radioterapijo v delih tumorja, kjer je zmanjšana perfuzija povzročila lokalno hipoksijo (199). Tako bi lahko sklepali, da sta perfuzija in heterogenost perfuzije, ovrednoteni z UZ-KS, uporabni

za napovedovanje rezultatov antiangiogenih zdravljenj, vendar ju ni mogoče uporabiti za vse vrste onkoloških zdravljenj.

Napovedovanje izida zdravljenja je zahtevno, še posebej v luči, da ga med zdravljenjem izvedemo čim prej, kadar so ciljno prilagojene terapije učinkovitejše (199, 200). Naši rezultati heterogenosti perfuzije tumorjev kažejo, da je za oceno izida zdravljenja EKT mogoče uporabiti ne samo intenzivnost perfuzije tumorja, temveč tudi heterogenost perfuzije; če so tumorji po zdravljenju še vedno heterogeni, je morebiti potrebno razmisliti o ponovni terapiji. V raziskavi na mišjem modelu, zdravljenem z EKT z BLM in GEP pIL-12, je heterogenost perfuzije korelirala z rastjo tumorja samo v dveh časovnih točkah; zato so potrebne nadaljnje raziskave, da se oceni, ali GEP p-IL12 vpliva na ožilje tumorja tako, da je heterogenost perfuzije tumorja manj prediktivna za rast tumorja.

4 SKLEPI

- V naših predkliničnih raziskavah smo potrdili, da rezultati UZ-KS pokažejo značilno zmanjšano perfuzijo jeter prašiča po EP/EKT ter mišjih induciranih tumorjev, zdravljenih z metodo, ki temelji na EP. Enako smo ugotovili tudi v klinični raziskavi pri pasjih tumorjih, zdravljenih s kombinacijo EKT in GEP pIL-12.

- Naši rezultati potrjujejo, da je EKT varna za zdravljenje tumorjev, ki mejijo na velike jetrne žile ali se vanje vraščajo, saj slikovno-diagnostične ugotovitve po EP/EKT prašičjih jeter niso pokazale klinično pomembnih poškodb velikih jetrnih žil in parenhima; stene žil in njihova prehodnost so bile nespremenjene.

- Z raziskavami na miših in psih smo z UZ-KS dokazali heterogeni pretok skozi tumorje potrdili, da je heterogenost perfuzije povezana z izidom zdravljenja.

- Tako v predkliničnih raziskavah na induciranih mišjih tumorjih kot pri spontanih tumorjih psov smo potrdili, da rezultati UZ-KS korelirajo z lokalnim odgovorom na zdravljenje s terapijami, ki temeljijo na uporabi EP. Perfuzija tumorjev je po terapiji večja pri tumorjih, ki so se odzvali z nepopolnim odgovorom, kot pri tistih s popolnim odgovorom.

- Prediktivno vrednost UZ-KS smo potrdili s statistično značilnimi Pearsonovimi koeficienti: večja kot je bila perfuzija tumorja, krajši je bil pričakovani čas podvojitve tumorja.

- Na kliničnih pacientih smo ugotovili razlike v intenzivnosti in heterogenosti perfuzije med tumorji s popolnim odgovorom in tumorji, ki se niso odzvali ali se niso odzvali popolnoma vse preiskovane dni po zdravljenju, zato predlagamo, da bi v prihodnjih raziskavah izvajali UZ-KS tumorjev psov pred in takoj po terapiji ter v nekajdnevnih razmikih.

5 POVZETEK

Reverzibilna EP je metoda, ki z izpostavitvijo celic kratkim visokonapetostnim električnim pulzom začasno poveča prepustnost celične membrane in omogoča molekulam vstop v celico. Reverzibilna EP se uporablja pri dveh načinih zdravljenja bolnikov s tumorji: pri EKT, kjer se omogoči vstop v celice kemoterapevtikom, in pri GEP, kjer se omogoči vnos genetskega materiala za proizvodnjo želenega proteina. Kljub klinični učinkovitosti zdravljenj na osnovi EP pa še vedno primanjkuje podatkov o varnostnih vidikih EKT tumorjev jeter ter o parametrih, ki bi lahko napovedali izid zdravljenja, zato je bil namen doktorskega dela ovrednotenje rezultatov slikovno-diagnostičnih metod po EP in EKT jeter zdravih prašičev ter po EKT in GEP induciranih mišjih in spontanih pasjih tumorjev.

Radiološke spremembe jeter zdravih prašičev po EP in EKT z BLM in varnostni vidik potencialno nevarne vstavitve elektrod v velike jetrne žile smo preučili z UZ-KS takoj po EKT ter s CT-KS od 60 do 90 minut in en teden po EKT. Kot model preiskovanja uporabnosti UZ-KS kot prediktivnega dejavnika zdravljenja s terapevtskimi metodami, ki temeljijo na EP, smo izbrali miši z induciranimi melanomi B16F10. V prvi raziskavi na mišjem modelu smo tumorje zdravili z obsevanjem in GEP plazmida, ki utiša MCAM, v drugi raziskavi pa z EKT z BLM in GEP pIL-12. Pri psih s spontanimi tumorji, ki so bili zdravljeni z EKT v kombinaciji z GEP, smo primerjali rezultate UZ-KS tumorjev, ki so se odzvali na zdravljenje s popolnim odgovorom, s tistimi, ki se na zdravljenje niso odzvali ali se niso odzvali popolnoma.

Rezultati slikovno-diagnostičnih metod jeter prašičev po EP in EKT z BLM so pokazali značilno zmanjšano perfuzijo tretiranega področja. Spremembe niso bile posledica uporabe BLM, saj so bile enake pri poskusni in kontrolni skupini, kjer smo aplicirali samo električne pulze. Namerna vstavitev elektrod in aplikacija električnih pulzov neposredno v svetlino velikih žil ni povzročila tromboz, krvavitev ali drugih hemodinamsko pomembnih poškodb. V prvi raziskavi na mišjem modelu smo opazili zmanjšanje perfuzije tumorjev v terapevtskih skupinah v primerjavi s kontrolnimi skupinami in rezultati UZ-KS so korelirali z zmanjšano gostoto žil. Povprečne vrednosti parametra, ki opisuje volumen pretoka, ki smo ga izračunali kot razliko med vrhom intenzitete signala ter osnovno vrednostjo intenzitete signala, tj. vrh ločljivosti oz. maksimalno ojačanje kontrasta (PE), so bile značilno nižje pri tumorjih, ki so se odzvali na terapijo s popolnim

odgovorom, in vrednosti PE so pokazale trend korelacije s protitumorsko učinkovitostjo. V drugi raziskavi na mišjih melanomih, zdravljenih z EKT v kombinaciji z GEP pIL-12, je UZ-KS pokazal zmanjšano perfuzijo v skupinah z daljšim časom podvojitve volumna tumorja in prediktivno vrednost UZ-KS smo potrdili z značilnimi Pearsonovimi koeficienti: višja kot je bila vrednost PE, krajši je bil pričakovani čas podvojitve volumna tumorja. Nadalje, s krajšim časom podvojitve volumna je bila značilno povezana tudi večja heterogenost perfuzije tumorja. Tudi v klinični raziskavi pri psih smo ugotovili številne razlike v parametrih UZ-KS med tumorji s popolnim odgovorom in tumorji z nepopolnim odgovorom: perfuzija in heterogenost perfuzije sta bili manjši pri tumorjih s popolnim odgovorom.

Z raziskavo na prašičih smo prvi natančno opisali akutne slikovno-diagnostične spremembe jeter po EKT z BLM in pričakujemo, da bomo z rezultati doprinesli, da bo EKT globoko ležečih tumorjev bolj varna in učinkovita. V dveh raziskavah na mišjem modelu in v klinični raziskavi na psih smo prvi pokazali, da lahko rezultate UZ-KS uporabimo za napovedovanje izida zdravljenja s terapijami, ki temeljijo na EP. Tudi o rezultatih UZ-KS, ki kažejo, da je heterogenost tumorjev povezana z rastjo tumorja, do sedaj drugi avtorji niso poročali. Tako smo potrdili vse zastavljene hipoteze in pričakujemo, da bomo z rezultati doktorske disertacije pripomogli k optimizaciji protokolov zdravljenja z EKT in GEP tako v veterinarski kot humani medicini. Rezultati UZ-KS so neraziskan klinični parameter zdravljenja z EKT in GEP in imajo znaten potencial v kliničnem ocenjevanju učinka zdravljenja, saj nam zaradi takojšnjih rezultatov in možnosti večkratnega ponavljanja postopka omogočajo personalizirani pristop k zdravljenju s terapijami, ki temeljijo na EP.

6 SUMMARY

Reversible EP is a method that allows molecules to enter the cell because exposure of the cells to short high-voltage electrical pulses temporarily increases cell membrane permeability. Reversible EP is used in two types of treatment of tumor patients: ECT, which allows chemotherapeutic drugs to enter cells, and GET, which allows the entry of genetic material to produce the desired protein. Despite the clinical efficacy of EP-based treatments, there is still insufficient data on the safety aspects of ECT of liver tumors and on parameters that could predict the outcome of treatment. Therefore, the aim of this dissertation was to evaluate the results of diagnostic imaging methods after EP and ECT of healthy porcine liver, when the electrodes are inserted and the electrical pulses are applied directly into the lumen of the major hepatic vessels, and after ECT and GET of induced murine and spontaneous canine tumors, to investigate the applicability of DCE-US as a predictive factor of ECT and GET treatment.

Radiological changes in the liver parenchyma of healthy pigs and in the large blood vessels after ECT with BLM with potentially dangerous insertion of electrodes into the large hepatic vessels were studied by DCE-US immediately after and DCE-CT 60 to 90 min and one week after treatment. Mice with induced B16F10 melanoma were selected as a model to investigate the utility of DCE-US as a predictor of EP-based treatment. In the former study on a mouse model, tumors were treated with irradiation and GEP of the MCAM silencing plasmid; in the latter study mice were treated with ECT with BLM and/or GEP pIL-12. In dogs with spontaneous tumors treated with ECT and GET, we compared the DCE-US results of tumors that responded to treatment with a complete response to those that did not respond or did not respond completely.

Porcine liver results of diagnostic imaging after ECT showed decreased blood flow in the treated area. The changes were not due to the use of BLM, as they were the same in the experimental groups and the control groups in which only electrical pulses were administered. Intentional insertion of electrodes and application of electrical pulses directly into the lumen of large vessels did not result in thrombosis, haemorrhage, or other hemodynamically significant injury. In the first study in a mouse model, we observed a decrease in tumor perfusion in the treatment groups compared with the control groups, and the results of DCE-US correlated with decreased

vessel density. The mean value of the parameter describing flow volume, calculated as the difference between peak signal intensity and baseline signal intensity, i.e., peak enhancement (PE), was significantly lower in tumors that responded to therapy with complete response, and the values of PE showed a trend toward correlation with antitumor efficacy. In the study on mouse melanomas treated with ECT with BLM in combination with GET pIL-12, DCE-US showed lower perfusion in groups with longer tumor volume doubling time, and the predicted DCE-US value was confirmed by statistically significant Pearson coefficients: the higher the PE value, the shorter the expected tumor volume doubling time. In addition, greater tumor perfusion heterogeneity was associated with shorter volume doubling time. In our clinical study, we also found a number of differences in DCE-US parameters between tumors with complete response and tumors with incomplete response: perfusion and perfusion heterogeneity were lower in tumors with complete response.

The study in pigs is the first to accurately describe acute imaging changes in the liver after ECT with BLM, and we expect the results will help make ECT of deep-seated tumors safer and more effective. In two studies using a mouse model and in the canine clinical study, we were the first to demonstrate that DCE-US results can be used to predict treatment outcome for EP-based therapies. DCE-US results showing that tumor heterogeneity is associated with tumor growth have not been previously reported by other authors, either.

DCE-US results are unexplored parameters of ECT and GET treatments. They allow us to take a personalized approach to treatment with EP-based therapies because the results are immediate and there is the possibility of repeating the DCE-US procedures. Therefore, we believe that DCE-US has significant potential for clinical evaluation of treatment efficacy, and we expect that the results of the dissertation will help to optimize the treatment approach with ECT and GET in both animal and human medicine.

7 ZAHVALE

Mentorici, doc. dr. Darji Pavlin: kaj vse si naredila zame! Veliko potrpežljivosti in naklonjenosti premoreš. Tudi kadar nisem znala narediti, kot sva se dogovorili, ali tudi kadar sem poslala delovno verzijo brez glave in repa, si mi dala zagon s konstruktivnimi predlogi in komentarji, ki niso vsebovali slabe volje ali neobčutljive kritike, ki bi mi dodatno jemali veselje do dela. Hvala, da si mi razložila, kako se lotiti znanstveno-raziskovalnega dela, še pomembneje, kako v njem uživati, vztrajati in ga objaviti, torej tudi kako se pogovarjati z recenzenti in, tečnobnim popravkom navkljub, z obilico humorja uspeti. Veselim se, da nama ne bo nikoli dolgčas, in upam, da je sodelovanje v času doktorske disertacije šele začetek skupnih projektov, saj je sodelovati s tabo prijetno; zapleti se rešujejo zlahka in zato kmalu zbledijo, ostane pa občutek, da je naše delo opravljeno učinkovito, dobro in vsem v zadovoljstvo. Hvala tudi za pomoč pri delu s kliničnimi pacienti in študenti ter neštetih osebnih zagatah, ki se bi zdele mnogo večje, če ne bi bilo tvoje pragmatičnosti, razumevanja in naklonjenosti.

Somentorici, višji znan. sod. dr. Simoni Kranjc Brezar: prijazna si na vsakem koraku, ne vem, kako bi brez tvojega empatičnega čuta miške! Hvala, da si me uvedla v svet raziskovanja in mi približala zahtevno in odgovorno delo z eksperimentalnimi živalmi v najboljši možni luči. Izredno me je veselilo opazovati tvoje usklajeno sodelovanje z drugimi raziskovalci; iz tebe so sijali izkušenost, marljivost in nalezljivo navdušenje. Brez tebe bi nad mišjimi poskusi prav gotovo obupala že na začetku, pa potem še neštetokrat, a vedno znova so tvoji razmisleki, ideje in izkušnje ponujali sprejemljive rešitve, ki so me opogumile, da sem trmasto vztrajala odporu, lenobi in padcem navkljub.

Doktorski komisiji:

prof. dr. Robertu Frangežu hvala za pomoč pri prvih korakih znanstvenega pisanja, prijava teme doktorske disertacije bi bila brez vas bolj pomanjkljiva, doktorska disertacija pa manj imenitna. Najlepše se vam zahvaljujem tudi za postavljanje vzgleda visokošolskega učitelja;

prof. dr. Igorju Kocjančiču hvala za komentarje, radiološke presoje in terminološke rešitve;

doc. dr. Ani Nemec hvala za pripravljenost na hitro ukrepanje, vse strokovne debate in dolgoletno izmenjavo mnenj, obogatenih s tvojo pogumno specialistično izkušnjo v tujini.

Sodelavcem na Onkološkem inštitutu:

prof. dr. Maji Čemažar hvala za spoznavanje znanosti in pridobivanje neprecenljivih izkušenj v eksperimentalnem svetu. Hvala za planiranje, diskusije in konstruktivno sodelovanje pri znanstvenih objavah, prav tako pa tudi za zaupanje vame in prijazne naklonjene besede, ki so omilile najtežje trenutke težav s kontrastom in z razvozlavanjem pridobljenih rezultatov;

prof. dr. Gregorju Serši hvala za priložnost znanstveno-raziskovalnega dela, za inspirativne debate o vaskularnih učinkih elektrokemoterapije in za vso pomoč pri piljenju znanstvenih člankov;

specialistki radiologije Nini Boc hvala za obsežno podajanje znanja na vseh področjih slikovne diagnostike, hvala za tvoj prosti čas, ko sva razvozlavali rezultate pujskov in mišk, hvala tudi za iskrene besede in podporo v mnogih zapletenih in manj prijetnih situacijah;

dr. Maši Bošnjak hvala za dobro voljo, celodnevna druženja z miškami in da si s takšnim veseljem delila znanje predklinične onkologije;

dr. Urši Lampreht Tratar se zahvaljujem za navdušenje nad raziskovalnim delom, prijazne besede ter klinične podatke in slike tumorjev psov;

dr. Moniki Savarin hvala za takojšnje prijazne odzive in histološke rezultate tumorjev miši;

Miri Lavric hvala za nešteto celic, ki so zrastle v tumorje mišk;

radioinženirju Janiju Izlakarju se zahvaljujem za mnoge popoldneve, dobro voljo in številne CT & MRI posnetke;

Sodelavcem na Kliniki za male živali:

prof. dr. Nataši Tozon hvala za komentarje in onkološke presoje, ki so k doktorski disertaciji dodali poglobljeni uvid v kontekst primarne teme. Hvala tudi za zanimivo podajanje znanj in za prijazno naklonjenost v trenutkih osebnih stisk;

dr. Nini Milevoj hvala za prijetno sodelovanje, strokovno pomoč in vse nasvete v zvezi s formalnimi čermi pisanja doktorske disertacije;

anestezistkam izr. prof. dr. Alenki Seliškar, dr. Barbari Lukanc in dr. Katerini Tomsic hvala, da so psi in pujsi zadovoljno spali, da smo lahko v miru izpeljali dodatne preiskave slikovne diagnostike.

Radiološkemu oddelku veterinarske fakultete v Zürichu najlepša hvala, da sem vas lahko obiskala, prof. dr. Stefanie Ohlerth, dipl. ECVDI hvala za izkušnje in poduke v zvezi s kontrastnim ultrazvokom in doc. dr. Francesci Del Chicca, dipl. ECVDI za vse koristne nasvete v nepreglednih dilemah radiološke diagnostike.

Statističarkam mag. Mateji Nagode, doc. dr. Nataši Kejžar in dr. Tanji Knific najlepša hvala za natančne izračune in razlage; brez tako obsežne, natančne in pravilne statistike bi težko uspeli.

Lektorici dr. Mateji Gaber se zahvaljujem za neverjetno hitro odzivnost, razumevanje, da so že vsi roki pretečeni in natančno lekturo, ki je popravila tek pripovedi.

Anglistki Aleksandri Žerjav hvala za ekspeditiven pregled angleškega izvlečka in povzetka.

Knjižničarki mag. Brigiti Grecs Smole hvala za hitre odzive, mnoga pojasnila, popravke literature in bibliografske podatke disertacije.

Centru za podiplomski študij, Biljani Grubišić in dr. Mateji Stvarnik, hvala za številne obrazložitve, hitro odzivnost in mnoge spodbude.

Brez ultrazvočnih aparatov podjetja DIPROS disertacija ne bi bila mogoča; Mihi Melincu hvala za večno podporo in vero vame in Tonetu Jamniku za neskončne razlage o delovanju ultrazvočnih naprav, za primerne nastavitve aparatov in takojšnje odzive ob vseh možnih časih.

Psom in njihovim lastnikom, ki ste sodelovali v raziskavi, se iz srca zahvaljujem za udeležbo, zlasti za velikodušnost v naknadnem prihajanju na kliniko za ultrazvočne preiskave po že opravljenem posegu.

Vsem mojim, ki ste me bodrili in mi vedno stali ob strani ter potrpežljivo čakali, da bom spet z vami; Karmen, hvala za skrb, pozornost in vzor, brez tebe bi bilo več bušk in ponižanj, želja po vednosti pa bolj nedosegljiva.

8 LITERATURA

1 Yarmush ML, Golberg A, Serša G, Kotnik T, Miklavčič D. Electroporation-based technologies for medicine: Principles, applications, and challenges. Annu Rev Biomed Eng 2014; 16(1): 295–320. doi: 10.1146/annurev-bioeng-071813-104622.

2 Gehl J. Electroporation: theory and methods, perspectives for drug delivery, gene therapy and research. Acta Physiol Scand 2003; 177: 437–47. doi: 10.1046/j.1365-201X.2003.01093.x.

3 Cemazar M, Tamzali Y, Sersa G, et al. Electrochemotherapy in veterinary oncology. J Vet Intern Med 2008; 22(4): 826–31. doi: 10.1111/j.1939-1676.2008.0117.x.

4 Mali B, Jarm T, Snoj M, Sersa G, Miklavcic D. Antitumor effectiveness of electrochemotherapy: A systematic review and meta-analysis. Eur J Surg Oncol 2013a; 39(1): 4–16. doi: 10.1016/j.ejso.2012.08.016.

5 Čemažar M, Serša G. Recent advances in electrochemotherapy. Bioelectricity 2019; 1(4): 204–13. doi: 10.1089/bioe.2019.0028.

6 Campana LG, Edhemovic I, Soden D, et al. Clinical electrochemotherapy – emerging applications. Eur J Surg Oncol 2019; 45(2): 92–102. doi: 10.1016/j.ejso.2018.11.023.

7 Tozon N, Serša G, Čemažar M. Electrochemotherapy: potentiation of local antitumour effectiveness of cisplatin in dogs and cats. Anticancer Res 2001; 21(4A): 2483–8.

8 Barabas K, Milner R, Lurie D, Adin C. Cisplatin: a review of toxicities and therapeutic applications. Vet Comp Oncol 2008; 6(1): 1–18. doi: 10.1111/j.1476-5829.2007.00142.x.

9 Spugnini EP, Baldi A. Electrochemotherapy in veterinary oncology: state-of-the-art and perspectives. Vet Clin North Am Small Anim Pract 2019; 49(5): 967–79. doi: 10.1016/j.cvsm.2019.04.006.

10 Umezawa H, Maeda K, Takeuchi T, Okami Y. New antibiotics, bleomycin A and B. J Antibiot 1966; 19(5): 200–9.

11 Domenge C, Orlowski S, Luboinski B, et al. Antitumor electrochemotherapy: new advances in the clinical protocol. Cancer 1996; 77(5): 956–63. doi: 10.1002/(sici)1097-0142(19960301)77:5<956::aid-cncr23>3.0.co;2-1.

12 Tozon N, Lampreht Tratar U, Žnidar K, et al. Operating procedures of the electrochemotherapy for treatment of tumor in dogs and cats. J Vis Exp 2016; (116): e54760 (9 str.). doi: 10.3791/54760.

13 Serša G, Čemažar M, Miklavčič D, Mir LM. Electrochemotherapy: variable anti-tumor effect on different tumor models. Bioelectrochem Bioenerg 1994; 35: 23–7. doi: 10.1016/0302-4598(94)87006-3.

14 Gehl J, Skovsgaard T, Mir LM. Vascular reactions to in vivo electroporation: characterization and consequences for drug and gene delivery. Biochim Biophys Acta 2002; 1569(1/3): 51–8. doi: 10.1016/s0304-4165(01)00233-1.

15 Jaroszeski MJ, Dang V, Pottinger C, et al. Toxicity of anticancer agents mediated by electroporation *in vitro*. Anticancer Drugs 2000; 11(3): 201–8. doi: 10.1097/00001813-200003000-00008.

16 Heller R, Jaroszeski MJ, Reintgen DS, et al. Treatment of cutaneous and subcutaneous tumors with electrochemotherapy using intralesional bleomycin. Cancer 1998; 83(1): 148–57. doi: 10.1002/(sici)1097-0142(19980701)83:1<148::aid-cncr20>3.0.co;2-w.

17 Sersa G, Stabuc B, Cemazar M, Miklavcic D, Rudolf Z. Electrochemotherapy with cisplatin: clinical experience in malignant melanoma patients. Clin Cancer Res 2000; 6(3): 863–7.

18 Byrne CM, Thompson JF, Johnston H, et al. Treatment of metastatic melanoma using electroporation therapy with bleomycin (electrochemotherapy). Melanoma Res 2005; 15(1): 45–51. doi: 10.1097/00008390-200502000-00008.

19 Gaudy C, Richard MA, Folchetti G, Bonerandi JJ, Grob JJ. Randomized controlled study of electrochemotherapy in the local treatment of skin metastases of melanoma. J Cutan Med Surg 2006; 10(3): 115–21. doi: 10.2310/7750.2006.00037.

20 Marty M, Sersa G, Rémi Garbay J, et al. Electrochemotherapy – an easy, highly effective and safe treatment of cutaneous and subcutaneous metastases: results of ESOPE (European Standard Operating Procedures of Electrochemotherapy) study. Eur J Cancer Suppl 2006; 4(11): 3–13. doi: 10.1016/j.ejcsup.2006.08.002.

21 Mir LM, Gehl J, Sersa G, et al. Standard operating procedures of the electrochemotherapy: instructions for the use of bleomycin or cisplatin administered either systemically or locally and electric pulses delivered by Cliniporator by means of invasive or non-invasive electrodes. Eur J Cancer Suppl 2006; 4: 14–25. doi: 10.1016/j.ejcsup.2006.08.003.

22 Bertino G, Serša G, De Terlizzi F, et al. European research on electrochemotherapy in head and neck cancer (EURECA) project: results of the treatment of skin cancer. Eur J Cancer 2016; 63: 41–52. doi: 10.1016/j.ejca.2016.05.001.

23 Bigi L, Galdo G, Cesinaro AM, et al. Electrochemotherapy induces apoptotic death in melanoma metastases: a histologic and immunohistochemical investigation. Clin Cosmet Investig Dermatol 2016; 9: 451–9. doi: 10.2147/CCID.S115984.

24 Campana LG, Marconato R, Valpione S, et al. Basal cell carcinoma: 10-year experience with electrochemotherapy. J Transl Med 2017; 15(1): 122. doi: 10.1186/s12967-017-1225-5.

25 Gehl J, Sersa G, Matthiessen LW, et al. Updated standard operating procedures for electrochemotherapy of cutaneous tumours and skin metastases. Acta oncol 2018; 57(7): 874–82. doi: 10.1080/0284186X.2018.1454602.

26 Tafuto S, von Arx C, De Divitiis, et al. Electrochemotherapy as a new approach on pancreatic cancer and on liver metastases. Int J Surg 2015; 21: S78–82. doi: 10.1016/j.ijsu.2015.04.095.

27 Granata V, Fusco R, Piccirillo M, et al. Electrochemotherapy in locally advanced pancreatic cancer: preliminary results. Int J Surg 2015; 18: 230–6. doi: 10.1016/j.ijsu.2015.04.055.

28 Bimonte S, Leongito M, Granata V, et al. Electrochemotherapy in pancreatic adenocarcinoma treatment: pre-clinical and clinical studies. Radiol Oncol 2016; 50(1): 14–20. doi:10.1515/raon-2016-0003.

29 Dežman R, Čemažar M, Serša G, et al. Safety and feasibility of electrochemotherapy of the pancreas in a porcine model. Pancreas 2020; 49(9): 1168–73. doi: 10.1097/MPA.0000000000001642.

30 Edhemovic I, Gadzijev EM, Brecelj E, et al. Electrochemotherapy: a new technological approach in treatment of metastases in the liver. Technol Cancer Res Treat 2011; 10(5): 475–85. doi: 10.7785/tcrt.2012.500224.

31 Edhemovic I, Brecelj E, Gasljevic G, et al. Intraoperative electrochemotherapy of colorectal liver metastases. J Surg Oncol 2014; 110(3): 320–7. doi: 10.1002/jso.23625.

32 Edhemovic I, Brecelj E, Cemazar M, et al. Intraoperative electrochemotherapy of colorectal liver metastases: a prospective phase II study. Eur J Surg Oncol 2020; 46(9): 1628–33. doi: 10.1016/j.ejso.2020.04.037.

33 Colletti L, Battaglia V, De Simone P, et al. Safety and feasibility of electrochemotherapy in patients with unresectable colorectal liver metastases: a pilot study. Int J Surg 2017; 44: 26–32. doi: 10.1016/j.ijsu.2017.06.033.

34 Ruers T, van Coevorden F, Punt CJA, et al. Local treatment of unresectable colorectal liver metastases: results of a randomized phase II trial. J Natl Cancer Inst 2017; 109(9): djx015 (10 str.). doi: 10.1093/jnci/djx015.

35 Djokic M, Cemazar M, Popovic P, et al. Electrochemotherapy as treatment option for hepatocellular carcinoma, a prospective pilot study. Eur J Surg Oncol 2018; 44(5): 651–7. doi: 10.1016/j.ejso.2018.01.090.

36 Campana LG, Valpione S, Falci C, et al. The activity and safety of electrochemotherapy in persistent chest wall recurrence from breast cancer after mastectomy: a phase-II study. Breast Cancer Res Treat 2012; 134(3): 1169–78. doi: 10.1007/s10549-012-2095-4.

37 Sersa G, Cufer T, Paulin SM, Cemazar M, Snoj M. Electrochemotherapy of chest wall breast cancer recurrence. Cancer Treat Rev 2012; 38(5): 379–86. doi: 10.1016/j.ctrv.2011.07.006.

38 Glass LF, Pepine ML, Fenske NA, Jaroszeski M, Reintgen DS, Heller R. Bleomycin-mediated electrochemotherapy of metastatic melanoma. Arch Dermatol 1996; 132(11): 1353–7. doi:10.1001/archderm.1996.03890350095015.

39 Kishida T, Asada H, Itokawa Y, et al. Electrochemo-gene therapy of cancer: intratumoral delivery of interleukin-12 gene and bleomycin synergistically induced therapeutic immunity and suppressed subcutaneous and metastatic melanomas in mice. Mol Ther 2003; 8(5): 738–45. doi: 10.1016/j.ymthe.2003.08.002.

40 Heller LC, Heller R. Electroporation gene therapy preclinical and clinical trials for melanoma. Curr Gene Ther 2010; 10(4): 312–7. doi: 10.2174/156652310791823489.

41 Sedlar A, Dolinšek T, Markelc B, et al. Potentiation of electrochemotherapy by intramuscular IL-12 gene electrotransfer in murine sarcoma and carcinoma with different immunogenicity. Radiol Oncol 2012; 46(4): 302–11. doi: 10.2478/v10019-012-0044-9.

42 Sersa G, Teissie J, Cemazar M, et al. Electrochemotherapy of tumors as in situ vaccination boosted by immunogene electrotransfer. Cancer Immunol Immunother 2015; 64(10): 1315–27. doi: 10.1007/s00262-015-1724-2.

43 Cemazar M, Jarm T, Sersa G. Cancer electrogene therapy with interleukin-12. Curr Gene Ther 2010; 10(4): 300–11. doi: 10.2174/156652310791823425.

44 Rosazza C, Meglic SH, Zumbusch A, Rols MP, Miklavcic D. Gene electrotransfer: a mechanistic perspective. Curr Gene Ther 2016; 16(2): 98–129. doi: 10.2174/1566523216666160331130040.

45 Heller L, Todorovic V, Cemazar M. Electrotransfer of single-stranded or double-stranded DNA induces complete regression of palpable B16.F10 mouse melanomas. Cancer Gene Ther 2013; 20(12): 695–700. doi: 10.1038/cgt.2013.71.

46 Pavlin D, Tozon N, Serša G, Čemažar M. Efficient electrotransfection into canine muscle. Technol Cancer Res Treat 2008; 7: 45–54. doi: doi: 10.1177/153303460800700106.

47 Tevz G, Pavlin D, Kamensek U, et al. Gene electrotransfer into murine skeletal muscle: a systematic analysis of parameters for long-term gene expression. Technol Cancer Res Treat 2008; 7(2): 91–101. doi: 10.1177/153303460800700201.

48 Tevz G, Kranjc S, Cemazar M, et al. Controlled systemic release of interleukin-12 after gene electrotransfer to muscle for cancer gene therapy alone or in combination with ionizing radiation in murine sarcomas. J Gene Med 2009; 11(12): 1125–37. doi: 10.1002/jgm.1403.

49 Trollet C, Bloquel C, Scherman D, Bigey P. Electrotransfer into skeletal muscle for protein expression. Curr Gene Ther 2006; 6(5): 561–78. doi: 10.2174/156652306778520656.

50 Pavselj N, Préat V. DNA electrotransfer into the skin using a combination of one high- and one low-voltage pulse. J Control Release 2005; 106(3): 407–15. doi: 10.1016/j.jconrel.2005.05.003.

51 Cui Z, Dierling A, Foldvari M. Non-invasive immunization on the skin using DNA vaccine. Curr Drug Deliv 2006; 3(1): 29–35. doi: 10.2174/156720106775197538.

52 Vandermeulen G, Staes E, Vanderhaeghen ML, Bureau MF, Scherman D, Préat V. Optimisation of intradermal DNA electrotransfer for immunisation. J Control Release 2007; 124(1-2): 81–7. doi: 10.1016/j.jconrel.2007.08.010.

53 Heller R, Schultz J, Lucas ML, et al. Intradermal delivery of interleukin-12 plasmid DNA by in vivo electroporation. DNA Cell Biol 2001; 20(1): 21–6. doi: 10.1089/10445490150504666.

54 Pavlin D, Cemazar M, Kamensek U, Tozon N, Pogacnik A, Sersa G. Local and systemic antitumor effect of intratumoral and peritumoral IL-12 electrogene therapy on murine sarcoma. Cancer Biol Ther 2009; 8: 2114–22. doi: 10.4161/cbt.8.22.9734.

55 Cemazar M, Pavlin D, Kranjc S, Grosel A, Mesojednik S, Sersa G. Sequence and time dependence of transfection efficiency of electrically-assisted gene delivery to tumors in mice. Curr Drug Deliv 2006; 3(1): 77–81. doi: 10.2174/156720106775197556.

56 Del Vecchio M, Bajetta E, Canova S, et al. Interleukin-12: biological properties and clinical application. Clin Cancer Res 2007; 13(16): 4677–85. doi: 10.1158/1078-0432.CCR-07-0776.

57 Nguyen KG, Vrabel MR, Mantooth SM, et al. Localized Interleukin-12 for cancer immunotherapy. Front Immunol 2020; 11: 575597. doi: 10.3389/fimmu.2020.575597.

58 Chan SH, Perussia B, Gupta JW, et al. Induction of interferon gamma production by natural killer cell stimulatory factor: characterization of the responder cells and synergy with other inducers. J Exp Med 1991; 173: 869–79. doi: 10.1084/jem.173.4.869.

59 Trinchieri G. Interleukin-12: a cytokine produced by antigen-presenting cells with immunoregulatory functions in the generation of T-helper cells type 1 and cytotoxic lymphocytes. Blood 1994; 84(12): 4008–27. doi: 10.1182/blood.V84.12.4008.bloodjournal84124008.

60 Yoshida A, Koide Y, Uchijima M, Yoshida TO. IFN-γ induces IL-12 mRNA expression by a murine macrophage cell line, J774. Biochem Biophys Res Comm 1994; 198: 857–61. doi: 10.1006/bbrc.1994.1122

61 Pavlin D, Cemazar D, Sersa G, Tozon N. IL-12 based gene therapy in veterinary medicine. J Transl Med 2012; 10: 234–44. doi: 10.1186/1479-5876-10-234.

62 Pavlin D, Cemazar M, Cör A, Sersa G, Pogačnik A, Tozon N. Electrogene therapy with interleukin-12 in canine mast cell tumors. Radiol Oncol 2011; 45: 30–9. doi:10.2478/v10019-010-0041-9.

63 Cutrera J, King G, Jones P, et al. Safe and effective treatment of spontaneous neoplasms with interleukin 12 electro-chemo-gene therapy. J Cell Mol Med 2015; 19(3): 664–75. doi: 10.1111/jcmm.12382.

64 Daud AI, DeConti RC, Andrews S, et al. Phase I trial of interleukin-12 plasmid electroporation in patients with metastatic melanoma. J Clin Oncol 2008; 26(36): 5896–903. doi: 10.1200/JCO.2007.15.6794.

65 Kodre V, Cemazar M, Pecar J, Sersa G, Cor A, Tozon N. Electrochemotherapy compared to surgery for treatment of canine mast cell tumours. In Vivo 2009; 23: 55–62.

66 Reed SD, Fulmer A, Buckholz J, et al. Bleomycin/interleukin-12 electrochemogenetherapy for treating naturally occurring spontaneous neoplasms in dogs. Cancer Gene Ther 2010; 17: 571–8. doi: 10.1038/cgt.2010.13.

67 Tozon N, Kodre V, Juntes P, Sersa G, Cemazar M. Electrochemotherapy is highly effective for the treatment of canine perianal hepatoid adenoma and epithelioma. Acta Vet (Beograd) 2010; 60(2/3): 285–302. doi: 10.2298/AVB1003285T.

68 Spugnini EP, Vincenzi B, Citro G, Dotsinsky I, Mudrov T, Baldi A, 2011. Evaluation of cisplatin as an electrochemotherapy agent for the treatment of incompletely excised mast cell tumors in dogs. J Vet Intern Med 2011; 25: 407–11. doi: 10.1111/j.1939-1676.2011.0678.x.

69 Spugnini EP, Di Tosto G, Salemme S, Pecchia L, Fanciulli M, Baldi A. Electrochemotherapy for the treatment of recurring aponeurotic fibromatosis in a dog. Can Vet J 2013; 54: 606–9.

70 Impellizeri J, Aurisicchio L, Forde P, Soden DM. Electroporation in veterinary oncology. Vet J 2016; 217: 18–25. doi: 10.1016/j.tvjl.2016.05.015.

71 Salvadori C, Svara T, Rocchigiani G, et al. Effects of electrochemotherapy with cisplatin and peritumoral il-12 gene electrotransfer on canine mast cell tumors: a histopathologic and immunohistochemical study. Radiol Oncol 2017; 14; 51(3): 286–94. doi: 10.1515/raon-2017-0035.

72 Milevoj N, Lampreht Tratar U, Nemec A, et al. A combination of electrochemotherapy, gene electrotransfer of plasmid encoding canine IL-12 and cytoreductive surgery in the treatment of canine oral malignant melanoma. Res Vet Sci 2019; 122: 40–9. doi: 10.1016/j.rvsc.2018.11.001.

73 Milevoj N, Tozon N, Licen S, Lampreht Tratar U, Sersa G, Cemazar M. Health-related quality of life in dogs treated with electrochemotherapy and/or interleukin-12 gene electrotransfer. Vet Med Sci 2020; 6: 290–8. doi: 10.1002/vms3.232.

74 Maglietti F, Tellado M, De Robertis M, et al. Electroporation as the immunotherapy strategy for cancer in veterinary medicine: state of the art in Latin America. Vaccines (Basel) 2020; 8(3): e537. doi: 10.3390/vaccines8030537.

75 Nemec A, Milevoj N, Lampreht Tratar U, Sersa G, Cemazar M, Tozon N. Electroporation-based treatments in small animal veterinary oral and maxillofacial oncology. Front Vet Sci 2020; 7: 575911. doi: 10.3389/fvets.2020.575911.

76 Tellado MN, Maglietti FH, Michinski SD, Marshall GR, Signori E. Predictive factors of response to electrochemotherapy in canine oral malignant melanoma. Radiol Oncol 2020; 54(1): 68–78. doi: 10.2478/raon-2020-0014.

77 Cemazar M, Ambrozic Avgustin J, Pavlin D, et al. Efficacy and safety of electrochemotherapy combined with peritumoral IL-12 gene electrotransfer of canine mast cell tumours. Vet Comp Oncol 2017; 15(2): 641–54. doi: 10.1111/vco.12208.

78 Tozon N, Pavlin D, Sersa G, Dolinsek T, Cemazar M. Electrochemotherapy with intravenous bleomycin injection: An observational study in superficial squamous cell carcinoma in cats. J Feline Med Surg 2014; 16: 291–9. doi: 10.1177/1098612X13507071.

79 Spugnini EP, Vincenzi B, Carocci F, Bonichi C, Menicagli F, Baldi A. Combination of bleomycin and cisplatin as adjuvant electrochemotherapy protocol for the treatment of incompletely excised feline injection-site sarcomas: a retrospective study. Open Vet J 2020; 10(3): 267–71. doi: 10.4314/ovj.v10i3.4.

80 Racnik J, Svara T, Zadravec M, et al. Electrochemotherapy with bleomycin of different types of cutaneous tumours in a ferret (*Mustela Putorius Furo*). Radiol Oncol 2017; 52(1): 98–104. doi: 10.1515/raon-2017-0057.

81 Tamzali Y, Borde L, Rols MP, Golzio M, Lyazrhi F, Teissie J. Successful treatment of equine sarcoids with cisplatin electrochemotherapy: a retrospective study of 48 cases. Equine Vet J 2012; 44: 214–20. doi: 10.1111/j.2042-3306.2011.00425.x.

82 Tozon N, Kramaric P, Kos Kadunc V, Sersa G, Cemazar M. Electrochemotherapy as a single or adjuvant treatment to surgery of cutaneous sarcoid tumours in horses: a 31-case retrospective study. Vet Rec 2016; 179: 1–6. doi: 10.1136/vr.103867.

83 Racnik J, Svara T, Zadravec M, Gombac M, Cemazar M, Sersa G, Tozon N. Electrochemotherapy with cisplatin for the treatment of a non-operable cutaneous fibroma in a cockatiel (*Nymphicus hollandicus*). N Z Vet J 2019; 67(3): 155–8. doi: 10.1080/00480169.2018.1564393.

84 Racnik J, Svara T, Zadravec M, Gombac M, Cemazar M, Sersa G, Tozon N. Electrochemotherapy with bleomycin in the treatment of squamous cell carcinoma of the uropygial gland in a cockatiel (*Nymphicus Hollandicus*). J Exotic Pet Med 2019; 29: 217–21. doi:10.1053/j.jepm.2018.04.020

85 Groselj A, Kranjc S, Bosnjak M, et al. Vascularization of the tumours affects the pharmacokinetics of bleomycin and the effectiveness of electrochemotherapy. Basic Clin Pharmacol Toxicol 2018; 123(3): 247–56. doi: 10.1111/bcpt.13012.

86 Čemažar M, Miklavčič D, Serša G. Intrinsic sensitivity of tumor cells to bleomycin as an indicator of tumor response to electrochemotherapy. Jpn J Cancer Res 1998; 89: 328–33. doi: 10.1111/j.1349-7006.1998.tb00566.x.

87 Mali B, Miklavcic D, Campana LG, et al. Tumor size and effectiveness of electrochemotherapy. Radiol Oncol 2013; 47(1): 32–41. doi: 10.2478/raon-2013-0002.

88 Mesojednik S, Pavlin D, Serša G, et al. The effect of the histological properties of tumors on transfection efficiency of electrically assisted gene delivery to solid tumors in mice. Gene Ther 2007; 14(17): 1261–9. doi: 10.1038/sj.gt.3302989.

89 Markelc B, Sersa G, Cemazar M. Differential mechanisms associated with vascular disrupting action of electrochemotherapy: intravital microscopy on the level of single normal and tumor blood vessels. PLoS One 2013; 8: e59557. doi: 10.1371/journal.pone.0059557.

90 Sersa G, Cemazar M, Miklavcic D, Chaplin DJ. Tumor blood flow modifying effect of electrochemotherapy with bleomycin. Anticancer Res 1999; 19: 4017–22. doi: 10.1007/978-3-540-73044-6 152.

91 Sersa G, Cemazar M, Parkins CS, Chaplin DJ. Tumour blood flow changes induced by application of electric pulses. Eur J Cancer 1999; 35: 672–7. doi: 10.1016/S0959-8049(98)00426-2.

92 Jarm T, Cemazar M, Miklavcic D, Sersa G. Antivascular effects of electrochemotherapy: implications in treatment of bleeding metastases. Expert Rev Anticancer Ther 2010; 10(5): 729–46. doi: 10.1586/era.10.43.

93 Bellard E, Markelc B, Pelofy S, et al. Intravital microscopy at the single vessel level brings new insights of vascular modification mechanisms induced by electropermeabilization. J Control Release 2012; 163: 396–403. doi: 10.1016/j.jconrel.2012.09.010.

94 Markelc B, Bellard E, Serša G, et al. In vivo molecular imaging and histological analysis of changes induced by electric pulses used for plasmid DNA electrotransfer to the skin: a study in a dorsal window chamber in mice. J Membr Biol 2012; 245(9): 545–54. doi: 10.1007/s00232-012-9435-5.

95 Sersa G, Beravs K, Cemazar M, Miklavcic D, Demsar F. Contrast enhanced MRI assessment of tumor blood volume after application of electric pulses. Electro- Magnetobiol 1998; 17: 229–306. doi: 10.3109/15368379809022574.

96 Sersa G, Krzic M, Sentjurc M, et al. Reduced blood flow and oxygenation in SA-1 tumours after electrochemotherapy with cisplatin. Br J Cancer 2002; 87: 1047–54. doi.org/10.1038/sj.bjc.6600606.

97 Sersa G, Cemazar M, Miklavcic D. Tumor blood flow modifying effects of electrochemotherapy: a potential vascular targeted mechanism. Radiol Oncol 2003; 37: 43–8. doi: 10.1007/978-3-540-73044-6_153.

98 Sersa G, Jarm T, Kotnik T, et al. Vascular disrupting action of electroporation and electrochemotherapy with bleomycin in murine sarcoma. Br J Cancer; 2008: 98(2): 388–98. doi: 10.1038/sj.bjc.6604168.

99 Raesi E, Firoozabadi SMP, Hajizadeh S, Rajabi H, Hassan ZM. The effect of high-frequency electric pulses on tumor blood flow *in vivo*. J Membrane Biol 2010; 236(1): 163–6. doi: 10.1007/s00232-010-9288-8.

100 Cemazar M, Parkins CS, Holder AL, et al. Electroporation of human microvascular endothelial cells: evidence for an anti-vascular mechanism of electrochemotherapy. Br J Cancer 2001; 84(4): 565–70. doi: 10.1054/bjoc.2000.1625.

101 Charpentier KP, Wolf F, Noble L, Winn B, Resnick M, Dupuy DE. Irreversible electroporation of the liver and liver hilum in swine. HPB (Oxford) 2011; 13(3): 168–73. doi: 10.1111/j.1477-2574.2010.00261.x.

102 Appelbaum L, Ben-David E, Sosna J, Nissenbaum Y, Goldberg SN. US findings after irreversible electroporation ablation: radiologic-pathologic correlation. Radiology 2012; 262(1): 117–25. doi: 10.1148/radiol.11110475.

103 Kasivisvanathan V, Thapar A, Oskrochi Y, Picard J, Leen EL. Irreversible electroporation for focal ablation at the porta hepatis. Cardiovasc Intervent Radiol 2012; 35: 1531–4. doi: 10.1007/s00270-012-0363-7.

104 Kingham TP, Karkar AM, D'Angelica MI, Allen PJ, DeMatteo RP, Getrajdman GI. Ablation of perivascular hepatic malignant tumors with irreversible electroporation. J Am Coll Surg 2012; 215: 379–87. doi: 10.1016/j.jamcollsurg.2012.04.029.

105 Abdelsalam ME, Chetta JA, Harmoush S, et al. CT findings after irreversible electroporation ablation in a porcine model: Radiologic-pathologic correlation. J Vasc Interv Radiol 2013; 24(4): S161. doi:10.1016/j.jvir.2013.01.405.

106 Au JT, Kingham TP, Jun K, et al. Irreversible electroporation ablation of the liver can be detected with ultrasound B-mode and elastography. Surgery 2013; 153(6): 787–93. doi: 10.1016/j.surg.2012.11.022.

107 Lee EW, Chen C, Prieto VE, Dry SM, Loh CT, Kee ST. Advanced hepatic ablation technique for creating complete cell death: irreversible electroporation. Radiology 2010; 255(2): 426–33. doi: 10.1148/radiol.10090337.

108 Lee YJ, Lu DS, Osuagwu F, Lassman C. Irreversible electroporation in porcine liver: short- and long-term effect on the hepatic veins and adjacent tissue by CT with pathological correlation. Invest Radiol 2012; 47(11): 671–5. doi: 10.1097/RLI.0b013e318274b0df.

109 Lee YJ, Lu DS, Osuagwu F, Lassman C. Irreversible electroporation in porcine liver: acute computed tomography appearance of ablation zone with histopathologic correlation. J Comput Assist Tomogr 2013; 37(2): 154–8. doi: 10.1097/RCT.0b013e31827dbf9b.

110 Narayanan G, Bhatia S, Echenique A, Suthar R, Barbery K, Yrizarry J. Vessel patency post irreversible electroporation. Cardiovasc Intervent Radiol 2014; 37(6): 1523–9. doi: 10.1007/s00270-014-0988-9.

111 Chung DJ, Sung K, Osuagwu FC, Wu HH, Lassman C, Lu DS. Contrast enhancement patterns after irreversible electroporation: experimental study of CT perfusion correlated to histopathology in healthy porcine liver. J Vasc Interv Radiol 2016; 27(1): 104–11. doi: 10.1016/j.jvir.2015.09.005.

112 Cannon R, Ellis S, Hayes D, Narayanan G, Martin RCG. Safety and early efficacy of irreversible electroporation for hepatic tumors in proximity to vital structures. J Surg Oncol 2013; 107(5): 544–9. doi: 10.1002/jso.23280.

113 Boc N, Edhemovic I, Kos B, et al. Ultrasonographic changes in the liver tumors as indicators of adequate tumor coverage with electric field for effective electrochemotherapy. Radiol Oncol 2018; 52(4): 383–91. doi: 10.2478/raon-2018-0041.

114 Tozer GM, Kanthou C, Baguley BC. Disrupting tumour blood vessels. Nat Rev Cancer 2005; 5(6): 423–35. doi: 10.1038/nrc1628.

115 Jain RK. Normalization of tumor vasculature: an emerging concept in antiangiogenic therapy. Science 2005; 307(5706): 58–62. doi: 10.1126/science.1104819.

116 Siemann DW. The unique characteristics of tumor vasculature and preclinical evidence for its selective disruption by tumor-vascular disrupting agents. Cancer Treat Rev 2011; 37(1): 63–74. doi: 10.1016/j.ctrv.2010.05.001.

117 Ohlerth S, Wergin M, Bley CR, Del et al. Correlation of quantified contrast-enhanced power Doppler ultrasonography with immunofluorescent analysis of microvessel density in spontaneous canine tumours. Vet J 2010; 183(1): 58–62. doi: 10.1016/j.tvjl.2008.08.026.

118 Schärz M, Ohlerth S, Aschermann R, et al. Evaluation of quantified contrast-enhanced color and power Doppler ultrasonography for the assessment of vascularity and perfusion of naturally occurring tumors in dogs. Am J Vet Res 2005; 66(1): 21–9. doi: 10.2460/ajvr.2005.66.21.

119 Lyshchik A, Moses R, Barnes SL, Higashi T, Asato R, Miga MI, Gore JC, Fleischer AC. Quantitative analysis of tumor vascularity in benign and malignant solid thyroid nodules. J Ultrasound Med 2007; 26(6): 837–46. doi: 10.7863/jum.2007.26.6.837.

120 Brustmann H, Riss P, Naudé S. The relevance of angiogenesis in benign and malignant epithelial tumors of the ovary: a quantitative histologic study. Gynecol Oncol 1997; 67(1): 20–6. doi: 10.1006/gyno.1997.4815.

121 Ziegler L, O'Brien RT. Harmonic ultrasound: a review. Vet Radiol Ultrasound 2002; 43(6): 501–9. doi: 10.1111/j.1740-8261.2002.tb01040.x.

122 Katayama Y, Uchino J, Chihara Y, et al. Tumor neovascularization and developments in therapeutics. Cancers (Basel) 2019; 11(3): e316. doi: 10.3390/cancers11030316.

123 Kranjc Brezar S, Mrak V, Bosnjak M, Savarin M, Sersa G, Cemazar M. Intratumoral gene electrotransfer of plasmid DNA encoding shRNA against melanoma cell adhesion molecule radiosensitizes tumors by antivascular effects and activation of an immune response. Vaccines (Basel) 2020; 8(1): 135. doi: 10.3390/vaccines8010135.

124 Savarin M, Kamensek U, Cemazar M, Heller R, Sersa G. Electrotransfer of plasmid DNA radiosensitizes B16F10 tumors through activation of immune response. Radiol Oncol 2017; 51(1): 30–9. doi: 10.1515/raon-2017-0011.

125 Claudon M, Dietrich CF, Choi BI, et al. Guidelines and good clinical practice recommendations for contrast enhanced ultrasound (CEUS) in the liver–update 2012: a WFUMB-EFSUMB initiative in cooperation with representatives of AFSUMB, AIUM, ASUM, FLAUS and ICUS. Ultrasound Med Biol 2013; 39(2): 187–210. doi: 10.1016/j.ultrasmedbio.2012.09.002.

126 Erlichman DB, Weiss A, Koenigsberg M, Stein MW. Contrast enhanced ultrasound: A review of radiology applications. Clin Imaging 2019; 60(2): 209–15. doi: 10.1016/j.clinimag.2019.12.013.

127 Ziegler LE, O'Brien RT, Waller KR, Zagzebski JA. Quantitative contrast harmonic ultrasound imaging of normal canine liver. Vet Radiol Ultrasound 2003; 44(4): 451–4. doi: 10.1111/j.1740-8261.2003.tb00484.x.

128 Blomley MJ, Cooke JC, Unger EC, Monaghan MJ, Cosgrove DO. Microbubble contrast agents: a new era in ultrasound. BMJ 2001; 322(7296): 1222–5. doi: 10.1136/bmj.322.7296.1222.

129 Fetzer DT, Rafailidis V, Peterson C, Grant EG, Sidhu P, Barr RG. Artifacts in contrast-enhanced ultrasound: a pictorial essay. Abdom Radiol 2018; 43(4): 977–97. doi: 10.1007/s00261-017-1417-8.

130 Westwood M, Joore M, Grutters J, et al. Contrast-enhanced ultrasound using SonoVue® (sulphur hexafluoride microbubbles) compared with contrast-enhanced computed tomography and contrast-enhanced magnetic resonance imaging for the characterisation of focal liver lesions and detection of liver metastases: a systematic review and cost-effectiveness analysis. Health Technol Assess 2013; 17(16): 1–243. doi: 10.3310/hta17160.

131 Ohlerth S, O'Brien RT. Contrast ultrasound: general principles and veterinary clinical applications. Vet J 2007; 174(3): 501–12. doi: 10.1016/j.tvjl.2007.02.009.

132 Hyvelin JM, Gaud E, Costa M, Helbert A, Bussat P, Bettinger T, Frinking P. Characteristics and echogenicity of clinical ultrasound contrast agents: an *In vitro* and *In vivo* comparison study. J Ultrasound Med 2017; 36(5): 941–53. doi: 10.7863/ultra.16.04059.

133 Dijkmans PA, Juffermans LJM, Musters RJP, et al. Microbubbles and ultrasound: from diagnosis to therapy. Eur J Echocardiogr 2004; 5, 245–56. doi: 10.1016/j.euje.2004.02.001.

134 Denham SL, Alexander LF, Robbin ML. Contrast-enhanced ultrasound: practical review for the assessment of hepatic and renal lesions. Ultrasound Q 2016; 32(2): 116–25 . doi: 10.1097/RUQ.0000000000000182.

135 Seiler GS, Brown JC, Reetz JA, et al. Safety of contrast-enhanced ultrasonography in dogs and cats: 488 cases (2002-2011). J Am Vet Med Assoc 2013; 242: 1255–9. doi: 10.2460/javma.242.9.1255.

136 Dolan MS, Gala SS, Dodla S, et al. Safety and efficacy of commercially available ultrasound contrast agents for rest and stress echocardiography: a multicenter experience. J Am Coll Cardiol 2009; 53: 32–8. doi: 10.1016/j.jacc.2008.08.066.

137 O'Brien RT, Holmes SP. Recent advances in ultrasound technology. Clin Tech Small Anim Pract 2007; 22(3): 93–103. doi: 10.1053/j.ctsap.2007.05.003.

138 Leinonen MR, Raekallio MR, Vainio OM, et al. The effect of the sample size and location on contrast ultrasound measurement of perfusion parameters. Vet Radiol Ultrasound 2011; 52(1): 82–7.

139 O'Brien RT, Iani M, Matheson J, Delaney F, Young K. Contrast harmonic ultrasound of spontaneous liver nodules in 32 Dogs. Vet Radiol Ultrasound 2004; 45(6): 547–53. 10.1111/j.1740-8261.2004.04094.x.

140 Kutara K, Asano K, Kito A, et al. Contrast harmonic imaging of canine hepatic tumors. J Vet Med Sci 2006; 68(5): 433–8. doi: 10.1292/jvms.68.433.

141 Ivancic M, Long F, Seiler GS. Contrast harmonic ultrasonography of splenic masses and associated liver nodules in dogs. J Am Vet Med Assoc 2009; 234(1): 88–94. doi: 10.2460/javma.234.1.88.

142 Kanemoto H, Ohno K, Nakashima K, et al. Characterization of canine focal liver lesions with contrast-enhanced ultrasound using a novel contrast agent-sonazoid. Vet Radiol Ultrasound 2009; 50(2): 188–94. doi: 10.1111/j.1740-8261.2009.01515.x.

143 Nakamura K, Takagi S, Sasaki N, et al. Contrast-enhanced ultrasonography for characterization of canine focal liver lesions. Vet Radiol Ultrasound 2010; 51(1): 79–85. doi: 10.1111/j.1939-1676.2010.0609.x.

144 Nakamura K, Sasaki N, Yoshikawa M, et al. Quantitative contrast-enhanced ultrasonography of canine spleen. Vet Radiol Ultrasound 2009; 50(1): 104–8. doi: 10.1111/j.1740-8261.2008.01499.x.

145 Rossi F, Leone VF, Vignoli M, Laddaga E, Terragni R. Use of contrast-enhanced ultrasound for characterization of focal splenic lesions. Vet Radiol Ultrasound 2008; 49(2): 154–64. doi: 10.1111/j.1740-8261.2008.00343.x.

146 Taeymans O, Penninck D. Contrast enhanced sonographic assessment of feeding vessels as a discriminator between malignant vs. benign focal splenic lesions. Vet Radiol Ultrasound 2011; 52(4): 457–61. doi: 10.1111/j.1740-8261.2011.01815.x.

147 Mangano C, Macrì F, Di Pietro S, et al. Use of contrast-enhanced ultrasound for assessment of nodular lymphoid hyperplasia (NLH) in canine spleen. BMC Vet Res 2019; 15(1): e196. doi: 10.1186/s12917-019-1942-5.

148 Ohlerth S, Dennler M, Rüefli E, et al. Contrast harmonic imaging characterization of canine splenic lesions. J Vet Intern Med 2008; 22(5): 1095–102. doi: 10.1111/j.1939-1676.2008.0154.x.

149 Haers H, Vignoli M, Paes G, et al. Contrast harmonic ultrasonographic appearance of focal space-occupying renal lesions. Vet Radiol Ultrasound 2010; 51(5): 516–22. doi: 10.1111/j.1740-8261.2010.01690.x.

150 Bargellini P, Orlandi R, Paloni C, et al. Contrast-enhanced ultrasonographic characteristics of adrenal glands in dogs with pituitary-dependent hyperadrenocorticism. Vet Radiol Ultrasound 2013; 54(3): 283–92. doi: 10.1111/vru.12018.

151 Bargellini P, Orlandi R, Dentini A, et al. Use of contrast-enhanced ultrasound in the differential diagnosis of adrenal tumors in dogs. J Am Anim Hosp Assoc 2016; 52(3): 132–43. doi: 10.5326/JAAHA-MS-6363.

152 Salwei RM, O'Brien RT, Matheson JS. Characterization of lymphomatous lymph nodes in dogs using contrast harmonic and Power Doppler ultrasound. Vet Radiol Ultrasound 2005; 46(5): 411–6. doi: 10.1111/j.1740-8261.2005.00075.x.

153 Gaschen L, Angelette N, Stout R. Contrast-enhanced harmonic ultrasonography of medial iliac lymph nodes in healthy dogs. Vet Radiol Ultrasound 2010; 51(6): 634–7. doi: 10.1111/j.1740-8261.2010.01707.x.

154 Wisner ER, Ferrara KW, Short RE, Ottoboni TB, Gabe JD, Patel D. Sentinel node detection using contrast-enhanced power Doppler ultrasound lymphography. Invest Radiol 2003; 38(6): 358–65. doi: 10.1097/01.rli.0000065423.05038.88.

155 Lurie DM, Seguin B, Schneider PD, Verstraete FJ, Wisner ER. Contrast-assisted ultrasound for sentinel lymph node detection in spontaneously arising canine head and neck tumors. Invest Radiol 2006; 41(4): 415–21. doi: 10.1097/01.rli.0000201230.29925.95.

156 Fournier Q, Thierry F, Longo M, et al. Contrast-enhanced ultrasound for sentinel lymph node mapping in the routine staging of canine mast cell tumours: a feasibility study. Vet Comp Oncol 2020 Avg. 24. doi: 10.1111/vco.12647.

157 Donelly EF, Geng L, Wojcicki WE, Fleischer AC, Hallahan DE. Quantified power Doppler US of tumor blood flow correlates with microscopic quantification of tumor blood vessels. Radiology 2001; 219(1): 166–70. doi: 10.1148/radiology.219.1.r01ap38166.

158 Zhou JH, Cao LH, Liu JB, et al. Quantitative assessment of tumor blood flow in mice after treatment with different doses of an antiangiogenic agent with contrast-enhanced destruction-replenishment US. Radiology 2011; 259(2): 406–13. doi: 10.1148/radiol.10101339.

159 Zhou JH, Cao LH, Zheng W, Liu M, Han F, Li AH. Contrast-enhanced gray-scale ultrasound for quantitative evaluation of tumor response to chemotherapy: preliminary results with a mouse hepatoma model. AJR Am J Roentgenol 2011; 196(1): W13-7. doi: 10.2214/AJR.10.4734.

160 Arteaga-Marrero N, Mainou-Gomez JF, Rygh CB, et al. Radiation treatment monitoring with DCE-US in CWR22 prostate tumor xenografts. Acta Radiol 2019; 60(6): 788–97. doi: 10.1177/0284185118798167.

161 Sedelaar JP, van Leenders GJ, Hulsbergen-van de Kaa CA, et al. Microvessel density: correlation between contrast ultrasonography and histology of prostate cancer. Eur Urol 2001; 40(3): 285–93. doi: 10.1159/000049788.

162 Leng X, Huang G, Ma F, Yao L. Regional contrast-enhanced ultrasonography (DCE-US) characteristics of breast cancer and correlation with microvessel density (MVD). Med Sci Monit 2017; 23: 3428–36. doi: 10.12659/MSM.901734.

163 Li X, Li Y, Zhu Y, Fu L, Liu P. Association between enhancement patterns and parameters of contrast-enhanced ultrasound and microvessel distribution in breast cancer. Oncol Lett 2018; 15(4): 5643–9. doi: 10.3892/ol.2018.8078.

164 Nierman KJ, Fleischer AC, Huamani J, et al. Measuring tumor perfusion in control and treated murine tumors: correlation of microbubble contrast-enhanced sonography to dynamic contrast-enhanced magnetic resonance imaging and fluorodeoxyglucose positron emission tomography. J Ultrasound Med 2007; 26: 749–56. doi: 10.7863/jum.2007.26.6.749.

165 Lamuraglia M, Escudier B, Chami L, et al. To predict progression-free survival and overall survival in metastatic renal cancer treated with sorafenib: pilot study using dynamic contrast- enhanced Doppler ultrasound. Eur J Cancer 2006; 42(15): 2472–9. doi: 10.1016/j.ejca.2006.04.023.

166 Escudier B, Lassau N, Angevin E, et al. Phase I trial of sorafenib in combination with IFN alpha-2a in patients with unresectable and/or metastatic renal cell carcinoma or malignant melanoma. Clin Cancer Res 2007; 13(6): 1801–9. doi: 10.1158/1078-0432.CCR-06-1432.

167 Lassau N, Chebil M, Chami L. A new functional imaging technique for the early functional evaluation of antiangiogenic treatment: dynamic contrast-enhanced ultrasonography (DCE-US). Target Oncol 2008 3: 111–7. doi: 10.1007/s11523-008-0081-x.

168 Lassau N, Chebil M, Chami L, Bidault S, Girard E, Roche A. Dynamic contrast-enhanced ultrasonography (DCE-US): a new tool for the early evaluation of antiangiogenic treatment. Target Oncol 2010; 5(1): 53–8. doi: 10.1007/s11523-010-0136-7.

169 Lassau N, Koscielny S, Albiges L, et al. Metastatic renal cell carcinoma treated with sunitinib: early evaluation of treatment response using dynamic contrast-enhanced ultrasonography. Clin Cancer Res 2010; 16(4): 1216–25. doi: 10.1158/1078-0432.CCR-09-2175.

170 Lassau N, Koscielny S, Chami L, et al. Advanced hepatocellular carcinoma: early evaluation of response to bevacizumab therapy at dynamic contrast-enhanced US with quantification – preliminary results. Radiology 2011; 258(1): 291–300. doi: 10.1148/radiol.10091870.

171 Lassau N, Chapotot L, Benatsou B, et al. Standardization of dynamic contrast-enhanced ultrasound for the evaluation of antiangiogenic therapies: the French multicenter support for innovative and expensive techniques study. Invest Radiol 2012; 47(12): 711–6. doi: 10.1097/RLI.0b013e31826dc255.

172 Lassau N, Cosgrove D, Armand JP. Early evaluation of tarGEPed drugs using dynamic contrast-enhanced ultrasonography for personalized medicine. Future Oncol 2012; 8(10): 1215–8. doi: 10.2217/fon.12.114.

173 Lassau N, Bonastre J, Kind M, et al. Validation of dynamic contrast-enhanced ultrasound in predicting outcomes of antiangiogenic therapy for solid tumors: the French multicenter support for innovative and expensive techniques study. Invest Radiol 2014; 49(12): 794–800. doi: 10.1097/RLI.0000000000000085.

174 Lassau N, Coiffier B, Kind M, et al. Selection of an early biomarker for vascular normalization using dynamic contrast-enhanced ultrasonography to predict outcomes of metastatic patients treated with bevacizumab. Ann Oncol 2016; 27(10): 1922–8. doi: 10.1093/annonc/mdw280.

175 Kim Y, Kim SH, Song BJ, et al. Early prediction of response to neoadjuvant chemotherapy using dynamic contrast-enhanced MRI and ultrasound in breast cancer. Korean J Radiol 2018; 19: 682–91. doi: 10.3348/kjr.2018.19.4.682.

176 Cicchelero L, Denies S, Vanderperren K, et al. Intratumoural interleukin 12 gene therapy stimulates the immune system and decreases angiogenesis in dogs with spontaneous cancer. Vet Comp Oncol 2017; 15: 1187–205. doi: 10.1111/vco.12255.

177 Cicchelero L, Denies S, Vanderperren K, et al. Immunological, anti-angiogenic and clinical effects of intratumoral interleukin 12 electrogene therapy combined with metronomic cyclophosphamide in dogs with spontaneous cancer: a pilot study. Cancer Lett 2017; 400: 205–18. doi: 10.1016/j.canlet.2016.09.015.

178 Eisenhauer EA, Therasse P, Bogaerts J, Schwartz LH, Sargent D, Ford R, Dancey J, Arbuck S, Gwyther S, Mooney M, Rubinstein L, Shankar L, Dodd L, Kaplan R, Lacombe D, Verweij J. New response evaluation criteria in solid tumours: revised RECIST guideline (version 1.1). Eur J Cancer 2009; 45(2): 228–47. doi: 10.1016/j.ejca.2008.10.026.

179 Nguyen SM, Thamm DH, Vail DM, London CA. Response evaluation criteria for solid tumours in dogs (v1.0): a Veterinary Cooperative Oncology Group (VCOG) consensus document. Vet Comp Oncol 2015; 13(3): 176–83. doi: 10.1111/vco.12032.

180 Schwarz LH, Litiere S, de Vries E, et al. RECIST 1.1 – update and clarification: from the RECIST Committee. Eur J Cancer 2016; 62: 132–7. doi: 10.1016/j.ejca.2016.03.081.

181 Seymour K, Bogaerts J, Perrone A, et al. iRECIST: guidelines for response criteria for use in trials testing immunotherapeutics. Lancet Oncol 2017; 18(3): e143–52. doi: 10.1016/S1470-2045(17)30074-8.

182 Zhu AX, Holalkere NS, Muzikansky A, et al. Early antiangiogenic activity of bevacizumab evaluated by computed tomography perfusion scan in patients with advanced hepatocellular carcinoma. Oncologist 2008; 13(2): 120–5. doi: 10.1634/theoncologist.2007-0174.

183 Dietrich CF, Averkiou MA, Correas JM, Lassau N, Leen E, Piscaglia F. An EFSUMB introduction into dynamic contrast- enhanced ultrasound (DCE-US) for quantification of tumour perfusion. Ultraschall in Med 2012; 33(4): 344–51. doi: 10.1055/s-0032-1313026.

184 Lencioni R, Llovet JM. Modified RECIST (mRECIST) assessment for hepatocellular carcinoma. Semin Liver Dis 2010; 30(1): 52–60. doi: 10.1055/s-0030-1247132.

185 Paoloni M, Khanna C. Translation of new cancer treatments from pet dogs to humans. Nat Rev Cancer 2008; 8(2): 147–56. doi: 10.1038/nrc2273.

186 Maio M. Melanoma as a model tumour for immuno-oncology. Ann Oncol 2012; 23 (Suppl 8): viii10–4. doi: 10.1093/annonc/mds257. doi: 10.1093/annonc/mds257.

187 Böck BC, Stein U, Schmitt CA, Augustin HG. Mouse models of human cancer. Cancer Res 2014; 74(17): 4671–5. doi: 10.1158/0008-5472.CAN-14-1424.

188 Hernandez B, Adissu HA, Wei BR, et al. Naturally occurring canine melanoma as a predictive comparative oncology model for human mucosal and other triple wild-type melanomas. Int J Mol Sci 2018; 19(2): e394 (19 str.). doi: 10.3390/ijms19020394.

189 Lampreht Tratar U, Horvat S, Cemazar M. Transgenic mouse models in cancer research. Front Oncol 2018; 8: e268. doi: 10.3389/fonc.2018.00268.

190 Gardner HL, Fenger JM, London CA. Dogs as a model for cancer. Annu Rev Anim Biosci 2016; 4: 199–222. doi: 10.1146/annurev-animal-022114-110911.

191 Costa E, Ferreira-Gonçalves T, Chasqueira G, et al. Experimental models as refined translational tools for breast cancer research. Sci Pharm 2020; 88: e32. doi:10.3390/scipharm88030032.

192 Rowell JL, McCarthy DO, Alvarez CE. Dog models of naturally occurring cancer. Trends Mol Med 2011; 17: 380–8. doi: 10.1016/j.molmed.2011.02.004.

193 Khanna C, Lindblad-Toh K, Vail D, et al. The dog as a cancer model. Nat Biotechnol 2006; 24(9): 1065–6. doi: 10.1038/nbt0906-1065b.

194 Gillies RJ, Schornack PA, Secomb TW, Raghunand N. Causes and effects of heterogeneous perfusion in tumors. Neoplasia 1999; 1(3): 197–207. doi: 10.1038/sj.neo.7900037.

195 Graff BA, Benjaminsen IC, Melas EA, Brurberg KG, Rofstad EK. Changes in intratumor heterogeneity in blood perfusion in intradermal human melanoma xenografts during tumor growth assessed by DCE-MRI. Magn Reson Imaging 2005; 23(9): 961–6. doi: 10.1016/j.mri.2005.09.006.

196 Graff BA, Benjaminsen IC, Brurberg KG, Ruut EBM, Rofstad EK. Comparison of tumor blood perfusion assessed by dynamic contrast-enhanced MRI with tumor blood supply assessed by invasive imaging. J Magn Reson Imaging 2005; 21(3): 272–81. doi: 10.1002/jmri.20265.

197 Yankeelov TE, Niermann KJ, Huamani J, et al. Correlation between estimates of tumor perfusion from microbubble contrast-enhanced sonography and dynamic contrast-enhanced magnetic resonance imaging. J Ultrasound Med 2006; 25: 487–97. doi: 10.7863/jum.2006.25.4.487.

198 Gaustad JV, Benjaminsen IC, Ruud EB, Rofstad EK. Dynamic contrast-enhanced magnetic resonance imaging of human melanoma xenografts with necrotic regions. J Magn Reson Imaging 2007; 26(1): 133–43. doi: 10.1002/jmri.20939.

199 Mayr NA, Huang Z, Wang JZ, et al. Characterizing tumor heterogeneity with functional imaging and quantifying high-risk tumor volume for early prediction of treatment outcome: cervical cancer as a model. Int J Radiat Oncol Biol Phys 2012; 83(3): 972–9. doi: 10.1016/j.ijrobp.2011.08.011.

200 Hayano K, Lee SH, Yoshida H, Zhu AX, Sahani DV. Fractal analysis of CT perfusion images for evaluation of antiangiogenic treatment and survival in hepatocellular carcinoma. Acad Radiol 2014; 21(5): 654–60. doi: 10.1016/j.acra.2014.01.020.

201 Ong SL, Gravante G, Metcalfe MS, Dennison AR. History, ethics, advantages and limitations of experimental models for hepatic ablation. World J Gastroenterol 2013; 19(2): 147–54. doi: 10.3748/wjg.v19.i2.147.

202 Nykonenko A, Vavra P, Zonca P. Anatomic Peculiarities of Pig and Human Liver. Exp Clin Transplant 2017; 15: 21–6. doi: 10.6002/ect.2016.0099.

203 Zmuc J, Gasljevic G, Sersa G, et al. Large liver blood vessels and bile ducts are not damaged by electrochemotherapy with bleomycin in pigs. Sci Rep 2019: 9(1): e3649. doi: 10.1038/s41598-019-40395-y.

204 Miklavcic D, Sersa G, Brecelj E, Gehl J, Soden D, Bianchi G. Electrochemotherapy: technological advancements for efficient electroporation-based treatment of internal tumors. Med Biol Eng Comput 2012; 50: 1213–25. doi: 10.1007/s11517-012-0991-8.

205 Gasljevic G, Edhemovic I, Cemazar M, et al. Histopathological findings in colorectal liver metastasis after electrochemotherapy. PloS One 2017; 12(7): e0180709. doi: 10.1371/journal.pone.0180709.

206 Tarantino L, Busto G, Nasto A, et al. Percutaneous electrochemotherapy in the treatment of portal vein tumor thrombosis at hepatic hilum in patients with hepatocellular carcinoma in cirrhosis: a feasibility study. World J Gastroenterol 2017; 23(5): 906–18. doi: 10.3748/wjg.v23.i5.906.

207 Kos B, Voigt P, Miklavcic D, Moche M. Careful treatment planning enables safe ablation of liver tumors adjacent to major blood vessels by percutaneous irreversible electroporation (IRE). Radiol Oncol 2015; 49: 234–41. doi: 10.1515/raon-2015-0031.

208 Faroja M, Ahmed M, Appelbaum L, Ben-David E, Moussa M, Sosna J. Irreversible electroporation ablation: is all the damage non thermal? Radiology 2013; 266: 462–70. doi: 10.1148/radiol.12120609.

209 Ivanusa T, Beravs K, Cemazar M, Jevtic V, Demsar F, Sersa G. MRI macromolecular contrast agents as indicators of changed tumor blood flow. Radiol Oncol 2001; 35(2): 139–47.

210 Markelc B, Bellard E, Sersa G, et al. Increased permeability of blood vessels after reversible electroporation is facilitated by alterations in endothelial cell-to-cell junctions. J Control Release 2018; 276: 30–41. doi: 10.1016/j.jconrel.2018.02.032.

211 Miklavcic D, Mali B, Kos B, Heller R, Sersa G. Electrochemotherapy: from the drawing board into medical practice. Biomed Eng Online 2014; 13(1): e29. doi: 10.1186/1475-925X-13-29.

212 Miklavcic D, Semrov D, Mekid H, Mir LM. A validated model of in vivo electric field distribution in tissues for electrochemotherapy and for DNA electrotransfer for gene therapy. Biochim Biophys Acta 2000; 1523(1): 73–83. doi:10.1016/s0304-4165(00)00101-x.

213 Prosen L, Markelc B, Dolinsek T, Music B, Cemazar M, Sersa G. Mcam silencing with RNA interference using magnetofection has antitumor effect in murine melanoma. Mol Ther Nucleic Acids 2014; 3: e205. doi: 10.1038/mtna.2014.56.

214 Wang F, Nojima M, Inoue Y, Ohtomo K, Kiryu S. Assessment of MRI contrast agent kinetics via retro-orbital injection in mice: comparison with tail vein injection. PLoS One 2015; 10(6): e0129326. doi: 10.1371/journal.pone.0129326.

215 Yardeni T, Eckhaus M, Morris HD, Huizing M, Hoogstraten-Miller S. Retro-orbital injections in mice. Lab Anim (NY) 2011; 40(5): 155–60. doi: 10.1038/laban0511-155.

216 Li YJ, Wen G, Wang Y, et al. Perfusion heterogeneity in breast tumors for assessment of angiogenesis. J Ultrasound Med 2013; 32(7): 1145–55. doi: 10.7863/ultra.32.7.1145.

217 Rohrer Bley C, Laluhova D, Roos M, Kaser-Hotz B, Ohlerth S. Correlation of pretreatment polarographically measured oxygen pressures with quantified contrast-enhanced power Doppler ultrasonography in spontaneous canine tumors and their impact on outcome after radiation therapy. Strahlenther Onkol 2009; 185(11): 756–62. doi: 10.1007/s00066-009-1988-6.

218 Ohlerth S, Bley CR, Laluhová D, Roos M, Kaser-Hotz B. Assessment of changes in vascularity and blood volume in canine sarcomas and squamous cell carcinomas during fractionated radiation therapy using quantified contrast-enhanced power Doppler ultrasonography: a preliminary study. Vet J 2010; 186(1): 58–63. doi: 10.1016/j.tvjl.2009.07.006.

219 Siemann DW, Chaplin DJ, Horsman MR. Realizing the potential of vascular targeted therapy: the rationale for combining vascular disrupting agents and anti-angiogenic agents to treat cancer. Cancer Invest 2017 14; 35(8): 519-534. doi: 10.1080/07357907.2017.1364745.

220 Sedlar A, Kranjc S, Dolinsek T, Cemazar M, Coer A, Sersa G. Radiosensitizing effect of intratumoral interleukin-12 gene electrotransfer in murine sarcoma. BMC Cancer 2013; 13: e38. doi: 10.1186/1471-2407-13-38.

221 Stimac M, Kamensek U, Cemazar M, Kranjc S, Coer A, Sersa G. Tumor radiosensitization by gene therapy against endoglin. Cancer Gene Ther 2016; 23(7): 214–20. doi: 10.1038/cgt.2016.20.

222 Savarin M, Prevc A, Rzek M, et al. Intravital monitoring of vasculature after targeted gene therapy alone or combined with tumor irradiation. Technol Cancer Res Treat 2018; 17(2): 1533033818784208. doi: 10.1177/1533033818784208.

223 Kalbasi A, Haas N, June CH, Vapiwala N. Radiation and immunotherapy: a synergistic combination. J Clin Invest 2013; 123(7): 2756–63. doi: 10.1172/JCI69219.

224 Kong WT, Wang WP, Huang BJ, Ding H, Mao F. Value of wash-in and wash-out time in the diagnosis between hepatocellular carcinoma and other hepatic nodules with similar vascular pattern on contrast-enhanced ultrasound. J Gastroenterol Hepatol 2014; 29(3): 576-80. doi: 10.1111/jgh.12394.

9 PRILOGE

9.1 Priloga 1. Dovoljenje za objavo članka 2.1

RADIOLOGY AND ONCOLOGY, Association of Radiology and Oncology,
Zaloska 2, P.O.Box 2217, SI-1000 Ljubljana, Slovenia, T/F: +386 1 5879 434, e: gsersa@onko-i.si www.degruyter.com/view/j/raon

Maja Brložnik

Spoštovani,

voljuje objavo rezultatov članka »
«

v doktorske delu Maja Brložnik

Članek objavljen

Digitally signed
by GREGOR SERSA
Date: 2021.06.15
10:53:19 +02'00'

š

Radiology and Oncology (**ISSN 1318-2099**) is a multidisciplinary journal devoted to-the publishing of original and high quality articles in diagnostic and interventional radiology, computerized tomography, ultrasound, magnetic resonance, nuclear medicine, radiotherapy, clinical and experimental oncology, radiobiology, radiophysics, and radiation protection. Therefore, the scope of the journal is to cover diagnostic and therapeutic aspects in oncology, which distinguishes it from other journals in the field.

Open access on the web: ISSN 1518-3207 www.degruyter.com/view/j/raon www.radioloncol.com

9. 2 Priloga 2. Dopolnilni podatki članka 2.2

Ultrazvočni pregled s kontrastnim sredstvom za oceno perfuzije tumorjev in izida zdravljenja na modelu mišjih melanomov

SUPPLEMENTARY INFORMATION

CONTRAST-ENHANCED ULTRASOUND FOR EVALUATION OF TUMOR PERFUSION AND OUTCOME FOLLOWING TREATMENT IN A MURINE MELANOMA MODEL

Supplementary Figure Legends

Supplementary Figure S1: Histological staining for blood vessels and associated CEUS perfusion evaluation in melanoma B16F10 after treatment with GET pMCAM and irradiation.

Supplementary Figure S2: Analysis of B16F10 tumor perfusion (CEUS PE) and vascular density after silencing of MCAM and irradiation.

Supplementary Figure S3: Contrast-enhanced ultrasonography (CEUS) of melanoma B16F10. The mouse was treated with electrical pulses only (EP group) and CEUS carried out on day 6.

Supplementary Figure S4: CEUS results after combined treatment of GET and irradiation in B16F10 melanoma. Based on CEUS measurements, peak enhancement (PE) was calculated as the difference between peak intensity (PI) and base intensity (BI).

Supplementary Figure S5: CEUS perfusion curves of a complete response tumor treated with gene electrotransfer of control plasmid DNA and irradiation. A = day 0, B = day 1, C = day 2, D = day 5, E = day 7, and F = day 10.

Supplementary Table Legends

Supplementary Figure S6: Growth of B16F10 melanomas after silencing of MCAM and irradiation. CTRL = control, EP = application of electrical pulses; GET = gene electrotransfer; IR = single-dose irradiation, 15 Gy; pC = intratumoral injection of control plasmid; pMCAM = intratumoral injection of plasmid DNA encoding shRNA for MCAM. Data represent mean and standard error of the mean (mean±SE) of tumors that did not show a complete response (n=3-7).

Supplementary Figure S7: Correlation of B16F10 tumor perfusion (CEUS PE) and vascular density, as assessed by histological analysis, after silencing MCAM and irradiation. In the treatment groups with the therapeutic plasmid; i.e. GET pMCAM and GET pMCAM IR, vascular density and PE were determined in the same mice, Pearson correlation coefficient was 0.45 (95% confidence interval [-0.57, 0.92]). GET = gene electrotransfer; IR = single-dose irradiation, 15 Gy; pMCAM = intratumoral injection of plasmid DNA encoding shRNA for MCAM.

Supplementary Table S1. Comparison of mean peak enhancement between complete responders (CR) and mice with tumor growth (non-CR). Mean (SD) for PE values and the number of mice for each group. P-values correspond to t-tests for each day, with Hommel correction for family-wise error rate when data are non-negatively associated (adjusted P).

Supplementary Table S2. Linear regression coefficients for each measurement day associating PE with log transformed DT.

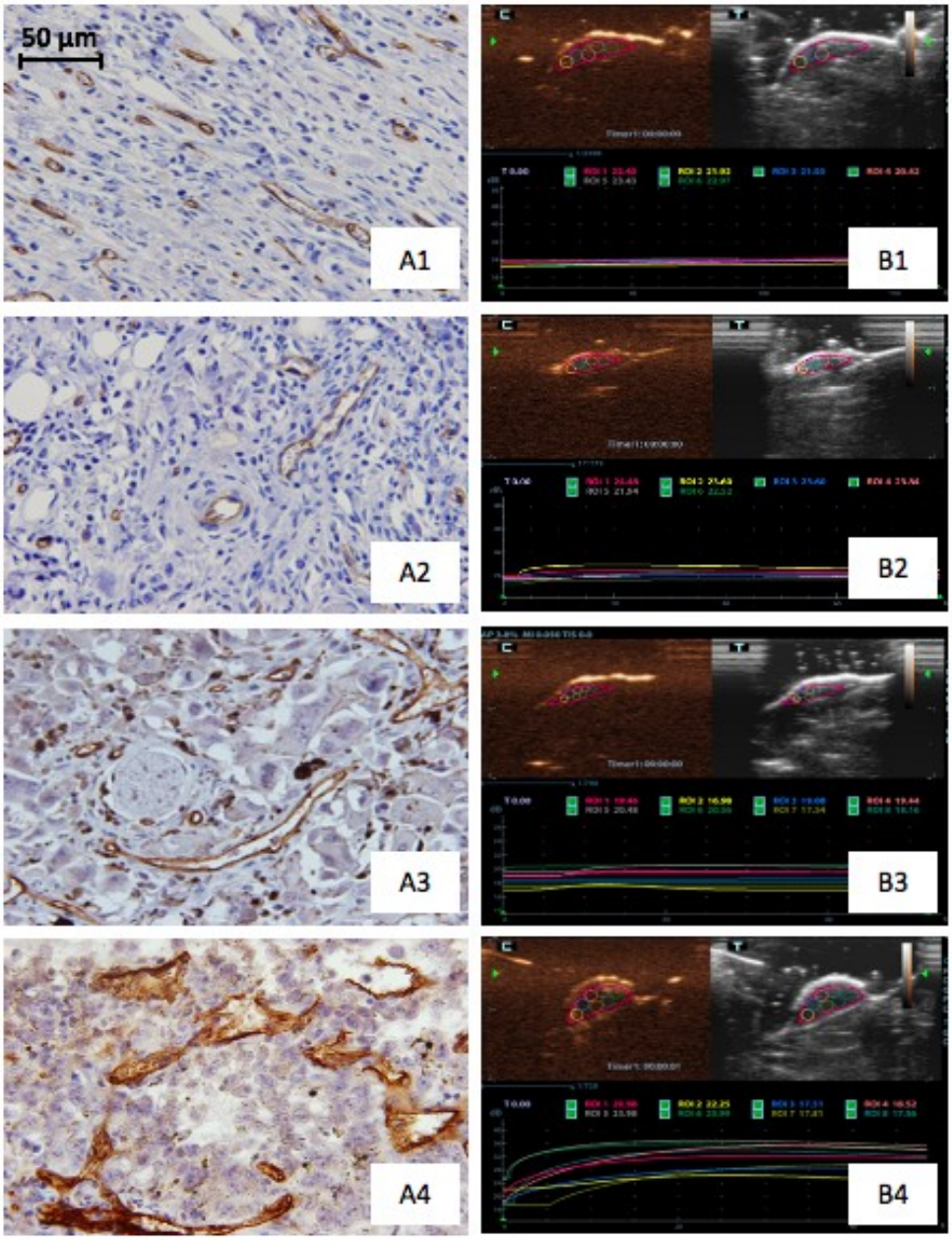

Supplementary Figure S1: Histological staining for blood vessels and associated CEUS perfusion evaluation in melanoma B16F10 after treatment with GET pMCAM and irradiation. Representative histological images are shown on the left (A1–A4), 40x, brown staining shows CD31-positive tumor vessels. Associated CEUS perfusion curves are shown on the right (B1–B4). Pink curve indicates perfusion of whole tumor and other curves show perfusion of individual regions of interest. The three combined therapeutic groups (1–3) and untreated control group (4) are presented: 1 = GET pMCAM IR (gene electrotransfer of plasmid DNA encoding shRNA against MCAM and irradiation), 2 = GET pMCAM (gene electrotransfer of plasmid DNA encoding shRNA against MCAM), 3 = GET pC IR (gene electrotransfer of control plasmid DNA and irradiation), 4 = CTRL (untreated control). Note the lower vessel density (brown stained blood vessels) in the histological images of A1-A3 compared to image A4 and the correlating CEUS perfusion curves showing decreased perfusion (B1–B3) compared to B4.).

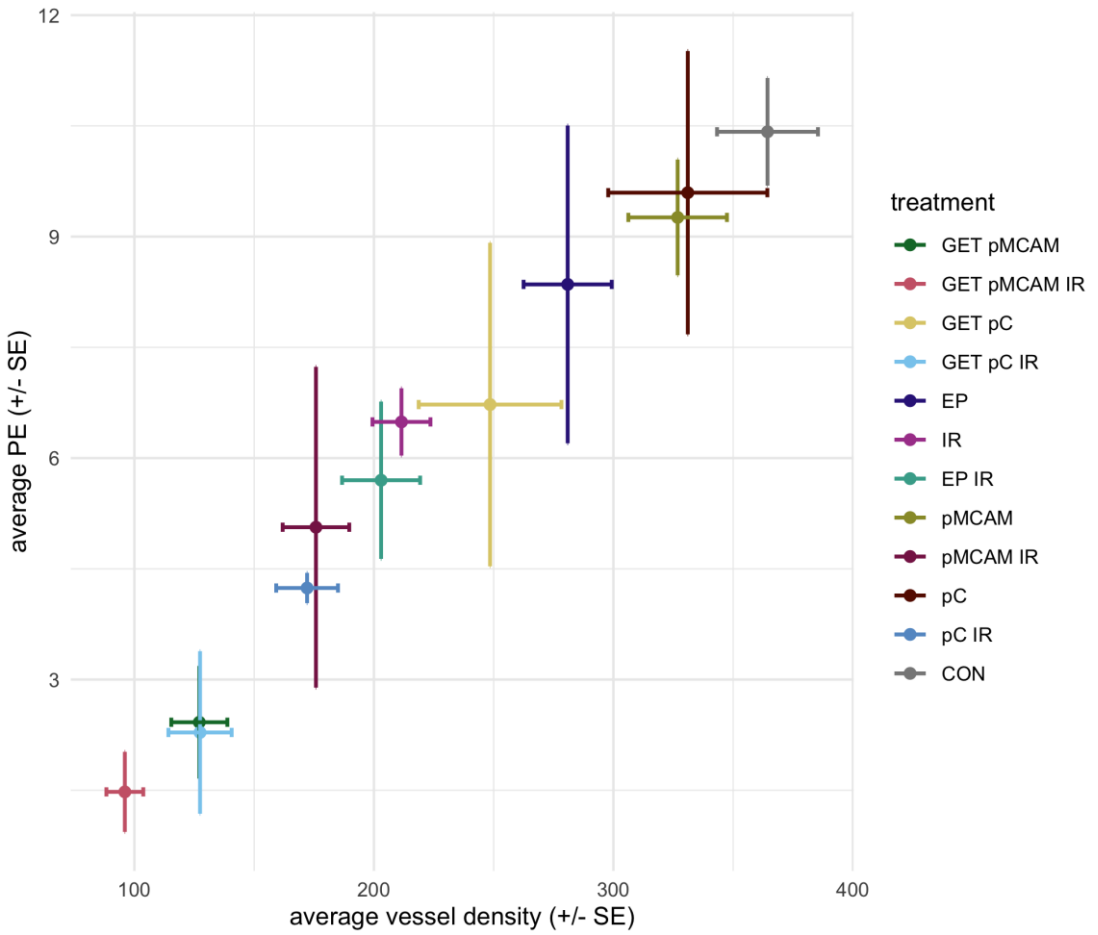

Supplementary Figure S2: Analysis of B16F10 tumor perfusion (CEUS PE) and vascular density after silencing of MCAM and irradiation. Note that there is a correlation between the average histological vascular density and the average CEUS results for each treatment. CTRL = control, EP = application of electrical pulses; GET = gene electrotransfer; IR = single-dose irradiation, 15 Gy; pC = intratumoral injection of control plasmid; pMCAM = intratumoral injection of plasmid DNA encoding shRNA for MCAM.

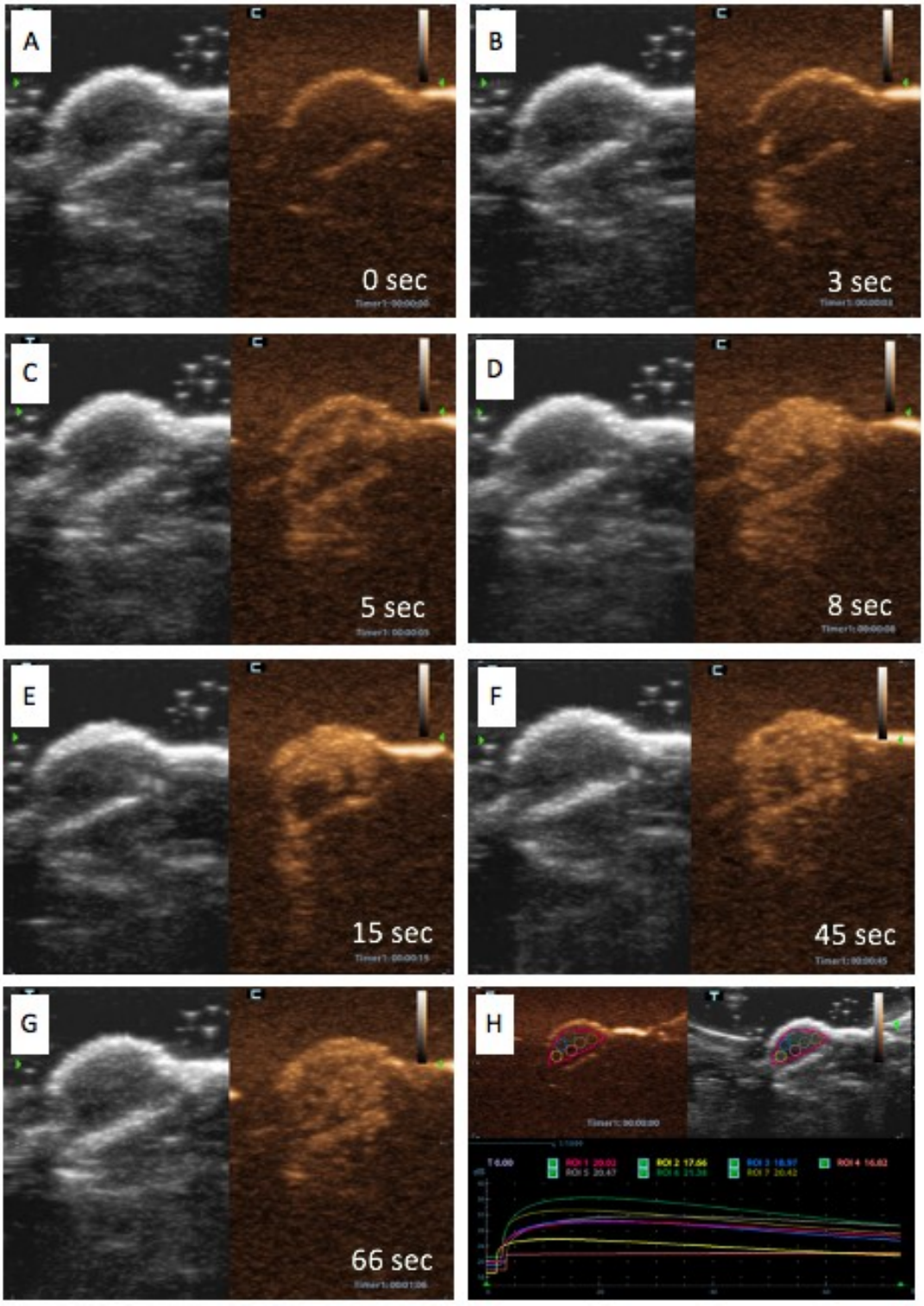

Supplementary Figure S3: Contrast-enhanced ultrasonography (CEUS) of melanoma B16F10. The mouse was treated with electrical pulses only (EP group) and CEUS carried out on day 6. Representative images at different time points (A – G), with the non-linear contrast mode seen to the right of each image. Note that tumors start filling with microbubbles 3 seconds after administration. Perfusion curves for the whole tumor (pink curve) and different ROIs are shown in H.

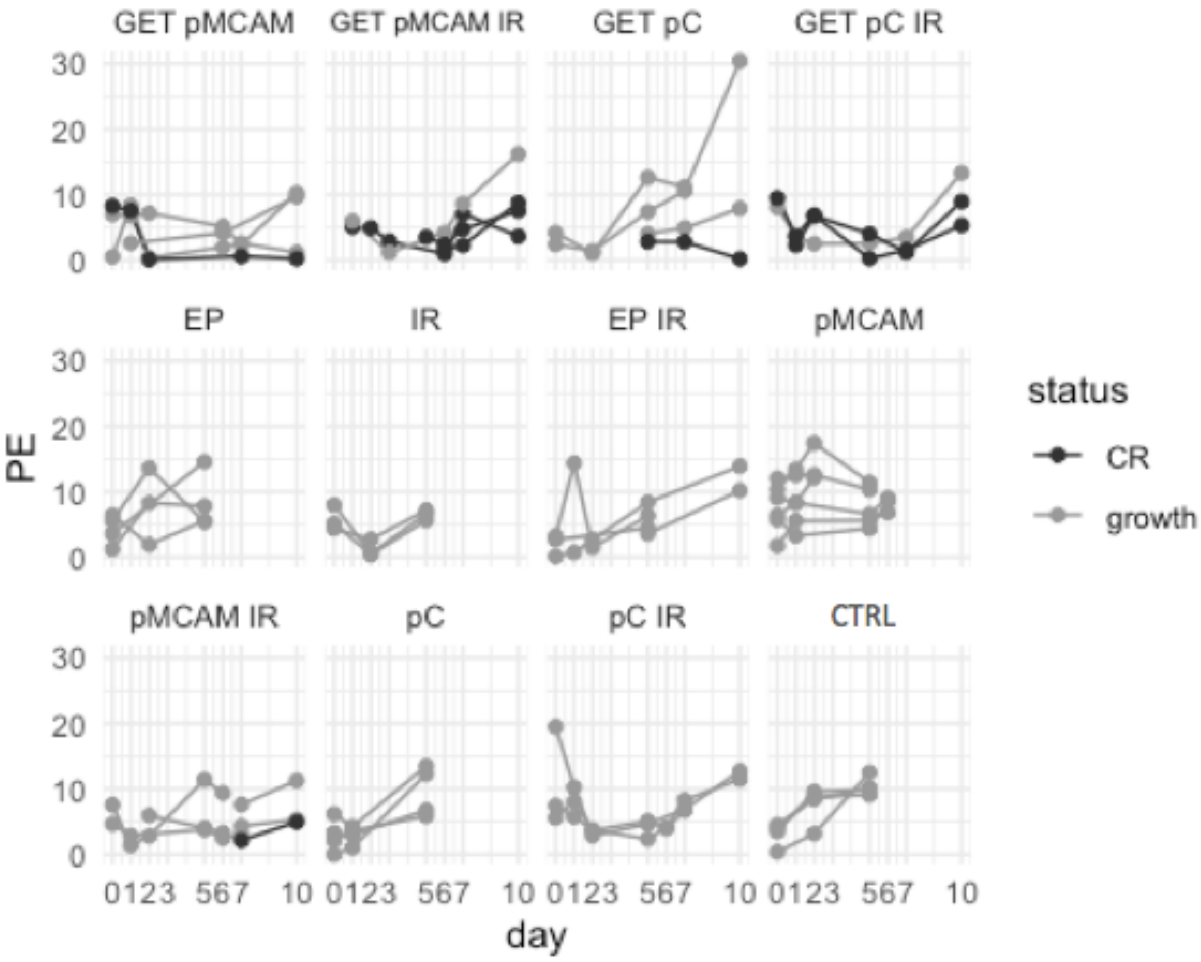

Supplementary Figure S4: CEUS results after combined treatment of GET and irradiation in B16F10 melanoma. Based on CEUS measurements, peak enhancement (PE) was calculated as the difference between peak intensity (PI) and base intensity (BI). Data represent individual measurements for each animal in the group at a given time point. All 12 groups are shown. CTRL = control, CR = complete responder; EP = application of electrical pulses; GET = gene electrotransfer; IR = single-dose irradiation, 15 Gy; pC = intratumoral injection of control plasmid; pMCAM = intratumoral injection of plasmid DNA encoding shRNA for MCAM.

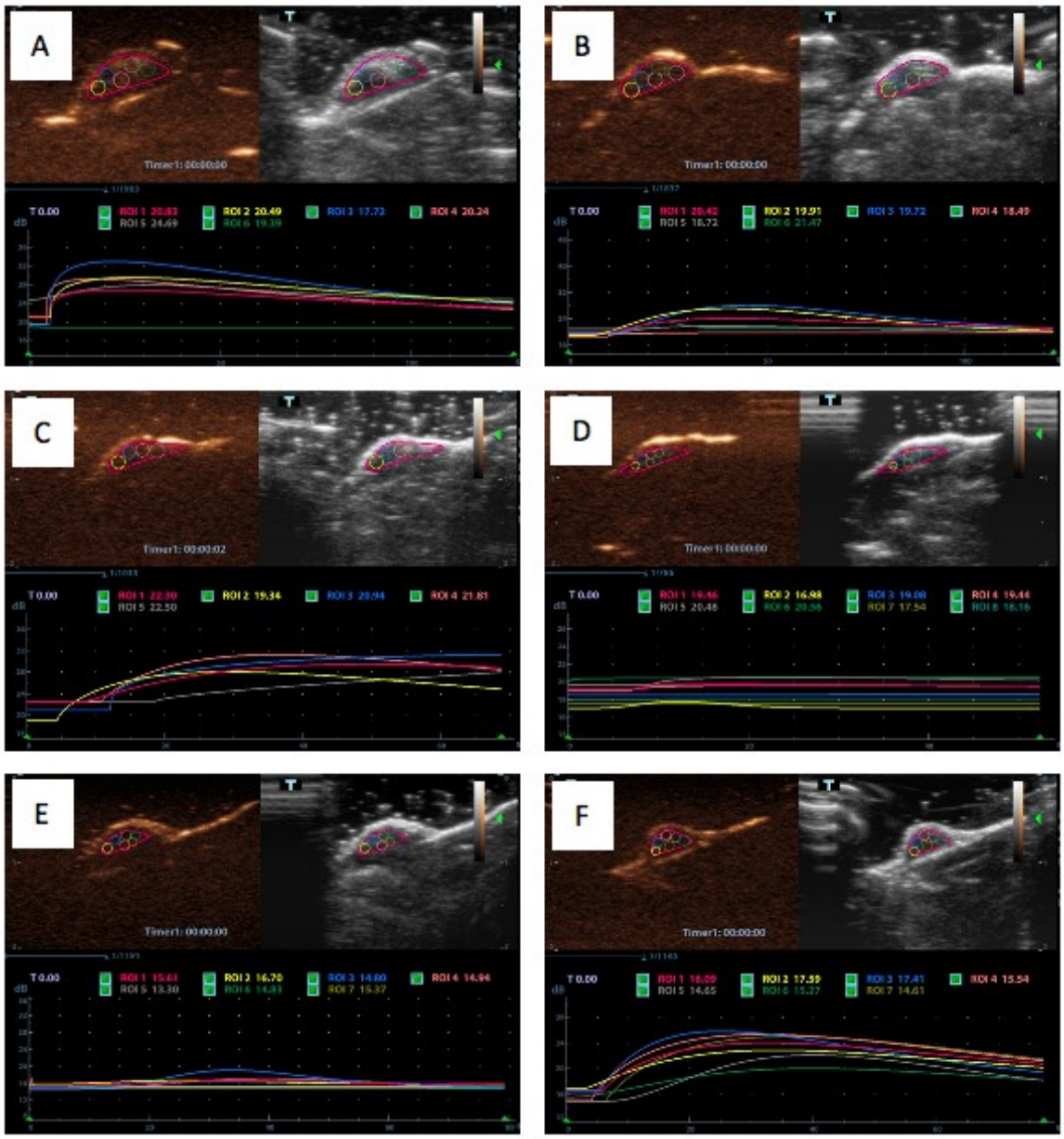

Supplementary Figure S5: CEUS perfusion curves of a complete response tumor treated with gene electrotransfer of control plasmid DNA and irradiation. A = day 0, B = day 1, C = day 2, D = day 5, E = day 7, and F = day 10. Peak enhancement (PE) values of the whole tumor (represented by the pink curve) on these days were 9.5 (A), 3.7 (B), 6.9 (C), 0.3 (D), 1.6 (E) and 5.4 (F). Pink curve indicates perfusion of whole tumor and other curves show perfusion of individual regions of interest. Note the heterogeneity of perfusion on days 0, 1, 2 and 10.

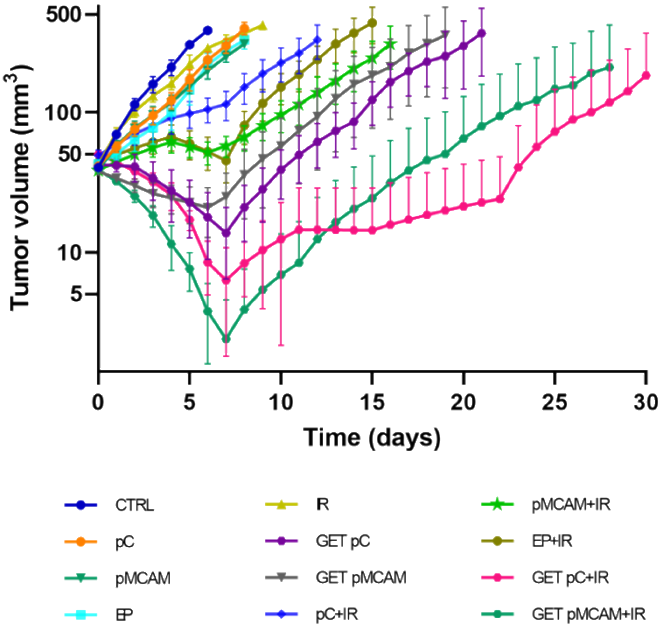

Supplementary Figure S6: Growth of B16F10 melanomas after silencing of MCAM and irradiation. CTRL = control, EP = application of electrical pulses; GET = gene electrotransfer; IR = single-dose irradiation, 15 Gy; pC = intratumoral injection of control plasmid; pMCAM = intratumoral injection of plasmid DNA encoding shRNA for MCAM. Data represent mean and standard error of the mean (mean±SE) of tumors that did not show a complete response (n=3-7).

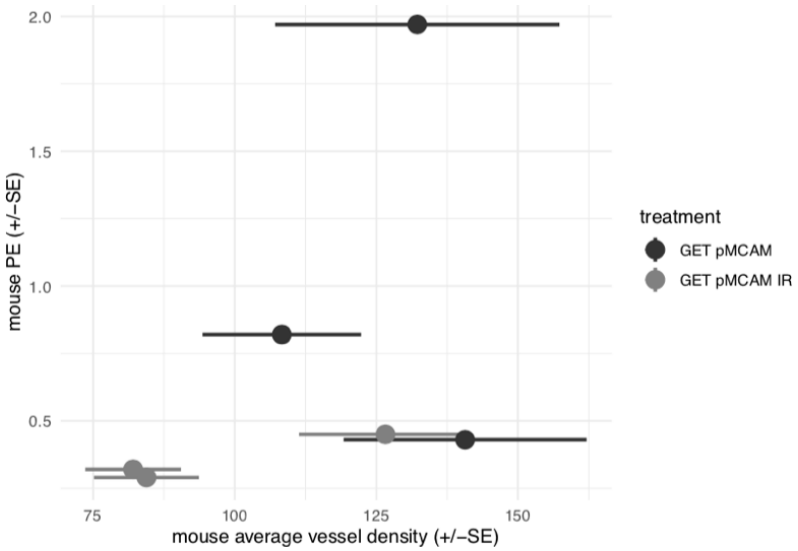

Supplementary Figure S7: Correlation of B16F10 tumor perfusion (CEUS PE) and vascular density, as assessed by histological analysis, after silencing MCAM and irradiation. In the treatment groups with the therapeutic plasmid; i.e. GET pMCAM and GET pMCAM IR, vascular density and PE were determined in the same mice, Pearson correlation coefficient was 0.45 (95% confidence interval [-0.57, 0.92]). GET = gene electrotransfer; IR = single-dose irradiation, 15 Gy; pMCAM = intratumoral injection of plasmid DNA encoding shRNA for MCAM.

Supplementary Table S1. Comparison of mean peak enhancement between complete responders (CR) and mice with tumor growth (non-CR). Mean (SD) for PE values and the number of mice for each group. P-values correspond to t-tests for each day, with Hommel correction for family-wise error rate when data are non-negatively associated (adjusted P).

day	CR	n	non-CR	n	P	adjusted P
0	8.88 (0.85)	2	5.21 (3.86)	34	0.011	0.032
1	4.66 (2.24)	4	6.10 (3.99)	22	0.340	0.680
2	4.67 (3.17)	4	5.42 (4.75)	25	0.698	0.698
5	2.66 (1.68)	4	7.42 (3.36)	34	0.003	0.015
6	1.70 (0.71)	3	5.27 (2.57)	12	0.001	0.007
7	2.82 (2.14)	8	6.21 (2.99)	13	0.007	0.021

Supplementary Table S2. Linear regression coefficients for each measurement day associating PE with log transformed DT.

day	regression coefficient (PE)	P	adjusted P
0	0.043	0.410	0.740
1	-0.026	0.740	0.740
2	-0.085	0.168	0.503
5	-0.208	<0.001	0.002
6	-0.384	0.003	0.015
7	-0.217	0.012	0.048

9. 3 Priloga 3. Dopolnilni podatki članka 2.3

Tumorska perfuzija, ovrednotena z dinamično ultrazvočno kontrastno preiskavo kot prediktivni dejavnik mišjih melanomov, zdravljenih z elektrokemoterapijo in genskim elektroprenosom plazmidne DNA z zapisom za mišji interlevkin-12

SUPPLEMENTARY INFORMATION

TUMOR PERFUSION EVALUATION USING DYNAMIC CONTRAST-ENHANCED ULTRASOUND AFTER ELECTROCHEMOTHERAPY AND IL-12 PLASMID ELECTROTRANSFER IN MURINE MELANOMA

Supplementary Figure Legends

Supplementary Figure S1: Dynamic contrast-enhanced magnetic resonance imaging (DCE-MRI) in B16F10 melanoma after electrochemotherapy with bleomycin (ECT BLM). A = untreated control, B = immediately after ECT BLM, C = 6 hours after ECT BLM, D = 36 hours after ECT BLM. To the left, the perfusion curve is presented and to the right, contrast-enhanced T1-weighted image is shown. Note that signal intensity increases for only 70 arbitrary units (a.u.) in B and 110 a.u. in C, while it increases by more than 500 a.u. in A and D.

Supplementary Figure S2: Dynamic contrast-enhanced ultrasound (DCE-US) examination of melanoma B16F10; untreated control on day 6: representative images at different times (A = at 3 sec, B = at 6 sec, C = at 20 sec, D = at 40 sec, E = at 80 sec), where the nonlinear contrast mode is shown to the right of each image. Perfusion curves for the whole tumor and different regions of interest (ROIs) are presented in F.

Supplementary Figure S3: Schedule for the combined treatment of electrochemotherapy with bleomycin (ECT BLM) and gene electrotransfer of plasmid DNA encoding mouse interleukin-12 (ECT BLM GET pIL-12).

Supplementary Figure S4: Schedule for dynamic contrast-enhanced ultrasound (DCE-US) examinations.

Supplementary Figure S5: Dynamic contrast-enhanced ultrasound (DCE-US) perfusion curve with a schematic presentation of dynamic parameters. Raw data and fitting curves are presented by M9 (Mindray) ultrasound machine built-in machine software. Peak enhancement (PE) is the difference between peak (PI) and base intensity (BI). The arrival time (AT) is the time after contrast injection until the appearance of contrast. Time to peak (TTP) is the time when the contrast intensity reaches a peak

value. Descend time to one-half (DT/2) is the time when the intensity is half the value of the peak intensity. Ascending and descending slopes (AS and DS) refer to slope coefficients. Area under the curve (AUC) is area under the perfusion curve.

Supplementary Table Legends

Supplementary Table S1: Tumor growth delay (GD) and doubling time (DT) after electrochemotherapy with bleomycin (ECT BLM) and gene electrotransfer of plasmid DNA encoding mouse interleukin-12 (GET pIL-12) in the melanoma B16F10 model.

Supplementary Table S2: Mean peak enhancement (PE) values and their standard error after electrochemotherapy with bleomycin (ECT BLM) and gene electrotransfer of plasmid DNA encoding mouse interleukin-12 (GET pIL-12) in the melanoma B16F10 model. Note that on days 7 and 10, only mice in the therapeutic groups (ECT BLM and ECT BLM combined with GET pIL-12) were measured because mice in the control groups were humanely sacrificed on day 6 due to the disease burden.

Supplementary Table S3: Pearson correlation coefficients for each day of the dynamic contrast-enhanced ultrasound (DCE-US) measurement, associating peak enhancement (PE) with logarithmically transformed tumor doubling time (DT). Note that data for mice in all groups are presented.

Supplementary Table S4: Pearson correlation coefficients for each day of the dynamic contrast-enhanced ultrasound (DCE-US) measurement, associating peak enhancement (PE) with logarithmically transformed tumor doubling time (DT). Note that only data for mice in the therapeutic groups (ECT BLM and ECT BLM combined with GET pIL-12) are presented.

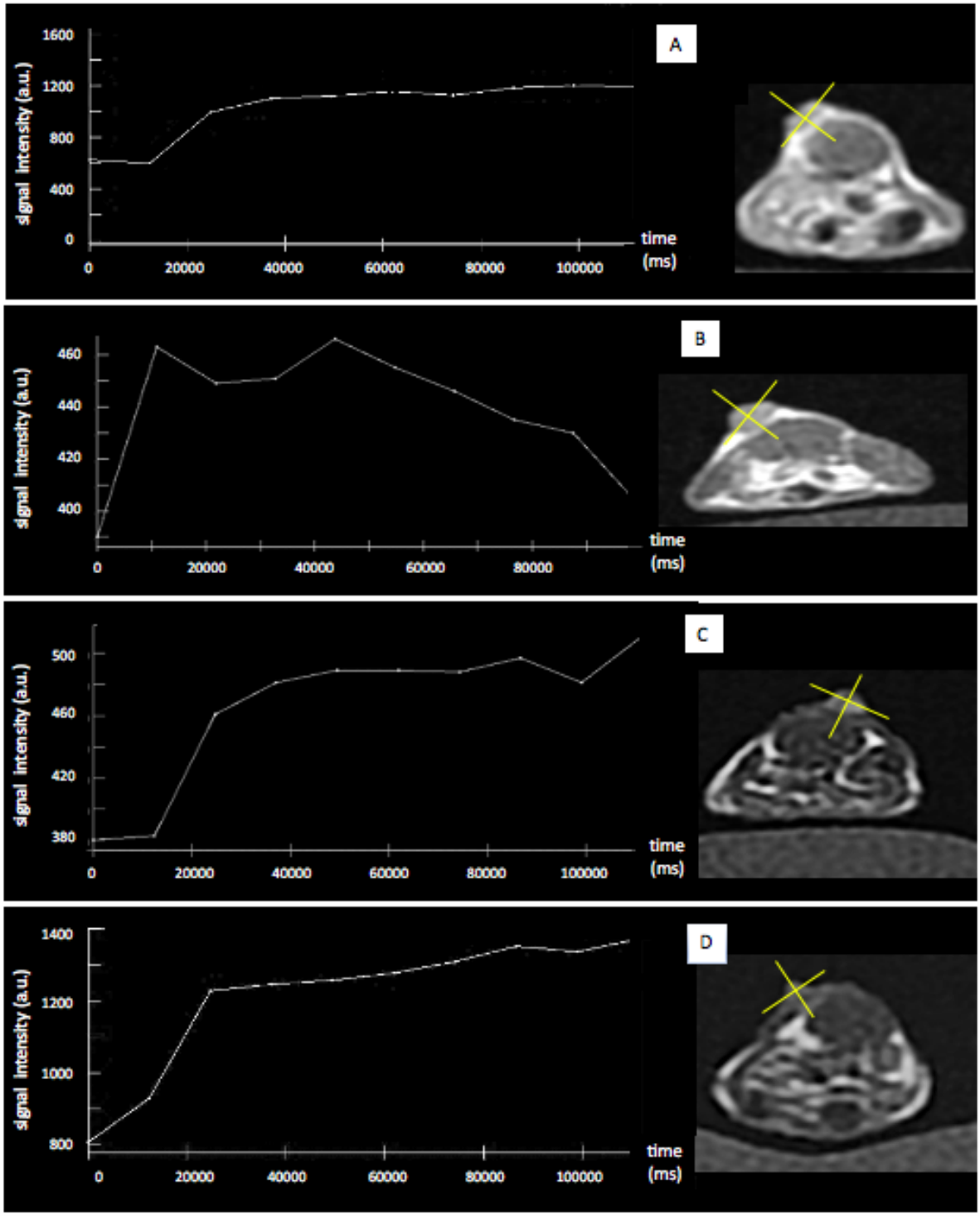

Supplementary Figure S1: Dynamic contrast-enhanced magnetic resonance imaging (DCE-MRI) in B16F10 melanoma after electrochemotherapy with bleomycin (ECT BLM). A = untreated control, B = immediately after ECT BLM, C = 6 hours after ECT BLM, D = 36 hours after ECT BLM. To the left, the perfusion curve is presented and to the right, contrast-enhanced T1-weighted image is shown. Note that signal intensity increases for only 70 arbitrary units (a.u.) in B and 110 a.u. in C, while it increases by more than 500 a.u. in A and D.

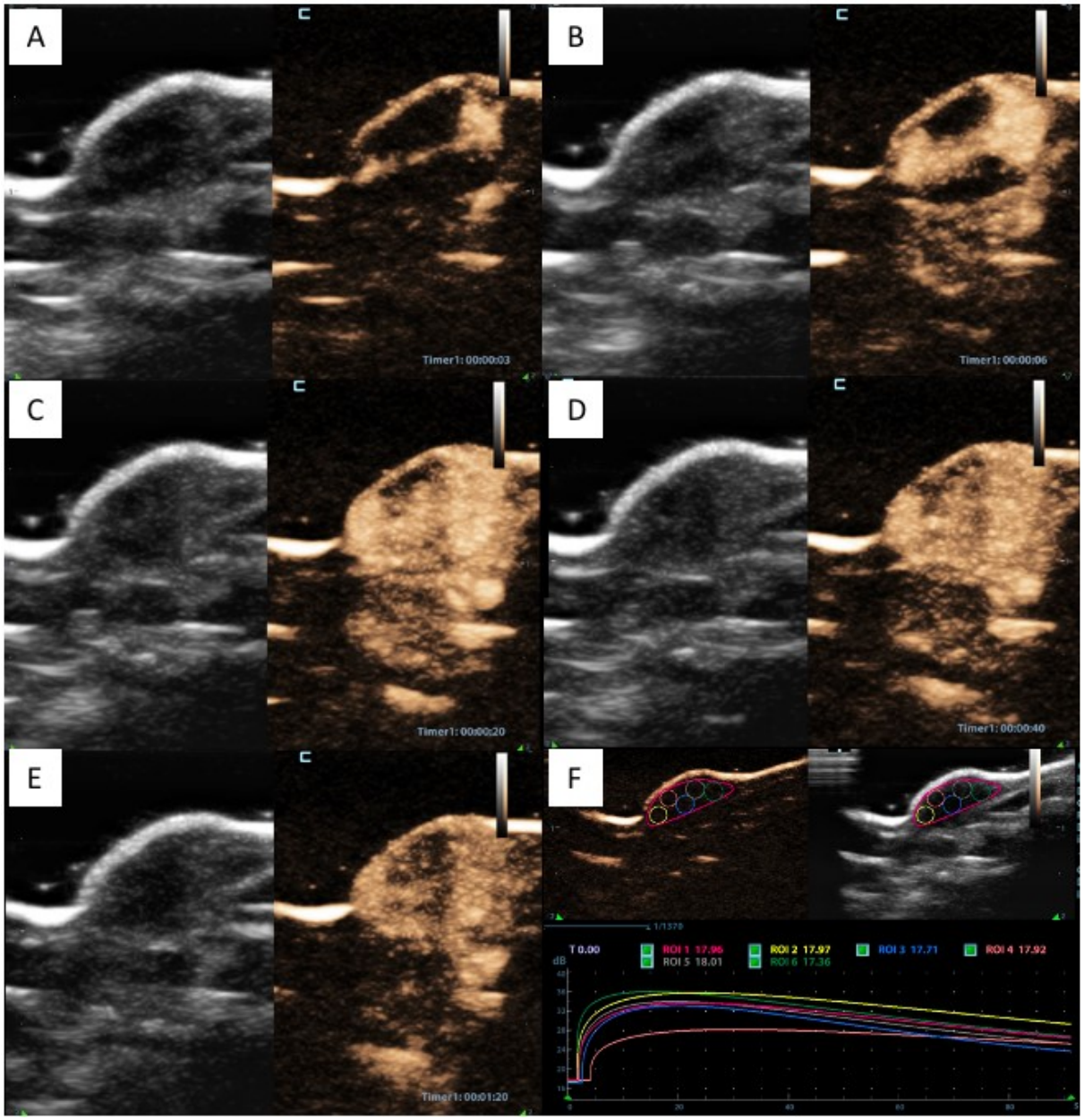

Supplementary Figure S2: Dynamic contrast-enhanced ultrasound examination (DCE-US) of melanoma B16F10; untreated control on day 6: representative images at different times (A = at 3 sec, B = at 6 sec, C = at 20 sec, D = at 40 sec, E = at 80 sec), where the nonlinear contrast mode is shown to the right of each image. Perfusion curves for the whole tumor and different regions of interest (ROIs) are presented in F.

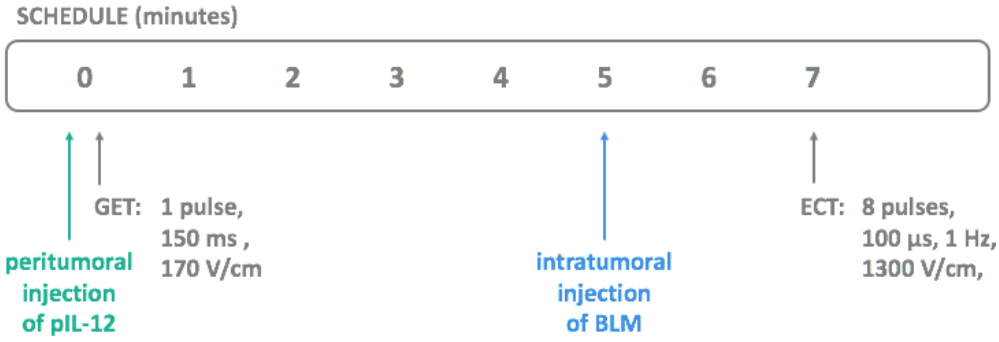

Supplementary Figure S3: Schedule for the combined treatment of electrochemotherapy with bleomycin (ECT BLM) and gene electrotransfer of plasmid DNA encoding mouse interleukin-12 (ECT BLM GET pIL-12).

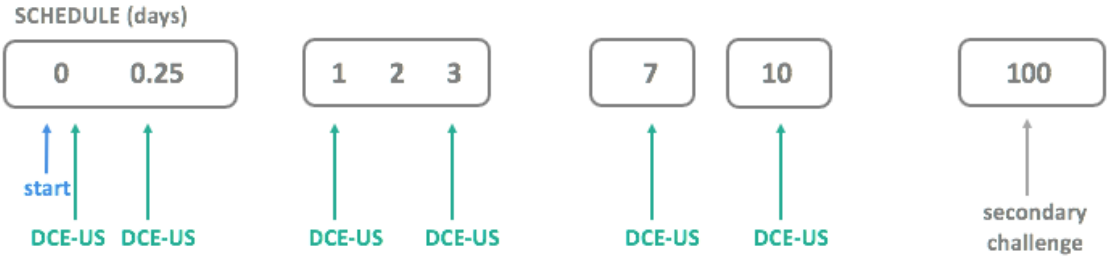

Supplementary Figure S4: Schedule for dynamic contrast-enhanced ultrasound (DCE-US) examinations.

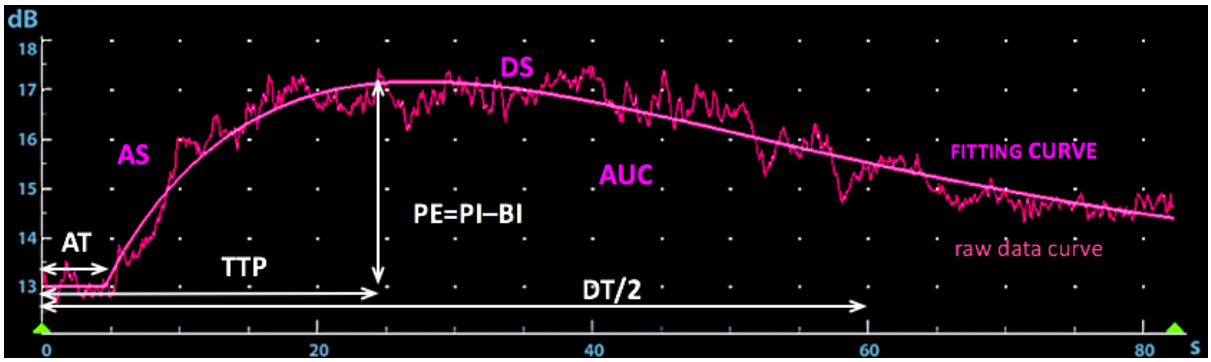

Supplementary Figure S5: Dynamic contrast-enhanced ultrasound (DCE-US) perfusion curve with a schematic presentation of dynamic parameters. Raw data and fitting curves are presented by M9 (Mindray) ultrasound machine built-in machine software. Peak enhancement (PE) is the difference between peak (PI) and base intensity (BI). The arrival time (AT) is the time after contrast injection until the appearance of contrast. Time to peak (TTP) is the time when the contrast intensity reaches a peak value. Descend time to one-half (DT/2) is the time when the intensity is half the value of the peak intensity. Ascending and descending slopes (AS and DS) refer to slope coefficients. Area under the curve (AUC) is area under the perfusion curve.

Supplementary Table S1: Tumor growth delay (GD) and doubling time (DT) after electrochemotherapy with bleomycin (ECT BLM) and gene electrotransfer of plasmid DNA encoding mouse interleukin-12 (GET pIL-12) in the melanoma B16F10 model.

Group	n	DT (days) mean±SE	GD (days) mean±SE
Control	8	1.5±0.2	/
EP (ECT pulses)	8	3.2±0.3	1.7±0.3
EP (GET pulses)	8	2.1±0.1	0.6±0.1
BLM	8	2.2±0.1	0.7±0.1
pIL-12	8	1.9±0.1	0.4±0.1
GET pIL-12	8	3.4±0.3	1.9±0.3
ECT BLM	8	15.5±1.6*	14.0±1.6*
ECT BLM GET pIL-12	10	28.2±3.6*	26.7±3.6*

BLM = bleomycin, 7.5 µg/mouse; ECT = electrochemotherapy; EP = electric pulses; GET = gene electrotransfer; pIL-12 = plasmid DNA encoding mouse interleukin-12; SE = standard error of arithmetic mean; * = $p<0.05$, statistically significant difference compared to all other group; / = not applicable.

Supplementary Table S2: Mean peak enhancement (PE) values and their standard error after electrochemotherapy with bleomycin (ECT BLM) and gene electrotransfer of plasmid DNA encoding mouse interleukin-12 (GET pIL-12) in the melanoma B16F10 model. Note that on days 7 and 10, only mice in the therapeutic groups (ECT BLM and ECT BLM combined with GET pIL-12) were measured because mice in the control groups were humanely sacrificed on day 6 due to the disease burden.

Group	n	PE 0 (a.u.) mean±SE	PE 0.25 (a.u.) mean±SE	PE 1 (a.u.) mean±SE	PE 3 (a.u.) mean±SE	PE 7 (a.u.) mean±SE	PE 10 (a.u.) mean±SE
Control	8	6.5±0.7◎	6.5±1.12◎	6.4±1.0◎	8.9±1.1◎	/	/
EP (ECT pulses)	4	2.1±0.6*◊	2.8±0.5✦	3.7±0.9	6.6±0.9◊✦	/	/
EP (GET pulses)	4	3.8±0.7	2.9±0.4	2.9±0.5	6.3±0.9	/	/
BLM	3	3.8±0.6	4.7±1.0	3.8±0.6	3.6±1.0	/	/
pIL-12	4	5.8±1.3	2.4±1.0	4.1±0.6	6.0±1.2	/	/
GET pIL-12	8	3.8±0.8	3.7±0.9	6.2±1.6	4.7±0.9*	/	/
ECT BLM	8	2.4±0.8*	1.6±0.4*⊡	2.2±0.3*	2.2±0.5*	3.0±0.8	5.9±1.3⊡
ECT BLM GET pIL-12	8	1.7±0.5*	1.8±0.4*	2.1±0.6*	2.5±0.6*	2.1±0.6	2.9±0.5*

BLM = bleomycin, 7.5 µg/mouse; ECT = electrochemotherapy; EP = electric pulses; GET = gene electrotransfer; pIL-12 = plasmid DNA encoding mouse interleukin-12; PE 0 = peak enhancement immediately after the therapy; PE 0.25 = peak enhancement 6 hours after therapy, PE 1 = peak enhancement 24 hours after therapy, PE 3 = peak enhancement 3 days after therapy, PE 7 = peak enhancement 7 days after therapy , PE 10 = peak enhancement 10 days after therapy, SE = standard error of arithmetic mean; * = $p<0.05$, statistically significant difference compared to group ◎; / = not applicable, ✦⊡◊ = statistical significance between two groups of mice.

Supplementary Table S3: Pearson correlation coefficients for each day of the dynamic contrast-enhanced ultrasound (DCE-US) measurement, associating peak enhancement (PE) with logarithmically transformed tumor doubling time (DT). Note that data for mice in all groups are presented.

day	r	95% CI	R^2	P
0	-0.5871	-0.7482 to -0.3608	0.2492	< 0.001
0.25	-0.4510	-0.6535 to -0.1882	0.2034	0.002
1	-0.4423	-0.6472 to -0.1777	0.1956	0.002
3	-0.5976	-0.7552 to -0.3747	0.3571	< 0.001
7	-0.6067	-0.8475 to -0.1587	0.3681	0.013
10	-0.7691	-0.9157 to -0.4419	0.5916	< 0.001

r = Pearson correlation coefficient, CI = confidence interval, R^2 = coefficient of determination

Supplementary Table S4: Pearson correlation coefficients for each day of the dynamic contrast-enhanced ultrasound (DCE-US) measurement associating peak enhancement (PE) with logarithmically transformed tumor doubling time (DT). Note that only data for mice in the therapeutic groups (ECT BLM and ECT BLM combined with GET pIL-12) are presented.

day	r	95% CI	R^2	P
0	-0.7746	-0.7482 to -0.3608	0.5999	< 0.001
0.25	-0.4729	-0.7847 to -0.0297	0.2237	0.005
1	-0.2580	-0.66683 to -0.2725	0.0666	0.335
3	-0.5478	-0.8206 to -0.0715	0.3001	0.028
7	-0.6067	-0.8475 to -0.1587	0.3681	0.013
10	-0.7691	-0.9157 to -0.4419	0.5916	< 0.001

r = Pearson correlation coefficient, CI = confidence interval, R^2 = coefficient of determination